

**TECHNICAL REPORT ON THE EXPLORATION HISTORY
AND CURRENT STATUS OF THE STORM PROJECT,
SOMERSET ISLAND, NUNAVUT**

NTS Sheets 58C/10, 11, 13, 14
(73°39' N Latitude and 94°20' W)
UTM: 8173459N 458108E NAD83z15
Prospecting Permits: 7547, 7548, 7549, 7880, 8340, 8341, 8342, 8343

prepared for:
Aston Bay Ventures Ltd.
222 – 400 E Evergreen Blvd.
Vancouver, WA, USA
98660



prepared by:
Aurora Geosciences Ltd.¹
3506 McDonald Drive
Yellowknife, NT, Canada
X1A 2H1

and



APEX Geoscience Ltd.²
#200 9797 45 Avenue
Edmonton, AB, Canada
T6E 5V8

¹Jim Robinson, B.Sc., P. Geol.

²Bryan Atkinson, B.Sc., P. Geol.

October 31, 2012
Yellowknife, Northwest Territories
Canada

CERTIFICATE OF QUALIFICATIONS, CONSENT AND DATE AND SIGNATURES

I, Ronald James Robinson residing at 3506 McDonald Drive, Yellowknife, Northwest Territories, Canada hereby certify that:

I am presently employed by Aurora Geosciences Ltd. of Yellowknife, Northwest Territories, Canada as a senior resource geologist;

I am a graduate of the University of British Columbia (1985) and hold a B.Sc. degree in geology. I have been employed in my profession by various mining and consulting companies since my graduation. I have produced and supervised the production of mineral resource estimates and mineral reserve documents on numerous deposits and deposit types for the past twenty years. I am a “qualified person” for the purposes of National Instrument 43-101;

I am a member of the Northwest Territories Association of Professional Engineers, Geologists, and Geophysicists (Member #1662).

I visited and inspected the property on August 4, 2012;

I have had no involvement with Aston Bay Ventures Ltd., its predecessors or subsidiaries. nor in the Aston Bay Property prior to visiting the property and researching and writing this report, and I am independent of the issuer applying all of the tests in section 1.4 of National Instrument 43-101;

I have not received nor expect to receive any interest, direct or indirect, in Aston Bay Ventures Ltd., its subsidiaries, affiliates and associates;

I have read “Standards of Disclosure for Mineral Projects”, National Instrument 43-101 and Form 43-101F1, and the Report has been prepared in compliance with this Instrument and that Form;

I am responsible for the preparation of the complete report;

As of the date of this certificate, to the best of my knowledge, information and belief, I am not aware of any material fact or material change with respect to the subject matter of the Report that is not reflected in the Report, the omission or addition of which would make the Report misleading;

This certificate applies to the NI 43-101 compliant technical report titled “Technical Report On The Exploration History And Current Status Of The Storm Project, Somerset Island, Nunavut, ” dated October 31, 2012; and

I consent to the public filing of this technical report with any stock exchange and any regulatory authority and consent to the publication for regulatory purposes, including electronic publication in the public company files of their websites accessible to the public, of extracts from the technical report by Aston Bay Ventures Ltd.

Dated at Yellowknife, Northwest Territories, this 31st day of October, 2012.



R. J. Robinson, P. Geol.

Northwest Territories and Nunavut Association of Professional Engineers and Geoscientists

Senior Resource Geologist

Aurora Geosciences Ltd.

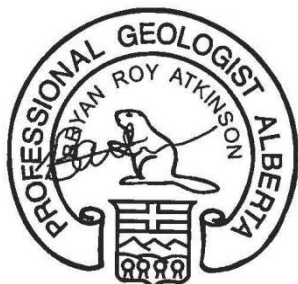
Certificate of Author

I, Bryan Roy Atkinson, B.Sc., P.Geol., MAusIMM, do hereby certify that:

1. I am a senior geologist with: APEX Geoscience Ltd.
Suite 200, 9797 – 45th Avenue
Edmonton, Alberta T6E 5V8
Phone: 780-439-5380
2. I graduated with a B.Sc. with Specialization in Geology from the University of Alberta in 2004.
3. I am and have been registered as a Professional Geologist with the Association of Professional Engineers, Geologists and Geophysicists of Alberta since 2008.
4. I have worked as a geologist and practiced my profession for more than eight years since my graduation from university and have been involved in mineral exploration, mine site geology and operations and mineral resource estimations on numerous projects and deposits in Canada, the United States, Mexico, South America, Africa, Australia, Indonesia and Saudi Arabia.
5. I have read the definition of “Qualified Person” set out in National Instrument 43-101 (“NI 43-101”) and certify that by reason of my education, affiliation with a professional association (as defined in NI 43-101) and past relevant work experience, I fulfill the requirements to be a “Qualified Person” for the purpose of NI 43-101.
6. I am responsible for and have supervised the 2012 exploration and preparation of the Technical Report titled *“Technical Report on the Exploration History and Current Status of the Storm Project, Somerset Island, Nunavut”*, and dated October 31st, 2012 (the “Technical Report”). I visited the Property between July 28th and August 31st, 2012.
7. Prior to the completion of this report I have not had prior involvement with the property that is the subject of the Technical Report.
8. I am not aware of any scientific or technical information with respect to the subject matter of the Technical Report that is not reflected in the Technical Report, the omission to disclose which makes the Technical Report misleading.
9. I own 25,000 shares of Aston Bay Ventures Ltd. The level of investment does not compromise my independence as set out in sections 1.5.1 and 1.5.2 of NI 43-101. I have read National Instrument 43-101 and Form 43-101F1, and the Technical Report has been prepared with that instrument and form.
10. I consent to the filing of the Technical Report with the regulatory authority and any publication by them for regulatory purposes, including electronic publication in the public company files or their websites.

Dated this October 31st, 2012

Edmonton, Alberta, Canada



Bryan R. Atkinson, B.Sc., P.Geol., MAusIMM

TECHNICAL REPORT ON THE EXPLORATION HISTORY AND CURRENT STATUS OF THE STORM PROJECT, SOMERSET ISLAND, NUNAVUT

TABLE OF CONTENTS

| | |
|---|------|
| CERTIFICATE OF QUALIFICATIONS, CONSENT AND DATE AND SIGNATURES | ii |
| Certificate of Author | iv |
| TABLE OF CONTENTS..... | v |
| LIST OF FIGURES..... | vii |
| LIST OF TABLES..... | viii |
| APPENDICES (At end of document) | viii |
| 1: SUMMARY | 1 |
| 1.1 Introduction | 1 |
| 1.2 Location and Ownership | 1 |
| 1.3 Geology | 2 |
| 1.4 History and Mineralization..... | 2 |
| 1.5 Work Completed | 3 |
| 1.6 Conclusions | 3 |
| 1.7 Recommendations | 4 |
| 2: INTRODUCTION..... | 5 |
| 3: RELIANCE ON OTHER EXPERTS..... | 9 |
| 4: PROPERTY DESCRIPTION AND LOCATION..... | 9 |
| 5: ACCESSIBILITY, CLIMATE, LOCAL RESOURCES, INFRASTRUCTURE AND PHYSIOGRAPHY | 14 |
| 5.1 Access, Local Resources, and Infrastructure..... | 14 |
| 5.2 Climate and Physiography..... | 15 |
| 6: HISTORY | 16 |
| 7: GEOLOGICAL SETTING AND MINERALIZATION | 24 |
| 7.1 Regional Geology | 24 |
| 7.2 Local Geology | 26 |
| 7.3 Property Geology | 27 |
| 7.4 Mineralization | 33 |
| 7.4.1 Seal Zinc | 33 |

| | | |
|-------|--|----|
| 7.4.2 | Storm Copper | 34 |
| 8: | DEPOSIT TYPES | 37 |
| 8.1 | Mississippi Valley-Type Lead Zinc Deposits | 37 |
| 8.2 | Sediment-Hosted Stratiform Copper Deposits | 38 |
| 8.2.1 | Kupferscheifer type..... | 38 |
| 8.2.2 | Kipushi-type | 38 |
| 9: | EXPLORATION | 39 |
| 9.1 | Introduction | 39 |
| 9.2 | VTEM Airborne Geophysical Survey | 39 |
| 9.3 | Airborne Geophysical Interpretation..... | 42 |
| 9.4 | Surface Sampling & Mapping..... | 45 |
| 9.5 | Historical Diamond Drill Core Resampling and Collar Surveying..... | 45 |
| 10: | DRILLING | 49 |
| 11: | SAMPLE PREPARATION, ANALYSES AND SECURITY | 49 |
| 11.1 | Sample Collection and Shipping..... | 49 |
| 11.2 | Sample Preparation, Analyses and Security..... | 49 |
| 12: | DATA VERIFICATION..... | 51 |
| 13: | MINERAL PROCESSING AND METALLURGICAL TESTING..... | 51 |
| 14: | MINERAL RESOURCE ESTIMATES | 52 |
| 15: | ADJACENT PROPERTIES | 52 |
| 16: | OTHER RELEVANT DATA AND INFORMATION | 52 |
| 17: | INTERPRETATION AND CONCLUSIONS..... | 52 |
| 18: | RECOMMENDATIONS..... | 55 |
| 19 | REFERENCES..... | 58 |

LIST OF FIGURES

| | |
|--|----|
| Figure 1 Storm Property Location Map..... | 8 |
| Figure 2 Prospecting Permit and Claim Location Map..... | 10 |
| Figure 3 Seal Zone Historic Drillhole Collars | 17 |
| Figure 4 Storm Showing Historic Drillhole Collars | 18 |
| Figure 5 Regional Geology | 25 |
| Figure 6 Seal Zinc Showing Property Geology..... | 29 |
| Figure 7 Storm Copper Showing Property Geology | 30 |
| Figure 8 Stratigraphic Column, Northwest Somerset Island..... | 32 |
| Figure 9 Storm Property VTEM Survey | 40 |
| Figure 10 Storm Property Airborne Total Magnetic Intensity | 41 |
| Figure 11 Multiscale Edge Detection (Worms) with Interpreted Major Linears | 43 |
| Figure 12 Storm Property RDI Clipped to 500 ohm-m | 44 |
| Figure 13 2012 Grab Sample Locations..... | 47 |
| Figure 14 Historic Drilling Re-sampled Core Locations | 48 |
| Figure 15 Storm Property VTEM Survey Prospective Target Zones..... | 54 |

LIST OF TABLES

| | |
|---|----|
| Table 1 List of Abbreviations..... | 7 |
| Table 2 Storm Property Prospecting Permit and Mineral Claim Details..... | 11 |
| Table 3 Selected Historic Climate Statistics for Resolute Bay, NU (Environment Canada, 2012)..... | 15 |
| Table 4 Storm Property Historical Exploration Summary | 19 |
| Table 5 Seal Zone Significant Drill Hole Intersections..... | 21 |
| Table 6 Storm Zone Significant Historic Drill Hole Intersections | 22 |
| Table 7 2012 Seal Zone Significant Assay Highlights From Historic Drill Holes | 46 |
| Table 8 2012 Storm Prospect Significant Assay Highlights From Historic Drill Holes | 46 |
| Table 9 Comparison of Historic to 2012 Assay Results for Selected Intervals..... | 55 |
| Table 10 Estimated cost to conduct Stage 1 and 2 exploration programs during 2013..... | 56 |

APPENDICES (At end of document)

Appendix 1 Aston Bay APEX Costs 2011-2012

Appendix 2 Airborne Geophysical Interpretation of the Storm Copper Property

Appendix 3 Grab Sample Results

Appendix 4 Core Intervals and Descriptions

1: SUMMARY

1.1 Introduction

In 2012, Aston Bay Ventures Ltd. (Aston Bay) commissioned APEX Geoscience Ltd. (APEX) to complete a field based sampling program and, in conjunction with Aurora Geosciences Ltd. (Aurora), prepare an independent, Canadian National Instrument 43-101 (NI 43-101) Technical Report, for the Storm Property (“the Property”), located on Somerset Island, in Nunavut, Canada. The Storm Property contains the Seal zinc-silver prospect and multiple copper-silver showings that collectively represent the Storm prospect. This report provides details of historic and recent base metal exploration conducted at the Property to date, which includes a recent airborne geophysical survey and follow-up interpretation during 2011, and a field based surface and historic core sampling program along with ground truthing of the recently identified geophysical anomalies during 2012.

A detailed post-processing study carried out on the 2011 airborne VTEM data indicated that the mineralized zones of the Storm deposit can be accurately mapped and modeled. Analysis of the resistivity depth imaging (RDI) inversions in conjunction with the historical drilling suggests that there remain several zones that have not been drill tested adequately. Further, the deep (100 to 200 m below sea level) conductive trends shown to be extending southward from the 4100N Zone have not been tested at all. Additional modeling of the VTEM data using the Maxwell plate modelling software should permit precise drill targeting for these bodies.

A further nine secondary anomalous areas were identified through inversion modeling of the VTEM data. These zones do not have characteristics similar to those of the main Storm deposits, but do represent areas of surficial or near surface conductivity, and merit further investigation.

The 2012 drill core resampling program indicates that the 2012 assay values agree very well with the historic data. Sampling of selected, previously untested sections of the stored drill core commonly yielded copper assays in the range of 0.1 to 0.3% copper.

This report provides details of base metals exploration conducted to date in order to indicate that the Storm property is a property of merit, suitable for further advancement.

1.2 Location and Ownership

The property is located 112 km south of the community of Resolute Bay, Nunavut on Somerset Island and centred geographically at approximately 73°39’ North latitude and 94°20’ West longitude. The property is a land package consisting of four Commander prospecting permits totaling 195,438.9 acres or 79,091 hectares, along with four prospecting permits held by Michael Dufresne on behalf of Aston Bay, totaling 167,598 acres or 67,825 hectares. The total property area is 363,037 acres or 146,916 hectares.

The Storm property covers an area roughly 63 kilometres long by 42 kilometres wide. The known Storm Copper showings and geophysical anomalies cover a broad area east of Aston Bay. The

showings extend east/west 34 km from 450000E to 484000E and north/south 20 km from 8165000N to 8185000N. The Seal Zinc showings cover a smaller area 6 km north/south and 2 km east /west on a peninsula and island in Aston Bay

With respect to the four (4) permits held by Commander there is an option agreement with Aston Bay whereby the latter can earn a 70% ownership stake by becoming publicly listed, transferring 3,000,000 common shares and \$150,000 to Commander, plus incurring \$15 million in exploration expenditures to advance the property, including delivery of an Indicated Resource as defined by NI 43-101, before December 31, 2019.

1.3 Geology

The Storm property covers a portion of the Cornwallis Fold and Thrust Belt which affects sediments of the Arctic Platform deposited on a stable, passive continental margin that existed from Late Proterozoic to Late Silurian time. The oldest rocks in the sedimentary sequence are intruded by 1,270 Ma MacKenzie diabase dykes and 623 Ma Franklin diabase dykes.

The Late Silurian to Early Devonian Caledonian Orogeny shed clastic sediments onto the Arctic Platform from the east and created localized, basement-cored uplifts. The most significant basement uplift is the Boothia Uplift, a north-south trending basement feature 125 km wide by 1,000 km long and possibly rooting the Sverdrup Basin to the north.

Southward compression during the Ellesmerian Orogeny in Late Devonian to Early Carboniferous time produced a fold and thrust belt north and west of the former continental margin, effectively ending carbonate sedimentation throughout the region. It is this tectonic event that is believed to have generated the ore-bearing fluids responsible for Zn-Pb deposits in the region.

1.4 History and Mineralization

Historical exploration around the Storm Property has defined two distinct styles of mineralization, each associated with its own specific stratigraphic horizon. The stratabound Seal Zinc (Zn) showing occur in Early to Middle Ordovician Ship Point Formation rocks. The stratigraphic and structurally controlled Storm Copper (Cu) showings occur at least 800 m higher in the stratigraphic column in the Late Ordovician to Late Silurian Allen Bay Formation (Cook and Moreton, 2000).

Mineralization at the Seal Zn showings is primarily hosted within a quartz arenite unit with interbedded dolostone and sandy dolostone of the Ordovician Ship Point Formation. Mineralization at the Storm Cu showings is epigenetic, carbonate-hosted and lies within an intracratonic rift basin that has been modified by folding and faulting. The mineralization is spatially associated with the north and south boundary faults of the Central Graben. This structure is interpreted as a pull-apart basin developed as a result of translational movement along basement-rooted faults. The basal Aston Formation red beds are thought to be a plausible source of metals for the mineralization at both the Seal Zn and Storm Cu showings.

The area has been an exploration target since 1960 when mineralization was first discovered by Bankeno Ltd. while conducting oil and gas exploration in the region. Bankeno entered into a 25% joint venture with Cominco Ltd. in 1964 to explore properties in the Cornwallis Zn-Pb district, including the area of the Storm showings. From early 1964 until 2007, Cominco was actively conducting exploration within the Storm Property. A joint venture agreement with Noranda Inc. covered exploration from 1999 to 2001. Commander Resources acquired Prospecting Permits in the area after the land package held by Cominco had substantially lapsed in 2007.

In writing this report the authors relied upon government research, personal communications, assessment reports and historical internal reports summarized by and on behalf of Cominco, Noranda and Commander. The author also utilized information from Cominco, later Teck-Cominco Ltd. (Teck), who had maintained mineral tenure in the region since 1964.

1.5 Work Completed

The 2012 program involved interpretation of the VTEM and aeromagnetic survey from 2011 by Intrepid Geophysics. This was followed by a property visit, prospecting, surface sampling, resampling of historical diamond drill core and ground truthing of the VTEM anomalies by APEX and Aurora personnel. Resurveying of the drill collars was necessary as it had been noted that previously published collar locations did not correspond to the actual locations of the drillhole collars in the field.

The drill core resampling program was aimed to validate historical results, extend several of the mineralized, historically sampled intervals and infill data missing (not reported) from previous drill programs. Approximately 30% of the previously un-split core which was sampled and assayed during 2012 yielded assay results in the 0.1 to 0.3% range for Cu. Most of these sample intervals were shoulder samples, or samples from between previously recognized mineralized zones.

Prospecting confirmed the presence, location and extent of known historic zinc and copper mineralization at the Seal Zinc and Storm Copper showings, respectively and their correlation with geophysical anomalies. A total of 14 rock grab samples were collected from the Storm Copper, Seal Zinc and from Seal Island. Two samples were collected from two discrete zones, 2750N and 2200N, within the overall Storm Copper zone, both assayed greater than 40% Cu. Six samples were collected along the trend of known mineralization at the Seal Zinc showing, returning assays up to greater than 30% Zn. On Seal Island, six samples were collected from areas of historically reported mineralized outcrops and anomalous assays; none of the 2012 returned anomalous assays.

The 2012 Storm exploration expenditures were approximately CDN \$448,000.

1.6 Conclusions

The combination of terrain, climate and remote location are challenges to the effective determination of the size and characteristics of the Seal Zn and Storm Cu mineral deposits. At the

Seal Zn showings, steep terrain makes it problematic to place drill holes in the optimum locations for drill testing the stratabound mineralization. At the Storm Cu showings, essentially most of the mineralization in the largest zone is covered or masked by complexly faulted units lying within the Central Graben. However, soil geochemistry, geophysical surveys and drilling results to date indicate that further work is warranted to outline and better define both showings.

Enhanced derivative grids of the airborne magnetic data were generated and imaged as part of this study. These have highlighted a limited number of structural orientations and trends. The aeromagnetic data is primarily reflecting very long wavelength, buried features believed to be sourced in the Proterozoic basement at some depth. Significant linear features are mapped based upon analysis of all derivatives; these are interpreted as most likely occurring within the sedimentary section (based on frequency content) and may be related to equivalent horizons to the known Storm copper zones. These features are presented as possible structural controls impacting the stratiform sulphide mineralization.

A comprehensive post-processing study carried out on the 2011 airborne VTEM data shows that the mineralized zones of the Storm deposit can be accurately mapped and modeled. Analysis of the resistivity depth imaging (RDI) inversions in conjunction with the historical drilling suggests that there remain portions of the 4100N, ST97-15, ST99-34, 3500N, 2750N and 2200N zones that have not been drill tested adequately. Furthermore, the deep (100 to 200 m below sea level) conductive trends shown to be extending southward from the 4100N Zone have not been tested at all. Additional modeling of the VTEM data using the Maxwell plate modelling software should permit precise drill targeting for these bodies.

An additional nine secondary anomalous areas were identified through inversion modeling of the VTEM data. These zones do not have characteristics similar to those of the main Storm deposits, but do represent areas of surficial or near surface conductivity, and merit further investigation.

The 2012 drill core resampling program did not include samples from core for which historic detailed sample data are available. However, in comparing assay results from the 2012 program with intervals mentioned in other reports and documents, it can be seen that the 2012 assay values agree very well with the historic data. Sampling selected previously untested sections of the stored drill core commonly yielded copper assays in the range of 0.1 to 0.3% Cu. It was not possible to perform statistical analyses on the sample sets due to the sample intervals not exactly coinciding with historic intervals, but the results appear to agree within one to two standard deviations.

1.7 Recommendations

A reasonable Stage 1 exploration plan for the short term should entail a multi-faceted program to produce a resource estimate for the Seal Zinc deposit and good follow-up drill targets for a subsequent diamond drill program on the Storm Copper showings. The original Seal drilling data should be acquired from Teck along with follow-up geological and engineering studies leading to the determination of a NI 43-101 compliant mineral resource for the prospect.

Concurrent with the Seal planned work, exploration for the Storm showings should comprise; the completion of the reprocessing of the airborne VTEM data using the Maxwell plate modelling software, ground electromagnetic, magnetic and induced polarization surveying, and prospecting, mapping and geochemical sampling. This program is recommended to further delineate the conductive zones and possibly identify disseminated sulphides which in turn could indicate additional anomalous Cu mineralization. This Stage 1 exploration program is estimated at \$1,200,000 (not including GST) and would result in the location and prioritization of prospective targets to be drilled at the Seal and Storm areas in a subsequent Stage 2 program. It is anticipated that a follow-up Stage 2 drilling program could also be completed during 2013. A program of 1,200 m of diamond drilling tagged onto the Stage 1 field based exploration program is estimated at \$1,100,000 not including GST. However, the Stage 2 drilling program is contingent upon the results of the Stage 1 field work.

2: INTRODUCTION

In 2012, Aston Bay Ventures Ltd. (Aston Bay) commissioned APEX Geoscience Ltd. (APEX) to complete a field based sampling program and in conjunction with Aurora Geosciences Ltd. (Aurora), prepare an independent, Canadian National Instrument 43-101 (NI 43-101) Technical Report, for the Storm Property (“the Property”), located on Somerset Island, Nunavut, Canada. located, Nunavut. This Report is a technical summary, and is written to comply with the standards set out in NI 43-101 for the Canadian Securities Administration (CSA), and presents the results and expenditures of the work done on behalf of Aston Bay by APEX and Aurora in 2012.

The Storm Property, located east of Aston Bay on northwestern Somerset Island, Nunavut, Canada, is approximately 112 km south of the community of Resolute Bay on Cornwallis Island and 1,500 km northwest of Iqaluit, the capital of Nunavut (Figure 1). The Storm Property (the “Property” or the “Storm Property”), is comprised of 8 prospecting permits, including four permits, numbered 7547, 7548, 7549, 7880, which are 100% owned by Commander Resources Ltd. (Commander) and four permits, numbered 8340, 8341, 8342, and 8343, which are 100% owned by Michael Dufresne on behalf of Aston Bay. On November 17, 2011, Aston Bay entered into an option agreement with Commander whereby Aston Bay can earn up to a 70% interest in Commander’s portion of the Storm Property land package.

The lead author, Mr. Jim Robinson, P.Geol., a senior geologist with Aurora, and an independent and Qualified Person as defined in National Instrument 43-101, has prepared a compilation of proprietary and publicly available information for Storm. Mr. Robinson visited the property on August 4th, 2012.

The second author, Mr. Bryan Atkinson, B.Sc., P.Geol., a senior geologist with APEX, and a Qualified Person, conducted a field visit to the property between July 28th and August 3rd, 2012. This report summarizes the available historic geological, geophysical, and geochemical information for the property along with the results of the 2011 VTEM airborne survey and the 2012 field work conducted by APEX

and Aurora personnel and has been prepared on behalf of Aston Bay. APEX personnel were involved in all aspects of the 2012 field work.

The authors, in writing this report, use sources of information as listed in the references. The report is a compilation of proprietary and publicly available information as well as information obtained during property visits, and research by government and university geoscientists. Government reports were prepared by qualified persons holding post-secondary geology, or related university degree(s), and are therefore deemed to be accurate. For those reports which were written by others who may or may not be qualified persons, the information in those reports is assumed to be reasonably accurate, based on the data review and field visits conducted by the authors. However, they are not the basis for this report.

Unless otherwise stated, all units used in this report are metric, all dollar amounts (\$) are in Canadian currency, and Universal Transverse Mercator (UTM) co-ordinates in this report and accompanying illustrations are referenced to the North American Datum 1983 (NAD83), Zone 15 North.

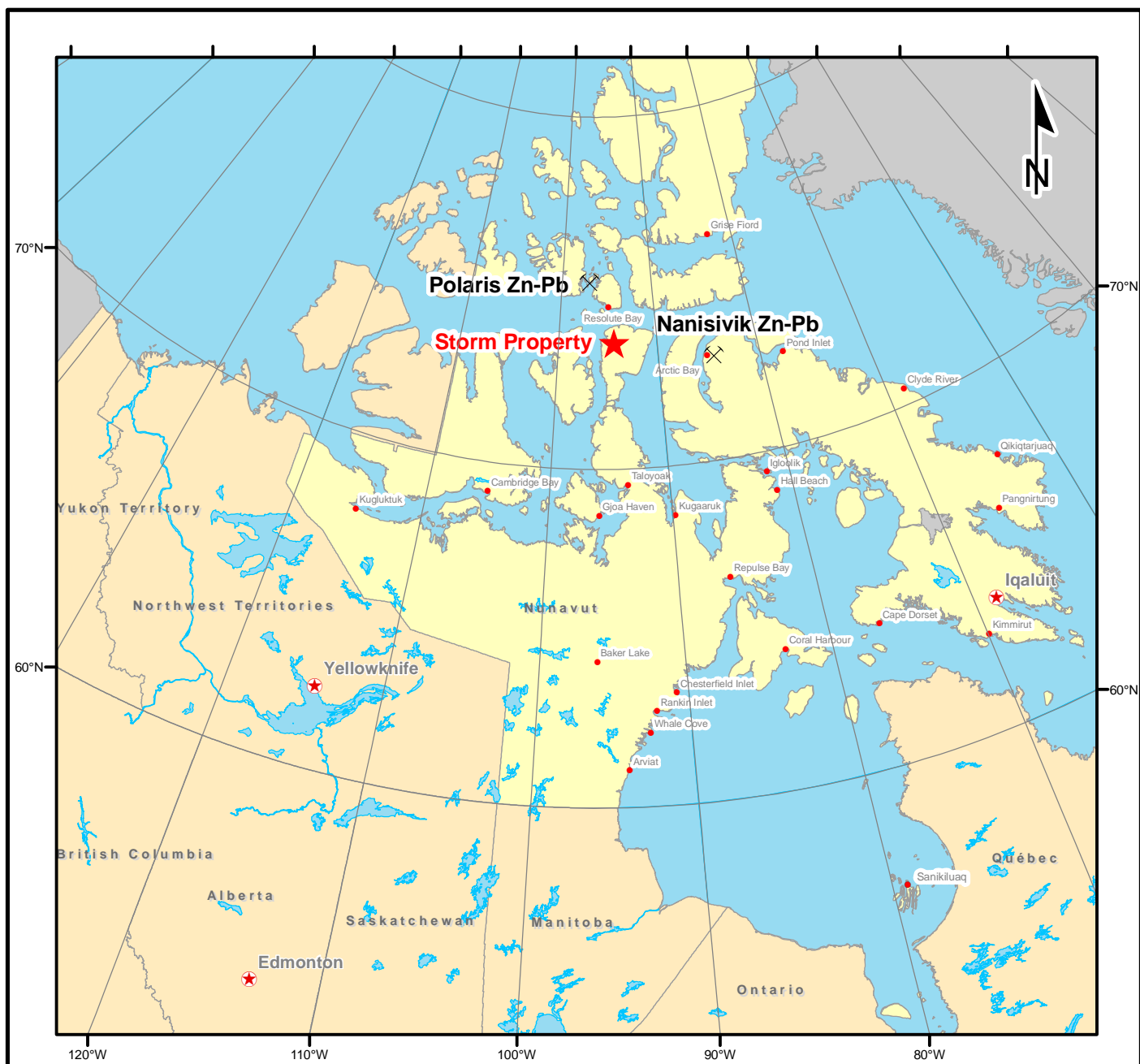
For the convenience of the reader, the following table lists common units and abbreviations employed in the SI (metric) system of measurement.

Table 1 List of Abbreviations

Units of measurement used in this report conform to the SI (metric) system.

| | | | |
|---------------------|-----------------------------|-------------------|--------------------------------|
| μ | micron | kPa | kilopascal |
| °C | degree Celsius | kVA | kilovolt-amperes |
| °F | degree Fahrenheit | kW | kilowatt |
| °K | degree Kelvin | kWh | kilowatt-hour |
| μg | microgram | L | litre |
| μm | micrometre | L/s | litres per second |
| A | ampere | M | mega (million) |
| ASL | Above Sea Level | m | metre |
| a | annum (year) | m ² | square metre |
| bbl | barrel | m ³ | cubic metre |
| Btu | British thermal unit | MASL | metres above sea level |
| cal | calorie | mi. | statute mile |
| cfm | cubic feet per minute | min. | minute |
| cm | centimetre | mm | millimetre |
| cm ² | square centimetre | mph | miles per hour |
| d | day | MVA | megavolt-amperes |
| dia. | diameter | MWh | megawatt-hour |
| dmt | dry metric tonne | MW | megawatt |
| dwt | dead-weight ton | m ³ /h | cubic metres per hour |
| ft. | foot | opt | Troy ounce per short ton |
| ft./s | foot per second | oz. | Troy ounce (31.1035g) |
| ft. ² | square foot | oz/dmt | ounce per dry metric tonne |
| ft. ³ | cubic foot | ppb | parts per billion |
| g | gram | ppm | parts per million |
| G | giga (billion) | psia | pound per square inch absolute |
| Gal | Imperial gallon | psig | pound per square inch gauge |
| g/L | gram per litre | RL | relative elevation |
| g/t | gram per tonne | s | second |
| gpm | Imperial gallons per minute | st | short ton |
| gr/ft. ³ | grain per cubic foot | stpa | short ton per year |
| ha | hectare | t | metric tonne |
| hp | horsepower | tpa | metric tonne per year |
| hr. | hour | tpd | metric tonne per day |
| in. | inch | US\$ | United States dollar |
| in. ² | square inch | USg | United States gallon |
| J | joule | USgpm | US gallon per minute |
| k | kilo (thousand) | V | volt |
| kcal | kilocalorie | W | watt |
| kg | kilogram | wmt | wet metric tonne |
| km | kilometre | yd ³ | cubic yard |
| km/h | kilometre per hour | yr. | year |
| km ² | square kilometre | ‰ | per mille |

Figure 1, below, shows the general location of the Storm property on the northern end of Somerset Island.



Legend



Storm Property



Provincial / Territorial
Capital



Past Producer



Provincial / Territorial
Boundary



Nunavut Communities



Water Body

ASTON BAY VENTURES LTD.

Somerset Island, Nunavut, Canada

Storm Property Location

0 1,000 Km



1:20,000,000 Scale

Projection: Lambert Conformal Conic
Derived from Horizontal Datum NAD83

APEX Geoscience Ltd.
Edmonton, AB

Figure 1
October 10, 2012

3: RELIANCE ON OTHER EXPERTS

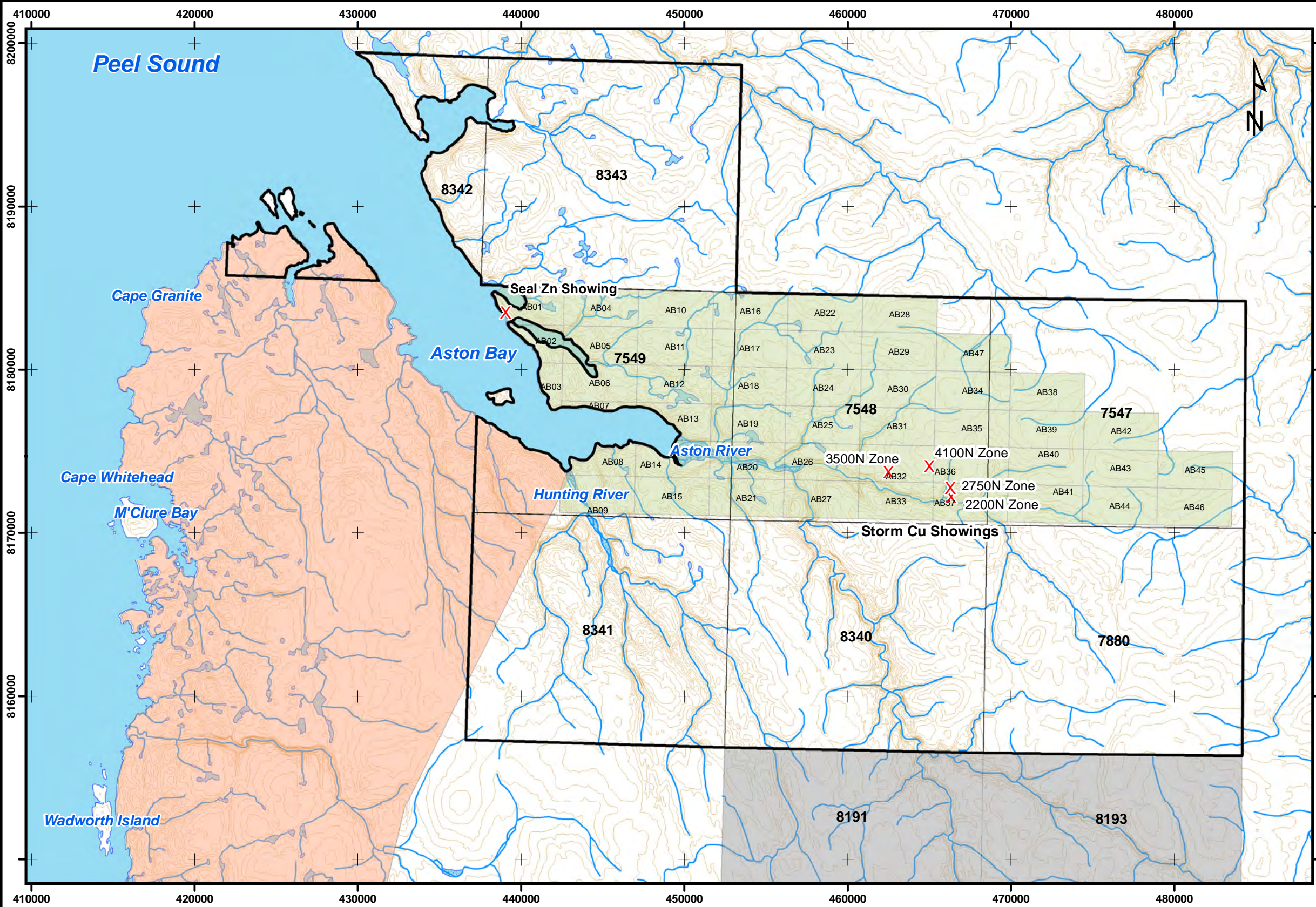
The authors have made no attempt to verify the legal status and ownership of the Property, nor are they qualified to do so. The Property comprises 8 prospecting permits, 7547, 7548, 7549, 7880, 8340, 8341, 8342, and 8343 that are shown as “Active” online on the Government’s (Aboriginal Affairs and Northern Development Canada’s) mineral rights viewing website (<http://ism-sid.inac.gc.ca/website/sidvh1/viewer.htm>). Permits 7547, 7548, 7549, and 7880 are listed as being in good standing in the name of Commander Resources Ltd. Additionally, FMC Law has provided Aston Bay with written confirmation that these permits are held in good standing by Commander. Permits 7547, 7548, and 7549 are set to expire on January 31, 2013. Within these permits 47 mineral claims have been staked and are listed as pending in the name of Commander Resources Ltd. The claims have a record date of September 19, 2012 and an anniversary date of September 12, 2014. The claims have not been legally surveyed and will come into effect once the permits lapse. Permit 7880 has an expiry date of January 31, 2013. Permits 8340, 8341, 8342, and 8343 are listed as being in good standing in the name of Michael Dufresne (on behalf of Aston Bay). Permits 8340 to 8343 have an expiry date of January 31, 2017.

4: PROPERTY DESCRIPTION AND LOCATION

The Storm Property is located in the general area of Aston Bay, on northwestern Somerset Island, Nunavut, Canada (Figure 1). The property is approximately 112 km south of Resolute Bay on Cornwallis Island, the nearest community. It is 1,500 km northwest of Iqaluit, the capital of Nunavut and ~1,500 km northeast of Yellowknife, NT. It is located in the Qikiqtaaluk Region of Nunavut, within the 1:50,000 scale NTS (National Topographic System) map sheets 058C10, C11, C13 and C14.

The Storm Property is comprised of eight contiguous prospecting permits, numbered 7547, 7548, 7549, 7880, 8340, 8341, 8342, and 8343, covering a combined area of approximately 363,037 acres (146,916 hectares; Table 2, Figure 2). The Property is bounded by latitudes 73°30’ N and 73°52.5’ N, and longitudes 93°30’ W and 95°30’ W, and is centred at approximately 73°39’ N latitude and 94°20’ W longitude (Figure 2). Commander currently maintains 100% interest in permits 7547, 7548, 7549, and 7880; permits 8340, 8341, 8342, and 8343 are held 100% by Michael Dufresne on behalf of Aston Bay.

During July and August 2012, APEX, on behalf of Commander and Aston Bay, staked 47 mineral claims, totalling 113,632 acres (45,985.4 ha), within permits 7547, 7548, and 7549 which are due to be expire January 31, 2013 (Figure 2). These claims are currently Pending. They have a record date of September 19, 2012 and an anniversary date of September 12, 2014 and will come into effect once the permits lapse.



Legend

- X Showing
- Storm Property Outline
- Storm Prospecting Permit
- Storm Mineral Claim
- Other Prospecting Permit
- Inuit Owned Land
- Topographic Contour
- Drainage
- Water Body



ASTON BAY VENTURES LTD.

Somerset Island, Nunavut, Canada

Storm Property Map

0 10 Km

1:250,000 Scale
UTM NAD 83 Zone 15N

APEX Geoscience Ltd.
Edmonton, AB

Figure 2
November, 2012

Table 2 Storm Property Prospecting Permit and Mineral Claim Details

| Permit Number | Owner | NTS Sheet | Area (acres) | Date Issued | Expiry Date |
|---------------|--------------------------|---------------------|-------------------|--------------|---------------|
| 7547 | Commander Resources Ltd. | 058C10 | 51,040.00 | Feb. 1, 2008 | Jan. 31, 2013 |
| 7548 | Commander Resources Ltd. | 058C11 | 51,040.00 | Feb. 1, 2008 | Jan. 31, 2013 |
| 7549 | Commander Resources Ltd. | 058C11 | 42,318.89 | Feb. 1, 2008 | Jan. 31, 2013 |
| 7880 | Commander Resources Ltd. | 058C10 | 51,040.00 | Feb. 1, 2010 | Jan. 31, 2015 |
| 8340 | Aston Bay Ventures Inc. | 058C11 | 51,040.00 | Feb. 1, 2012 | Jan. 31, 2017 |
| 8341 | Aston Bay Ventures Inc. | 058C11 | 51,040.00 | Feb. 1, 2012 | Jan. 31, 2015 |
| 8342 | Aston Bay Ventures Inc. | 058C13 | 15,285.07 | Feb. 1, 2012 | Jan. 31, 2017 |
| 8343 | Aston Bay Ventures Inc. | 058C14 | 50,233.00 | Feb. 1, 2012 | Jan. 31, 2017 |
| | | Total Acres: | 363,036.96 | | |
| | | Total Ha: | 146,915.84 | | |

| Tag Number | Claim Name | Date Staked | Record Date | Expiry Date | Area (acres) | Owner |
|------------|------------|-------------|-------------|-------------|--------------|--------------------------|
| 16471 | AB1 | 24/07/2012 | 12/09/2012 | 12/09/2014 | 2237 | Commander Resources Ltd. |
| 16472 | AB2 | 24/07/2012 | 12/09/2012 | 12/09/2014 | 1331 | Commander Resources Ltd. |
| 16473 | AB3 | 24/07/2012 | 12/09/2012 | 12/09/2014 | 895.2 | Commander Resources Ltd. |
| 16474 | AB4 | 24/07/2012 | 12/09/2012 | 12/09/2014 | 2582.5 | Commander Resources Ltd. |
| 16475 | AB5 | 24/07/2012 | 12/09/2012 | 12/09/2014 | 2582.5 | Commander Resources Ltd. |
| 16476 | AB6 | 24/07/2012 | 12/09/2012 | 12/09/2014 | 2582.5 | Commander Resources Ltd. |
| 16477 | AB7 | 24/07/2012 | 12/09/2012 | 12/09/2014 | 550.7 | Commander Resources Ltd. |
| 16478 | AB8 | 24/07/2012 | 12/09/2012 | 12/09/2014 | 1506 | Commander Resources Ltd. |
| 16479 | AB9 | 24/07/2012 | 12/09/2012 | 12/09/2014 | 2545 | Commander Resources Ltd. |
| 16480 | AB10 | 24/07/2012 | 12/09/2012 | 12/09/2014 | 2582.5 | Commander Resources Ltd. |
| 16481 | AB11 | 24/07/2012 | 12/09/2012 | 12/09/2014 | 2582.5 | Commander Resources Ltd. |
| 16482 | AB12 | 24/07/2012 | 12/09/2012 | 12/09/2014 | 2582.5 | Commander Resources Ltd. |
| 16483 | AB13 | 24/07/2012 | 12/09/2012 | 12/09/2014 | 1661 | Commander Resources Ltd. |
| 16484 | AB14 | 24/07/2012 | 12/09/2012 | 12/09/2014 | 2189 | Commander Resources Ltd. |
| 16485 | AB15 | 24/07/2012 | 12/09/2012 | 12/09/2014 | 2582.5 | Commander Resources Ltd. |
| 16486 | AB16 | 25/07/2012 | 12/09/2012 | 12/09/2014 | 2582.5 | Commander Resources Ltd. |
| 16487 | AB17 | 25/07/2012 | 12/09/2012 | 12/09/2014 | 2582.5 | Commander Resources Ltd. |
| 16488 | AB18 | 25/07/2012 | 12/09/2012 | 12/09/2014 | 2582.5 | Commander Resources Ltd. |
| 16489 | AB19 | 25/07/2012 | 12/09/2012 | 12/09/2014 | 2582.5 | Commander Resources Ltd. |
| 16490 | AB20 | 25/07/2012 | 12/09/2012 | 12/09/2014 | 2582.5 | Commander Resources Ltd. |
| 16491 | AB21 | 25/07/2012 | 12/09/2012 | 12/09/2014 | 2582.5 | Commander Resources Ltd. |
| 16492 | AB22 | 25/07/2012 | 12/09/2012 | 12/09/2014 | 2582.5 | Commander Resources Ltd. |
| 16493 | AB23 | 25/07/2012 | 12/09/2012 | 12/09/2014 | 2582.5 | Commander Resources Ltd. |
| 16494 | AB24 | 25/07/2012 | 12/09/2012 | 12/09/2014 | 2582.5 | Commander Resources Ltd. |
| 16495 | AB25 | 25/07/2012 | 12/09/2012 | 12/09/2014 | 2582.5 | Commander Resources Ltd. |
| 16496 | AB26 | 25/07/2012 | 12/09/2012 | 12/09/2014 | 2582.5 | Commander Resources Ltd. |
| 16497 | AB27 | 25/07/2012 | 12/09/2012 | 12/09/2014 | 2582.5 | Commander Resources Ltd. |
| 16498 | AB28 | 25/07/2012 | 12/09/2012 | 12/09/2014 | 2582.5 | Commander Resources Ltd. |

| Tag Number | Claim Name | Date Staked | Record Date | Expiry Date | Area (acres) | Owner |
|------------|------------|-------------|-------------|-------------|-----------------------|--------------------------|
| 16499 | AB29 | 25/07/2012 | 12/09/2012 | 12/09/2014 | 2582.5 | Commander Resources Ltd. |
| 16500 | AB30 | 25/07/2012 | 12/09/2012 | 12/09/2014 | 2582.5 | Commander Resources Ltd. |
| 16501 | AB31 | 25/07/2012 | 12/09/2012 | 12/09/2014 | 2582.5 | Commander Resources Ltd. |
| 16502 | AB32 | 26/07/2012 | 12/09/2012 | 12/09/2014 | 2582.5 | Commander Resources Ltd. |
| 16503 | AB33 | 26/07/2012 | 12/09/2012 | 12/09/2014 | 2582.5 | Commander Resources Ltd. |
| 16504 | AB34 | 26/07/2012 | 12/09/2012 | 12/09/2014 | 2582.5 | Commander Resources Ltd. |
| 16505 | AB35 | 26/07/2012 | 12/09/2012 | 12/09/2014 | 2582.5 | Commander Resources Ltd. |
| 16506 | AB36 | 26/07/2012 | 12/09/2012 | 12/09/2014 | 2582.5 | Commander Resources Ltd. |
| 16507 | AB37 | 26/07/2012 | 12/09/2012 | 12/09/2014 | 2582.5 | Commander Resources Ltd. |
| 16508 | AB38 | 26/07/2012 | 12/09/2012 | 12/09/2014 | 2582.5 | Commander Resources Ltd. |
| 16509 | AB39 | 26/07/2012 | 12/09/2012 | 12/09/2014 | 2582.5 | Commander Resources Ltd. |
| 16510 | AB40 | 26/07/2012 | 12/09/2012 | 12/09/2014 | 2582.5 | Commander Resources Ltd. |
| 16511 | AB41 | 26/07/2012 | 12/09/2012 | 12/09/2014 | 2582.5 | Commander Resources Ltd. |
| 16512 | AB42 | 26/07/2012 | 12/09/2012 | 12/09/2014 | 2582.5 | Commander Resources Ltd. |
| 16513 | AB43 | 26/07/2012 | 12/09/2012 | 12/09/2014 | 2582.5 | Commander Resources Ltd. |
| 16514 | AB44 | 26/07/2012 | 12/09/2012 | 12/09/2014 | 2582.5 | Commander Resources Ltd. |
| 16515 | AB45 | 26/07/2012 | 12/09/2012 | 12/09/2014 | 2582.5 | Commander Resources Ltd. |
| 16516 | AB46 | 26/07/2012 | 12/09/2012 | 12/09/2014 | 2582.5 | Commander Resources Ltd. |
| 16517 | AB47 | 01/08/2012 | 12/09/2012 | 12/09/2014 | 2582.5 | Commander Resources Ltd. |
| | | | | | Total Acres | 113632.4 |
| | | | | | Total Hectares | 45985.4 |

On November 17, 2011, Aston Bay entered into an option agreement with Commander whereby Aston Bay can earn up to a 70% interest in the 4 permits held by Commander and a 5 km area of interest that buffers the these permits by: becoming publicly listed, issuing a total of 3 million shares to Commander, making total cash payments of \$150,000 and funding \$15 million in exploration, including delivery of an Indicated Resource, as defined in NI 43-101, by December 31, 2019. The first \$6 million in expenditures must be completed by the end of 2015 in a stepwise fashion, \$1 million in expenditures in both 2012 and 2013, rising to \$2 million in expenditures in 2014 and 2015. Aston Bay can purchase the remaining 30% interest in the property by either paying \$15 million to Commander or transferring 20% of the outstanding Aston Bay shares to Commander. Commander's interest in the property reverts to a 0.875% Gross Overriding Royalty (GOR) if their ownership of the property drops below 10%.

Under the current Nunavut mining law prospecting permits are valid for either three or five years depending on whether they are located below or above the 68th parallel (68° north latitude). All permits comprising the Storm Property are north of this administrative boundary. The holder of an active prospecting permit has exclusive rights to stake mineral claims within the permit area. There are no surface rights associated with a prospecting permit.

For Prospecting permits representative work equivalent to \$0.10 per acre is required during the first work period (1 or 2 years depending on whether the permit is valid for 3 or 5 years), during the second

work period (again either 1 or 2 years) representative work equivalent to \$0.20 per acre is required. In the final year of the prospecting permit, representative work totalling \$0.40 per acre is required. A deposit equal to the required expenditures must be submitted either as payment in lieu of, or work completed prior to the start of the work period. If a prospecting permit expires or is relinquished the holder cannot stake mineral claims in the area for a period of one year. Where Prospecting Permits include areas of ocean, these areas subtracted or 'clipped' from the total surface area.

Mineral claims can be staked by or on behalf of an individual or corporation that holds a valid prospecting licence. Claims must be rectangular in shape wherever possible, with north – south and east – west oriented boundaries. Claims cannot exceed 2,582.5 acres in size. Claims are valid for a total of 10 years. Mineral claims require representation work commitments of \$4/acre, due following the first two years of the claim's existence, and \$2/acre for each year thereafter. Representation work must be filed with the relevant Mining Recorder's office within 30 days of the anniversary date of the claim or within 60 days of the date of the issuance of a lapsing notice. Mineral claims can be grouped for the purposes of applying assessment credit. After the 10 year period, mineral claims are either relinquished or taken to lease. Conversion of a mineral claim to a mineral lease also requires that a legal survey of the claim be completed and registered. Once converted, a mineral lease can be maintained by making annual payments of \$1/acre with no further work and/or expenditure commitments. A mineral lease is valid for a period of 21 years and may be renewed indefinitely. Renewal of a mineral lease for subsequent 21 year periods requires a payment of \$2/acre.

A small portion of the western extents of permits 7549, 8341 and 8342 are located within Inuit owned Lands (IOL) surface rights land parcel RB-02. The remainder of the permit area and the entire area of the staked mineral claims lies on Crown owned land.

Water use activities (i.e. for camps and/or drilling) within Nunavut require a Water Licence to be granted by the Nunavut Water Board (Article 12 of Nunavut Land Claims Agreement). To establish an exploration camp on Crown Lands in Nunavut requires a land use permit issued by Indian and Northern Affairs Canada (INAC). All IOL licences, water licences and INAC land use applications are screened by the Nunavut Impact Review Board (NIRB) under Article 13 of Nunavut Land Claim Agreement. NIRB screens project proposals to determine whether they may have significantly adverse environmental and socio-economic impact potential. Surface access to lands within the IOL surface parcel requires permission from the Qikiqtani Inuit Association (QIA).

An INAC land use permit for a camp and drilling in the name of Commander is active and in good standing. A camp has not been constructed and nor has drilling been conducted to date under the permit. A Nunavut Water Licence has been recently issued to Commander that allows for a camp to be established and drilling to be conducted. The author is not aware of any agreements, encumbrances or environmental liabilities to which the Property is subject to or any other reasons that would prevent Aston Bay from acquiring the necessary permits to conduct the work described in the 'Recommendations' section of this report.

5: ACCESSIBILITY, CLIMATE, LOCAL RESOURCES, INFRASTRUCTURE AND PHYSIOGRAPHY

5.1 Access, Local Resources, and Infrastructure

The Storm Property is located on northwestern Somerset Island, in the Canadian Arctic Archipelago. Due to the Property's remote location, access is typically restricted to charter air service from Resolute Bay, located 112 km north of the property. Resolute Bay has a modern airport facility with a 1,982 m (6,504 ft.) gravel runway. Daily commercial air service to Resolute Bay is available via Iqaluit, with connections from Ottawa or Montreal. A weekly service between Yellowknife, NT and Resolute Bay is also available. Chartered air service can be obtained from either Yellowknife or Iqaluit.

Hotel accommodations, groceries, camp outfitters, and construction supplies can be acquired locally in Resolute Bay; however food and other supplies can be sourced more cost-effectively from Yellowknife or Ottawa. There is a health clinic in Resolute Bay, the closest hospitals are in Iqaluit, 1,500 km southeast, and Yellowknife, 1,500 km southwest of the Property. Local labour is available from surrounding Inuit communities. Industry services are typically contracted out of Yellowknife or southern Canada, with limited services available out of Iqaluit.

Infrastructure at the Storm Property is limited to an unmaintained 192 m (630 ft.) airstrip, located adjacent to an old Cominco exploration camp site at approximately 73°42' N latitude and 94°43' W longitude. In its current condition, the airstrip is suitable for landing Single or Twin Otter aircraft. Several lakes on the Property are large enough to land small float-equipped aircraft during the summer months. During the winter, a Twin Otter or DC-3 aircraft fitted with skis can be landed on the sea ice in Aston Bay, allowing for off-season stocking of fuel and other supplies. A prepared ice strip on Aston Bay would be able to accommodate DHC-5 Buffalo, Dash 7 or C-130J Super Hercules aircraft. The current airstrip at the Storm Property is located in an area with the potential for expansion to accommodate larger aircraft. Furthermore, several areas east of the current airstrip would be suitable for construction of a longer airstrip.

Fifty kilometres to the northeast of the property at Cumberland Sound, is Arctic Watch Lodge, a wilderness adventure resort. The lodge maintains a 1,036 m (3,400 ft.) gravel airstrip and is also able to deliver other support services. The Arctic Watch airstrip is capable of handling various turboprop cargo aircraft, such as DHC-5 Buffalo, Dash 7 and C-130J Super Hercules, and could be used as a staging area for future exploration programs. During the 2012 exploration program, the field crew was based out of the Arctic Watch Lodge. The lodge provided accommodations and meals, as well as storage space for gear and samples, and is a viable alternative to establishing a stand-alone camp for small or short duration field programs.

The most efficient means of mobilizing fuel, heavy equipment, and supplies to the Storm Property is by sea-lift. Ocean shipping lanes servicing Resolute Bay and the former Polaris Mine operation run

in close proximity to the Storm Property (Figure 1). The west end of the Property borders the tidewater of Aston Bay on Peel Sound, part of the Northwest Passage (Figures 1 and 2). Desgagnés Transarctik Inc. and NEAS offer an annual sea-lift service to a number of coastal northern communities, including Resolute Bay. Because Aston Bay is free of sea ice for 8 to 10 weeks per year, the option of direct offloading at Aston Bay is available. Furthermore, in the future, a protected, deep water port could be constructed along the northern shore of Aston Bay.

5.2 Climate and Physiography

The property is located in the Northern Arctic Ecozone consisting of plateaux and rocky hills. Coastal areas typically constitute wide plains ‘fenced’ by boulders carried onshore by sea ice, strong tidal currents and storm waves. The Northern Arctic Ecozone is characterized by low mean temperatures and minor precipitation, mainly falling as snow. Daylight hours vary dramatically from 24 hour darkness in the middle of winter to 24 hour sunlight at the height of summer. Table 3 summarizes historic climate statistics for Resolute Bay, the nearest community. January and February are the coldest months, with average temperatures below -30°C. Summers are typically brief, cool, and damp with a mean temperature through July and August of under 3°C. Snow cover during winter months may be as little as 30 cm, however due to constant northwest winds, drift accumulations can be significant. The entire region is subject to continuous permafrost, extending to depths of 400 to 500 metres.

Table 3 Selected Historic Climate Statistics for Resolute Bay, NU (Environment Canada, 2012)

| | Jan | Feb | Mar | Apr | May | Jun | Jul | Aug | Sep | Oct | Nov | Dec | Year |
|--------------------|-------|-------|-------|-------|-------|------|------|------|------|-------|-------|-------|-------|
| Temperature | | | | | | | | | | | | | |
| Daily Average (°C) | -32.4 | -33.1 | -30.7 | -22.8 | -10.9 | -0.1 | 4.3 | 1.5 | -4.7 | -14.9 | -23.6 | -29.2 | -16.4 |
| Precipitation | | | | | | | | | | | | | |
| Rainfall (mm) | 0 | 0 | 0 | 0 | 0.5 | 6.5 | 15.7 | 21.8 | 5.4 | 0.5 | 0 | 0 | 50.3 |
| Snowfall (cm) | 4.7 | 3.7 | 7 | 6.6 | 11.1 | 8.7 | 4.2 | 13.1 | 21 | 16.2 | 8.6 | 5.5 | 110.3 |

The Storm Property is in a region characterized by rolling terrain with low relief. The topography initially rises abruptly from sea level to about 100 m, and then levels out eastward, to an average of roughly 200 to 300 m above sea level. The Aston River is the main watercourse in the area; it runs east-west through the Storm Property, draining into Aston Bay. The Aston River and other major drainages are characterized by steep incised canyons, typically exposing good outcrop along the canyon walls.

Flat areas are dominated by felsenmeer and cryoturbated soils. Cryoturbation produces features such as frost boils, ice-wedge polygons, stone nets and stone stripes.

Vegetation at the Storm Property consists mainly of moss, lichens, stunted plants and Arctic grasses. The grasses are typically observed growing at lower elevations in areas associated with river drainage basins. Muskox are commonly observed grazing in these areas. Arctic fox, hare, and lemmings have also been noted at the property. Polar bears and caribou are rarely observed.

6: HISTORY

Commander Resources Ltd. initially acquired the Storm Property as three contiguous Prospecting Permits in February 2008. One additional permit was added in February 2010. Much of the area covered by these permits was part of a larger mineral claim package, previously held by Cominco Ltd. ("Cominco"), and later Teck-Cominco Ltd. (now known as Teck Resources Ltd.). The last remnants of the Cominco land package lapsed in 2007. Exploration work in the areas around Aston Bay and the Storm Property has been carried out intermittently since the 1960s. Most of the historical work at the Storm Property was undertaken by, or on behalf of, Cominco. Figures 3 and 4 illustrate historic exploration drilling at the Seal and Storm showings respectively. A summary of historic work is provided in Table 4.

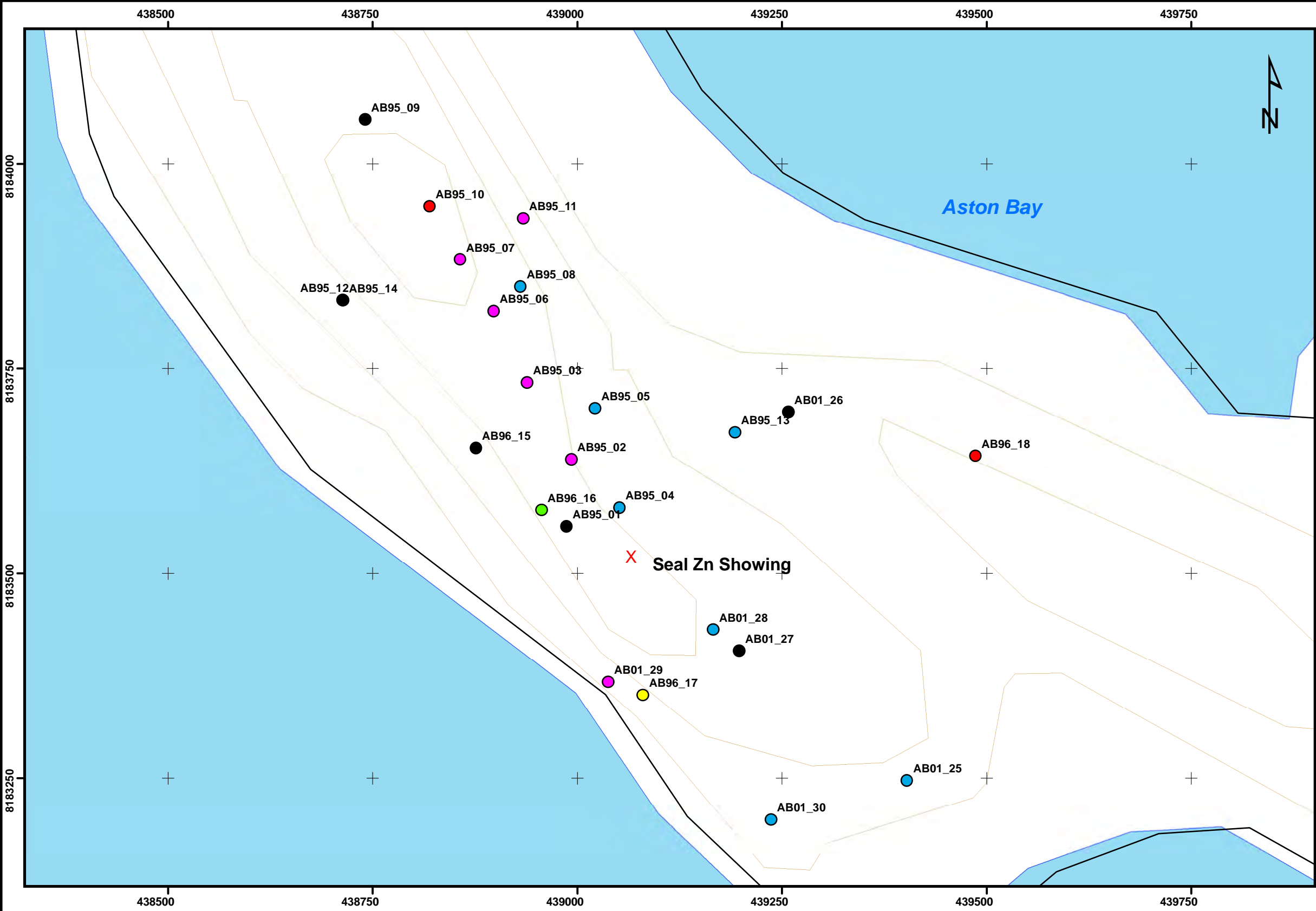
1966 Cominco: Stream geochemistry with a sample density of 1 per 2.4 square miles (6.2 square km) was conducted over parts of northwestern Somerset Island; reconnaissance prospecting was also undertaken. Three soil samples were taken from the area of the Seal showing (Whaley, 1975).

1970 J.C. Sproule and Associates Ltd.: Photogeological mapping, limited reconnaissance prospecting, and stream sediment geochemical sampling were conducted (Neale and Campbell, 1970). The geochemical survey included areas of the far eastern side of the current Storm Property and returned some anomalous copper assay values.

1973 Cominco: Geological mapping, prospecting, and soil sampling were carried out in the Aston Bay area as a follow up to 1966 work. Anomalous soil and rock samples were described with zinc values up to 5% in rubble at the main Seal showing. Consequently, claims PAT 1-10 were staked on September 24, 1973 (Whaley, 1974).

1974 Cominco: Geological mapping, prospecting and soil sampling were carried out on the Astec Property (Seal showing), consisting of the PAT 1-10 claim group. Fifteen soil samples were collected and analyzed for zinc and lead (Whaley, 1975).

1978 Esso Minerals: Prospecting, geological mapping, geochemical surveys and an airborne radiometric survey exploring for uranium mineralization were conducted at Aston Bay by Trigg, Woollett & Associates. Geochemical samples of lake and stream sediments were taken in the Aston Bay area (Cannuli and Olson, 1978).



Legend

X Showing

Storm Prospecting Permit

Water Body

Topographic Contour

Seal Zn Drill Collars

Zn % x m Values

> 5.0 % x m

1.0 - 5.0 % x m

0.50 - 1.0 % x m

0.25 - 0.50 % x m

< 0.25 % x m

No Data

ASTON BAY VENTURES LTD.

Somerset Island, Nunavut, Canada

Seal Zn Historic Drill Collars

Zn % x m Values

100 50 0 100 Metres

1:5,000 Scale

UTM NAD 83 Zone 15N

APEX Geoscience Ltd.

Edmonton, AB

Figure 3

October 10, 2012

Table 4 Storm Property Historical Exploration Summary

| Type of Work | Year | Target Area | Summary |
|--------------------|------|----------------|---|
| Diamond Drilling | 1995 | Seal Zn Zone | 14 holes, 2,465.7 m |
| | 1996 | Seal Zn Zone | 10 holes, 1,828 m |
| | 1996 | Storm Cu Zone | 1 hole, 290.3 m |
| | 1997 | Storm Cu Zone | 17 holes, 2,801.3 m |
| | 1999 | Storm Cu Zone | 41 holes, 4,593.4 m |
| | 2000 | Storm Cu Zone | 8 holes, 1,348.5 m |
| | 2001 | Seal Zn Zone | 6 holes, 822 m |
| Soil Sampling | 1973 | Aston Bay | 15 samples |
| | 1994 | Aston Bay | 434 samples North & South Peninsula, & Seal Island |
| | 1995 | Aston Bay | 225 samples from South Peninsula and Seal Island |
| | 1995 | Regional | Regional sampling in areas south of Aston Bay |
| | 1997 | Storm Cu Zone | 536 samples (grid) |
| | 1998 | Storm Cu Zone | 851 samples (grid) |
| | 1998 | Storm Property | 1338 samples (regional) |
| | 1999 | Storm Cu Zone | 750 samples (grid) |
| Stream Sediment | 1966 | Regional | Sample density 1 per 6.2 km ² |
| | 1970 | Regional | 198 samples taken on current Property |
| | 1993 | Aston Bay | No data available |
| | 1994 | Regional | 50 heavy mineral samples |
| Rock Sampling | 1973 | Aston Bay | Prospecting Seal showing and North Peninsula; no data available |
| | 1993 | Aston Bay | Prospecting in Aston Bay area; no data available |
| | 1994 | Aston Bay | 65 samples North & South Peninsula, & Seal Island |
| Geophysics | 1994 | Aston Bay | 168 line-km of IP and 62 line-km of gravity |
| | 1995 | Aston Bay | HLEM survey on North Peninsula |
| | 1997 | Storm Cu Zone | 89 line-km of IP and 71.75 line-km of HLEM |
| | 1997 | Storm Property | 10,741 line-km high-resolution aeromagnetic survey |
| | 1998 | Storm Cu Zone | 44.5 line-km of IP |
| | 1999 | Storm Cu Zone | 57.7 line-km of IP |
| | 1999 | Storm Property | Airborne hyperspectral survey |
| | 2000 | Storm Property | 3,260 line-km GEOTEM airborne survey |
| | 2000 | Storm Cu Zone | Ground geophysics: 100.5 km of UTEM, 69.2 km of gravity, 11 km of magnetics, and 6.5 km of HLEM |
| | 2011 | Storm Property | 3,970 line-km VTEM airborne survey |
| Geological Mapping | 1970 | Regional | Photogeological mapping of NW Somerset Island |
| | 1973 | Aston Bay | 1":1/4 mile mapping of North and South Peninsulas |
| | 1994 | Aston Bay | Detailed mapping of Seal Island and North and South Peninsulas |
| | 2000 | Storm Cu Zone | Detailed geological mapping |

1993 Cominco: Stream sediment geochemistry and prospecting were completed in the Aston Bay area. Nine mineral claims were staked, totalling 23,242.50 acres. Three prospecting permits, totalling 163,602 acres, were applied for (Leigh, 1996).

1994 Cominco: Detailed geological mapping was carried out on Seal Island and the North and South peninsulas of Aston Bay. (The North and South peninsulas refer to the north end and south end of the peninsula on which the Seal Zinc showing is located). Induced polarization (IP) and gravity geophysical surveys were conducted on Seal Island and the North Peninsula. A total of 168 line-km of IP and 62 line-km of gravity were completed. Soil geochemical sampling was conducted along the Seal Island and North Peninsula geophysical grids. Soil sampling, prospecting, and mapping were done on the South Peninsula. A total of 434 soil samples and 65 rock grab samples were analyzed. Soil sampling highlights included 15 samples with greater than 1% zinc (Zn), including a 1.06% Zn sample from the South Peninsula. Rock sampling highlights included 18 samples from Seal Island and the North Peninsula with greater than 1% Zn. Most of the high grade samples were found proximal to the Seal main showing; the highest value returned was 8.8% Zn in soils and 40% Zn with 200 grams per tonne (g/t) silver (Ag) in rock samples. Helicopter reconnaissance and heavy mineral sampling were conducted south of Aston Bay. The highest grade observed was 2,230 parts per million (ppm) Zn with 229 ppm lead (Pb). Twelve additional claims (SEAL 1-12), totalling 28,911.7 acres, were staked in the Aston Bay area. Two prospecting permits (1491, 1492), located southeast of Aston Bay, were granted, totalling 108,530 acres (Smith, 1995).

1995 Cominco: Fourteen diamond drill holes (AB95-1 to AB95-14) were completed on the North Peninsula of Aston Bay for a total of 2,465.7 m (Figure 3 and 4). Drill intersections of up to 10.5% Zn and 28 g/t Ag over 18 m core length were obtained for the Seal Zinc Deposit (Table 5). A horizontal-loop electromagnetic (HLEM) survey was also conducted on the North Peninsula. Results from the drill program and HLEM survey were not filed as assessment work and are not publicly available at this time. Regional scale soil sampling and prospecting was completed on the South Peninsula, Seal Island, and the area south of Aston Bay. Zinc values of up to 850 ppm were recorded in soils on the South Peninsula. All areas returned multiple samples with greater than 100 ppm Zn. Nine adjoining claims (SEAL 13-21) were staked in the Aston Bay area and 16 additional claims were staked to the south of, and adjoining, the prospecting permits (Leigh, 1995).

1996 Cominco: Ten diamond drill holes (AB96-15 to AB96-24), totalling 1,733.0 m were completed on the North and South peninsulas of Aston Bay (Figures 3 and 4). Four holes were drilled on the North Peninsula (841.0 m), and five holes were drilled on the South Peninsula (983.2 m). The best results were from the North Peninsula drill holes, including 1.8% Zn with 14 ppm Ag over 0.5 m in hole AB96-17; 2.8% Zn with 10 ppm Ag over 1 m and 2.2% Zn over 1 m in hole AB96-17 (Leigh, 1996). On July 14, 1996, during a regional reconnaissance program, Cominco geologists discovered large chalcocite boulders in Ivor Creek, about 20 km east of Aston Bay, at the subsequently named 2750 Zone at the Storm Copper Showing. Copper mineralization, hosted by Paleozoic dolostone and limestone, was found over a 7 km structural trend (Cook and Moreton, 2009). A single drill hole (330 m) was completed to test for economic copper mineralization (Smith, 2001). The exact collar location and analytical results from this

drill hole are not publicly available at this time. Claims STORM 1-19 were staked (Leigh and Lajoie, 1998).

Table 5 Seal Zone Significant Drill Hole Intersections

| Drill Hole ID | From (m) | To (m) | Length (m) | Zn (%) | Ag (g/t) |
|---------------|-----------------------|--------|------------|--------|----------|
| AB95-02* | 50.00 | 68.00 | 18.00 | 10.50 | 28.00 |
| AB96-17 | 28.50 | 29.00 | 0.50 | 1.80 | 14.00 |
| | 48.20 | 48.40 | 0.20 | 2.20 | 8.00 |
| AB96-18 | 144.00 | 147.00 | 3.00 | 2.00 | 6.00 |
| AB01-29 | 51.10 | 78.00 | 26.90 | 0.78 | 1.75 |
| | <i>includes</i> 51.10 | 54.60 | 3.50 | 2.73 | 9.55 |
| | <i>and</i> 74.30 | 78.00 | 3.70 | 1.06 | 0.99 |

* Historic assay certificates for intersection not available. Data taken from Cominco cross section (Grextan, 2009).

1997 Cominco: Sander Geophysics Ltd., on behalf of Cominco, conducted a high-resolution aeromagnetic survey over a 5,000 square kilometre area of northern Somerset Island. A total of 204 SW-NE oriented traverse lines and 21 NW-SE oriented control lines were flown for a total of 10,741 line-km. Traverse lines were spaced at 500 m and control lines were spaced at 2,500 m (O'Connor, 1997). Eighty-nine line-km of IP and 71.75 line-km of HLEM were completed, and 536 soil samples were collected at the Storm Copper showing. Seventeen diamond drill holes, for a total of 2,784 m, were completed in the central graben area of the Storm Zone. Assay highlights included: 49.71% copper (Cu) with 17.1 ppm Ag over 0.6 m and 19.87% Cu over 1.1 m in hole ST97-02; 4.67% Cu over 4.8 m and 4.13% Cu over 1.4 m in hole ST97-03; and 14.62% Cu with 23.5 g/t Ag over 1.3 m and 4.41% Cu with 12.4 g/t Ag over 1.4 m in hole ST97-13 (Table 6). The present day copper zones at the Storm Showing were established: the 2200N, 2750N, 3500N, and 4100N zones (Cook and Moreton, 2009). Claims STORM 20-89 were staked (Leigh, 1998).

1998 Cominco: A total of 44.5 line-km of IP were completed and 2,090 soil samples were collected at the Storm Zone. Eight-hundred fifty-one (851) soil samples were collected along the IP grid and 1,239 base-of-slope samples were collected during regional drainage prospecting traverses. An area 700 m by 100 m on the soil grid was found to contain >500 ppm Cu, trending parallel to the graben structure. The highest Cu value attained was 1,920 ppm. The anomalous area is centred over the 3500N Zone. Highlights from the regional soil survey included 458 ppm Cu with 856 ppm Zn and 221 ppm Cu with 508 ppm Zn, both related to rusty limonitic soils (Leigh, 1998b). Regional soil sampling was also conducted on Cominco's SEAL claims. A total of 209 samples were collected, with maximum values of 33 ppm Cu and 108 ppm Zn (Leigh, 1998a & 1998b).

1999 Cominco: A total of 57.7 line-km of IP were completed in the Storm Copper Zone. Seven-hundred fifty (750) soil samples were collected at the main Storm grid. The maximum Cu and Zn values achieved in the main grid were 592 ppm and 418 ppm, respectively (Leigh, 1999). Forty-one (41)

Table 6 Storm Zone Significant Historic Drill Hole Intersections

| Drill Hole ID | From (m) | To (m) | Length (m) | Cu (%) |
|-------------------------|---------------|---------------|--------------|--------------|
| ST97-02 <i>includes</i> | 0.00 | 15.00 | 15.00 | 4.24 |
| | 0.00 | 6.84 | 6.84 | 8.98 |
| | 0.00 | 4.30 | 4.30 | 13.76 |
| ST97-03 <i>includes</i> | 0.00 | 50.90 | 50.90 | 1.22 |
| | 0.00 | 6.40 | 6.40 | 3.96 |
| | 38.40 | 42.60 | 4.20 | 2.92 |
| ST97-05 | 28.50 | 38.20 | 9.70 | 1.22 |
| ST97-13 <i>includes</i> | 59.80 | 113.00 | 53.20 | 1.34 |
| | 59.80 | 70.00 | 10.20 | 2.89 |
| | 107.30 | 112.00 | 4.70 | 2.73 |
| ST97-14 | 92.30 | 98.20 | 5.90 | 1.07 |
| ST97-15 | 48.00 | 51.00 | 3.00 | 1.51 |
| ST99-19 <i>includes</i> | 12.20 | 68.50 | 56.30 | 3.07 |
| | 12.20 | 47.70 | 35.50 | 4.75 |
| | 33.30 | 46.60 | 13.30 | 10.06 |
| ST99-21 | 73.10 | 76.90 | 3.80 | 0.99 |
| ST99-22 | 44.30 | 58.40 | 14.10 | 1.56 |
| ST99-23 | 42.60 | 46.40 | 3.80 | 1.07 |
| ST99-31 <i>includes</i> | 4.60 | 59.70 | 55.10 | 1.23 |
| | 7.60 | 35.80 | 28.20 | 1.85 |
| | 7.60 | 11.80 | 4.20 | 4.72 |
| ST99-31 <i>includes</i> | 33.00 | 35.80 | 2.80 | 6.74 |
| | 0.00 | 19.30 | 19.30 | 0.57 |
| | 72.60 | 77.10 | 4.50 | 1.62 |
| ST99-43 <i>includes</i> | 41.00 | 77.40 | 36.40 | 0.96 |
| | 41.00 | 52.80 | 11.80 | 1.61 |
| ST99-47 <i>includes</i> | 43.40 | 111.00 | 67.60 | 1.34 |
| | 75.90 | 87.40 | 11.50 | 4.75 |
| ST99-53 <i>includes</i> | 17.30 | 43.00 | 25.70 | 1.66 |
| | 20.30 | 25.10 | 4.80 | 3.70 |
| | 38.60 | 43.00 | 4.40 | 4.62 |
| ST99-56 <i>includes</i> | 32.60 | 67.80 | 35.20 | 1.25 |
| | 52.40 | 62.60 | 10.20 | 3.25 |
| ST00-60 | 54.00 | 58.90 | 4.90 | 2.26 |
| | 73.40 | 78.30 | 4.90 | 2.32 |
| | 114.10 | 132.70 | 18.60 | 0.57 |
| ST00-61 <i>includes</i> | 50.3 | 70.1 | 19.80 | 1.10 |
| | 59.40 | 64.40 | 5.00 | 2.12 |
| ST00-62 <i>includes</i> | 60.00 | 106.00 | 46.00 | 1.25 |
| | 78.80 | 106.00 | 27.20 | 1.87 |
| | 96.50 | 106.00 | 9.50 | 2.32 |
| ST00-63 | 63.60 | 73.30 | 9.70 | 1.42 |
| ST00-64 | 56.60 | 76.25 | 19.65 | 1.40 |
| ST00-65 | 46.00 | 47.00 | 1.00 | 2.65 |
| | 66.00 | 67.00 | 1.00 | 1.86 |
| ST00-66 | 55.50 | 69.60 | 14.10 | 1.14 |
| | 102.45 | 103.20 | 0.75 | 20.07 |

diamond drill holes, for a total of 4,560.8 m, were completed at the Storm Copper showings, testing IP/Resistivity anomalies with the highlights presented in Table 6. Assay highlights included: 1.35% Cu over 3.8 m in hole ST99-23 (2200N Zone); 5.5% Cu over 28.7 m, including 9.56% Cu over 13.3 m in hole ST99-19 (2750N Zone); 2.9% Cu over 9.2 m, including 6.3% Cu over 2.8 m hole ST99-31 (3500N Zone); 4.9% Cu over 11 m in hole ST99-47 (4100N Zone); and 13.5% Cu with 23 g/t Ag over 1.9 m in hole ST99-56 (4100N Zone). As a result of the extensive 1999 drilling, Cominco geologists divided the upper Allen Bay Formation into three main stratigraphic marker units: alternating dolomicrite and dolowackestone (ADMW), brown dolopackstone and dolofloatstone (BPF), and varied stromatoporoid (VSM) (Leigh and Tisdale, 1999).

1999 Noranda Inc.: Noranda Inc. ("Noranda") entered into an option agreement with Cominco whereby Noranda could earn a 50% interest in the STORM property package (48 claims) by incurring exploration expenditures of \$7 million over a four year period, commencing in 1999. An airborne hyperspectral survey completed by Noranda identified 26 airborne electromagnetic and magnetic (AEM/MAG) and 266 colour anomalies (MacRobbie *et al.*, 2000).

2000 Noranda Inc.: A 3,260 line-km GEOTEM electromagnetic and magnetic airborne geophysical survey was flown over the Property at 250 m to 300 m line spacings. A total of 29 anomalies of interest were identified, including a conductor coincident with the 4100N Zone. Ground geophysical surveys were carried out as a follow up to the airborne surveys, including 100.5 line-km of UTEM, 69.2 line-km of gravity, 11 line-km of magnetics, and 6.5 line-km of HLEM. In addition to the geophysical surveys, geological mapping, prospecting, and soil sampling were carried out to evaluate the 2000 AEM and 1999 hyperspectral anomalies. Eleven diamond drill holes, for a total of 1,885.5 m, were completed; eight of the holes, for a total of 1,348.5 m, were completed within the current Storm Property, at the 4100N Zone showing (MacRobbie *et al.*, 2000).

2001 Noranda: The ASTON claims (7 claims) were added to the original option agreement with Cominco. Reconnaissance follow up on selected airborne targets from the 1999 and 2000 airborne surveys was completed. Six diamond drill holes, for a total of 822 m, were completed on the Seal Zinc showing. Assay highlights for 2001 drilling include: 7.65% Zn with 26.5 g/t Ag over 1.1 m in hole AB01-29 (Smith, 2001).

2007 The last of the original Cominco property package lapsed.

2008 Commander: Prospecting permits 7547, 7548, and 7549, comprising the Storm Property, were issued to Commander in February 2008. Scott Wilson Roscoe Postle Associates Inc. ("Scott Wilson RPA") was retained by Commander to prepare an independent Technical Report on the Property (Cook and Moreton, 2009). Field work included traversing geological contacts at the Seal, 2200N, 2750N, and 4100N showings to evaluate the accuracy of previous mapping. Collars for all the holes in the 4100N Zone were examined. Additionally, in order to verify historic drill results, core stored at the former Aston Bay camp site was selectively sampled. Seven holes were sampled, including two from the Seal occurrence and five from the Storm copper showings. Duplicate analyses for the Storm holes

corresponded well with original results. Original certificates of analysis for the Seal holes were not available; however, results confirmed good zinc and silver content in the drill core (Grextan, 2009).

2011 Commander: Geotech Ltd., on behalf of Commander, conducted a helicopter-borne versatile time domain electromagnetic (VTEM plus) and aeromagnetic survey over the Storm Property. A total of 3,969.7 line-km were flown. The primary VTEM survey flight lines were oriented 030/210 at 150 m spacing with parallel infill lines at 75 m spacing and orthogonal tie lines at 1,500 m spacing.

7: GEOLOGICAL SETTING AND MINERALIZATION

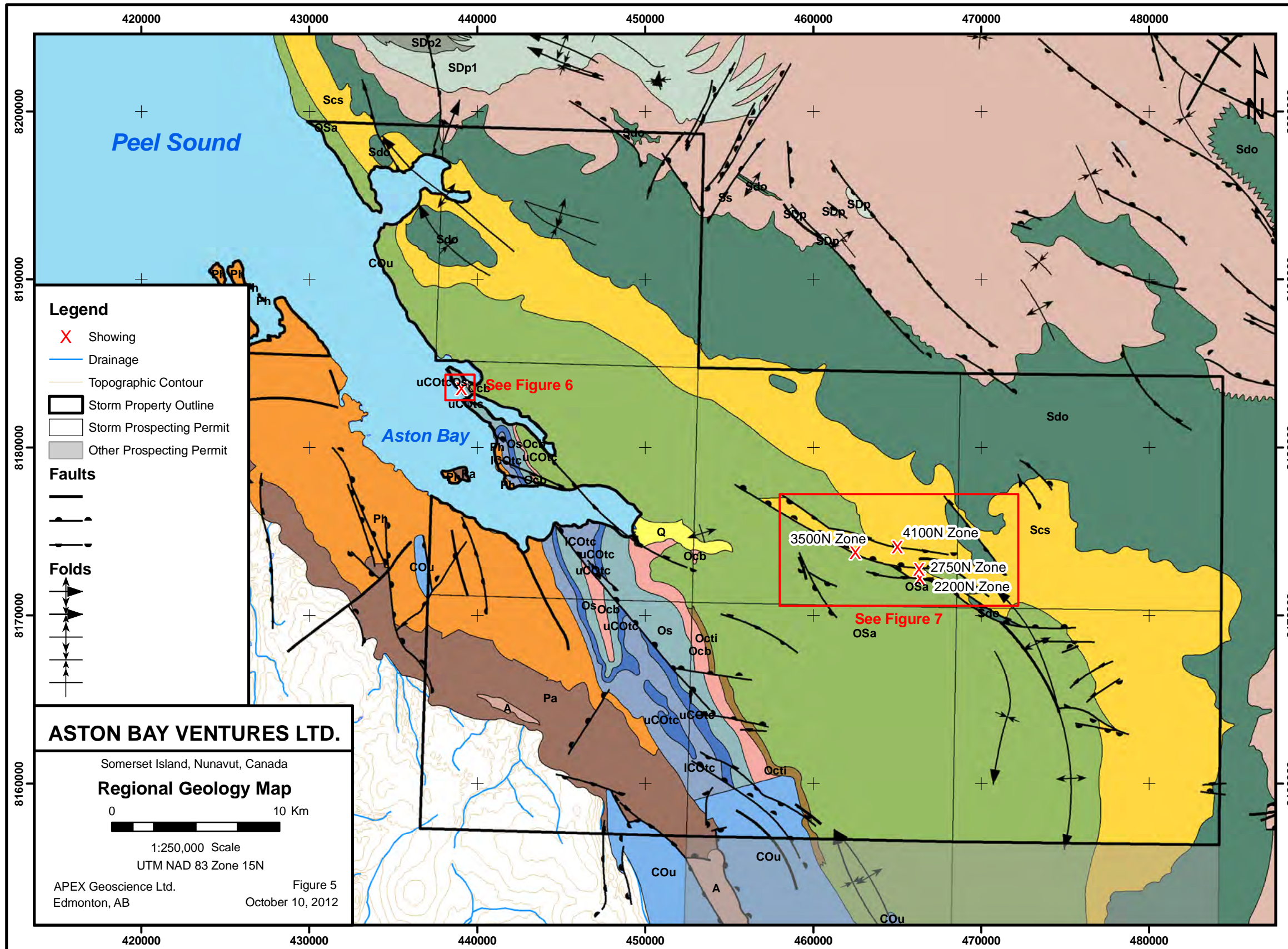
7.1 Regional Geology

The Boothia Uplift, which formed predominantly during the Late Silurian to Early Devonian Caledonian Orogeny, is a Precambrian basement high forming a major linear structural feature that dominates the regional geology of Somerset Island and the Boothia Peninsula (Okulitch, *et al.*, 1985). The Boothia Uplift extends 1,000 km northward from the Boothia Peninsula into the Arctic Archipelago and ranges from 80 to 125 km wide (Okulitch, *et al.*, 1985; Packard, *et al.*, 1987). The Boothia Uplift was formed by west-directed compressive stresses of the coeval late stages of the Caledonian (Taconic) Orogeny (Okulitch, *et al.*, 1985; de Freitas, *et al.*, 1999). Proterozoic stratigraphy on Victoria Island and Baffin Island shows broad folding indicative of another deformation event that may have affected Somerset Island rocks (Smith, 1995).

The core of the Boothia Uplift is composed of Archean and Aphebian granulite facies metasedimentary and metavolcanic crystalline rocks with near-vertical bedding and foliation reflecting north – south trending, tight, upright folds. The folded and faulted sequence of Late Proterozoic and Paleozoic carbonates and clastic rocks flanking the Boothia Uplift to the east and west constitute the Cornwallis Fold and Thrust Belt (Okulitch, *et al.*, 1985; Smith, 1995; Cook, *et al.*, 2009; Grextan, 2009).

The Cornwallis Fold and Thrust belt was formed by basement and platform rocks being thrust westward during the closing pulses of the Caledonian Orogeny, wherein forces in the crystalline basement extended upwards into the overlying carbonate and clastic rocks of the Late Proterozoic and Early Phanerozoic eras (Okulitch, *et al.*, 1985; Smith, 1995). Evaporite units in the stratigraphy may have acted as intermediate decollement zones. Fold structures exposed at surface within the Cornwallis Fold and Thrust Belt are largely broad open anticlines and synclines with north – south axes. The distribution of Paleozoic rocks on Somerset Island defines a large asymmetrical syncline with the youngest strata preserved in the center. Structures related to local block faulting, flexures and gentle folding overprint the main synclinorium. Three dominant fault orientations have been observed on Somerset Island; north – south, northwest – southeast and northeast – southwest.

Compressional stress from the Late Devonian Ellesmerian Orogeny, west of the Boothia Uplift, affected structures on Bathurst Island as well as Cornwallis Island and the Grinnell Peninsula of



Bedrock Geology

Quaternary

Q Stream, deltaic, glacial and marine beach sediments (mapped when underlying geology could not be inferred with reasonable certainty).

Early Tertiary

Te Eureka Sound Formation: Sandstone, siltstone, shale, minor conglomerate. Dominantly continental.

Late Silurian to (?) Early Devonian

SDp Peel Sound Formation-undivided

SDp4 Member 4: Conglomerate, polymictic, red; minor sandstone, red.

SDp3 Member 3: Sandstone and pebbly sandstone, red; minor conglomerate, polymictic.

SDp2 Member 2: Conglomerate, oligomictic, minor sandstone.

SDp1 Member 1: Sandstone, red, grey or green; interbedded siltstone and mudstone, red, green, or variegated.

Late Silurian

Somerset Island Formation-undivided

Upper member: Dolostone and limestone, grey, greenish, or buff, laminated; siltstone, rare bioclastic limestone.

Ss Lower member: Dolostone and limestone; grey, greenish, or buff, laminated; argillaceous or bioclastic limestone, rubbly weathering.

Sdo Douro Formation: Argillaceous and dolomitic limestone, grey to green, rubbly weathering; minor bioclastic limestone, distinct reefoid mounds.

Cape Storm Formation

Western areas: Grey, buff, or brown dolostone; lesser limestone and sandstone; minor siltstone and shale.

Scs East coast: Dolostone, buff brown, parts sandy; grey, partly sandy, dolomitic limestone; sandstone. All thin-medium bedded.

Late Ordovician To Late Silurian

OSa Allen Bay Formation: Buff to pale grey dolostone, crystalline, med-massive bedded, parts bioclastic, resistant.

Middle and Late Ordovician

Cornwallis Group

Irene Bay Formation: Limestone; green-grey shale.

Octi Thumb Mtn Formation: Limestone; dolostone, calcareous; pale grey, cream or greenish grey; fossiliferous; resistant.

Ocb Bay Fiord Formation: Dolostone, dark grey or greenish grey, fissile, very fine grained; recessive.

Early To Middle Ordovician

Os Ship Point Formation: Pale grey-buff, thin to med bedded dolostone, parts bioclastic, rare chert nodules; sandstone common locally.

Late Cambrian To Early Ordovician

Turner Cliffs Formations

uCOtc Upper member: Dolostone, grey-buff, cherty, thick to massive beds, resistant.

ICotc Lower member: Thin-med bedded, grey to buff dolostone; thinly bedded, greenish dolostone. Sandstone with intraformational conglomerate and breccia; highly variable laterally.

Proterozoic

Ph Hunting Formation: Thin to thick dolostone beds, commonly stromatolitic. Minor interbedded chert, shale and siltstone.

Pa Aston Formation: Sandstone, minor siltstone, shale, and conglomerate. Distinct red stromatolitic dolosiltite marker unit near base.

Archean-Aphebian

A Crystalline Rocks: Mainly gneiss, minor metapelite, metabasite, granite and diabase; distinct calc-silicate and marble bands.

Devon Island, where basement structures were reactivated to form complex interference patterns in the overlying sedimentary cover. The area south of Barrow Strait acted as a buttress for the Parry Island Fold Belt and therefore compressional stresses related to the Ellesmerian Orogeny are not believed to reach as far south as Somerset Island (Okulitch, *et al.*, 1985; Grexton, 2009; Smith, 1995).

The last major tectonic event that affected the region was the Tertiary - Eocene Eurekan Orogeny that reactivated older faults via compressional events in the Sverdrup Basin (Cook, *et al.*, 2009; Grexton, 2009), creating north-trending dextral strike-slip and dextral oblique reverse faults (Guest, *et al.*, 2011). Tertiary faulting along the Boothia Uplift resulted in the preservation of Tertiary and older strata by producing fault-bounded grabens (Okulitch, *et al.*, 1985; Smith, 1995).

7.2 Local Geology

Proterozoic carbonate rocks are not well exposed on Somerset Island, therefore most of their depositional history is derived from nearby Victoria and Baffin Islands. An 800 m thick sequence of Middle Proterozoic, red weathering fine- to medium-grained hematitic silica cemented sandstone and conglomerate comprising the Aston Formation sits unconformably atop the crystalline basement of Somerset Island (Okulitch *et al.*, 1991). Following a period of uplift, intrusion of the Mackenzie dyke swarm at 1.27 Ga (LeCheminant and Heaman, 1989), and erosion, the Huntington Formation was deposited unconformably atop the Aston Formation.

The Huntington Formation is a 2,100 m thick unit comprised of thin- to medium-bedded, locally stromatolitic dolostone with minor gypsum. The 1,400 m thick Patrick Formation, an informal formation name used by Cominco geologists, is comprised of shallow-water carbonates overlain by black shale, lying conformably over the Huntington Formation. The Patrick Formation is exposed on Seal Island in Aston Bay (Cook, *et al.*, 2009). The Patrick, Huntington and Aston formations show evidence of minor faulting and folding prior to the intrusion of the 723 Ma Franklin diabase dykes and sills (Heaman, *et al.*, 1992).

A sequence of Cambrian to Late Ordovician carbonate and clastic sedimentary rocks, that young to the east, unconformably overlie the Patrick Formation. The 350 m thick Turner Cliffs Formation sits directly atop the rocks of the Patrick Formation. The Turner Cliffs Formation is comprised of an upper massive cherty dolostone layer and a lower interbedded unit of sandy, dolomitic and argillaceous rocks (Miall and Kerr, 1980).

The Ship Point Formation (64 – 250 m thick) sits conformably above the Turner Cliffs Formation and is comprised of pale grey thin- to medium-bedded dolostone with local minor stromatolitic, oolitic, and bioturbated beds (Miall and Kerr, 1980). Dark grey to brownish grey recessive fissile dolostone of the Bay Fiord Formation (6 to 196 m thick) sits conformably upon the Ship Point Formation (Miall and Kerr, 1980).

The fossiliferous 0 – 115 m thick Thumb Mountain Formation consists of pale grey, thinly bedded dolomitic biomicrite which lies unconformably above the Bay Fiord Formation. Interbedded greenish grey recessive argillaceous dolomitic limestone and shales of the Irene Bay Formation (0-34 m thick) sit conformably atop the Thumb Mountain Formation. The Bay Fiord, Thumb Mountain and Irene Bay formations make up the Cornwallis Group.

The Allen Bay Formation, deposited during the Late Ordovician and Early Silurian, sits unconformably atop the Irene Bay Formation and is comprised of a basal unit of massive dolostone containing Arctic Ordovician Fauna and an upper crystalline dolomite unit with common stromatolitic and bioclastic horizons (Miall and Kerr, 1980).

The Silurian Cape Storm, Douro and Cape Crauford Formations constitute a succession which sits conformably upon the Allen Bay Formation. The Cape Storm Formation consists of thinly-bedded, flaggy dolostone and ranges between 120 and 240 m thick. The 170 – 240 m thick Douro Formation is dominated by nodular, argillaceous, fossiliferous limestone. The Cape Crauford Formation is an equivalent facies to the upper portion of the Allen Bay Formation on central Somerset Island and is comprised of evaporites and dolomites.

During the Late Silurian to Devonian, tectonic movement of the Boothia Uplift resulted in the deposition of a clastic wedge, markedly dolostone and limestone of the Somerset Island and the Peel Sound Formations, which is preserved in small areas of the northwestern portion of the Property. The clastic wedge lies conformably above the Douro Formation (MacRobbie *et al.*, 2000; Cook & Moreton, 2009).

During the Late Cretaceous (103 Ma – 94 Ma), kimberlite diatremes intruded the northeastern portion of Somerset Island (Wu *et al.*, 2012; Smith *et al.*, 1989). These bodies intruded along the dominant fault orientations in the region, in addition to following apparent dyke swarm orientations.

The Property and surrounding area underwent several distinct periods of major tectonic deformation from the Proterozoic through to the Tertiary, and the rocks within the Property show resultant complex folding and faulting (Grextan, Assessment Report Storm Property: 2008; Technical Evaluation, 2009; Smith, 1995). The most recent deformation event reactivated older structures and created large grabens during transtensional movement, while preserving Tertiary and older strata (Cook, *et al.*, 2009; Smith, 1995). The Central Graben structure on the Storm Property (Figure 5), bounded by north – south trending faults, preserves rocks of the down-dropped Douro Formation, indicating faults likely cut through the full stratigraphic column underlying the Silurian Douro Formation (Cook, *et al.*, 2009).

7.3 Property Geology

Property-scale geology for the areas of the Seal and Storm showings is illustrated in Figures 6 and 7, respectively. Geology unit abbreviations are illustrated on Figures, 5, 6 and 7. A stratigraphic

column which serves to illustrate and simplify the lithological relationships in the Property area is presented in Figure 8 for reference.

The material in this section is summarized from Dewing and Turner (*pers. comm.*, 2012), Leigh (1996), Leigh and Tisdale (1999), MacRobbie *et al.* (2000), and Smith (2001). The geological information has been gathered from both drill core and limited bedrock exposure throughout the property, though the focus is on the Seal and Storm mineralized zones.

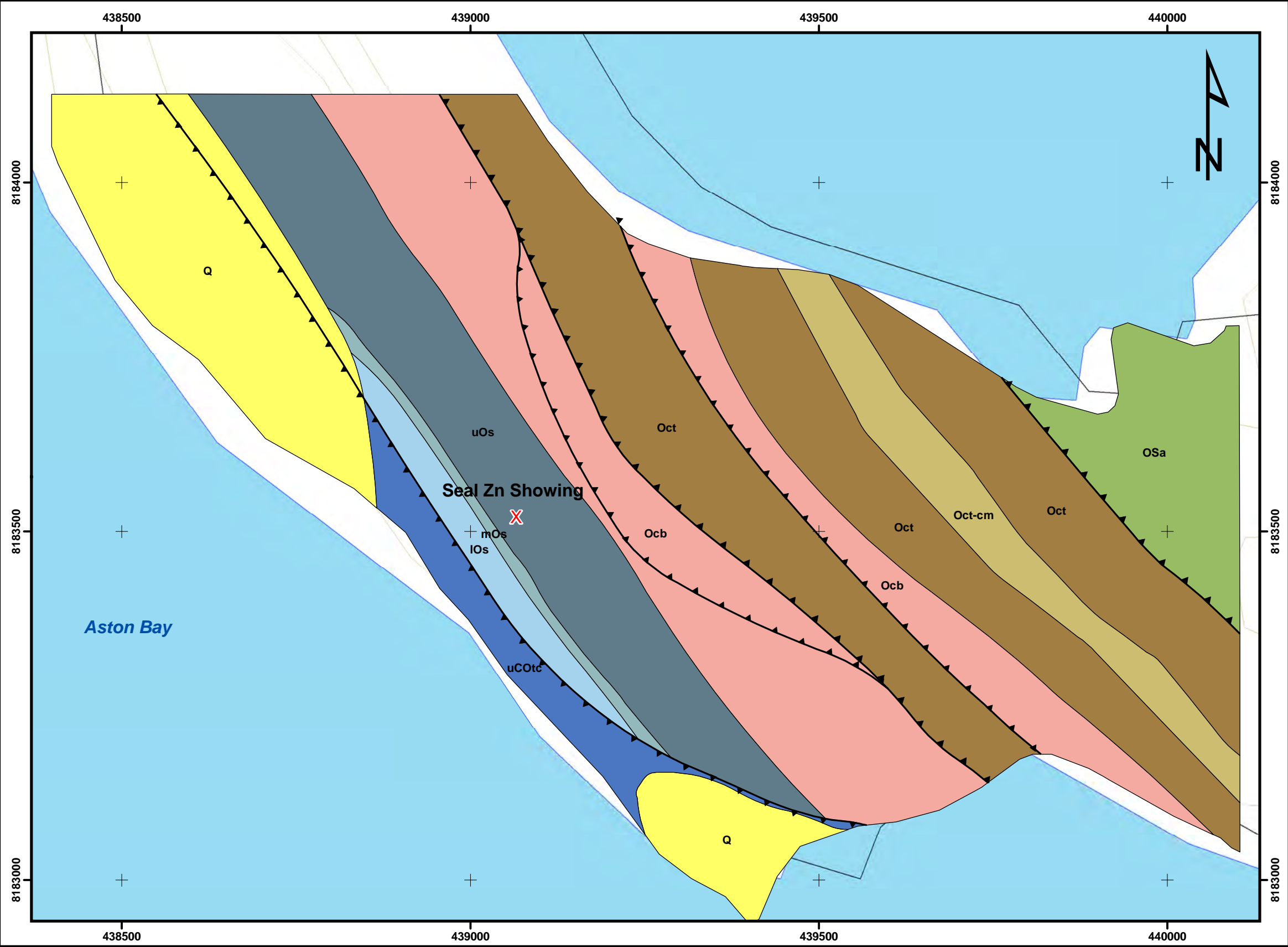
The oldest rocks observed on the property belong to the 200 m thick Turner Cliffs Formation (units uCOtc and ICOtc). The rocks of the Turner Cliffs Formation were deposited within and proximal to the intertidal zone. The unit consists of a series of interbedded cryptalgal laminates, stromatolites and flat pebble conglomerates. A leached dolostone with chert nodules occurs within the succession. It is described as a pseudobreccia, contains abundant white dolospar and calcite (making up 60% of the zone) with 5-20% of the rock being comprised of cavities. Locally, brown resinous sphalerite is present within the cavities of the pseudobreccia.

Lying conformably above the Turner Cliffs Formation within the property are rocks of the Ship Point Formation (Os). The contact between the Turner Cliffs and Ship Point formations is marked by the first occurrence of sandy dolostone and the disappearance of laminated dolomicrite. The Ship Point Formation is a resistant, ridge-forming rock unit which was deposited in a shelf environment and has a distinctive dull grey weathered colour. The base of the Ship Point Formation consists of a 1.5 – 2 m thick sandy dolostone bed which is overlain by a distinctive 8 – 10 m well-sorted quartz arenite with well-preserved planar cross-beds. The sandstone unit is locally pyritic with associated elevated zinc values. The upper 50 m plus of the Ship Point Formation is comprised of medium-bedded sandy dolostone, bioturbated mottled dolostone, cross-bedded arenaceous sandstone and local oolitic dolostone.

The Bay Fiord Formation (unit Ocb) lies conformably upon the Ship Point Formation and consists of green to grey to brown, thinly-bedded to laminated silty dolostone and shale. Conformably above the Bay Fiord Formation is the Ordovician Thumb Mountain Formation which is comprised of bioturbated argillaceous dolostone with abundant scattered chert nodules.

In the western portion of the Property the Thumb Mountain Formation (unit Octi) is in fault contact with the overlying Silurian Allen Bay Formation (unit OSa). Though the Allen Bay Formation is the youngest unit present in the western portion of the property, the same cannot be said in the eastern portion of the property where the Allen Bay Formation hosts the Storm copper mineralization.

The Allen Bay Formation in general consists of buff dolostone with common chert nodules and vuggy crinoidal dolowackestone along with carbonate muds. The upper Allen Bay Formation has been subdivided into three members. The 150 m plus thick buff to light-grey, lower Varied Stromatoporoid (VSM) unit is comprised of interbedded dolofloatstone, dolorudstone, stromatoporoid boundstone, framestone and thinly-bedded to laminated dolomicrite.



Legend

X

Showing

Topographic Contour

Water Body

Storm Prospecting Permit

Faults

Bedrock Geology

Quaternary

Q

Stream, deltaic, glacial and marine beach sediments (mapped when underlying geology could not be inferred with reasonable certainty).

Late Ordovician To Late Silurian

OSa

Allen Bay Formation: Buff to pale grey dolostone, crystalline, med-massive bedded, parts bioclastic,

Middle and Late Ordovician

Cornwallis Group

Octi

Irene Bay Formation: Limestone. Green-grey shale.

Thumb Mtn Formation: Limestone; dolostone; calcareous; pale grey, cream or greenish grey; fossiliferous; resistant.

Ocb

Bay Fiord Formation: Dolostone, dark grey or greenish grey, fissile, very fine grained; recessive.

Early To Middle Ordovician

Os

Ship Point Formation: Pale grey-buff, thin to med bedded dolostone, parts bioclastic, rare chert nodules; sandstone common locally.

Late Cambrian To Early Ordovician

Turner Cliffs Formations

uCOtc

Upper member: Dolostone, grey-buff, cherty, thick to massive beds, resistant.

ICOTc

Lower member: Thin-med bedded, grey to buff dolostone; thinly bedded, greenish dolostone. Sandstone with intraformational conglomerate and breccia; highly variable laterally.

ASTON BAY VENTURES LTD.

Somerset Island, Nunavut, Canada

Local Geology Map

Seal Zn Showing

150750150

Metres

1:6,000

Scale

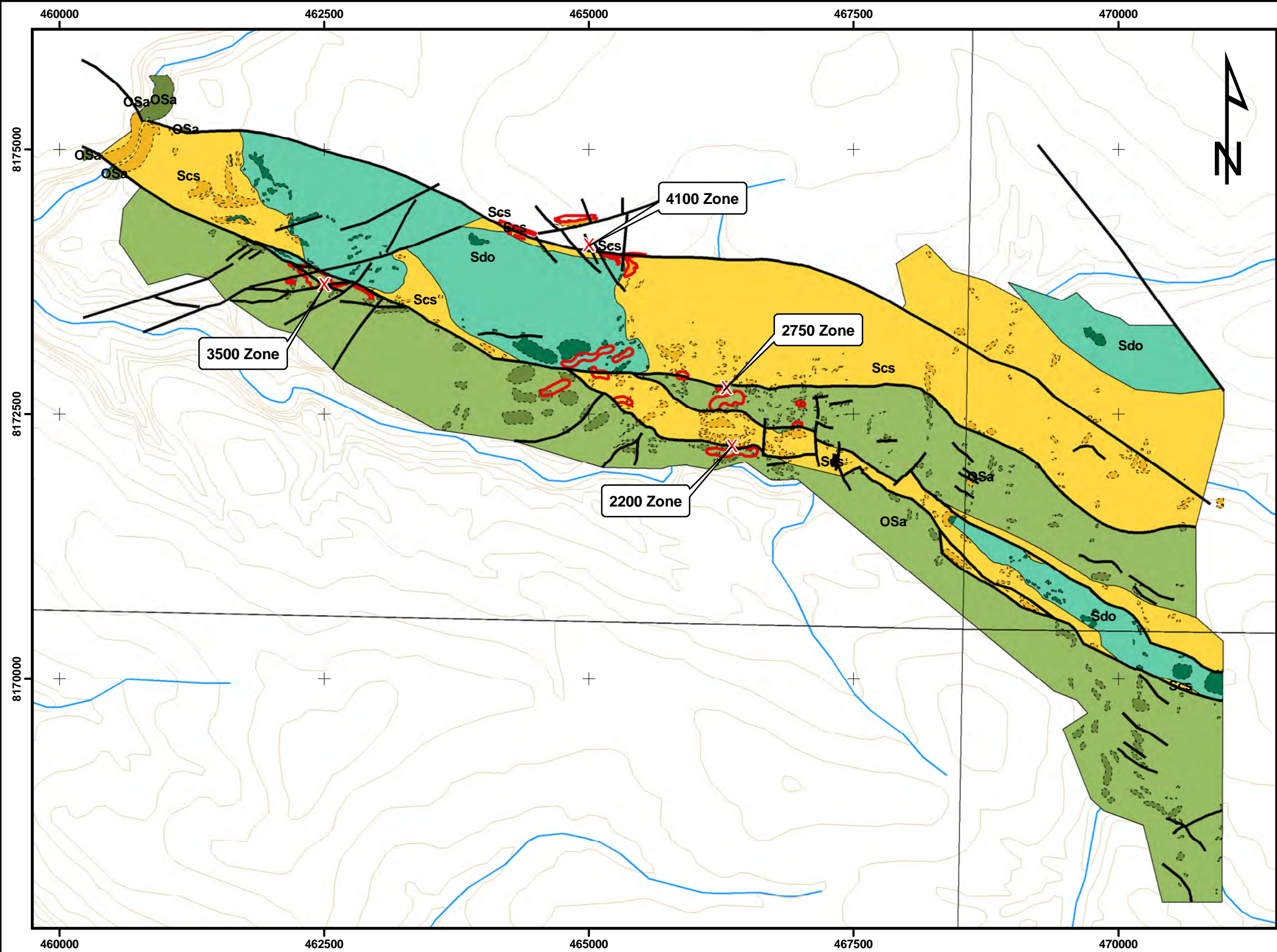
UTM NAD 83 Zone 15N

APEX Geoscience Ltd.

Edmonton, AB

Figure 6

October 10, 2012



Bedrock Geology

Late Silurian

Sdo Douro Formation: Argillaceous and dolomitic limestone, grey to green, rubbly weathering; minor bioclastic limestone, distinct reefoid mounds.

Cape Storm Formation

Scs Western areas: Grey, buff, or brown dolostone; lesser limestone and sandstone; minor siltstone and shale.
East coast: Dolostone, buff brown, parts sandy; grey, partly sandy, dolomitic limestone; sandstone. All thin-medium bedded.

Late Ordovician To Late Silurian

OSa Allen Bay Formation: Buff to pale grey dolostone, crystalline, med-massive bedded, parts bioclastic,

Legend

X Showing

Storm Prospecting Permit

Fault

Detailed outcrop

Surface mineralization

Topographic Contour

Drainage

ASTON BAY VENTURES LTD.

Somerset Island, Nunavut, Canada

Local Geology Map

Storm Showing

1,000 500 0 1,000 Metres

1:40,000 Scale
UTM NAD 83 Zone 15N

APEX Geoscience Ltd.
Edmonton, AB

Figure 7
October 10, 2012

Three marker horizons are present within the VSM,: the Oolitic Marker (OP), the Rudstone Chip Marker (RCM) and the Stromatoporoid Boundstone/Framestone Marker (SBFM). The OP occurs 40 m from the top of the VSM and is made up of 1 to 2 reverse-graded oolitic to oncolitic packstone beds. The RCM is less than 1 m in thickness and consists of a coarse mixture of elongate fossil fragments. Five metres above the RCM is the 6 m thick SBFM which occurs near the top of the VSM. The SBFM contains light brown digitate stromatoporoids in growth position.

The 35 m thick middle unit of the upper Allen Bay Formation is termed the Brown Dolopackstone and Dolofloatstone (BPF). The BPF is medium to dark brown comprised of coral-rich dolofloatstone and dolopackstone, with scattered fragmented stromatolites and local dolomicrite interbeds. Chert nodules are common in two horizons within the BPF. Thirty-five to fifty metres of Alternating Dolomicrite and Dolowackestone (ADMW) makes up the upper unit of the upper Allen Bay Formation. The ADMW is made up of thickly-bedded to massive dolomicrite with common internal laminations and metre-scale beds of dolowackestone with fossil debris.

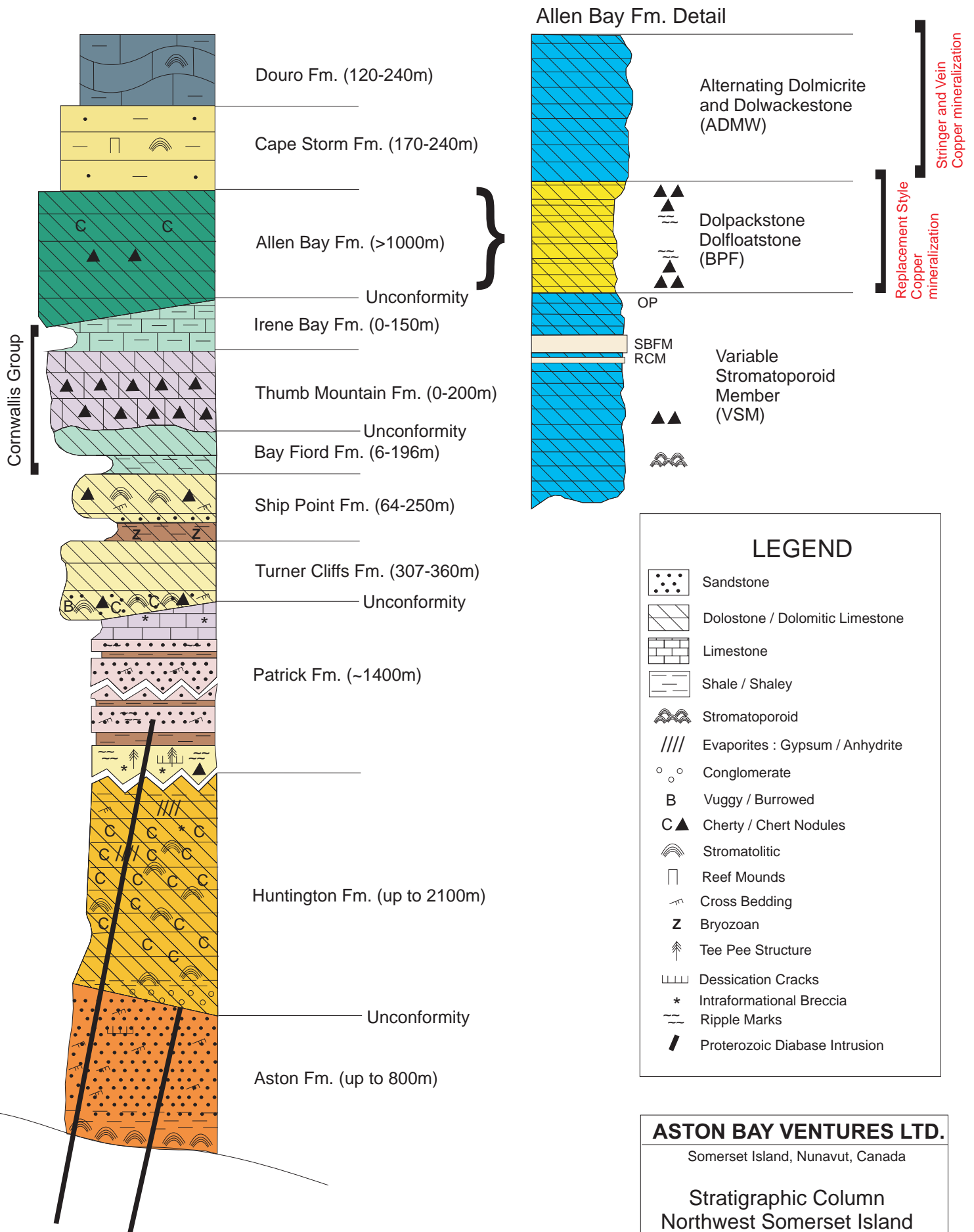
The Cape Storm and the Duoro formations conformably overlie the Allen Bay Formation. The Cape Storm Formation (unit ScS) was deposited in a shallow water to emergent environment and is comprised of platy light- to medium-grey dolostone with widely spaced argillaceous interbeds. The dark green colour of the Duoro Formation (unit Sdo) distinguishes this unit from the others within the eastern portion of the Property. The Duoro Formation consists of nodular argillaceous limestone containing fossilized bivalves, rugose and colonial corals.

The dominant structural feature in the eastern portion of the property is the ESE trending Central Graben. It appears that the Storm copper mineralization was deposited early in the formation of the graben and later structurally modified.

According to Dewing and Turner (*pers. comm.*, 2012), bedding at the Seal Zinc showing forms a northeast-dipping monocline. On Aston Peninsula, beds dip 14° closest to the ocean, increasing to 34° in the Thumb Mountain Formation, then decreasing northeastward. The monocline is in faulted contact with the Proterozoic Thumb Mountain Formation and locally folded into anticline-syncline pairs with northeast-trending fold axes and plunges. There are small normal faults which offset rock units on Aston Peninsula and near the Seal showing; however there appears to be no direct correlation between mineralization and structure.

The Storm Copper showings are located along faults that define the east-west trending Central Graben. This structure is about 1 km across at the western end, widening to 2 km across where the axis of the graben turns towards a northwest-southeast orientation. The faults are sub-vertical or dip slightly in towards the graben. Local fault juxtaposition of the Allen Bay and Duoro formations indicate a minimum throw of 250 m. Besides the main graben boundary faults, smaller fault splays and sub-grabens exist (Dewing and Turner, *pers. comm.*, 2012).

The Central Graben is similar to structural sandbox models of pull-apart basins described by Dooley and McLay (1997). The authors modeled a number of releasing bends in strike-slip structural



settings. The underlapping, 30° releasing sidestep model in Dooley and McLay (1997) bears a strong resemblance to the Central Graben at the Storm showing.

7.4 Mineralization

Base metal mineralization has been identified within the Property in two distinct areas namely the Seal zinc showing and the Storm copper showing. The Seal zinc showing occurs within the lower portion of the Early Ordovician Ship Point Formation, proximal to Aston Bay. The Storm copper showing is comprised of four distinct zones surrounding the Central Graben and is hosted within the upper 80 metres of the Late Ordovician to Early Silurian Allen Bay Formation.

7.4.1 Seal Zinc

The Seal Zinc showing is located in the northwestern part of the Property at the base of a small peninsula immediately northwest of the Aston Peninsula on Aston Bay. It occurs on a steep, southwest facing hill as scree, as minor outcrop of disseminated sphalerite in pseudo brecciated Turner Cliffs Formation, and as massive sphalerite and pyrite in the Ship Point Formation. Scattered blocks containing sphalerite occur along the 1,500 m length of this peninsula. The Aston Peninsula proper contains small patches of rusty sandstone and sandy limestone in a similar stratigraphic position, but no sphalerite was found.

Strata on the north side of Aston Bay span the Gallery to Allen Bay formations and consist of the Gallery, Turner Cliffs, Ship Point, Bay Fiord, Thumb Mountain, Irene Bay and Allen Bay formations. Similar rock types in the Thumb Mountain, Irene Bay and Allen Bay formations make differentiating them problematic. For mapping purposes, a recessive weathering interval between the Thumb Mountain and Allen Bay formations was interpreted to be the Irene Bay Formation.

The mineralization is hosted in an 8-10 m thick porous and permeable basal quartz-arenite with interbeds of dolostone and sandy dolostone (Cook and Moreton, 2009; Smith, 2001). Zinc mineralization is present in two forms within the Seal Zinc showing, firstly as coarse-grained, reddish-brown blackjack sphalerite and secondly as honey yellow, colloform sphalerite. The zinc mineralization occurs as local to complete replacement of the sandy dolostone interbeds as well as interstitial disseminations in massive sandstone beds (Cook and Moreton, 2009).

The known mineralization extends for 400 m along strike and is 50-100 m in width and upwards of 20 m in thickness, containing 7-8% Zn and 23-27 g/t Ag (Cook and Moreton, 2009). Fine-grained marcasite is the dominant sulphide with lesser amounts of coarse pyrite associated with the dolostone interbeds. Post-mineralization faulting may have resulted in repetition and thickening of the mineralized zone (Cook and Moreton, 2009). Although the mineralization appears to be lensoid, it is believed to be stratabound.

The footwall of the mineralization is marked by a large hydrothermal alteration zone within the Turner Cliffs Formation. This alteration zone is described as a pseudobreccia and pervasive solution breccia cemented with coarse-grained white dolospar (Leigh, 1996). The northwest-trending alteration zone has a strike length of over 600 m and a stratigraphic thickness of 150 m (Smith, 2001). Minor mineralization is evident within the alteration zone expressed as disseminated sphalerite filling voids and veins and associated with the dolospar cement (Cook and Moreton, 2009).

The pseudobreccia alteration zone has a sharp upper contact with a laminated dolomicrite unit and a sharp lower contact with argillaceous nodular dolostone (Smith, 2001). The upper and lower contacts of the pseudobreccia zone likely represent aquitards focussing the flow of the hydrothermal alteration (Leigh, 1996). Cook and Moreton (2009) suggest that the alteration zone represents the feeder zone for the Seal Zinc mineralization.

7.4.2 Storm Copper

The Storm Copper mineralization is located adjacent to, and offset by, the north and south bounding faults of the Central Graben structure and includes four discrete zones of copper mineralization: 2200N, 2750N, 3500N and 4100N. The first three zones outcrop at surface whereas zone 4100N is blind, covered by a veneer of the Cape Storm Formation (Cooke and Moreton, 2009; Grexton, 2008; Leigh and Tisdale, 1999).

Three formations are exposed in the vicinity of the Storm Copper showings, the Allen Bay, Cape Storm and Duoro formations. The Allen Bay Formation hosts the majority of the mineralization at the Storm Copper showing. It is conformably overlain by the Cape Storm Formation, which is in turn, conformably overlain by the Duoro Formation.

The Storm Copper mineralization is hosted within the upper 80 metres of the Silurian Allen Bay Formation. The mineralization occurs within an alternating sequence of recrystallized and variably fossiliferous dolostones lying above a thick reef unit (Cook and Moreton, 2009). Copper mineralization is largely located within structurally prepared ground occurring within crackle breccia, solution breccia, solution crackle breccia and tectonic breccias (Cook & Moreton, 2009; Grexton, 2008). Mineralization is most common within crackle breccia horizons. The crackle breccia is monomictic with angular to subangular, centimetre-scale clasts cemented with *in situ* micritic dolomite, lime mud and calcite with lesser copper and iron sulphides (Cook and Moreton, 2009).

Copper mineralization occurs as breccia cement and fracture fill within brecciated, recrystallized and locally silicified Allen Bay Formation dolostone. Pyrite and marcasite are the principal sulphides; these are locally replaced by copper sulphides. Copper mineralization within the fossiliferous units is typically disseminated, void-filling and net textured replacement of the host, whereas the mineralization in the less porous units is within crackle breccia, stringers and veins (Cook and Moreton, 2009).

Chalcocite, covellite and bornite, with lesser chalcopyrite, are the dominant copper sulphides present within the Storm copper zones. Accessory cuprite, azurite, covellite and native copper are also present (Grextan, 2008). Alteration within the Storm copper showing is expressed as sucrosic recrystallization and local dedolomitization of the host dolostone, along with local strong hematite and limonite with irregular pockets of silicification (Cook and Moreton, 2009).

Low-grade copper mineralization extends over a distance of five kilometres in the four main zones which are referenced by their UTM northings (2200N, 2750N, 3500N and 4100N). The 2200N, 2750N and 3100N zones occur in outcrop. The 4100N zone lies largely beneath the Cape Storm Formation with only minor mineralization noted at surface. Mineralization occurs within the upper 80 m of the Allen Bay Formation. Alteration and minor copper sulphides occur in the Cape Storm and Duoro formations. This alteration includes moderate to intense fracturing, small zones of mosaic packbreccias with calcite, pyrite and subordinate chalcocite cement, pervasive hematite staining and rare malachite/chalcocite in fractures.

The 2200N and 2750N zones show evidence of vertical plumbing and the copper mineralization does not appear to be stratabound. The 4100N zone is again fault proximal and vertically plumbed though the dominant copper mineralization is stratabound (Cook and Moreton, 2009). The 4100N zone has less pyrite and marcasite than the other Storm Copper zones.

A genetic link between the Storm Copper zones and the Central Graben has been outlined by Cook and Moreton (2009). The west-directed Caledonian compressional event (Taconic Orogeny) resulted in a recharge of fluids from adjacent highlands through the evaporite hosting basin and circulation of deep basinal fluids through red beds of the Aston Formation. The Aston Formation red beds appear to be the source of metals for both the Storm and Seal mineralized systems.

The 2200N zone is exposed along the Aston River ridge proximal to the 2200N fault. Soil geochemical anomalies extend 600 m with subsurface continuity of mineralization mapped by IP and HLEM surveys. Drilling has defined a 300 m long, 40 m thick and 60 m wide mineralized zone. Poddy to net-textured chalcocite and bornite occurring as breccia cement, fracture fill and veins replacing iron sulphides and *in situ* organic matter are the dominant copper minerals (Cook and Moreton, 2009; Grextan, 2008). Semi-massive sulphide zones are separated by wide intervals containing sporadic stringers and veins. Fine-grained, disseminated native copper occurs in near vertical, irregular wavy stringers and net textured veinlets proximal to the 2200N fault (Cook and Moreton, 2009).

The surface exposure of the 2750N zone consists of a 100 m long, east-west trending malachite-stained gossan adjacent to the 2750 Fault (or South Boundary Fault) of the Central Graben. This is also referenced as the Southern Fault of the Central Graben (Cook and Moreton, 2009). Drilling indicates that the mineralized zone continues from surface to 80 m depth, the zone narrows from 50 m width at surface to 25 m at depth, and occurs in an area of complex faulting.

Massive chalcocite along with pervasive low grade bornite in crackle breccia comprise the mineralization within the 2750N zone. Areas on surface closest to the fault are silicified. Hematite-cemented breccia zones are a common feature of the 2750N zone.

Cook and Moreton (2009) note a progressive zonation of copper minerals both vertically and laterally away from the 2750 fault. A chalcocite-bornite zone dominates from surface to 50 m depth; this gives way to a chalcopyrite zone which dominates to 70 m depth. Cook and Moreton (2009) report that a silicified, pervasive solution breccia occurs as a broad envelope beneath the mineralization, whereas hematite cemented crackle breccia occurs marginal to the mineralization and adjacent to the 2750 Zone.

Mineralization at 3500N is expressed as a 300 m rubble and outcrop zone of copper oxides and rusty limonitic recrystallized rocks of the Allen Bay Formation (Leigh and Tisdale, 1999). Drilling indicates that the zone is extremely erratic and discontinuous with an overall strike length of 200 m and is upwards of 75 m thick with an undetermined width (Cook and Moreton, 2009). Mineralization occurs within a complex of intersecting faults that juxtapose the Allen Bay and Duoro formations. Chalcocite and bornite occur as disseminations, stringers and veins within coarsely recrystallized dolostone.

The 4100N zone has a limited surface expression and is located at the intersection of the North Boundary fault with three or more subtle northwest structural lineaments. The mineralized zone defined to date extends over 1000 m strike and 400 m width with the potential for deep extensions to the south of the 4100N fault (Leigh and Tisdale, 1999). The zone is open to the north, east and west (Cook and Moreton, 2009). Previous authors have noted that the zone is irregular though persistent and occurs in a predictable stratigraphic position (Cook and Moreton, 2009; Grexton, 2008).

Copper mineralization dominated by chalcocite occurs in steeply dipping veins and breccias as well as stratabound disseminations filling voids and replacing organic partings and macrofossils. Copper mineralization extends through 80 metres of stratigraphy from the basal, hematite-altered Cape Storm Formation into the ADMW and BPF units of the upper Allen Bay Formation (Cook & Moreton, 2009; Grexton, 2008). The 4100N occurrence also exhibits a vertical copper mineralization zonation from top to bottom of chalcocite-bornite-chalcopyrite-native copper. In the west end of the 4100N zone an outer lead-zinc zone of galena-sphalerite-chalcopyrite in the footwall adjacent to copper mineralization is present (Cook and Moreton, 2009; Grexton, 2008; MacRobbie *et al.*, 2000).

There were two main diagenetic events. The first was dolomitization accompanying the precipitation of pyrite and chalcocite with bornite intergrowths. Silica, occurring as cryptocrystalline quartz, minor sphalerite and galena were deposited at the margins of the alteration system. The second diagenetic event consists of minor dissolution and dedolomitization of dolomite, dissolution of galena and the precipitation of zinc oxides.

Oxidation of chalcopyrite-bornite and pyrite led to their replacement by chalcocite, covellite and native copper. Chalcopyrite and bornite occur as remnants with chalcocite and covellite. Hematite staining is commonly associated with the zones of chalcocite. The second event was accompanied by calcite precipitation. Copper mineral surfaces were subsequently altered to malachite and azurite.

8: DEPOSIT TYPES

8.1 Mississippi Valley-Type Lead Zinc Deposits

Mississippi Valley Type (MVT) deposits are epigenetic, stratabound deposits that occur in unmetamorphosed platform carbonate rocks with a particular affinity to dolomites. The majority of the host rocks to MVT deposits are Cambrian – Ordovician and Carboniferous in age, and are believed to have formed as part of the normal evolution of a sedimentary basin. Mississippi Valley Type deposits typically occur at or near basin edges or along arches between basins, though they can also be associated with foreland fold and thrust belts and rift zones (Leach and Sangster, 1993).

Individual MVT deposits typically form in clusters creating mineral districts. Typical alterations associated with MVT deposits are dolomitization, brecciation, local recrystallization and dissolution (Leach and Sangster, 1993). Ore fluids are low temperature basinal brines: 75 – 200°C, dense, highly saline with 10-30 wt.% salts dominated by Na, Ca (Anderson and Macqueen, 1982). Groundwater is recharged within the orogenic flank during uplift and migrates through the deep portions of the basin via topographically driven fluid flow acquiring heat and leaching metals (Anderson and Macqueen, 1982; Leach and Sangster, 1993). These metals are carried as chloride complexes and precipitate as sulphides.

Ore formation has been attributed to three genetic models, or a combination of the models. The reduced sulphur or “non-mixing” model requires that the metals and reduced sulphur travel together in a single fluid, precipitation of sulphides occurs during cooling, dilution or changes in pH. The sulphate reduction model is a variation of the reduced sulphur model. Again both reduced sulphur and metals are transported in the same fluid, addition of reduced sulphur at the deposition site from the presence of methane or other organic material reduces the sulphate to precipitate sulphides (Leach and Sangster, 1993). The “mixing” model involves the interaction between a metal-rich brine and an H₂S-rich fluid at the deposition site (Anderson and Macqueen, 1982; Leach and Sangster, 1993). MVT deposits are typically small (<10 Mt ore) and combined Pb + Zn grades seldom exceed 10%, though their tendency to occur as clusters forming districts greatly aids in the economics (Leach and Sangster, 1993). One relevant exception to this is the Polaris mine which produced 22 Mt of ore grading 18% combined lead and zinc.

8.2 Sediment-Hosted Stratiform Copper Deposits

Sediment-hosted stratiform copper deposits occur throughout the world in variable host rocks. Several key features typify the deposit type, including: stratiform configuration of the ore zone; fine-grained, disseminated sulphides forming the ore zone; zonation of metals; and red beds present in the footwall and located within or associated with rift basins. The footwall red bed unit is the source for the metals which are leached and transported by circulating brines.

These brines then cross a redox boundary into a typically fine-grained, porous and permeable, sulphur-enriched reducing unit which causes the metals to precipitate as sulphides (Brown, 1992). As copper is the least soluble base metal it is the first to form sulphides and precipitate, starting with copper-rich phases of chalcocite and bornite and later chalcopyrite. Lead and zinc, being more soluble, are transported further in solution and are precipitated closer to the margins of the ore zone as the brine migrates (Brown, 1992). This results in an overprinting of the syn-diagenetic iron sulphides and sulphates in the host rock by base metal sulphides. Sediment-hosted stratiform copper deposits are related to the normal evolution of a continental rift basin. Two applicable sub-types, Kupferscheifer and Kipushi, are discussed below.

8.2.1 Kupferscheifer type

Kupferscheifer type deposits are typically hosted in epicontinental, shallow marine-derived sedimentary rocks such as carbonaceous shales, mudstones and siltstones. Red beds, evaporites and lesser rift-related mafic volcanic rocks are associated. The ore zone of Kupferscheifer deposits is hosted within fine-grained clastic rocks, and is typically stratiform and tabular, though it may be irregular in shape and cross cut several lithologies.

The main ore minerals are chalcopyrite, bornite, chalcocite and native copper with minor galena and sphalerite, which are present as fine-grained disseminations or veinlets. There is a lateral and vertical zonation upwards and away from the base of the ore zone. Copper concentrations are elevated at the base of the ore zone with lead and zinc concentrations increasing towards the margin. Silver, cobalt, lead and zinc are all important by-products. Alteration associated with Kupferscheifer deposits is limited to a strong hematite zone at the base of the ore zone. The ore zone is hosted within a reducing lithological unit.

8.2.2 Kipushi-type

Kipushi type deposits are formed along continental margin platforms or within deeper portions of intracratonic basins. Dolomites are the typical host rock for Kipushi deposits. This type of deposit is associated with mafic volcanic rocks. Host rocks have high porosity and permeability due to karst formation or brecciation, and are spatially related to transcurrent rift faults. A regional transition from platform carbonates to basinal shales is evident. The presence of stromatolites or reef complexes is common.

Kipushi deposits occur proximal to dolomitization fronts with limestone. The formation of these deposits requires a shale or other impermeable layer within the carbonate sequence to trap and focus fluid flow. Kipushi-type deposits are strongly associated with hydrocarbons. The ore zone consists of structurally controlled, stratiform stockwork veins. Within the ore zone there are abundant open vugs resulting in colloform textures and common rosettes and blades.

The main ore minerals are bornite, chalcocite, chalcopyrite, carrollite, sphalerite, galena and tennantite. Surficial supergene malachite and azurite caps are common. A lateral and vertical zonation away from the core of the mineralized zone is evident. The highest concentration of copper is at the core, with lead, zinc and iron concentrations increasing towards the margins. Geochemically, Kipushi-type deposits show high Co/Ni, As/Sb and Ag/Au ratios. Alteration is expressed as dolomitization, sideritization and silicification.

9: EXPLORATION

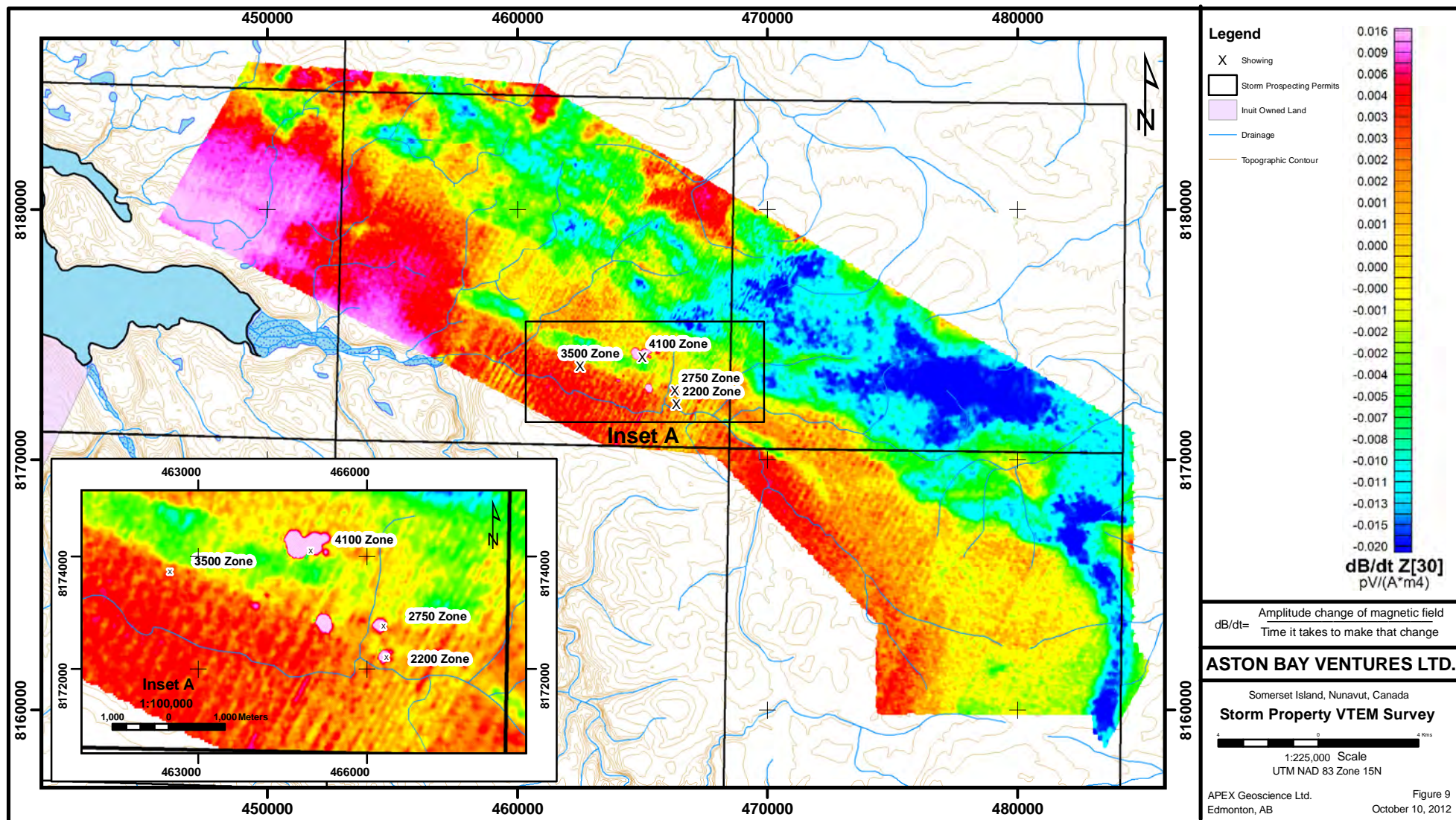
9.1 Introduction

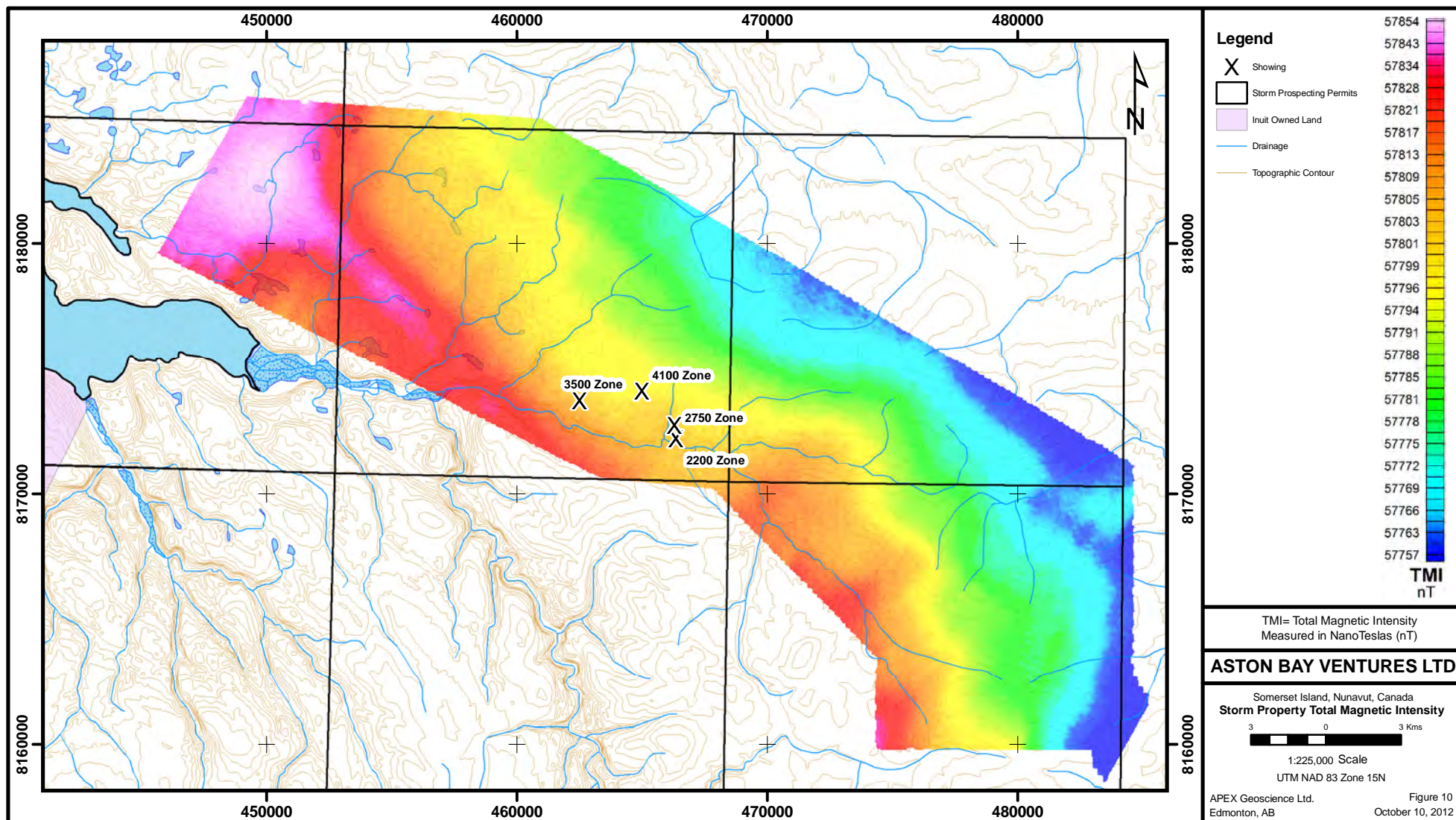
In 2012 APEX was retained by Aston Bay to conduct an exploration program on the Storm Property. The 2012 program involved interpretation of the VTEM and aeromagnetic survey from 2011 by Intrepid Geophysics. This was followed by a property visit, prospecting, surface sampling and resampling of existing diamond drill core and ground truthing of the VTEM anomalies by APEX and Aurora personnel. The resampling of historic drill core was intended to validate the historical results and fill data missing from the historic record. The cost to complete the Storm Property exploration in 2012 totalled approximately \$448,000 (Appendix 1).

9.2 VTEM Airborne Geophysical Survey

In July 2011 Commander retained Geotech Ltd. (Geotech) to complete a helicopter-borne Versatile Time-Domain Electromagnetic (VTEM) and aeromagnetic survey over the Storm Property (Figure 9). Between July 6th and July 24th 2011, a total of 3,969.7 line-km were flown. The primary VTEM survey flight lines were oriented 030°/210° and spaced at 150 m with parallel infill lines spaced at 75 m and orthogonal tie lines spaced at 1,500 m. The helicopter-borne survey measured electromagnetics (EM; Figure 9) and magnetics (Figure 10) using a Geotech Time Domain EM (VTEM plus) system and a Geometrics optically pumped caesium vapour magnetic field sensor mounted at 35 m and 13 m, respectively, below the aircraft. E M and magnetic readings were taken every 0.1 seconds (sec). The helicopter, a Eurocopter Aerospatiale (A-Star) 350 B3 owned and operated by Geotech, maintained a mean altitude of 77 m above ground with a survey airspeed of 80 km/h. A combined Geometrics caesium vapour magnetometer/GPS base station was used to compensate and correct for background magnetic field and GPS variations.

Data quality and completeness were verified through field data processing and analysis on a daily basis. Maps displaying magnetic and conductive properties of the surveyed areas were produced





from the data. Accurate positioning of the data was ensured through differential GPS navigational corrections.

9.3 Airborne Geophysical Interpretation

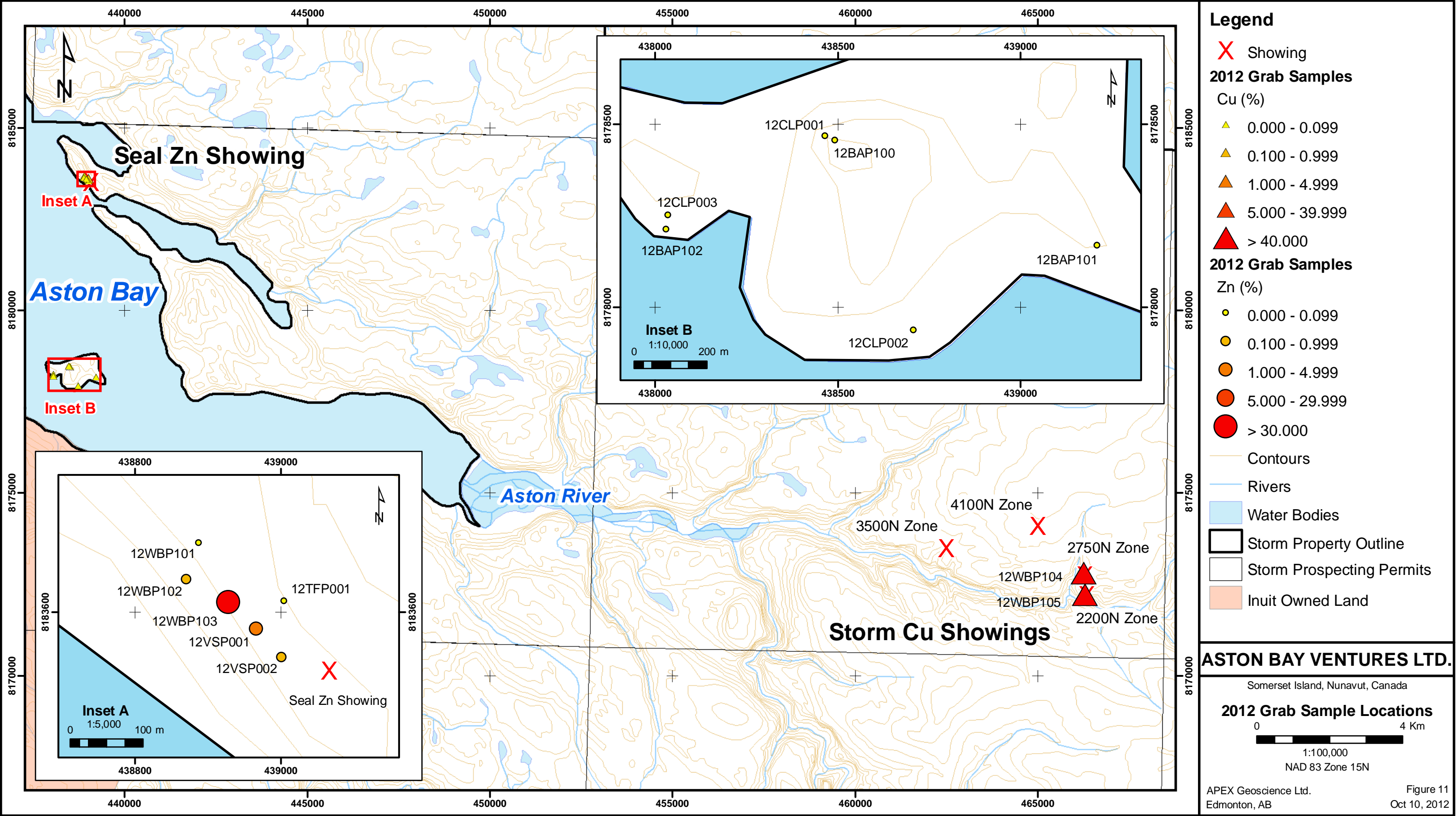
In 2011, Intrepid Geophysics Ltd. (Intrepid) was retained by Commander to provide an advanced interpretation of the geophysical data collected during the July 2011 VTEM survey. As part of this interpretation, enhanced derivative grids of the magnetics were generated and imaged, and a texture and phase analysis of the magnetics was undertaken in order to identify and map possible zones of structural complexity which may in turn indicate zones of favourable mineralization. A profile by profile review of all airborne electromagnetic anomalies was carried out preparatory to identifying high-priority areas of interest and zones for further investigation and ground follow-up.

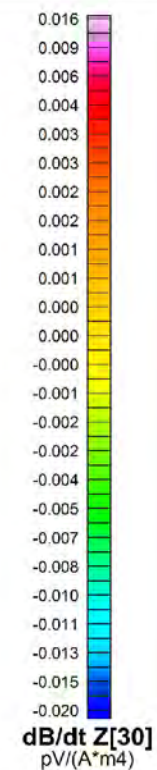
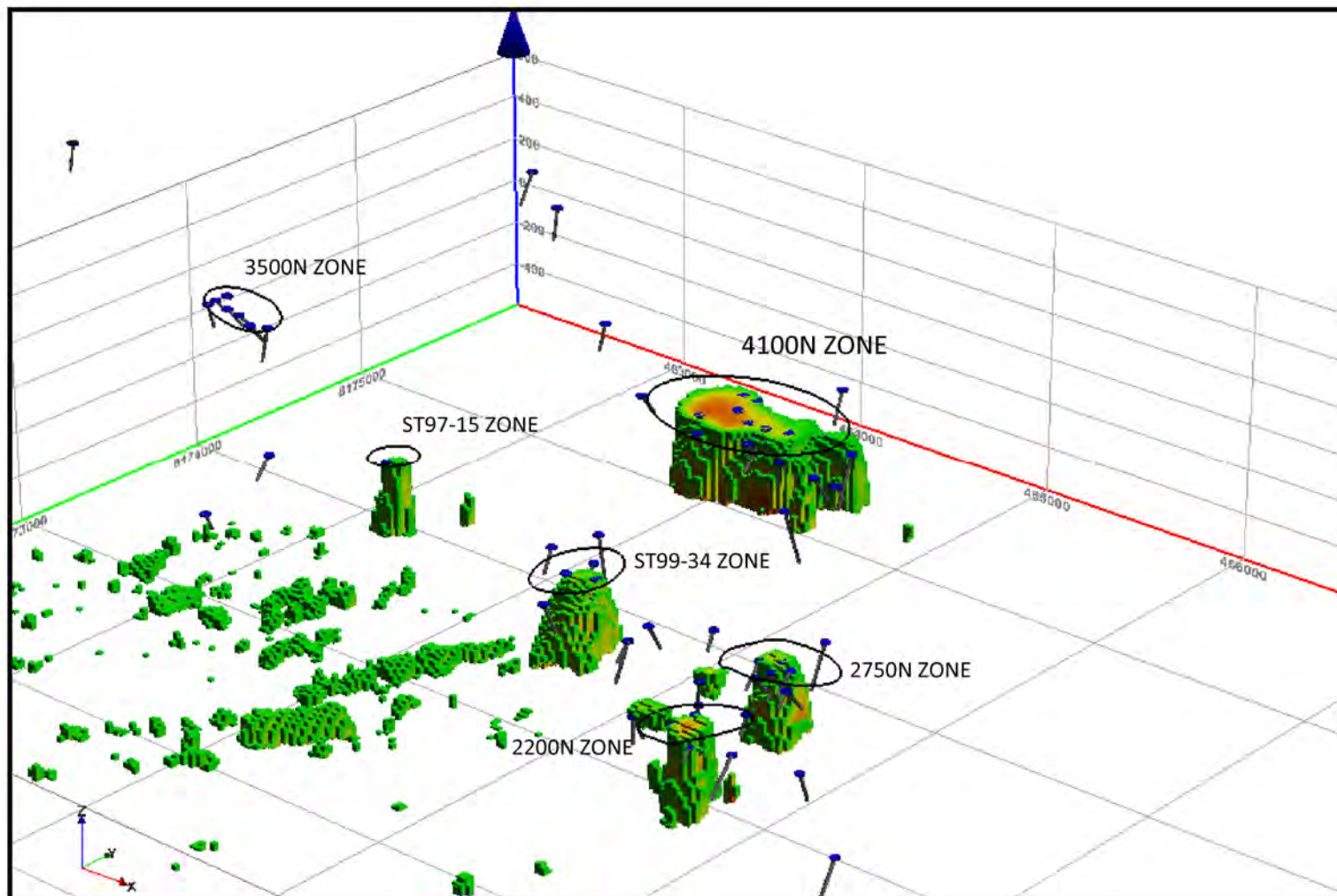
The following is a summary from the Intrepid report (Campbell, 2011) which is included as Appendix 2 at the end of this report.

Enhanced derivative grids of the airborne magnetic data were generated and imaged as part of the geophysical data reprocessing exercise and they have highlighted a limited number of structural orientations and trends. The aeromagnetic data is primarily reflecting very long wavelength, buried features believed to be sourced in the Proterozoic basement at some depth. A high-frequency, shallow component is however, evident throughout and is possibly related to detrital materials within the sedimentary rocks and perhaps related to variation in sea levels. Significant linear features are mapped based upon analysis of all derivatives; these are interpreted as most likely occurring within the sedimentary section (based on frequency content) and may be related to horizons equivalent to the known Storm Copper zones. These features are presented as possible structural controls impacting the stratiform sulphide mineralization (Campbell, 2011). Figure 11 shows all of the derivatives with interpreted structural features traced over the magnetic derivative map.

The principle anomalies of interest occur coincident to the known 4100N, 2750N and 2200N zones. Also responding well to the VTEM system are the ST97-15 and ST99-34 zones which were named during the course of the geophysical interpretation (see Figure 4); these 5 zones comprise the sole, unambiguous bedrock responses in the entire survey (Figure 9). The 3500N zone does not have a significant positive AEM response, but does lay right along the gradient edge from positive (extended and layered conductive zone) to negative response, apparently at the southern edge of the NW-trending graben. All of these conductive responses are distinguished by a complete lack of direct magnetic correlation.

Based on initial test modelling of selected lines, a consecutive series of 41 flight lines over the main Storm Copper zone were chosen for detailed resistivity depth imaging (RDI) by the airborne contractor. Results were provided as section images and grids for each line as well as a 3D voxel model of the apparent resistivity. These data were analyzed in 3D using Encom PA visualization and interpretation software. Analysis of the RDI inversions in conjunction with the historical drilling





dB/dt = $\frac{\text{Amplitude change of magnetic field}}{\text{Time it takes to make that change}}$

ASTON BAY VENTURES LTD.

Somerset Island, Nunavut, Canada

Storm Property
RDI clipped to 500 ohm-m

APEX Geoscience Ltd.
Edmonton, AB

Figure 12
October 10, 2012

suggests that there remain portions of the 4100N, ST97-15, ST99-34 and 2200N zones that have not been drill tested adequately. Figure 12 shows an inclined view of the voxel model clipped to 500 ohm-m for clarity and with the historic drillhole traces shown to illustrate the need for further drilling.

Furthermore, the deep (100 to 200 m below sea level) conductive trends shown to be extending southward from the 4100N zone have not been tested at all. Additional modeling of the VTEM data using the Maxwell plate modelling software should provide precise drill targeting for these bodies.

9.4 Surface Sampling & Mapping

The prospecting program confirmed the presence, location and extent of known historic zinc and copper mineralization at the Seal Zinc and Storm Copper showings, respectively and their correlation with geophysical anomalies. Rock grab samples were collected to verify historically reported values at the Seal Zinc and Storm Copper zones (Figure 13). A total of 14 rock grab samples were collected from the Storm Copper, Seal Zinc and from Seal Island (Figure 13). Two samples were collected from two discrete zones, 2750N and 2200N, within the overall Storm Copper zone, both assayed greater than 40% Cu. Six quartz arenite samples were collected along the trend of known mineralization at the Seal Zinc showing. Assays from the Seal zinc samples returned up to greater than 30% Zn. Copper and zinc over limit assays were still pending at the writing of this report. On Seal Island, areas of historically reported mineralized outcrops and anomalous assays were visited. Six samples were collected though none returned anomalous assays.

9.5 Historical Diamond Drill Core Resampling and Collar Surveying

A total of 399 drill core samples were collected from holes AB95-02, -03, -04, -05, -06, -07, -08, -10, -11, -12, and -13, and ST97-07, -08, -09, -10, and -11 (Appendix 4). The minimum sample length was 0.5 m, with a maximum sample length of 2.0 m, and an average sample length of 1.25 m. A summary of significant diamond drill sample composite length, weighted average grades is provided in Tables 7 and 8.

Diamond drill core samples were collected from historical drill core to fill in the gaps of unreported historic results. The sampling focused primarily on mineralized zones, and wherever possible, the original Cominco sample intervals were used. The majority of the drill core sampled in 2012 was previously sampled by Cominco, only half cores were remaining. The half core was again halved in order to obtain a representative (quarter core) sample over the desired intervals, while leaving a quarter core representative sample in the core box for further study if required. The samples were quartered using either a core splitter or a diamond bladed rock saw. For each sample, one quarter was left in its original position in the core box, on site, for future reference. The other quarter was placed, along with a numbered sample tag, into a labelled plastic sample bag, and sealed. Figure 14 shows the historic drillholes that were re-sampled during the 2012 exploration program.

In addition to resampling the previously sampled portions of the drill core, several samples were taken from previously un-sampled portions of the core. These samples were collected where copper mineralization was noted in visual examination of the core, and where shoulder samples were not collected around historic mineralized intervals, or where un-sampled intervals existed between mineralized zones. Approximately 30% of the previously un-split core which was sampled and assayed during 2012 yielded assay results in the 0.1 to 0.3% range for Cu.

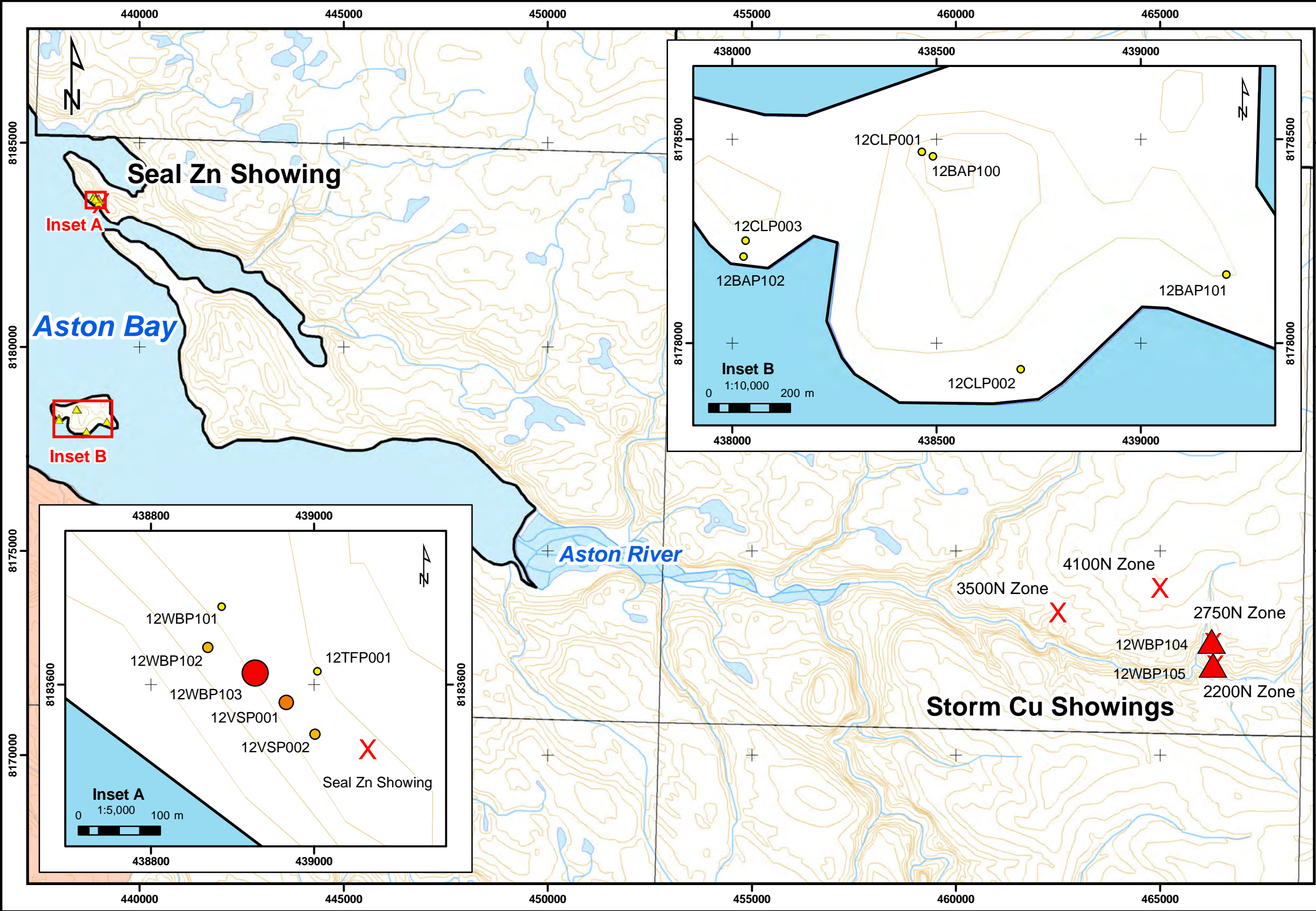
A total of eighty drillhole collars were located and re-surveyed using a handheld GPS unit. Seventeen of the holes were from the Seal Zinc showing, and sixty-three were from the Storm Copper showings. It was necessary to re-survey the drillholes as a discrepancy had been observed between locations reported by Cominco in assessment reports, and the actual locations of the collars in the field. There was some concern that the error in reported drillhole locations may have affected exploration results in the past. This is, however, unlikely as many of the historic drillholes were collared to intersect showings visible in outcrop, and in all likelihood, historic ground geophysical surveys and drill programs used the same local picketed grids for surveying and spotting drill collars.

Table 7 2012 Seal Zone Significant Assay Highlights From Historic Drill Holes

| Drill Hole ID | From (m) | To (m) | Length (m) | Zn (%) | Ag (g/t) |
|---------------|----------|--------|------------|--------|----------|
| AB95-02 | 51.8 | 70.6 | 18.8 | 8.46 | 24.2 |
| AB95-03 | 76.6 | 81 | 4.4 | 12.23 | 39.3 |
| AB95-03 | 88 | 101.7 | 13.7 | 6.74 | 34 |
| AB95-06 | 100 | 120.2 | 20.2 | 5.86 | 23.43 |
| AB95-06 | 127.3 | 134.5 | 7.2 | 3.71 | 30.18 |
| AB95-07 | 132 | 137 | 5 | 10.45 | 69.46 |
| AB95-10 | 140 | 146 | 6 | 1.76 | 30.98 |
| AB95-11 | 191 | 194 | 3 | 1.15 | 34.87 |
| AB95-11 | 203 | 208 | 5 | 1.79 | 53.58 |

Table 8 2012 Storm Prospect Significant Assay Highlights From Historic Drill Holes

| Drill Hole ID | From (m) | To (m) | Length (m) | Cu (%) |
|---------------|----------|--------|------------|--------|
| ST97-08 | 0 | 18.7 | 18.7 | 2.06 |
| ST97-08 | 25.2 | 58 | 32.8 | 3.78 |
| ST97-08 | 72 | 82.5 | 10.5 | 2.06 |
| ST97-09 | 62 | 86.5 | 24.5 | 2.03 |
| ST97-10 | 91.5 | 99 | 7.5 | 0.95 |



Legend

Showing

2012 Grab Samples
Cu (%)

- 0.000 - 0.099
- 0.100 - 0.999
- 1.000 - 4.999
- 5.000 - 39.999
- > 40.000

2012 Grab Samples
Zn (%)

- 0.000 - 0.099
- 0.100 - 0.999
- 1.000 - 4.999
- 5.000 - 29.999
- > 30.000

Contours

Rivers

Water Bodies

Storm Property Outline

Storm Prospecting Permits

Inuit Owned Land

ASTON BAY VENTURES LTD.

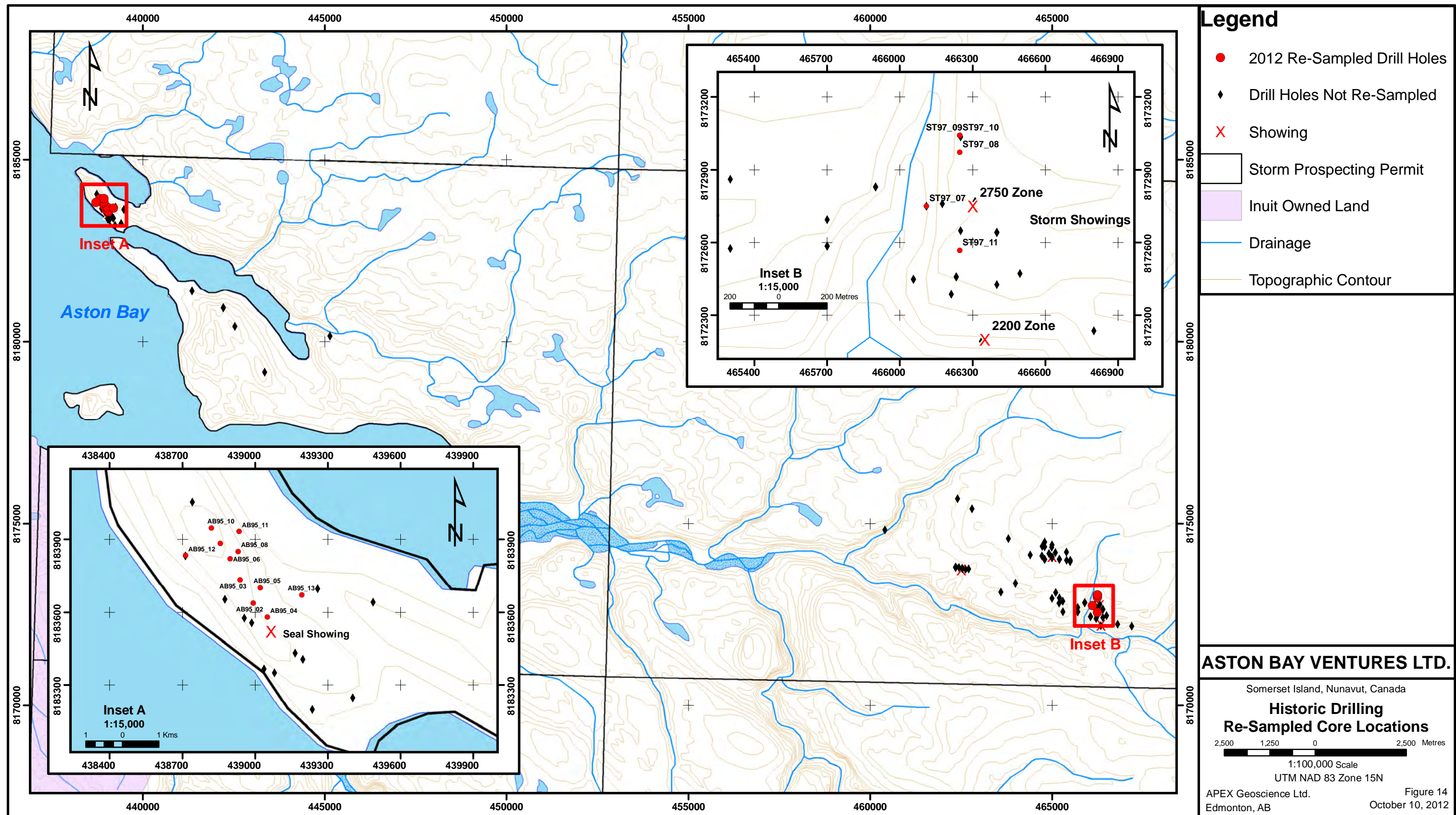
Somerset Island, Nunavut, Canada

2012 Grab Sample Locations

1:100,000
NAD 83 Zone 15N

APEX Geoscience Ltd.
Edmonton, AB

Figure 13
Oct 10, 2012



10: DRILLING

Previous drilling has been described and significant results listed in the History section. To date, Aston Bay Ventures Ltd. has not conducted any diamond drilling on the Storm Property

11: SAMPLE PREPARATION, ANALYSES AND SECURITY

11.1 Sample Collection and Shipping

Rock grab samples were collected from the Storm Copper and Seal Zinc showings and from Seal Island. The samples were described including by lithology, alteration, mineralogy, grain size, and texture. These observations were recorded in a fieldbook and later transcribed to an Excel spreadsheet (Appendix 3). The samples which were roughly fist-sized pieces of rock, each weighing no more than 5 kg, were placed into labelled plastic sample bags and sealed. Rock samples were collected such that the specimens represented the overall characteristics of mineralization from each particular location. Sample locations were recorded with a handheld GPS and marked with a labelled, representative sample in the field.

The drill core sampling focused primarily on mineralized zones, and wherever possible, the original Cominco sample intervals were used. The majority of the drill core intervals sampled in 2012 were previously sampled by Cominco resulting in only half cores remaining. The half core was again halved in order to obtain a representative (quarter core) sample over the desired intervals. In addition to resampling the previously sampled portions of the drill core, several samples were taken from previously un-sampled portions of the core. These samples were collected where copper mineralization was noted in visual examination of the core, and where shoulder samples were not collected around historic mineralized intervals, or where un-sampled intervals existed between mineralized zones. All sampled drill core was halved using either a core splitter or a diamond bladed rock saw. For each sample, half was left in its original position in the core box, on site, for future reference. The other half was placed, along with a numbered sample tag, into a labelled plastic sample bag, and sealed. The minimum sample length was 0.5 m, the maximum sample length was 2.0 m, and the average sample length was 1.25 m.

11.2 Sample Preparation, Analyses and Security

Individual rock grab and diamond drill core samples were placed into sealed plastic bags and then into poly woven (rice) bags for shipment to the independent laboratory immediately following collection. Numbered security tags were used to seal each rice bag prior to shipping. All rock samples were collected by APEX personnel and shipped to the ALS Minerals preparation lab in Yellowknife, NT.

Once received by ALS Minerals, rock and drill core samples were logged in to the ALS Minerals computerized tracking system and assigned bar code labels. Samples were dried prior to preparation and then crushed to pass a U.S. Standard No. 10 mesh, or 2 mm screen (70% minimum pass) using a mechanical jaw crusher. The samples were then split to 250 g using a riffle splitter, and sample splits were pulverized to pass a U.S. Standard No. 200 mesh, or 0.075 mm screen (85% minimum pass) using a steel ring mill (ALS Minerals, 2010).

The prepared samples were then shipped within the ALS Minerals network to the Vancouver Minerals Lab, located in North Vancouver, British Columbia. The Vancouver Minerals Lab facility is currently registered with ISO/IEC 17025:2005 accreditation from the Standards Council of Canada (SCC). ALS reported nothing unusual with respect to the shipment, once received. Security tags were reported to be intact and corresponded correctly with each bag of rock and drill core samples. The author did not have control over the samples at all times during transport, and therefore cannot personally verify what happened to the samples from shipping up to the time they were received by ALS. However, the author has no reason to believe that the security of the samples was compromised in any way once they entered the ALS chain of custody.

Rock grab sample pulps were subject to multi-element trace level analysis by Inductively Coupled Plasma - Atomic Emission Spectroscopy (ICP-AES) using nitric aqua regia digestion. A prepared sample is digested with aqua regia, diluted to 12.5 mL with deionized water, and analyzed by ICP-AES. The analytical results are corrected for inter-element spectral interference (ALS Minerals, 2009a). Samples that returned values greater than 100 ppm for Ag, and greater than 1% (10,000 ppm) Cu, Pb, or Zn were subjected to ore-grade (OG) ICP-AES analysis (ALS Minerals, 2009b). A prepared sample is digested with concentrated nitric acid and diluted with concentrated hydrochloric acid. The samples are then diluted with demineralized water in a 100 or 250 ml volumetric flask, and analyzed by ICP-AES or by atomic absorption spectrometry (AAS).

Diamond drill core sample pulps were subject to multi-element trace level analysis by ICP-AES using four acid digestion (ALS Minerals, 2009c). A prepared sample (0.25 g) is digested with perchloric, nitric, hydrofluoric, and hydrochloric acids. The residue is topped up with dilute hydrochloric acid and the resulting solution is analyzed by ICP-AES. Results are corrected for spectral interference. Samples that returned values greater than 100 ppm for Ag, and greater than 1% (10,000 ppm) Cu, Pb, or Zn were subjected to ore-grade (OG) element ICP-AES analysis (ALS Minerals, 2009b). A prepared sample is digested with nitric, perchloric, hydrofluoric, and hydrochloric acids, and then evaporated to incipient dryness. Hydrochloric acid and de-ionized water are added for further digestion, and the sample is heated for an additional allotted time. The sample is then cooled to room temperature and transferred to a 100 ml volumetric flask. The resulting solution is diluted to volume with de-ionized water, homogenized, and the solution is analyzed by ICP-AES or by ICP-AAS (ALS Minerals, 2009b).

12: DATA VERIFICATION

The authors conducted property visits to the Storm Property on August 4, 2012 (Mr. Robinson) and July 28 to August 3, 2012 (Mr. Atkinson) to supervise the 2012 exploration program and verify historical results. The authors visited the Seal, 2200N Zone, 2750N Zone, 3500N Zone, and 4100N Zone showings to verify the geology and mineralization reported at each showing. Rock grab samples were taken as samples to verify the mineralization at the Seal, 2200N Zone, and 2750N Zone showings. Additionally, the authors reviewed sections of mineralized drill core and collected drill core samples of several intervals which were historically reported to have anomalously high copper or zinc values.

At the ALS Minerals laboratory quality assurance and quality control (QA/QC) measures include routine screen tests to verify crushing and pulverizing efficiency, sample preparation duplicates (every 50 samples), and analytical quality controls (blanks, standards, and duplicates). Quality control samples are inserted with each analytical run, with the minimum number of QC samples dependant on the rack size specific to the chosen analytical method. Results for quality control samples that fall beyond the established limits are automatically red-flagged for serious failures and yellow-flagged for borderline results. Every batch of samples is subject to a dual approval and review process, both by the individual analyst and the Department Manager, before final approval and certification (ALS Minerals, 2012).

The QA/QC measures employed by APEX for the 2012 field program involved inserting blanks, analytical standards, and field duplicates in the diamond drill core sample stream. These QA/QC measures were completed as part of the drill core sampling program, prior to shipment to the laboratory, and are in addition to the normal QA/QC measures taken by the laboratory. Laboratory pulp standards inserted into the sample stream by APEX were compared to expected values, in order to ensure the lab results fell within the acceptable margin of error. Similarly, blanks were compared to expected values to ensure that contamination was not an issue.

It is the author's opinion that the sample preparation, security, analytical, and QA/QC procedures were more than adequate for this stage of exploration at the Storm Property.

Based on the property visit and the assay results, the authors have no reason to doubt the historic exploration results. Samples from the drill core yielded grade over width assays that were comparable to historically reported assays.

13: MINERAL PROCESSING AND METALLURGICAL TESTING

No mineral processing or metallurgical testing has been carried out by or on behalf of Aston Bay for the Storm property.

14: MINERAL RESOURCE ESTIMATES

Aston Bay has not yet produced a mineral resource estimate for the Storm property.

15: ADJACENT PROPERTIES

A group of eight contiguous prospecting permits abuts the property on the southern edge. These permits cover the eastern halves of NTS 1:50,000 map sheets 58C3 and 58C6, and the western halves of sheets 58C2 and 58C4. The northern block of four permits was issued in the name of David Dupre, and the southern four in the name of ColtStar Ventures (ColtStar). ColtStar refers to their permits as the Allen Bay property. The Nunavut Geoscience Nunavut minerals (NUMIN) database lists three showings on the ColtStar Allen Bay Property. These are the Peuyuk kimberlites, the Selatiavak kimberlite cluster, and the Typhoon zinc - lead showing. These showings have been the subject of sporadic exploration efforts in the past, but no diamonds or base metals of economic significance have been located.

16: OTHER RELEVANT DATA AND INFORMATION

The authors are not aware of any other information of a material nature relating to the Storm property. There is no information relating to the property, mineralization, metallurgical, environmental or social issues known to the authors not mentioned in this report.

17: INTERPRETATION AND CONCLUSIONS

The Storm Property is largely unexplored apart from the areas directly associated with the known showings. There have been several phases of airborne and ground geophysical surveying as well as a limited amount of diamond drilling. Of the 9000 m of drilling completed on the Storm showings, most were short holes (<150 m). Many of the mineralized zones intersected by drilling in the past are still open laterally and at depth, and none of the deeper VTEM anomalies have yet been drill tested. There has been some concern that the errors in the reported collar coordinates may have resulted in some of the holes not intersecting their intended targets, but this concern is probably overstated as discussed in section 9, above.

The remote location, challenging terrain and climate have thus far limited the effective determination of the size and characteristics of the Seal Zinc and Storm Copper ore bodies. At Seal Zinc, steep terrain makes it problematic to collar drill holes in the optimum locations for drill testing the stratabound mineralization. At Storm Copper, the majority of the mineralization in the largest zone is covered, or masked, by complexly faulted units lying within the Central Graben. Soil geochemistry, geophysical surveys and drilling results to date indicate that further work is warranted to outline and better define both showings.

Enhanced derivative grids of the airborne magnetic data were generated and imaged as part of the geophysical data reprocessing exercise and they have highlighted a limited number of structural orientations and trends. The aeromagnetic data is primarily reflecting very long wavelength, buried features believed to be sourced in the Proterozoic basement at some depth. A high-frequency, shallow component is however, evident throughout and is possibly related to detrital materials themselves related to variation in sea levels. Significant linear features are mapped based upon analysis of all of the derivatives. These are interpreted as most likely occurring within the sedimentary section (based on frequency content) and may be related to horizons equivalent to the known Storm Copper zones. These features are presented as possible structural controls impacting the stratiform sulphide mineralization (Campbell, 2011).

A comprehensive post-processing study carried out on the 2011 airborne VTEM data shows that the mineralized zones of the Storm deposit can be accurately mapped and modeled. The following is quoted from the Airborne Geophysical Interpretation Report by Christopher Campbell (Campbell, 2011) which is appended to this report and forms Appendix 2.

“Based on initial test modelling of selected lines, a consecutive series of 41 flight lines over the main Storm Copper zone were chosen for detailed resistivity depth imaging (RDI) by the airborne contractor; results were provided as section images and grids for each line as well as a 3D voxel model of the apparent resistivity. These data were analyzed in 3D using Encom PA (visualization and interpretation software). Analysis of the RDI inversions in conjunction with the historical drilling suggests that there remain portions of the 4100N, ST97-15, ST99-34 and 2200N Zones that have not been drill tested adequately. Further, the deep (100 to 200 m below sea level) conductive trends shown to be extending southward from the 4100N Zone have not been tested at all. Additional modeling of the VTEM data using the Maxwell plate modelling software should permit precise drill targeting for these bodies.”

An additional nine secondary anomalous areas were identified through inversion modeling of the VTEM data (Figure 15). These zones do not have characteristics similar to those of the main Storm deposits, but do represent areas of surficial or near surface conductivity, and merit further exploration.

In 2012, the resampling of historic drill core covered drill core intervals for which detailed sample data are unavailable. Comparison of the assay results from the 2012 resampling program against sample intervals mentioned in other reports and documents shows that the 2012 results (grade over width) are comparable to the historic data. It was not possible to perform statistical analyses on the sample sets due to sample intervals not exactly coinciding with historical sample intervals. Table 9 provides a comparison between historic and recent assay results. Prospecting in 2012 confirmed the location and surficial extent of historic mineralized zones at the Seal Zinc and Storm Copper showings. The 2012 rock grab samples from these areas returned highly anomalous results >30% Zn (Seal Zinc) and >40% Cu (Storm Copper). Overlimit assay results for these samples are still pending.

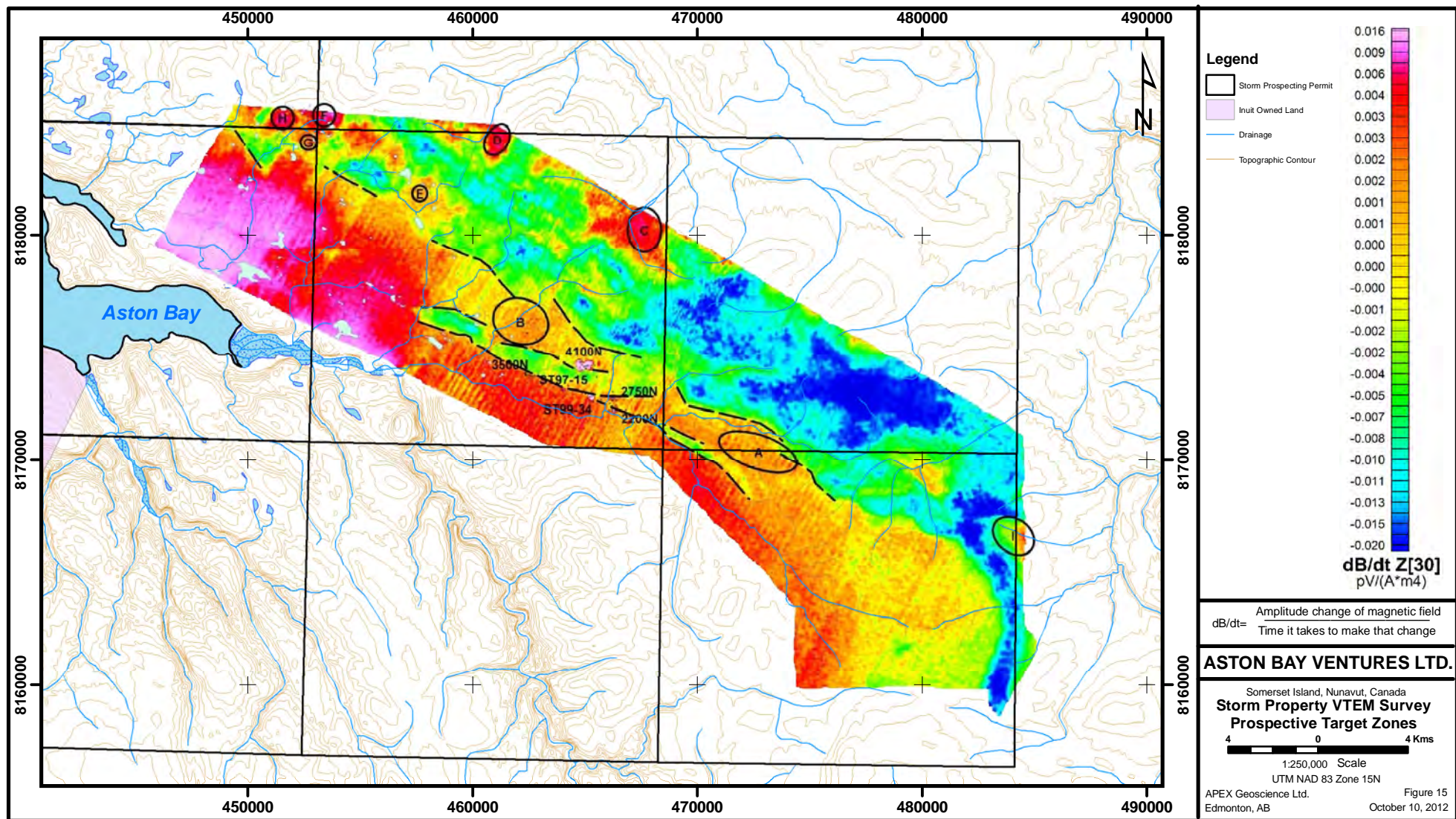


Table 9 Comparison of Historic to 2012 Assay Results for Selected Intervals

| Drill Hole | From (m) | To (m) | Length (m) | Ag (ppm) | | Zn (%) | |
|------------|----------|--------|------------|----------|-------|--------|-------|
| | | | | Hist | 2012 | Hist | 2012 |
| AB95-02 | 51.8 | 63 | 11.2 | 33.90 | 25.20 | 14.82 | 9.24 |
| AB95-02 | 65 | 70.6 | 5.6 | 39.53 | 35.10 | 11.58 | 10.53 |
| | | | | | | | |
| Drill Hole | From (m) | To (m) | Length (m) | Ag (ppm) | | Cu (%) | |
| | | | | Hist | 2012 | Hist | 2012 |
| ST97-08 | 5 | 110 | 105 | 4.95 | 3.40 | 2.92 | 2.09 |
| including | 5 | 58 | 53 | 5.66 | 4.20 | 5.09 | 3.18 |
| including | 27.8 | 29.1 | 1.3 | 14.80 | 21.90 | 18.74 | 13.65 |
| and | 50.3 | 54 | 3.7 | 2.68 | 4.20 | 14.68 | 9.67 |
| and | 72.5 | 82 | 9.5 | 7.82 | 5.20 | 4.04 | 1.98 |

18: RECOMMENDATIONS

Analysis of the RDI inversions on the airborne VTEM data, in conjunction with the historical drilling suggests that there are portions of the 4100N, ST97-15, ST99-34 and 2200N zones that have not been tested adequately by drilling. In addition, the deep (100 to 200 m below sea level) conductive trends shown to be extending southward from the 4100N zone have not been tested at all. Further modeling of the VTEM data using the Maxwell plate modelling software should be completed over the winter to precisely identify drill targets in the underexplored areas in and near the VTEM anomalies at the Storm deposit.

In addition to the known showings and their possible extensions, there are nine other areas of interest identified by examination of the geophysical data (Campbell, 2011). These targets do not have characteristics similar to the main Storm zones discussed above, but nonetheless present themselves as possible areas for ground follow-up and geochemical sampling. They may reflect sulphides deficient in copper, or sulphides dominant in zinc and/or lead mineralization and thus not amenable to direct detection by electromagnetic methods.

A program of geological prospecting, sampling and ground geophysics consisting of 3D induced polarization/resistivity is recommended to further delineate the conductive zones and possibly identify disseminated sulphides which in turn could indicate anomalous Cu mineralization. A reasonable Stage 1 exploration plan for the short term should entail a multi-faceted program to produce a resource estimate for the Seal Zinc deposit and good follow-up drill targets for a subsequent diamond drill program on the Storm Copper showings (Table 10). The original Seal drilling data should be acquired from Teck along with follow-up geological and engineering studies leading to a NI 43-101 compliant mineral resource for the prospect.

Table 10 Estimated cost to conduct Stage 1 and 2 exploration programs during 2013

| Item | Unit Cost | Units | Subtotal |
|--|-------------|---------|--------------------|
| 1 Stage 1: | | | |
| Accommodation: Camp, Food & Supplies | \$195,000 | 1 | \$195,000 |
| Geological Personnel & Camp Management | \$160,000 | 1 | \$160,000 |
| Geophysics Crew & Equipment | \$70,000 | 1 | \$70,000 |
| Fixed-Wing Aircraft Support | \$370,000 | 1 | \$370,000 |
| Includes Buffalo & Twin Otter mobilization of camp, supplies, fuel, weekly support & demob | | | |
| Helicopter | \$1,600 | 125 | \$200,000 |
| Fuel | \$35,000 | 1 | \$35,000 |
| Includes diesel, Jet A and propane | | | |
| Sample Assays: Core & Surface | \$35.00 | 600 | \$20,000 |
| Engineering & Environmental Studies | \$50,000 | 1 | \$50,000 |
| Administration, Reporting, Fees & Contingency | \$100,000 | 1 | \$100,000 |
| TOTAL STAGE 1 COSTS | | | \$1,200,000 |
| 2 Stage 2: | | | |
| Accommodation: Camp, Food & Supplies | \$95,000 | 1 | \$95,000 |
| Geological Personnel & Camp Management | \$80,000 | 1 | \$80,000 |
| Fixed-Wing Aircraft Support | \$315,000 | 1 | \$315,000 |
| Includes Buffalo & Twin Otter mobilization of camp, supplies, fuel, weekly support & demob | | | |
| Helicopter | \$1,800 | 105 | \$190,000 |
| Fuel | \$45,000 | 1 | \$45,000 |
| Includes diesel, Jet A and propane | | | |
| Drilling 1,200 m | \$175/m | 1200 | \$210,000 |
| Includes all drilling contract costs, including mob-demob meterage cost and man-hours | | | |
| Sample Assays: Core | \$35.00 | 1000 | \$35,000 |
| Engineering, Resource Studies & Tech Report | \$40,000 | 1 | \$40,000 |
| Administration, Reporting, Fees & Contingency | \$83,000 | 1 | \$90,000 |
| TOTAL STAGE 2 COSTS | | | \$1,100,000 |

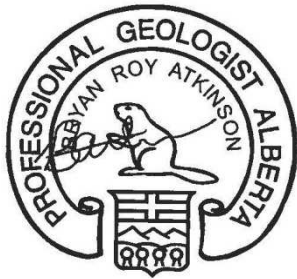
Concurrent with the Seal planned work, exploration for the Storm showings should comprise; the completion of the reprocessing of the airborne VTEM data using the Maxwell plate modelling software, ground electromagnetic, magnetic and induced polarization surveying, and prospecting, mapping and geochemical sampling. This program is recommended to further delineate the conductive zones and

possibly identify disseminated sulphides which in turn could indicate additional anomalous Cu mineralization. This Stage 1 program is estimated at \$1,200,000 (not including GST) and would result in the location and prioritization of prospective targets to be drilled at the Seal and Storm areas in a subsequent Stage 2 program (Table 10). Table 10 provides a best estimate of costs associated with the proposed, Stage 1 exploration program. It is anticipated that a follow-up Stage 2 drilling program could also be completed during 2013. A program of 1,200 m of diamond drilling tagged onto the Stage 1 field based exploration program is estimated at \$1,100,000 not including GST (Table 10). However, the Stage 2 drilling program is contingent upon the results of the Stage 1 field work.

Aurora Geosciences Ltd.



Jim Robinson, B.Sc., P.Geol.



Bryan Atkinson, B.Sc., P.Geol.

19 REFERENCES

ALS Minerals, 2012: Quality Management System ISO/IEC 17025:2005 & ISO 9001:2008. Minerals Technical Notes, 4 pp.

ALS Minerals, 2010: Standard Sample Preparation: Dry, Crush, Split and Pulverize. ALS Method Descriptions, Code PREP-31, 2 pp.

ALS Minerals, 2009a: Trace Level Methods Using Conventional ICP-AES Analysis (Nitric Aqua Regia Digestion). ALS Method Descriptions, Code ME-ICP41, 3 pp.

ALS Minerals, 2009b: Ore Grade Elements by Aqua Regia Digestion Using Conventional ICP-AES Analysis (HNO₃-HCl Digestion). ALS Method Descriptions, Code ME-OG46, 1 p.

ALS Minerals, 2009c: Trace Level Methods Using Conventional ICP-AES Analysis (HNO₃-HClO₄-HF-HCl Digestion). ALS Method Descriptions, Code ME-ICP61, 3 pp.

Aboriginal Affairs and Northern Development Canada, 2012: SID viewer; Commander prospecting permits <<http://ism-sid.inac.gc.ca/website/sidvh1/viewer.htm>> [July, 2012]. Online Federal Government mineral tenure database website.

Aulstead, K.L., Spencer, R.J., and Krouse, H.R., 1988: Fluid inclusion and isotopic evidence on dolomitization, Devonian of Western Canada: *Geochimica et Cosmochimica Acta*, v. 52, pp. 1027-1035.

Bethke, C.M., and Marshak, S., 1990: Brine migrations across North America the plate tectonics of groundwater: *Annual Review of Earth and Planetary Science*, v. 18, pp. 287–315.

Campbell, C., 2011: Airborne Geophysical Interpretation of the Storm Copper Property, Somerset Island, Qikiqtaaluk (Baffin) Region, Nunavut: Intrepid Geophysics Ltd., Unpublished Report, 111pp.

Cannuli, M.E. and Olson, R.A., 1978. Esso Minerals Canada, Exploration - 1978, Somerset Island and Prince of Wales Island, Arctic & Hudson Bay Mining District, NWT. Trigg, Woollett Consulting Ltd., Assessment Report 061797.

Cathles, L.M., and Smith, A.T., 1983: Thermal constraints on the formation of Mississippi Valley-type lead-zinc deposits and their implications for episodic basin dewatering and deposit genesis: *Economic Geology*, v. 78, pp. 983-1002.

Chi, G. and Savard, M., 2001: Mississippi Valley-type Zn-Pb Mineralization in Northern Cornwallis Fold Belt – Genetic Relationship between Ore-forming Fluids in Different Occurrences. Technical paper presented at Minespace 2001, Quebec CIM Technical Paper Library:

<http://www.cim.org/en/Publications-and-Technical-Resources/Publications/Technical_Papers.aspx>, [October, 2012]

Cook, B. and Moreton, C., 2009: Technical Report on the Storm Copper Project, Somerset Island, Nunavut, Canada: NI 43-101 Technical Report, 96 pp.

DeFreitas, T., Trettin, O. and Mallamo, M., 1999: Silurian System of the Canadian Arctic Archipelago. *Bulleting of Canadian Petroleum Geology*, v. 47, no. 2, pp. 136-193.

Dewing, K. and Turner, E.C., 2003: Structural setting of the Cornwallis lead-zinc district, Arctic Islands, Nunavut. *Geological Survey of Canada, Current Research 2003-B4*, 9 pp.

Dewing, K., Sharp, R. and Muraro, T., 2006: Exploration History and Mineral Potential of the Central Arctic Zn-Pb District, Nunavut. *The Arctic Institute of North America*, v. 59, no. 4, pp. 415– 427.

Dooley, T. and McLay, K., 1997: Analog modeling of pull-apart basins. *AAPG Bulletin* v. 81, No. 11, pp. 1804-1826.

Environment Canada Sea Ice Climatic Atlas 1981-2010, <http://www.ec.gc.ca/glaces-ice/default.asp?lang=En&n=090AF7D6-1>, 2012

Garven, G., 1985: The role of regional fluid flow in the genesis of the Pine Point deposit, Western Canada Sedimentary Basin. *Economic Geology*, v. 80, pp. 307-324.

Garven, G., and Freeze, R.A., 1984: Theoretical analysis of the role of groundwater flow in the genesis of stratabound ore deposits. 2. Quantitative results: *American Journal of Science*, v. 284, pp. 1125-1174.

Garven, G. and Raffensperger, J.P., 1997: Hydrogeology and geochemistry of ore genesis in sedimentary basins, *in* Barnes, H.L., ed., *Geochemistry of Hydrothermal Ore Deposits*, 3rd ed. New York, John Wiley and Sons, pp. 125–189.

Grextan, L. 2009: Storm Property, Somerset Island, Nunavut: Commander Resources Inc., Prospecting Permits 7547, 7548, 7549: Nunavut Mineral Assessment Report, 38 pp.

Guest, B., Hill, M. and Beauchamp, B., 2011: The Arctic Eureka Orogen: A plate tectonic conundrum. *Proceedings with Abstracts, American Geophysical Union, Fall 2011 Meeting*.

Heaman, L.M., LeCheminant, A.N. and Rainbird, R.H., 1992: Nature and timing of Franklin igneous events, Canada: Implications for a Late Proterozoic mantle plume and the break-up of Laurentia. *Earth and Planetary Science Letters*, v. 109 pp. 117-131.

Jackson, S.A., and Beales, F.W., 1967: An aspect of sedimentary basin evolution: The concentration of Mississippi Valley-type ores during the late stages of diagenesis. *Bulletin of Canadian Petroleum Geology*, v. 15, pp. 393-433.

Kerr, J. and DeVries, C., 1977: Structural Geology of Somerset Island and Boothia Peninsula, District of Franklin. Geological Survey of Canada, Paper 77-1A, pp. 107-111.

Leach, D.L., and Sangster, D.F., 1993: Mississippi Valley-type lead-zinc deposits, *in* Kirkham, R. V., Sinclair, W.D., Thorpe, R.I., and Duke, J.M., *eds.*, Mineral Deposit Modeling. Geological Association of Canada, Special Paper 40, pp. 289-314.

Leach, D., Taylor, D., Fey, D., Diehl, S., and Saltus, R., 2010: A Deposit Model for Mississippi Valley-Type Lead-Zinc Ores, Chap. A of Mineral Deposit Models for Resource Assessment. U.S. Geological Survey Scientific Investigations Report 2010-5070-A, 52 p.

LeCheminant, A.N. and Heaman, L.M., 1989: Mackenzie igneous events, Canada: Middle Proterozoic hotspot magmatism associated with ocean opening. *Earth and Planetary Science Letters*, v. 96 pp. 38-48.

Leigh, K.E. 1999: Geochemical and Geophysical Report on Claims Storm 1, 10, 12, 13, 18, 61, 62, 66, 75, 76 & 78. Cominco Ltd., Assessment Report 084241.

Leigh, K.E. 1998a: Geochemical and Geophysical Report on Claims Storm 1-44 and Seal 17, 1998. Cominco Ltd., Assessment Report 084128.

Leigh, 1998b: Geochemical Report on Claims Seal 1, Seal 11, Seal 15 and Seal 17. Cominco Ltd., Assessment Report 084108.

Leigh, K.E., 1996a: Aston Bay Diamond Drilling Assessment Report. Cominco Ltd., Assessment Report 083763.

Leigh, K.E., 1996b: Aston Bay Soil Geochemistry 1995 Assessment Report. Cominco Ltd., Assessment Report 083762.

Leigh, K.E., 1995: Assessment Report, Heavy Mineral Geochemical Survey, Aston Bay, Somerset Island, Claims Ast, Sound, Row, Par, Peel, Bay 1-3, Ton, Seal 1-12 and PP. 1491; 1492. Cominco Ltd., Assessment Report 083423.

Leigh, K.E. and Lajoie, J.J., 1999. Geophysical Report on the 1997 IP/Res Survey on Claims Storm 1, Storm 2 and Storm 3. Cominco Ltd., Assessment Report 084112.

Leigh, K. E. and Reid, C.J., 1998: Storm Year-End Report 1997, Somerset Island, Storm Property Technical Report

Nunavut Territory, NTS 58-C-11: Internal report Cominco Ltd., 30 pp., 1 Appendix.

Leigh, K.E. and Tisdale, D.L., 1999: Diamond Drilling Report on Claims Storm 1-15, 17-33, 40-42, 45-55, 57-59, 61-63, 65-67, 69-70, 73, 75-76, 78-79, 81-82 & 84-85. Cominco Ltd., Assessment Report 084243.

Leigh, K.E. and Tisdale, D.L., 2000: Year-End Report Storm Project; Internal Report Cominco Ltd., 20 pp.

MacRobbie, P., Hall, D., Rees, M. and Smith, A., 2000: Storm Property, 2000 Assessment Report: Airborne Electromagnetic and Magnetic Surveys, Ground Geophysical Surveys, Diamond Drilling, Regional Geological Mapping/Prospecting and Soil Geochemical Surveys. Cominco Ltd., Assessment Report 084328.

Morrow, D., 1998: Regional subsurface dolomitization; Models and constraints. Geoscience Canada, v. 25, pp. 57-70.

Morrow, D.W., Cumming, G.L., and Aulstead, K.L., 1990: The Gas-Bearing Devonian Manetoe Facies, Yukon and Northwest Territories. Geological Survey of Canada, Bulletin 400, 54 pp.

Neale, K.F. and Campbell, D.L., 1970. Report on Metallic Mineral Survey, Canadian Arctic Islands, 1970 Field Season. J.C. Sproule & Associates, Assessment Report 081987.

Nelson, J., Paradis, S., Christensen, J., and Gabites, J., 2002: Canadian Cordilleran Mississippi Valley-type deposits: A case for Devonian-Mississippian back-arc hydrothermal origin. Economic Geology, v. 97, pp. 1013-1036.

Nunavut Geoscience Nunavut Mineral (NUMIN) Database,
<<http://nunavutgeoscience.ca/apps/showing/showQuery.php>>, [October 2012]

O'Connor, K. 1997: High Resolution Airborne Geophysical Survey, Somerset Island NWT, Canada. Sanders Geophysics Ltd. for Cominco Ltd., Assessment Report 083920.

Okulitch, A., Packard, J. and Zolnai, A., 1985: Evolution of the Boothia Uplift, Arctic Canada. Canadian Journal of Earth Sciences, v. 23, no. 3, pp. 350-358.

Oliver, J., 1986: Fluids expelled tectonically from orogenic belts: Their role in hydrocarbon migration and other geologic phenomena. Geology, v. 14, pp. 99-102.

Packard, J. J., and Dixon, O. A., 1987: Tectonism and an Upper Silurian ramp-prodelta-rimmed shelf succession from Arctic Canada: An intracratonic product of Caledonian Compression. Program with Abstracts, AAPG Convention.

Sharp, J., 1978: Energy and momentum transport model of the Ouachita basin and its possible impact on formation of economic mineral deposits. *Economic Geology*, v. 73, pp. 1057-1068.

Smith, A., 2001: Storm-Seal Property, 2001 Assessment Report: Diamond Drilling and Regional Prospecting, Storm Claims: 53, 75, 76, 103 & 104; Aston Claims: Peel. Noranda Inc., Assessment Report 084444.

Smith, P.M., 1995: Assessment Report on 1994 Summer Field Work: Aston Bay Geology, Geochemistry, Geophysics and Mineralization. Cominco Ltd., Assessment Report 083570.

Smith, C.B., Allsopp, H.L., Garvie, O.G., Kramers, J.D., Jackson, P.F.S. and Clement, C.R., 1989: Note on the U-Pb perovskite method for dating kimberlites: Examples from the Wesselton and DeBeers Mines, South Africa, and Somerset Island, Canada. *Chemical Geology (Isotope Section)*, vol. 79, pp. 137-145.

Whaley, K.D.A., 1975: Cominco Ltd., Astec Property, Pat 1-10. Cominco Ltd., Assessment Report 061365.

Wu, F.-Y., Yang, Y.-H., Mitchell, R.H., Li, Q.-L., Yang, Q.-L. and Zhang, Y.-B., 2010: In site U-Pb age determination and Nd isotopic analysis of perovskites from kimberlites in southern Africa and Somerset Island, Canada. *Lithos*, vol. 115, pp. 205-222.

Appendix 1

Aston Bay APEX Costs 2011-2012

APEX Geoscience Ltd.
Profit & Loss Detail
January 2011 through December 2012

| Type | Date | Num | Memo | Amount |
|-------------------------------------|---|---------|---|-----------|
| Ordinary Income/Expense | | | | |
| Income | | | | |
| 4010 - Principals Directly Involved | | | | |
| | Total 4016 - Michael Dufresne - field | Invoice | Principal Directly Involved Field - Michael Dufresne (June 22-Aug 21/12) | 8,075.00 |
| | Total 4016 - Michael Dufresne - field | Invoice | Principal Directly Involved Office - Michael Dufresne (Sept 22/11-Oct 21/12) | 18,819.00 |
| | Total 4010 - Principals Directly Involved | | | 26,894.00 |
| 4020 - Geological field work | | | | |
| | Invoice | | Geological Services Performed Field - Warren Black (June 22-Aug 21/12) | 7,225.00 |
| | Invoice | | Geological Services Performed Field - Valene Sathiakanthan (June 22-Aug 21/12) | 7,225.00 |
| | Invoice | | Geological Services Performed Field - Travis Fulton (June 22-Aug 21/12) | 5,950.00 |
| | Invoice | | Geological Services Performed Field - Chris Livingstone (June 22-Aug 21/12) | 8,075.00 |
| | Invoice | | Geological Services Performed Field - Bryan Atkinson (July 22-Aug 21/12) | 6,500.00 |
| | Invoice | | Geological Services Performed Field - Perry Hohn (July 22-Aug 21/12) | 4,500.00 |
| | Total 4020 - Geological field work | | | 39,475.00 |
| 4030 - Geological office work | | | | |
| | Invoice | | Geological Services Performed Office - Amelie Dufresne (April 22-June 21/12) | 637.00 |
| | Invoice | | Geological Services Performed Office - Andrea De Stefano (May 22-June 21/12) | 1,452.75 |
| | Invoice | | Geological Services Performed Office - Andrew Turner Nov 22/11-July 21/12) | 1,821.25 |
| | Invoice | | Geological Services Performed Office - Anetta Banas (April 22-July 21/12) | 385.25 |
| | Invoice | | Geological Services Performed Office - Bryan Atkinson (June 22-Sept 21/12) | 5,785.00 |
| | Invoice | | Geological Services Performed Office - Casey Lunn (March 22-June 21/12) | 3,854.75 |
| | Invoice | | Geological Services Performed Office - Chris Atkins (Jan 1-July 21/12) | 3,334.50 |
| | Invoice | | Geological Services Performed Office - Chris Livingstone (Jan 1-Sept 21/12) | 22,122.75 |
| | Invoice | | Geological Services Performed Office - Eemeli Rantala (Oct 22/11-June 21/12) | 588.00 |
| | Invoice | | Geological Services Performed Office - Emily Laycock (March 22-April 21/12) | 1,537.25 |
| | Invoice | | Geological Services Performed Office - Godwin Mollel (June 22-Aug 21/12) | 4,595.50 |
| | Invoice | | Geological Services Performed Office - Josh Malkin (June 22-Aug 21/12) | 1,365.00 |
| | Invoice | | Geological Services Performed Office - Katie Salter (June 22-Aug 21/12) | 2,190.50 |
| | Invoice | | Geological Services Performed Office - Kevin Hon (June 22-July 21/12) | 720.00 |
| | Invoice | | Geological Services Performed Office - Kris Raffle (Oct 22-Aug 21/12) | 8,594.75 |
| | Invoice | | Geological Services Performed Office - Landon Mutch (July 22-Aug 21/12) | 100.00 |
| | Invoice | | Geological Services Performed Office - Mark Hanki (May 22-July 21/12) | 525.00 |
| | Invoice | | Geological Services Performed Office - Mollie McGrath (Jan 1-Feb 21/12) | 792.00 |
| | Invoice | | Geological Services Performed Office - Neil Krystowicz (June 22-July 21/12) | 450.00 |
| | Invoice | | Geological Services Performed Office - Nicole Rudolph (June 22-July 21/12) | 540.00 |
| | Invoice | | Geological Services Performed Office - Perry Hohn (July 22-Aug 21/12) | 42.25 |
| | Invoice | | Geological Services Performed Office - Philo Schoeman (April 22-June 21/12) | 1,028.50 |
| | Invoice | | Geological Services Performed Office - Rachelle Hough (Nov 22-Dec 21/11) | 28.00 |
| | Invoice | | Geological Services Performed Office - Roy Eccles (March 22-April 21/12) | 115.50 |
| | Invoice | | Geological Services Performed Office - Tara Gunson (Nov 22-Sept 21/12) | 2,089.50 |
| | Invoice | | Geological Services Performed Office - Travis Fulton (June 22-July 21/12) | 67.50 |
| | Invoice | | Geological Services Performed Office - Valene Sathiakanthan (June 22-Aug 21/12) | 1,161.00 |
| | Invoice | | Geological Services Performed Office - Warren Black (May 22-Aug 21/12) | 357.50 |
| | Invoice | | Geological Services Performed Office - Yuliana Proenza (Oct 22/11-June 21/12) | 5,384.00 |
| | Total 4030 - Geological office work | | | 71,665.00 |

APEX Geoscience Ltd.
Profit & Loss Detail
January 2011 through December 2012

| Type | Date | Num | Memo | Amount |
|--|---------|-----|--|------------|
| 4060 · HR & Safety | | | | |
| Total 4060 · HR & Safety | Invoice | | Human Resource and Safety Services Office - Sean Hawkes (June 22-Aug 21/12) | 207.75 |
| 4070 · Overhead & management fee | | | | |
| Total 4070 · Overhead & management fee | Invoice | | Operator's overhead and management fees (Nov 2011 to Oct 2012) | 15,000.28 |
| 4080 · Rentals & other project income | | | | |
| Total 4080 · Rentals & other project income | Invoice | | APEX rentals, accomodations, miscellaneous field equipment & supplies | 3,650.00 |
| 5000 · Third Party Reimbursable Income | | | | |
| 5010 · Assays & related costs 6010 | | | | |
| Total 5010 · Assays & related costs 6010 | Invoice | | ALS Canada: assay analysis 2012 Field Work | 10,877.94 |
| 5080 · Field supplies 6080 | | | | |
| Total 5080 · Field supplies 6080 | Invoice | | Field Supplies | 4,323.62 |
| 5110 · Freight - other 6110 | | | | |
| Total 5110 · Freight - other 6110 | Invoice | | Freight | 1,787.54 |
| 5260 · Rental - equipment 6260 | | | | |
| Total 5260 · Rental - equipment 6260 | Invoice | | Equipment Rentals | 764.00 |
| 5340 · Subcontract - consulting 6340 | | | | |
| | Invoice | | Geological Services Performed Office - Fred Welke (June 1-15/12) | 287.50 |
| | Invoice | | Intrepid Geophysics: geophysical consulting, June/12, inv 12-1426 | 250.00 |
| | Invoice | | Geological Services Performed Office - Steven Nicholls Micromine Modelling | 3,170.50 |
| Total 5340 · Subcontract - consulting 6340 | | | | 3,708.00 |
| 5360 · Subcontract other 6360 | | | | |
| Total 5360 · Subcontract other 6360 | | | Discovery Mining: expediting services, July & August 2012 | 980.00 |
| 5430 · Travel - accomodations 6430 | | | | |
| | Invoice | | Various Hotels - Vancouver, Yellowknife, Baker Lake etc | 4,106.99 |
| | Invoice | | Canadian Arctic Holidays: Field Accomodations & Food | 39,550.00 |
| Total 5430 · Travel - accomodations 6430 | | | | 43,656.99 |
| 5440 · Travel - airfare 6440 | | | | |
| | Invoice | | Various Airfares Field Crew to YK & Flights to Vancouver | 17,273.10 |
| | Invoice | | Canadian Arctic Holidays: Airfare, Freight July - Aug, 2012 - Yellowknife - Sommerset Island | 37,000.00 |
| | Invoice | | 953731 NWT Ltd: Dash 8 Charter, Somerset Island/Yellowknife, Aug 7/12 | 7,000.00 |
| | Invoice | | Great Slave Helicopters: airfare, July 17-Aug 5/12 | 117,427.70 |
| Total 5440 · Travel - airfare 6440 | | | | 178,700.80 |
| 5450 · Travel - food 6450 | | | | |
| Total 5450 · Travel - food 6450 | Invoice | | Various Meals Travel, Vancouver, Edmonton, Field | 2,918.54 |
| 5460 · Travel - fuel 6460 | | | | |
| | Invoice | | Other Travel | 115.00 |
| | Invoice | | Great Slave Helicopters: fuel, July 17-19/12, inv 61541 | 11,419.66 |
| Total 5460 · Travel - fuel 6460 | | | | 11,535.56 |

APEX Geoscience Ltd.
Profit & Loss Detail
January 2011 through December 2012

| | Type | Date | Num | Memo | Amount |
|--|---------|------------|----------|--|------------|
| 5470 - Taxi, parking & other 6470 | | | | | |
| Total 5470 - Taxi, parking & other 6470 | Invoice | | | Taxi, Parking & Other Travel | 1,638.31 |
| 5570 - Bank charges & interest 6570 | | | | | |
| Total 5570 - Bank charges & interest 6570 | Invoice | | | Wire Transfer Fees | 25.00 |
| 5610 - Computer supplies & software 6610 | | | | | |
| Total 5610 - Computer supplies & software 6610 | Invoice | | | Dangotec Solutions | 3,008.00 |
| 5690 - Licenses, permits & fees 6690 | | | | | |
| Total 5690 - Licenses, permits & fees 6690 | Invoice | | | Nunavut Water Board Fees | 92.05 |
| 5830 - Professional fees 6830 | | | | | |
| Total 5830 - Professional fees 6830 | Invoice | | | Tukilik Translation: Inuktitut translation, June/12, inv 1186 | 50.00 |
| 5930 - Telephone 6930 | | | | | |
| Total 5930 - Telephone 6930 | Invoice | | | Allstream LD and Telus Cell Phone Charges | 283.69 |
| Total 5000 - Third Party Reimbursable Income | | | | | 283,000.32 |
| Total Eligible APEX Expenses | | | | | 421,242.07 |
| Other Eligible Expenses | | | | | |
| Oren Inc | | | | | |
| | | | | MD Benjamin Cox Office and Fieldwork: 4 months @ \$2500/mth | 10,000.00 |
| | | | | Oren Inc. Other Employees: 4 months @ \$3500/mth | 14,000.00 |
| | | | | Airfare and Travel | 2,000.00 |
| Total - Oren Inc. Expenses | | | | | 26,000.00 |
| Total Eligible Project Expenses | | | | | 447,242.07 |
| Ineligible Expenses | | | | | |
| 5690 - Licenses, permits & fees 6690 | | | | | |
| | Invoice | 03/20/2012 | 2012-100 | Mining Recorder: prospecting permit applications, Nov 29/11 | 21,708.14 |
| | Invoice | 05/31/2012 | 2012-248 | Government of Canada: refund, Aston Bay Ventures prospecting permits, Storm project, May 30/12 | (3,894.52) |
| | Invoice | 09/30/2012 | 2012-507 | Receiver General: mineral claims, Sept 10/12 | 11,363.24 |
| Total 5690 - Licenses, permits & fees 6690 | | | | | 29,176.86 |
| 5830 - Professional fees 6830 | | | | | |
| | Invoice | 04/30/2012 | 2012-185 | Edwards, Kenny & Bray LLP: legal services, Aston Bay Ventures, Jan/12 | 5,896.20 |
| | Invoice | 04/30/2012 | 2012-185 | Edwards, Kenny & Bray LLP: legal services, Aston Bay Ventures, Feb/12 | 1,941.20 |
| | Invoice | 04/30/2012 | 2012-185 | Edwards, Kenny & Bray LLP: legal services, Aston Bay Ventures, March/12 | 2,099.28 |
| Total 5830 - Professional fees 6830 | | | | | 9,936.68 |
| Total Ineligible Expenses | | | | | 39,113.54 |

Appendix 2

Airborne Geophysical Interpretation of the Storm Copper Property

Airborne Geophysical Interpretation

of the

Storm Copper Property

**Somerset Island
Qikiqtaaluk (Baffin) Region, Nunavut**

NTS Map Sheets 058C/10–11 & 058C/14–15

for



by



Christopher Campbell, P. Geo.
November 18, 2011

4505 Cove Cliff Road
North Vancouver, BC
Canada V7G 1H7

Project no.10-247-CMD

Summary

A helicopter-borne electromagnetic and magnetic survey was flown by Geotech Ltd. in July 2011 over the Storm Copper Property on Somerset Island ~120 kilometres south-southeast of Resolute Bay. The survey is comprised of ~3,970 line-kilometres of data acquired on a grid pattern of 300 and 150 m spaced traverses oriented at N030°E, controlled by 1,500 m spaced tie lines oriented at right angles toward N120°E. The electromagnetic technology utilized is Geotech's *VTEM Plus* time-domain system in a towed-loop configuration. Products obtained from this airborne geophysical survey include the total magnetic intensity, calculated (magnetic) vertical derivative, dB/dt and B-field both X- and Z-components, both dB/dt and B-field calculated Time Constants Tau, and a digital elevation model. Resistivity depth imaging (RDI) sections and apparent resistivity depth slices were also subsequently supplied as part of the interpretation phase of this project. A geosoft-format database of the profile data, as well as grids of total magnetic intensity, calculated vertical derivative, a single mid-time B-field Z-axis component, dB/dt and B-field time constants and the digital elevation model were provided by the contractor.

Enhanced derivative grids of the magnetics were generated and imaged as part of this interpretation; a texture and phase analysis of the magnetics was also undertaken in order to identify and map possible zones of structural complexity which may in turn indicate zones of favourable mineralization. A profile by profile review of all AEM anomalies was carried out preparatory to identifying high-priority areas of interest and zones for further investigation and ground follow-up.

The original objectives of this survey were two-fold:

- Utilize a more detailed and higher resolution approach in terms of line spacing and survey elevation via a helicopter platform in order to facilitate mapping of bedrock lithologies and structure which in turn may influence the emplacement or hosting of stratabound copper mineralization, and
- Look for centres of conductivity along the extent of the Central Graben structure and particularly in the vicinity of the 4100N Zone, which may have been missed by the coarser-spaced although similar in terms of dipole moment (power) Geotem survey.

These objectives have been or are being met via this interpretation; the data has enabled both the mapping and delineation of controlling structures, and identification of anomalous conductivity suggesting sulphide mineralization.

The principle anomalies of interest occur coincident to the known 4100N, 2750N and 2200N; also responding well to the VTEM system are the ST97-15 and ST99-34 zones; these 5 zones comprise the sole, unambiguous bedrock responses in the entire survey. The 3500N zone does not have a significant positive AEM response, but does lay right along the gradient edge from positive (extended and layered conductive zone) to negative response, apparently at the southern edge of the NW-trending graben. All of these conductive responses are distinguished by a complete lack of direct magnetic correlation.

Table of Contents

| | |
|--|-----|
| 1. Introduction | 1 |
| 1.1. Location and Access | 2 |
| 1.2. Climate and Physiography | 4 |
| 1.3. Claims | 4 |
| 2. Geology | 5 |
| 2.1. Regional Geology | 5 |
| 2.2. Property Geology and Conceptual Models | 7 |
| 3. Airborne Geophysics | 9 |
| 3.1. Exploration Criteria | 9 |
| 3.2. Helicopter Frequency-Domain EM Overview | 11 |
| 3.3. Operations | 13 |
| 3.4. Data Presentation | 14 |
| 4. Data Interpretation | 23 |
| 4.1. Overview | 23 |
| 4.2. Magnetism | 23 |
| 4.2.1. Multiscale Edge Analysis | 26 |
| 4.3. Electromagnetics | 30 |
| 5. Conclusions and Recommendations | 37 |
| 6. Certificate of Professional Qualifications | 38 |
| 7. Appendix A. Airborne Contractor's Logistics and Processing Report | A-1 |

List of Tables

| | | |
|----------|--|----|
| Table 1 | Mineral Claims comprising Storm Property | 4 |
| Table 2. | VTEM Secondary 'areas of interest' | 34 |
| Table 3. | | |
| Table 4. | | |

List of Figures

| | | |
|-------------|---|----|
| Figure 1. | Storm Copper Project Location Map | 3 |
| Figure 2. | Storm Property Prospecting Licenses with VTEM flightpath | 5 |
| Figure 3. | Regional Geology | 6 |
| Figure 4a. | Local Geology | 7 |
| Figure 4b. | Legend | 8 |
| Figure 5. | Conductivity / resistivity of common rocks and minerals | 11 |
| Figure 6. | TEM transmitted and received signals | 12 |
| Figure 7. | VTEM receiver measured waveform | 12 |
| Figure 8. | An example of VTEM dB/dt and B-Field data | 13 |
| Figure 9. | Interactive review of profiles and images | 15 |
| Figure 10. | Regional Aeromagnetics – Boothia Uplift | 16 |
| Figure 11. | Digital Elevation Model | 18 |
| Figure 12. | Residual Magnetic Intensity | 19 |
| Figure 13. | B-Field Z[36] | 20 |
| Figure 14. | Tau calculated from dB/dt data | 21 |
| Figure 15. | Tau calculated from B-Field data | 22 |
| Figure 16a. | dB/dt Tau Storm Cu mineralization | 23 |
| Figure 16b. | B-field Tau Storm Cu mineralization | 23 |
| Figure 17. | QuickMag model – SE dyke feature | 24 |
| Figure 18. | Unsupervised Classification of Magnetic Intensity | 24 |
| Figure 19. | ZS Filter (magnetics) mosaic | 25 |
| Figure 20. | ZS Filter: Tilt Derivative | 27 |
| Figure 21. | ZS Filter: Area Derivative | 28 |
| Figure 22. | Multiscale edge detection with interpreted major linears | 29 |
| Figure 23. | Example of stacked RDIs | 31 |
| Figure 24. | RDI section – Line 2290 looking toward 160° | 32 |
| Figure 25. | RDI voxel model – overview using reverse colour lookup | 32 |
| Figure 26. | RDI voxel – close-in view toward 320° | 33 |
| Figure 27. | RDI voxel – close-in view toward 135° | 33 |
| Figure 28. | dB/dt Z[30] pseudocolour image with anomalous zones | 35 |
| Figure 29. | Final ‘areas of interest’ superimposed with high-priority AEM anomalies | 36 |

1. Introduction

The Storm Property is located on the northwest corner of Somerset Island, Nunavut. The property is 82,307.5 hectares in size and is centred at ~94° 03' 04" West, 73 39' 33" North; it is host to a large area of carbonate-hosted copper mineralization (Storm) as well as a zone of zinc-silver mineralization (Seal). The Seal zinc-silver zone sits on tidewater on a peninsula that extends into Aston Bay. The Storm copper zone is located ~20 kilometres inland from the Seal zone and is the focus of the present study. The property area was acquired by Commander Resources in 2008 through the award of four (4) Prospecting Permits, which are valid for a term of five (5) years.

Zinc mineralization was discovered in the early 1970s, but the first drilling on the property occurred in 1995 by Cominco Ltd (now Teck Ltd.). The second hole of the program in 1995 intersected 10.5% Zn, 28 g/t Ag over a drilled width of 18 metres. Additional drilling in 1995 and 1996 resulted in a small deposit described in the assessment reports as being about 2 Mt grading 8% Zn with some silver credits. This zone was named the "Seal Deposit" by Cominco geologists.

Cominco geologists discovered large chalcocite boulders in a stream bed about 20 km inland from the Seal deposit in 1996; copper mineralization was subsequently found over a seven (7) kilometre structural trend, hosted by Paleozoic dolomite and limestone. Exploration work by Cominco in 1997 and 1999 and later by Noranda (now Xstrata) in 2000 and 2001 led to the discovery of four centres of copper mineralization, the 4100N, 2750N, 2200N and 3500N zones.

Work previously conducted on the property at large has included airborne magnetic and electromagnetic surveys, extensive soil geochemistry, ground geophysics (IP, HLEM and UTEM) and diamond drilling. 17 holes were initially drilled in 1997 on the Storm copper project; a total of ~4,560 metres of diamond drilling was completed in 41 holes in 1999, and a further ~1,350 metres in eight holes was drilled in 2000. Following Noranda's program in 2000 and 2001, no further work was done on the property and the claims gradually lapsed.

Massive sulphides have been the most important exploration target for electromagnetics since the 1950s; in fact, the method was developed for this particular application. However, it needs to be recognized that a good understanding of the type of massive sulphide deposit being sought must be fully understood. Some sulphide deposits are highly conductive and magnetic, while other deposit types may not have any discernible geophysical signature. Fortunately in this case, ground electromagnetics (horizontal-loop e.m.) and induced-polarization carried out in 1997 and a subsequent airborne electromagnetic (Geotem) survey as well as further ground work completed in 2000 by Cominco indicated the presence of identifiable, highly conductive copper-sulphide targets which were in turn confirmed by drilling. Physical property testing completed by Cominco reported¹ "...mineralization in the holes could adequately explain the conductivities seen in the airborne and ground follow-up surveys.'

Given conductive cover, compact, low flying AEM systems such as the helicopter time domain systems currently in use have a considerable advantage over higher flying fixed-wing systems with towed birds. This statement² is based on four premises:

- a) as a transmitter is reduced in altitude, the footprint of the current system induced in the ground is also reduced
- b) compact current systems decay more quickly than large ones implying that conductors under cover appear earlier in time

¹ MacRobbie, P.A., Hall, D., Smith, A. and Rees, M., 2000, Storm Property Assessment Report, 152 p.

² Macnae, J., 2007, Developments in broadband airborne electromagnetics in the past decade *in* Advances in Airborne Geophysics, Proceedings of Exploration 07: Fifth Decennial International Conference on Mineral Exploration, edited by B. Milkereit, 2007, p. 387-398.

- c) the depth of penetration of a dipolar source through conductive cover is greater than that of a more uniform source, and
- d) the closer a receiver is to the transmitter, the less the effects of current gathering and the earlier in time a target response can be seen.

An HTEM system at 30 m altitude would therefore have an advantage in conductive cover penetration of at least a factor of 2 over an otherwise identical fixed-wing system at 120/90 m transmitter/receiver altitude.

Based on conclusions drawn from a re-assessment of the property by Commander Resources and a qualifying NI 43-101 report (Cook and Moreton, 2009), an airborne electromagnetic and magnetic survey was conceived and designed to cover the property and aid in the design of the 2011 exploration program. Overarching objectives of this survey were two-fold:

- Utilize a more detailed and higher resolution approach in terms of line spacing and survey elevation via a helicopter platform in order to facilitate mapping of bedrock lithologies and structure which in turn may influence the emplacement or hosting of stratabound copper mineralization, and
- Look for centres of conductivity along the extent of the Central Graben structure and particularly in the vicinity of the 4100N Zone, which may have been missed by the coarser-spaced although similar in terms of dipole moment (power) Geotem survey.

A helicopter-borne electromagnetic and magnetic survey (VTEM Plus) was subsequently carried out in July 2011 over a selected portion of the Storm Property; the interpretation of this survey is the focus of this report.

1.1. Location and Access

The Storm Property is located within the high Arctic Qikiqtaaluk (Baffin) Region of Nunavut approximately 120 south-southeast of Resolute Bay on Cornwallis Island, and is centered at ~94° 03' 04" West, 73 39' 33" North on NTS Sheets 058C/10–11 and 058C/14–15.

The property is practically accessible only by air from Resolute Bay, the closest permanent settlement; this trip necessitates an open-water crossing of approximately 70 kilometres in each direction. Daily air service to Resolute is available through Iqaluit, with connections from Ottawa and Montreal. Resolute also has service once a week from Yellowknife.



Figure 1. Storm Copper Project Location Map

Prime Minister Stephen Harper announced (August, 2007) the construction of a pair of multimillion-dollar military facilities within the contested waters of Canada's Arctic territory. The facilities consist of a new army training centre at Resolute, Nunavut, and a deep-sea port at Nanisivik Naval Facility. A statement issued by the Prime Minister says, "The Training Centre will be a year-round multi-purpose facility supporting Arctic training and operations, accommodating up to 100 personnel. Training equipment and vehicles stationed at the site will also provide an increased capability and faster response time in support of regional military or civilian emergency operations." Although not as busy as it once was, Resolute Bay Airport is still the core of the town, serving as an aviation hub for exploration in the region and connected by direct service to Iqaluit. The Tajaat Co-op, part of the Arctic Cooperative, runs a grocery and retail store, a hotel, a restaurant, cable TV service, Internet, snowmobile rental, and an airport gift shop. The town has four hotels - Narwhal Inn, Qausuittuq Inns North and South Camp Inn, and the Airport Hotel – all of which have fewer than 100 rooms each, and several lodges. Other facilities include a Royal Canadian Mounted Police Detachment, a school (which provides education from kindergarten to Grade 12) and a gym.

1.2. Climate and Physiography

The climate on Somerset Island and the surrounding Canadian High Arctic is that of high latitude, continental landmass characterized by low mean temperatures and low precipitation. Because of the high latitude, the sun sets completely in late October and only fully rises again in early March; the intervening period is without sunlight. Resolute Bay (nearest centre with reported climate data) has a polar arctic climate with long cold winters and short cool summers. Environment Canada reports Resolute's average high for the year a -13.3°C while the average low for the year is -19.5°C. Resolute has a very dry climate with an average precipitation of 150 mm a year, most of it falling as snow from August to September. The record high for Resolute is 18.4 °C on July 9, 2011. The record low for Resolute is -52.2 °C on January 7, 1966. The whole region is one of continuous permafrost, which extends to depths of 400–500 m.

Resolute is one of Canada's northernmost communities and is second only to Grise Fiord on Ellesmere Island (Alert and Eureka are more northerly but are not considered towns—just military outposts and weather stations). As of the 2006 census the population was 229. Like most other northern communities, the roads and most of the terrain are all gravel.

Geological field exploration is best conducted from mid-June to late-August. Local lakes, rivers, and streams are generally ice-free by mid-July and do not freeze again until the end of August when snow begins to fall. Peel Sound, to the west, and Barrow Strait, on the north coast of Somerset Island, are generally ice-free by mid-July; however, the ensuing large areas of open water often create frequent periods of heavy fog over the low-lying parts of the island. This problem abates when the ocean freezes over again.

1.3. Claims

The Storm Copper Property is currently owned 100% by Commander Resources Ltd., through the granting of 4 prospecting licenses which are valid for 5 years from date of issue:

| Permit | Area | Status | Issue_Date | Expiry_Date | Owner | Percentage |
|--------|---------|--------|------------|-------------|--------------------------|------------|
| 7547 | 21859.8 | Active | 01/02/2008 | 31/01/2013 | Commander Resources Ltd. | 100 |
| 7548 | 21860.3 | Active | 01/02/2008 | 31/01/2013 | Commander Resources Ltd. | 100 |
| 7549 | 16565.0 | Active | 01/02/2008 | 31/01/2013 | Commander Resources Ltd. | 100 |
| 7880 | 22022.3 | Active | 01/02/2010 | 31/01/2015 | Commander Resources Ltd. | 100 |

Table 1. Mineral Claims comprising Storm Property

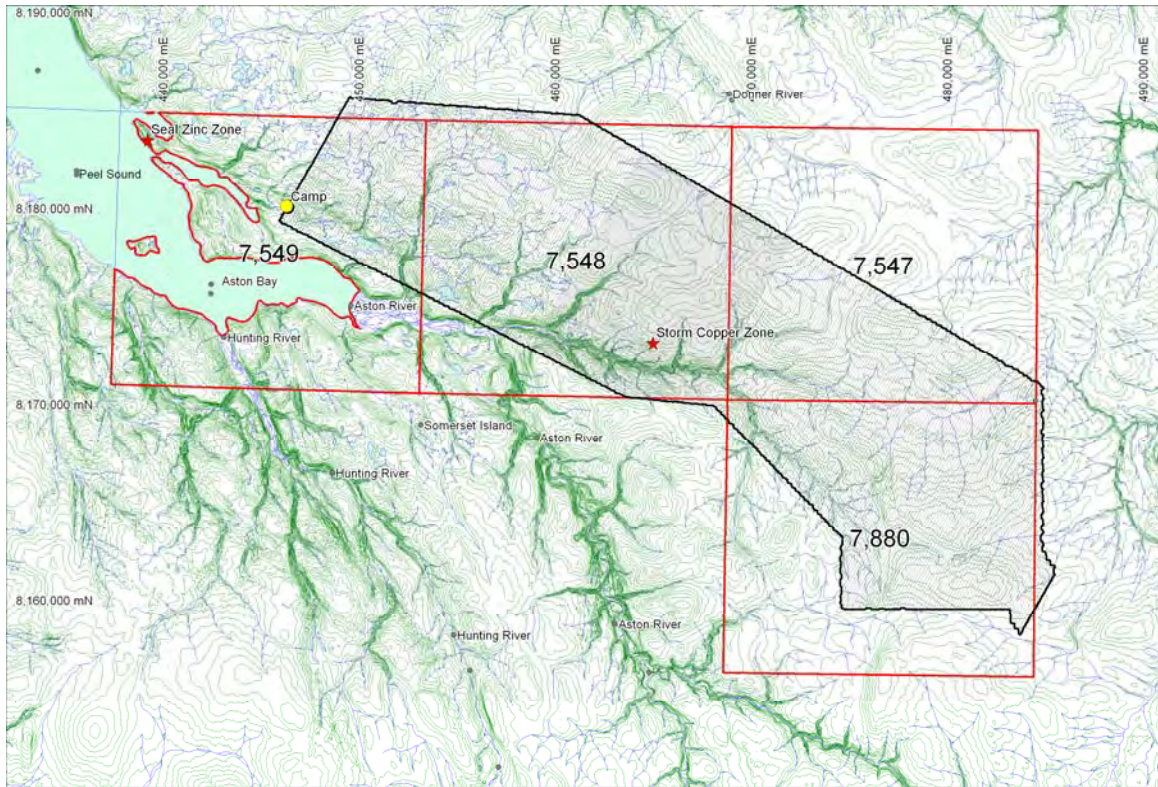


Figure 2. Storm Property Prospecting Licenses with VTEM flightpath

2. Geology

2.1. Regional Geology³

The geology of Somerset Island and the Boothia Peninsula is dominated by the Boothia Uplift, a major, positive, cratonic and supracrustal structural feature, formed mainly in the Late Silurian to Early Devonian. It extends due north for over 800 km from the Boothia Peninsula to the Grinnell Peninsula on Devon Island⁴ (Figure 3). The Boothia Uplift was linked kinematically to the stresses in the coeval Caledonian Orogen (to the east) and its structural-stratigraphic history in part resulted from basement anisotropies which developed during the latest (?) Proterozoic continental break-up⁵. According to Miall⁶, the uplift was formed by west-directed basement thrusting in response to the Caledonian Orogeny. The Archean-Aphebian crystalline core of the uplift is flanked on the east and west, and overlain to the north, by sedimentary rocks of the Arctic Platform⁷. In this part of the Archipelago, the Arctic Platform consists mainly of a structurally conformable, generally northward thickening succession of dominantly carbonate rocks ranging in

³ Cook, R.B. and Moreton, C, 2009, Technical report on the Storm Copper Project, Somerset Island, Nunavut. NI 43-101 Report prepared for Commander Resources Ltd., February 15, 2009, 96 p.

⁴ Okulitch, A.V., Packard, J.J., and Zolnai, A.J., 1991: Late-Silurian-Early Devonian Deformation of the Boothia Uplift; *in* Chapter 12 of *Geology of the Innuitian Orogen and Arctic Platform of Canada and Greenland*. H.P. Trettin (ed.) GSC, Geology of Canada, no. 3, pp.302-307.

⁵ De Freitas, T.A., Trettin, H.P., Dixon, O.A. and Mallamo, M., 1999: Silurian System of the Canadian Arctic Archipelago; *Bulletin of Canadian Petroleum Geology*, vol. 47; no. 2, pp. 136-193.

⁶ Miall, A.D. 1986: Effects of Caledonian tectonism in Arctic Canada; *Geology*, v14, pp. 904-907, Nov. 1986.

⁷ Stewart, W.O. 1987: Late Proterozoic to early Tertiary stratigraphy of Somerset Island and northern Boothia Peninsula, District of Franklin, NWT, GSC paper 83-26, 75 pp.

age from Early Cambrian to Early Devonian. The Storm Copper property is immediately underlain by Arctic Platform carbonates.

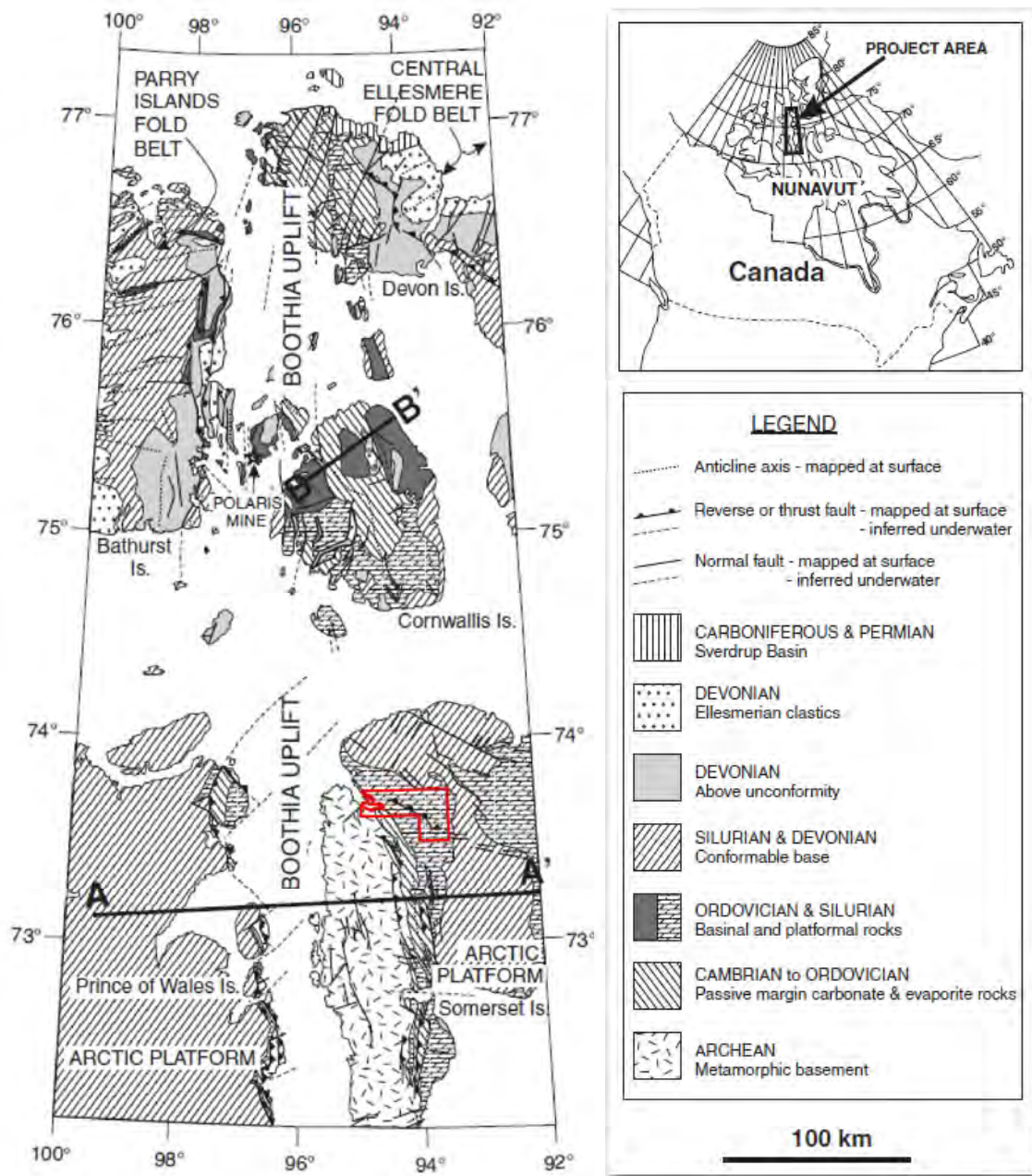


Figure 3. Regional Geology⁸

The core of the Boothia Uplift consists of near-vertical bedding/foliation reflecting north-south trending, tight, generally upright folds. Granulite-facies Archean and Early Proterozoic quartzofeldspathic, pelitic, calcareous and mafic rocks dominate. The overlying folded and faulted successions of Late Proterozoic and Paleozoic carbonate and clastic rocks on either side of the Boothia Uplift are termed the Cornwallis Fold and Thrust Belt. The fold structures exposed at surface in the Paleozoic rocks consist of broad open anticlines and synclines with predominantly

⁸ Dewing, K. and Turner, E.C., 2003, Structural setting of the Cornwallis lead-zinc district, Arctic Islands, Nunavut in Geological Survey of Canada Current Research 2003-B4, 9 p.

north-south axes. On Somerset Island, the distribution of Paleozoic rocks outlines a large asymmetrical syncline with the youngest formations preserved in the core. Superimposed on this main feature are structures related to local block faulting, flexures and relatively gentle folding. Prominent fault directions noted on northern Somerset Island run north-south, northwest-southeast, and northeast-southwest.

The final major tectonic event to affect the area occurred during the Eurekan Orogeny (Tertiary - Eocene) when generally north-trending, extensional, normal faults were created and older faults reactivated in response to the compressional events occurring in the Sverdrup Basin (500 km to the north).

2.2. Property Geology and Conceptual Models

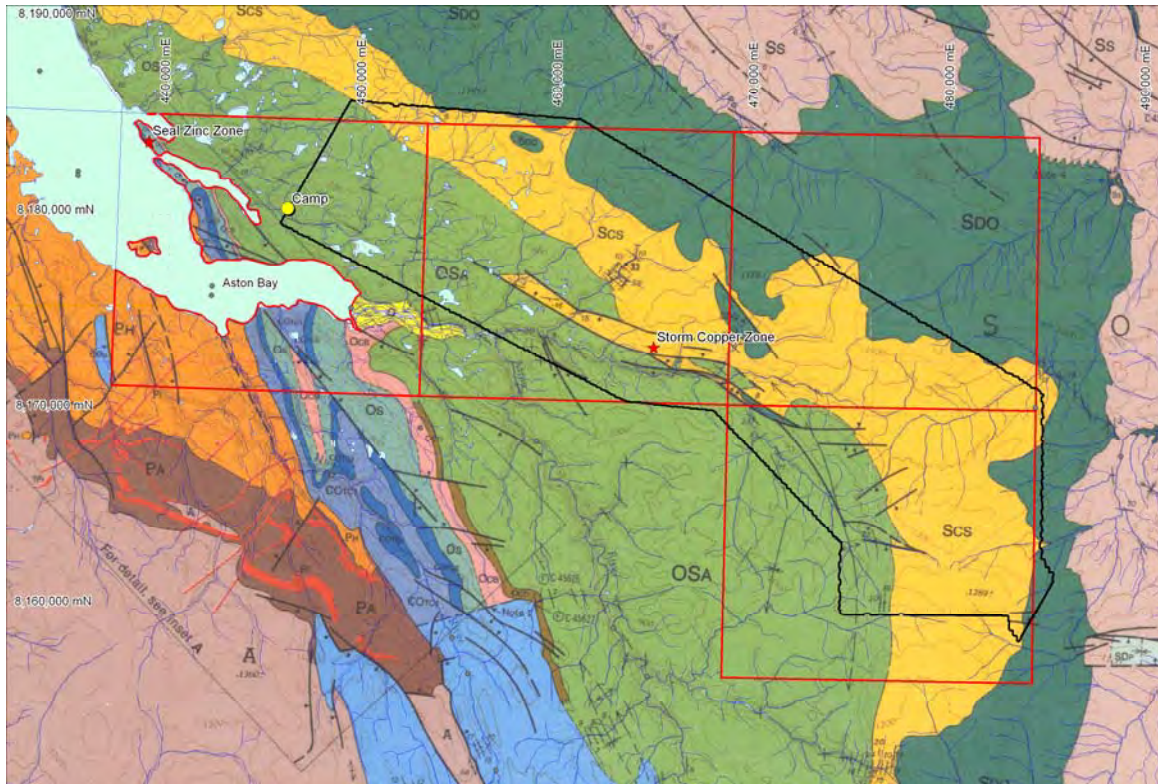


Figure 4a. Local Geology⁹

Cook and Moreton¹⁰ report the Storm Copper to be a variant on the classic sediment-hosted copper deposit; it is epigenetic, carbonate hosted and located within an intracratonic sedimentary basin which was subjected to folding and faulting. Local ground conditions, including faulting and brecciation, appears to have exerted a strong control on the localization of mineralization.

Examples of this deposit type include Redstone (Northwest Territories) and Kennecott (Alaska) although the type deposit is commonly regarded to be the Kupferschiefer district (Germany).

⁹ Stewart, W.D. and Kerr, J.Wm., 1984 Geology of Somerset Island North, District of Franklin. Geological Survey of Canada, Map 1595A, scale 1:250,000.

¹⁰ Cook, R.B. and Moreton, C, 2009, Technical report on the Storm Copper Project, Somerset Island, Nunavut. NI 43-101 Report prepared for Commander Resources Ltd., February 15, 2009, 96 p.

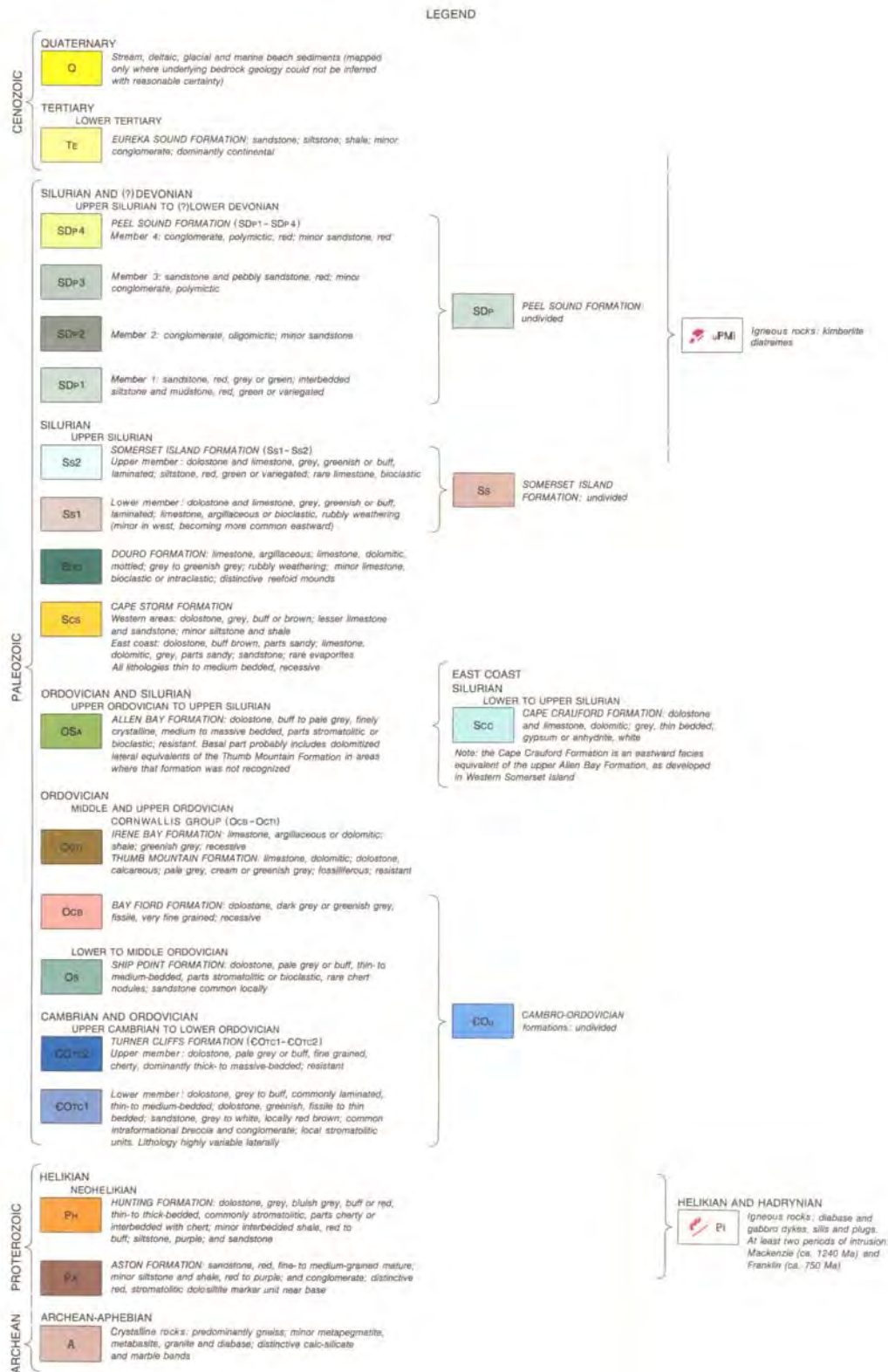


Figure 4b. Legend

These deposits are described by Lefebure and Alldrick¹¹ in brief as ‘...stratabound disseminations of native copper, chalcocite, bornite and chalcopyrite in a variety of continental sedimentary rocks including black shale, sandstone and limestone. These sequences are typically underlain by, or interbedded with, redbed sandstones with evaporite sequences. Sulphides are typically hosted by grey, green or white strata.’ Cox¹² more recently elaborates ‘...Sediment-hosted copper deposits are stratabound, that is, they are restricted to a narrow range of layers within a sedimentary sequence but do not necessarily follow sedimentary bedding. They are epigenetic and diagenetic, that is, they are formed after the host sediment is deposited, but in most cases, prior to lithification of the host. They form independently of igneous processes.’

3. Airborne Geophysics

3.1. Exploration Criteria

Historically, exploration geophysics applied toward sediment-hosted copper deposits appears to have not been particularly successful. The deposits have the form of concordant layers of sulphides, whose lateral extent is 10 to several 100s times the layer thickness. The most common ore minerals range into sphalerite (non-conductive) and galena (weak to moderately conductive); associated minerals include quartz, pyrrhotite, pyrite, chalcopyrite, marcasite, arsenopyrite and cassiterite. The most common rocks associated with the sulphide zone are wedges of sedimentary breccia and conglomerate; chert and barite are common in the overlying sequence of chemical sediments. Geological prospecting has been the most successful tool of exploration for these major deposits, although this is very possibly due to their size and lateral extent as well as timing of discovery. Nevertheless, geophysical methods in principle should be an effective tool for present and future exploration for high-grade, large tonnage sediment-hosted sulphide deposits in specific instances; for instance, airborne electromagnetics has been used successfully in Australia for Mt. Isa and McArthur River –type deposits (although these would properly be termed SEDEX lead-zinc deposits). A major phase of exploration in the late 1960s and 1970s made extensive use of IP/resistivity surveys which proved capable of detecting sulphide mineralization, although this was not necessarily copper-bearing. The poor conductivity of the mineralization and the generally conductive near surface has often precluded the use of EM methods. Gravity methods are typically ineffective for detecting mineralization, because responses associated with weathering and stratigraphy dominate the data. The mineralization itself is usually nonmagnetic.

The following (very general) exploration guides are provided by Lefebure and Alldrick (1996):

Geochemical Signature: Elevated values of Cu, Ag, Pb, Zn and Cd are found in host rocks, sometimes with weaker Hg, Mo, V, U, Co and Ge anomalies. Dark streaks and specks in suitable rocks should be analysed as they may be sulphides, such as chalcocite.

Geophysical Signature: Weak radioactivity in some deposits; resistivity, IP and gravity could also be useful but there are no definitive tools.

Other: Deposits often occur near the transition from redbeds to other units which is marked by the distinctive change in colour from red or purple to grey, green or black. The basal reduced unit within the stratigraphy overlying the redbeds will most often carry the highest grade mineralization.

¹¹ Lefebure, D.V. and Alldrick, D.J., 1996, Sediment-hosted Cu+/-Ag+/-Co, in Selected British Columbia Mineral Deposit Profiles, Volume 2 - Metallic Deposits, Lefebure, D.V. and Höy, T., Editors, British Columbia Ministry of Employment and Investment, Open File 1996-13, pages 13-16.

¹² Cox, D.P., Lindsey, Singer, D.A., Moring, B.C. and Diggles, M.F., 2007, Sediment-hosted copper deposits of the world: deposit models and database. US Geological Survey Open-File Report 03-107, 53 p.

Cominco's work in 1997–2000 successfully identified 4 zones of Cu mineralization within a wider-spread area of low-grade copper 'background.' These 4 zones contain locally high-grade intervals of chalcocite (79.85% Cu), bornite (63.31% Cu) and chalcopyrite (34.63% Cu) with local concentrations of accessory minerals, covellite (66.46% Cu), native copper, cuprite, malachite and azurite. Pyrite and marcasite occur as the main non-copper sulphides. The mineralization is hosted within the upper 80 metres of the Silurian Allen Bay Formation dolostone close to the conformable contact with the overlying Cape Storm Formation¹³.

More significantly, both ground and airborne electromagnetic surveys (Maxmin HLEM, UTEM and Geotem) isolated several conductive zones which were subsequently drilled and shown to have at least some degree of Cu mineralization. The 4100N Zone, comprising the strongest electromagnetic conductor, is essentially a blind outcrop beneath a veneer of Cape Storm Formation. The Storm area was initially tested by seventeen widely spaced drill holes, all of which are mineralized, is open in all directions and offers excellent exploration potential. It is evident that copper mineralization, exposed intermittently along a five-kilometre strike length, is preferentially located adjacent to the North and South (bounding) faults. The proximal disposition of the 4100N, and 2200N and 2750N zones on the north and south sides, respectively, of the Central Graben suggests that mineralization may have been more continuous across the graben stratigraphy prior to final movement along the bounding faults.

Geophysical signatures may include all or some of the following:

- direct electromagnetic response associated with anomalous conductivity arising from massive sulphides dominated by copper mineralization and a paucity of lead or zinc;
- magnetics to map controlling structure;
- induced polarization/resistivity surveys to outline disseminated sulphides and d.c. resistivity surveys to help map alteration zones; and
- airborne and ground radiometric surveys to help delineate alteration zones and anomalous gamma-ray radiation.

The main advantage of electromagnetic methods is their ability to distinguish between a very good conductor and one that is just slightly more conductive than the surrounding host rock. This is not as definite with dc resistivity methods due to their dynamic range limitations, and so the historically most successful applications of electromagnetics have been in finding highly conductive base metal deposits. The following figure illustrates how almost all of the ore minerals are electrically much more conductive than barren rocks.

¹³ Commander Resources Ltd. Internal Report, Storm Property Summary. www.commanderresources.com

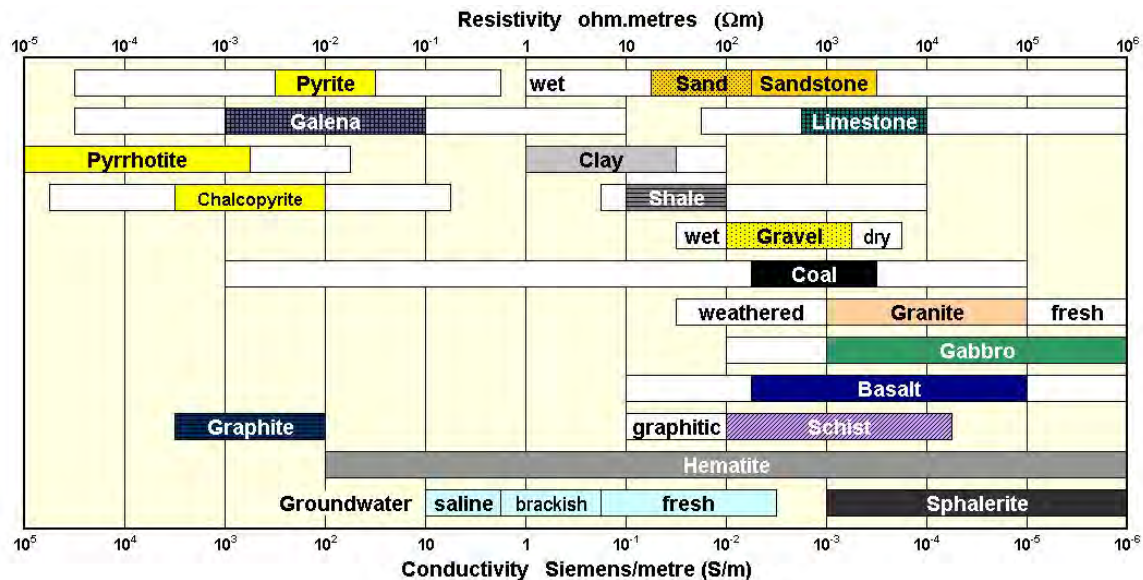


Figure 5. Conductivity / resistivity of common rocks and minerals

A conclusion is drawn whereby electromagnetics is or will be likely successful only in cases where copper sulphide dominates mineralization and the lead / zinc assemblage is not significant. Geological studies have shown that most of the copper deposits are structurally controlled at some scale. Analysis of modern regional airborne magnetic and radiometric datasets allows the structural and stratigraphic setting of the deposits to be determined, although weak overall levels of magnetization mean that intensive filtering/enhancement of the aeromagnetic data is required. Most deposits are associated with the intersection of linear magnetic anomalies, which are interpreted as faults. Units within the host succession have distinctive radiometric responses, allowing the stratigraphy to be mapped confidence. Regional to local airborne geophysical data provide a cost-effective means of identifying further occurrences of the structural/stratigraphic scenarios of the known deposits.

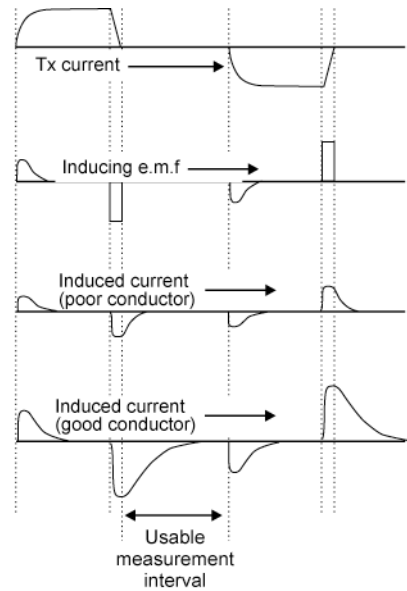
3.2. Time-Domain EM Overview

Electromagnetic induction is based on Faraday's law of induction which states that a changing magnetic field will produce an electric field, which in turn will create an electric current. Electromagnetic induction methods generate an electromagnetic field which induces current in the earth which in turn causes the subsurface to create a magnetic field; by measuring this magnetic field, subsurface properties and features can be deduced. This method measures the magnitude and phase of induced electromagnetic currents, which are related to the subsurface electrical conductivity. Electrical conductivity is a function of the soil and rock matrix, percentage of saturation, and the conductivity of the pore fluids. A transmitter (Tx) coil or loop is used to generate a time-varying magnetic field, the primary field, which induces an electromagnetic force in the neighbouring regions of space. This electromagnetic force drives eddy currents in the earth, and other conductive elements, which in turn produce a new magnetic field, the secondary field, registered by one or more receiver (Rx) coils. The secondary magnetic field contains information on the resistivity distribution in the ground, which can then be converted into geological knowledge because of the different electric properties of earth materials.

¹⁴A modified square wave of the type shown below flows in the transmitter circuits, and transients are induced in the ground on both the upgoing and downgoing 'ramps.' Only currents induced during the downgoing ramps are used, since only they can be observed in the absence of the

¹⁴ Milsom, J. and Erikson, A., 2011, Field Geophysics, 4th Edition, John Wiley & Sons Ltd. Press, p.165-166.

primary field. Ideally, the upramp transients should be small and decay quickly; the upramp is accordingly often 'tapered' to reduce induction. In contrast, the downramp current flow is terminated as quickly as possible to maximize induction. Transmitter self-induction must be minimized and single-turn loops are preferred to multi-turn loops (at least in principle).



Field Geophysics, Fourth Edition. John Milsom and Asger Eriksen.
© 2011 John Wiley & Sons, Ltd. Published 2011 by John Wiley & Sons, Ltd.

Figure 6. Transient electromagnetic (TEM) transmitted and received signals

Geotech's VTEM system uses an in-loop transmitter – receiver geometry to provide a symmetric response to allow for intuitive conductor interpretation. The coincident, vertical dipole transmitter – receiver configuration provides a symmetric system response. Any asymmetry in the measured EM profile is due to conductor dip, not the system, or direction of flying.

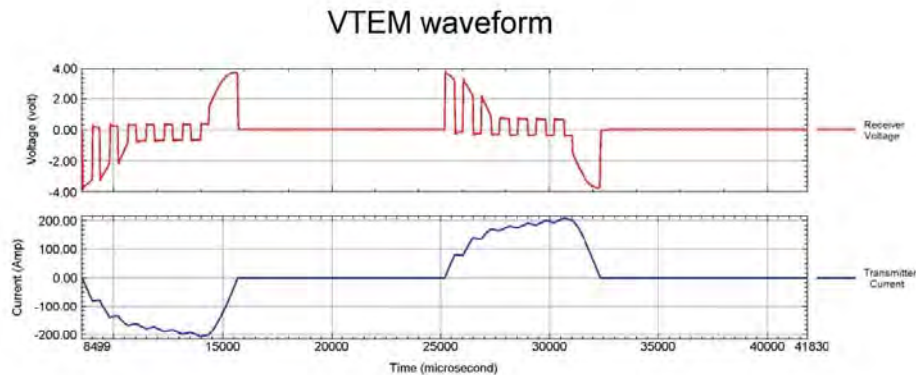


Figure 7. VTEM receiver measured waveform and the derived pulse shape

Geotech uses a complicated waveform which has been optimized to use as much of the helicopter's spare electrical power as possible. Depending on the requirement of the survey, the pulse width can be modified, i.e., lengthened, or shortened, or simplified. For a known transmitter – receiver geometry, the dB/dt seen in the receiver is proportional to the current in the transmitter. The current waveform in the transmitter is obtained by integrating the dB/dt receiver coil response

and then scaling to the maximum current. A typical receiver measured waveform and the derived pulse shape is shown in the preceding figure.

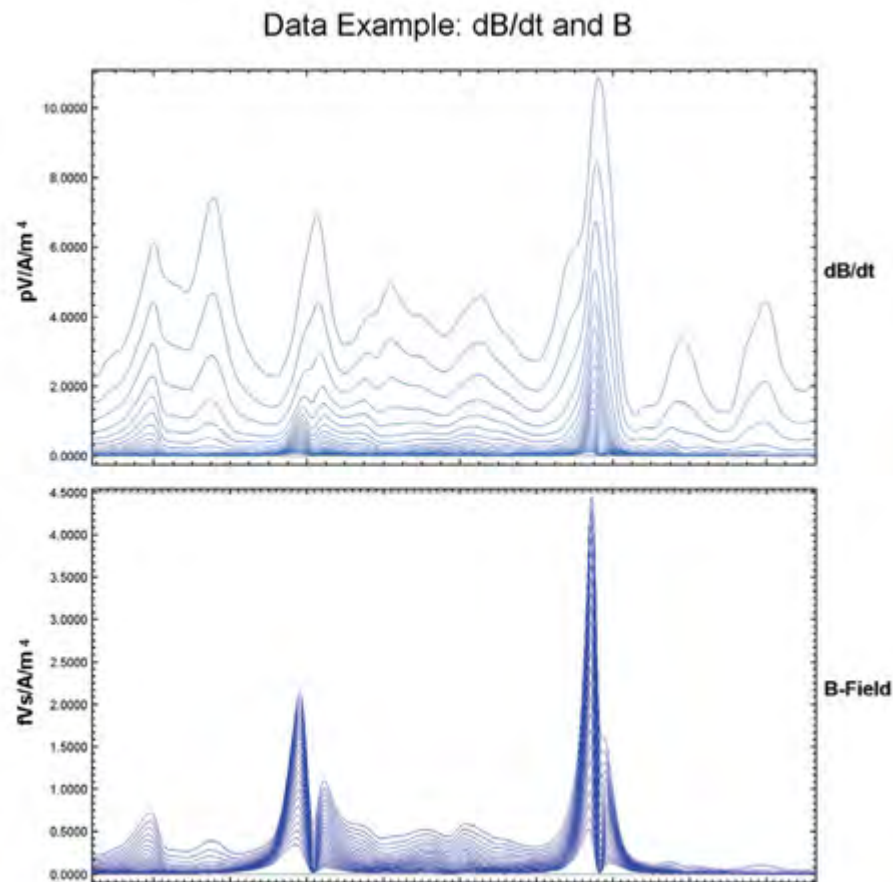


Figure 8. An example of VTEM dB/dt and B-Field data is shown.

It can be seen from the above figure that the B-Field data responds to the better conductors and that the overburden response is suppressed. This allows for easier interpretation of bedrock EM anomalies. The high signal-to-noise ratio of the system is also readily seen in the data.

3.3. Operations

Geotech Ltd. was contracted in June 2011 to fly an airborne electromagnetic and magnetic survey for Commander Resources Ltd. over the Storm Property on Somerset Island; operations were based out of Resolute Bay on Cornwallis Island as no camp facilities were in place on the property. Operations therefore involved a twice-daily open water crossing by helicopter and crew, some 70 km in each direction which necessitated appropriate equipment and protocols as per Transport Canada guidelines and regulations; a fuel cache located at the old Cominco site was utilized for daily re-fuelling. In the event, no problems were encountered and the survey was completed safely and without incident. Data acquisition occurred during the period July 2–24, 2011; 30 production flights were undertaken in 13 days with 10 days lost due to equipment and weather. Final survey coverage consisted of 3,969.647 line-kilometres, including tie lines. Flight lines were flown east-west (030°–210°) with a line separation of 150 m. Tie lines were flown orthogonal to the traverse lines (120°–300°) at intervals of 1,500 m; a central block of interest was in-filled resulting in an effective 75 m traverse line spacing.

The survey employed the VTEM Plus electromagnetic system. Ancillary equipment consisted of a caesium magnetometer, radar altimeter, GPS navigation system and a digital recording system. Ground equipment included GPS and magnetometer base stations for navigation control and monitoring of diurnal fluctuations. The instrumentation was installed by Geotech personnel in a Eurocopter Aerospatiale (AStar) 350 B3 helicopter, registration C-GXGX. The helicopter is owned and operated by Geotech Aviation. Although the stated nominal survey speed was 80 kph, the actual average ground speed achieved was 92.2 km/h (25.6 m/s); the average EM bird terrain clearance was 43.1 metres while the average magnetic sensor clearance was 62.1 metres.

A complete description of the field program is provided by the contractor's logistical report¹⁵, attached to this report as Appendix B.

3.4. Data Presentation

Electromagnetics

The VTEM electromagnetic system utilizes receiver and transmitter coils in concentric-coplanar and Z-direction oriented configuration. The receiver system for the project also included a coincident-coaxial X-direction coil to measure the in-line dB/dt and calculate B-Field responses. Thirty-two time measurement gates were used for the final data processing in the range from 96 to 7036 μ sec. A three stage digital filtering process was used to reject major spheric events and to reduce system noise. Results are presented as stacked profiles of EM voltages for the time gates, in linear-logarithmic scale for the B-field Z component and dB/dt responses in the Z and X components. B-field Z component time channel recorded at 2.021 milliseconds after the termination of the impulse is also presented as contour colour images. Calculated Time Constant (TAU) are presented for both B-field and dB/dt Z-component responses. Test resistivity depth images are presented for 4 selected lines; based on these initial tests, a further 41 lines over the central, in-fill zone were additionally processed through inversion and RDIs presented.

Magnetics:

The magnetic data was corrected for diurnal variations and then subjected to tie-line levelling; this data was then interpolated between survey lines using a random point gridding method to yield x-y grid values for a standard grid cell size of approximately 37.5 metres for the entire property and 15 metres for the in-fill area. A calculated vertical derivative (vertical gradient) was computed via a Fourier transformation and also mapped.

This airborne geophysical interpretation is based on an integrated analysis using a combination of GEOSOFT's integrated editors (spreadsheet and flight path), INTREPID's advanced Fourier filtering and multiscale edge detection, ER MAPPER's image enhancements and MAPINFO's GIS capability. All the final data is also presented as a series of digital maps and images generated at scale of 1:25,000. The airborne geophysical gridded data was analyzed using the following enhanced images:

- Total Magnetic Intensity; pseudocolour and colourdraped images
- Calculated Vertical Derivative; greyscale shaded-relief and colourdraped images
- Total Horizontal Derivative; colourdraped images
- Analytic Signal (total gradient); colourdraped images
- Tilt derivative; colourdraped images
- Total horizontal derivative of the tilt derivative; colourdraped images

¹⁵ Geotech Ltd., Project no. 11053. Report on a helicopter-borne versatile time domain electromagnetic (VTEM plus) and aeromagnetic geophysical survey, Storm Property, Resolute, Nunavut for Commander Resources Ltd., August, 2011, 68 p.

- B-Field and dB/dt Calculated Time Constants, pseudocolour images
- B-Field and dB/dt Z-Component, pseudocolour images
- Fraser Filter X Component dB/dt, colourdraped images
- Digital Elevation Model, colourdraped images
- Multiplots of magnetics and electromagnetics.

Projection Specifications:

| | |
|------------------|----------|
| Map projection | NUTM15 |
| Datum | NAD83 |
| Central meridian | 93° West |
| False Easting | 500000 m |
| False Northing | 0 m |
| Scale Factor | 0.9996 m |

In addition, the analysis and interpretation included a methodical review of the underlying profile data via both the contractor-supplied multiplots and an interactive review via GEOSOFT's integrated editors; example shown below in Figure 8.

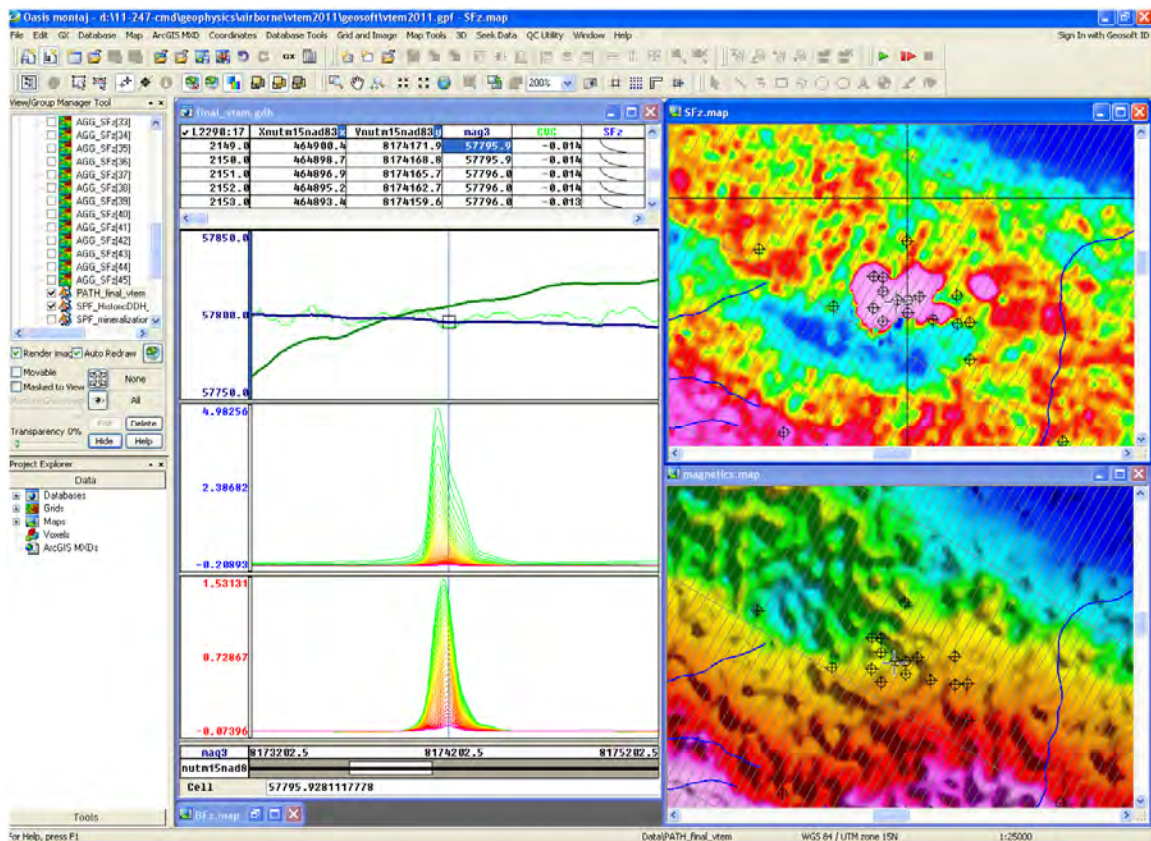


Figure 9. Interactive review of profiles and images

The subsequent analysis depends in part at least on the processing, visualization, mapping, and integration capabilities provided by specialized geophysical software. Discrete features and trends are checked on a profile by profile basis, linked to a variety of images and GIS layers, before final decisions as to interpretation and recommendations for ground follow-up are made.

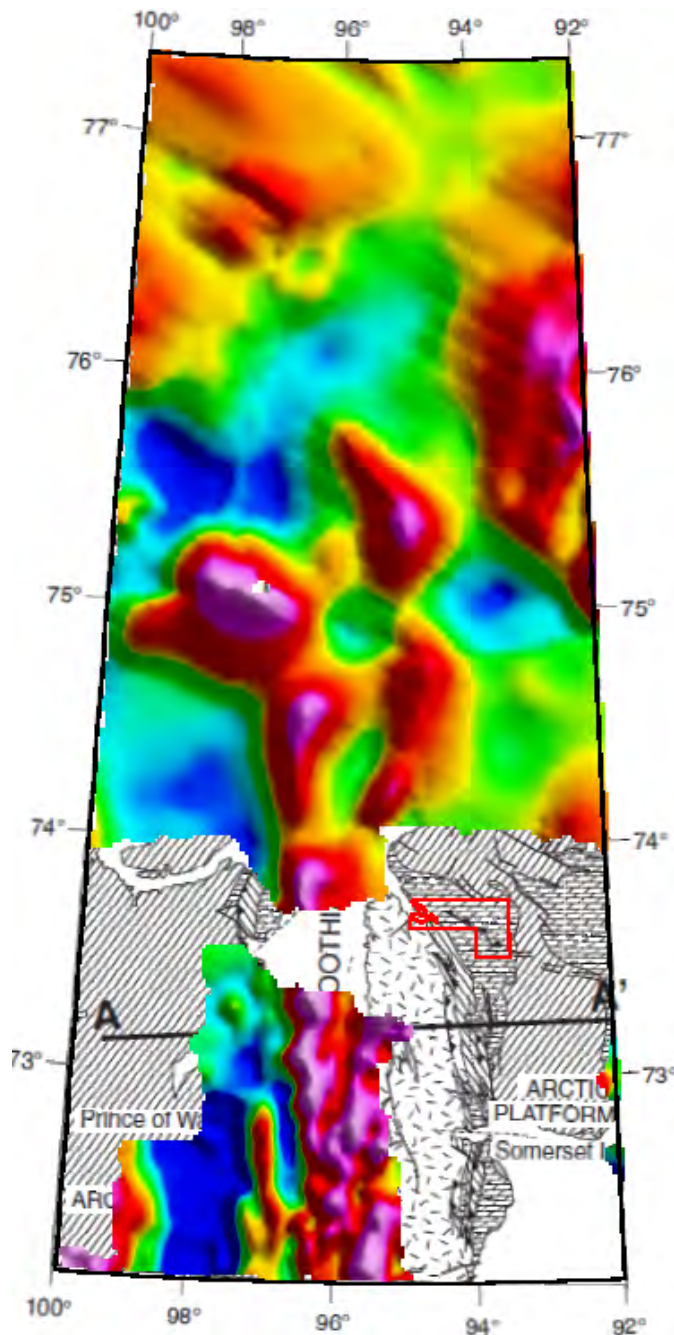


Figure 10. Regional Aeromagnetics (Natural Resources Canada) – Boothia Uplift

An image of the regional aeromagnetics (above) serves to place the Storm property in some context; in this case, the image is superimposed upon the Boothia Uplift regional geology previously shown (blank region in terms of coloured magnetics indicates unfortunately no data).

Modern high-resolution aeromagnetic data provides a clearer view of completely obscured rocks, allowing much finer divisions of provinces regionally, and units locally. As magnetic field compilations extend to greater scales, they may be used to tie existing isolated interpretations or maps together through continuous data coverage, provide continent-scale perspectives on geologic structure and evolution, and extend geological mapping of exposed (particularly Precambrian basement) regions into sediment-covered areas. A fundamental building block in these interpretations is the geophysical domain, distinguished on the basis of anomaly trend,

texture, and amplitude. Where basement is exposed, these domains often coincide with lithotectonic domains, geologic provinces, or cratons, depending on the scale of investigation. Delineating areas of magnetic anomalies having similar characteristics is intended, therefore, to isolate areas of crust having similar lithological, metamorphic, and structural character, and possibly, history. Anomaly trends may indicate the type of deformation undergone: for example, sets of parallel, narrow curvilinear anomalies may attest to penetrative deformation whereas broad ovoid anomalies might suggest relatively un-deformed plutons. The average anomaly amplitude within a domain reflects its bulk physical properties. For example, calc-alkaline magmatic arcs generally are marked by belts of high-amplitude positive magnetic anomalies while greenstone terranes commonly are associated with subdued magnetic fields. Additionally, where anomaly trends show abrupt changes in direction at domain boundaries, the relative age of the adjacent domains may also be inferred.

One of the by-products from the airborne geophysics program is a digital elevation model, derived from the GPS height and radar altimeter. Although not as accurate as a terrestrial geodetic survey, it remains a relatively inexpensive and accurate model of the topography of the study area. The errors contained in these sorts of DEMs are of the order of approximately 10 metres; the main contributions being from the radar altimeter data (1–2 metres) and the GPS height data (5–10 metres). When height comparisons are made in areas of flat terrain to elevations obtained during the course of third order gravity traverses and/or the elevations of geodetic stations, the errors are on the order of approximately 2 metres.

The final total magnetic intensity (Figure 12, following) has been corrected for parallax and diurnal, and a spike-removal filter applied. Additionally, the data was edited for abrupt elevation shifts which did cause some associated jumps or spikes. The data was then tie-line levelled and gridded using a bi-directional grid technique using a 37.5 m cell size, one-fourth of the nominal traverse line spacing. A correction for the regional reference field (IGRF) was applied.

Also shown on following figures are the B-field Z-component channel 36 as well as the B-Field and dB/dt calculated time constant (Tau, in ms). As concluded by Smith and Annan¹⁶, in cases when the exploration target is a highly conductive body, or at least more conductive than the surrounding host, B-field data will improve the chances of anomaly recognition. In cases where the exploration target is weakly conductive, the dB/dt response has a greater signal-to-noise ratio. In cases where the exploration target has an unknown conductance or conductivity, or when there are multiple targets which fall into both the above categories, a system utilizing both dB/dt and B-field is preferable.

- The response of poor conductors such as weakly conductive overburden is suppressed on B-field data
- The signal-to-noise ratio for good conductors (10–2,000 S) is greater on B-field data than dB/dt data.
- The response of conductive zones is frequently easier to interpret on B-field response profiles as larger amplitudes generally correspond to more conductive zones
- The effect of spherics is suppressed on B-field data
- The B-field response spans a smaller range of values than dB/dt, making it easier to plot or image; this tends to simplify the interpretation task.

¹⁶ Smith, R. and Annan, P., 1998, The use of B-field measurements in an airborne time-domain system: Part I Benefits of B-field versus dB/dt data. *Exploration Geophysics*, vol. 29, p. 24–29.

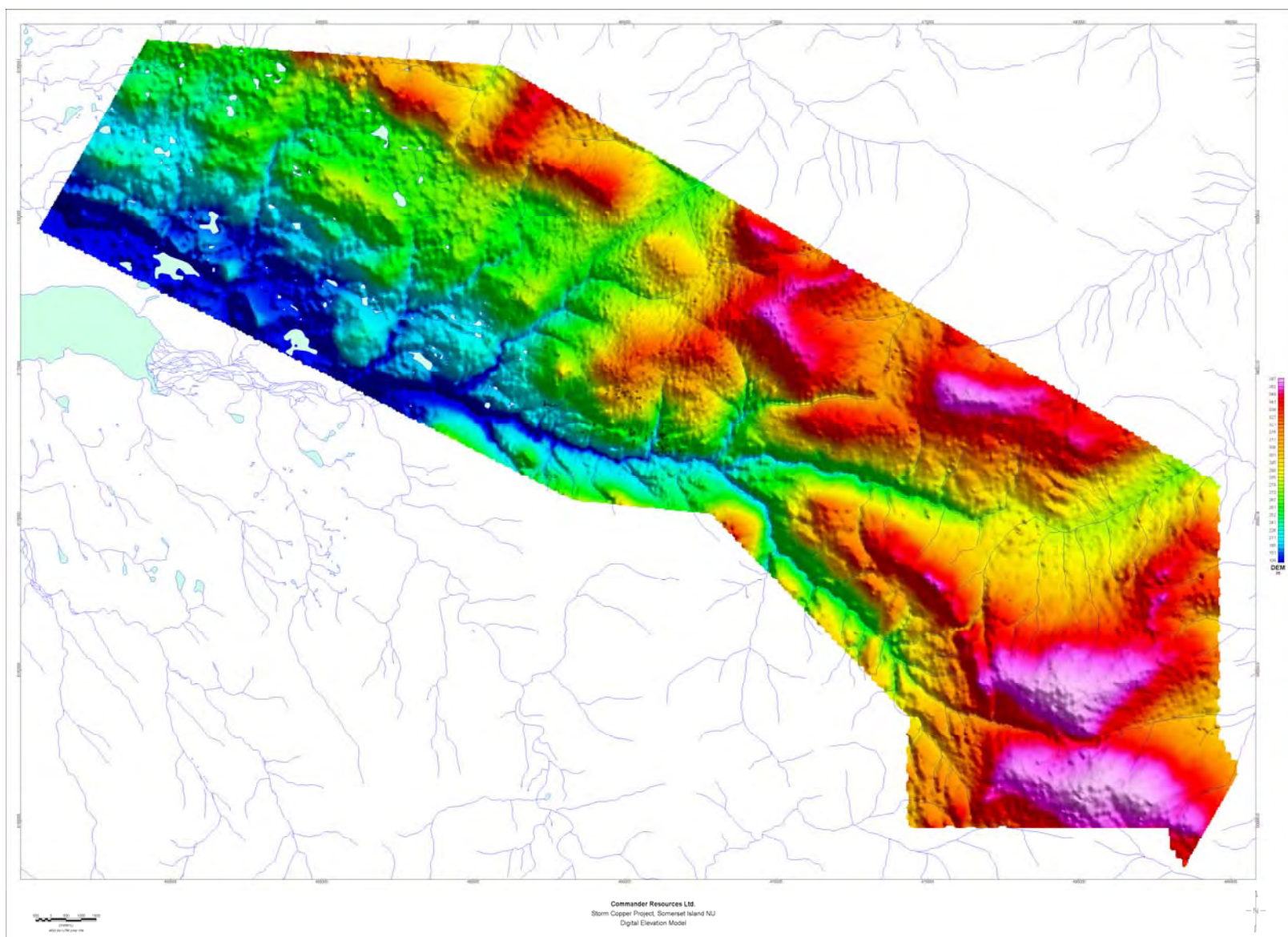


Figure 11. Digital Elevation Model (airborne geophysics)

The image above reflects the moderate topography of the survey block, with ~350 m relief being present.

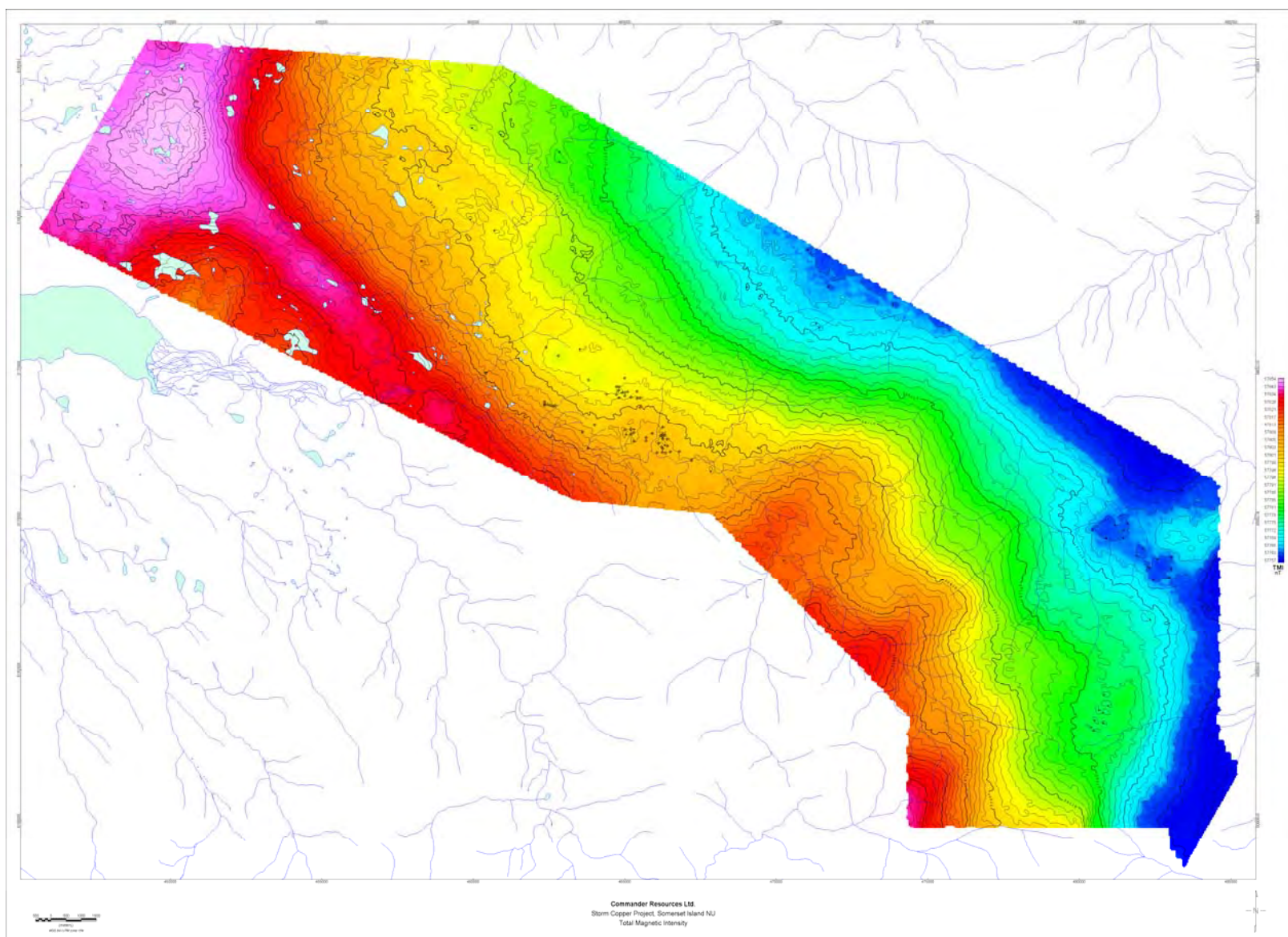


Figure 12. Residual Magnetic Intensity (2 nT contours)

The magnetic field is relatively quiet (dynamic range ~100 nT), in keeping with the platform carbonates and depth to crystalline basement.

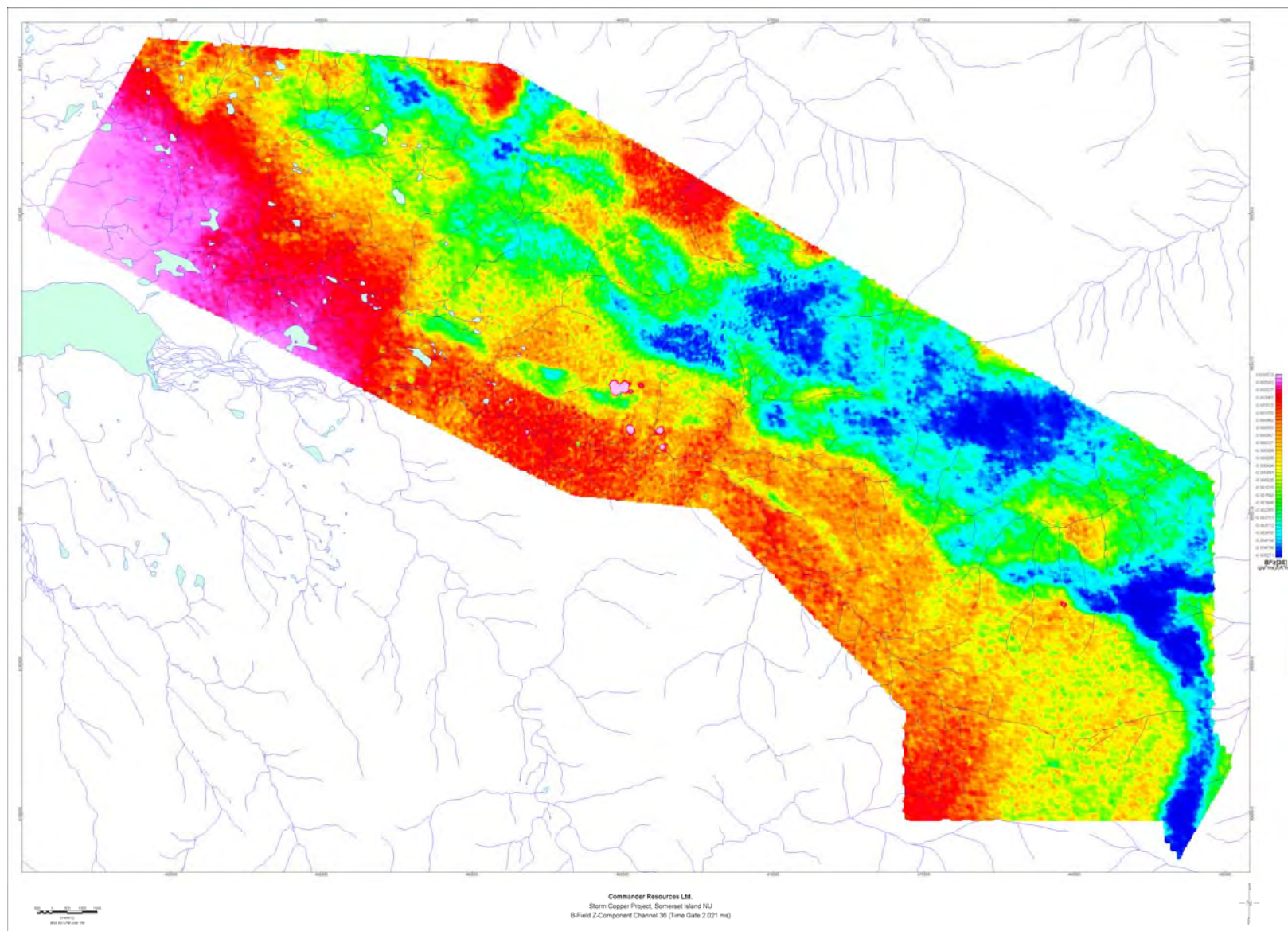


Figure 13. B-Field Z[36]

In this case, the historic drill collars are 'turned off' so that the strong conductive anomalies become more apparent.

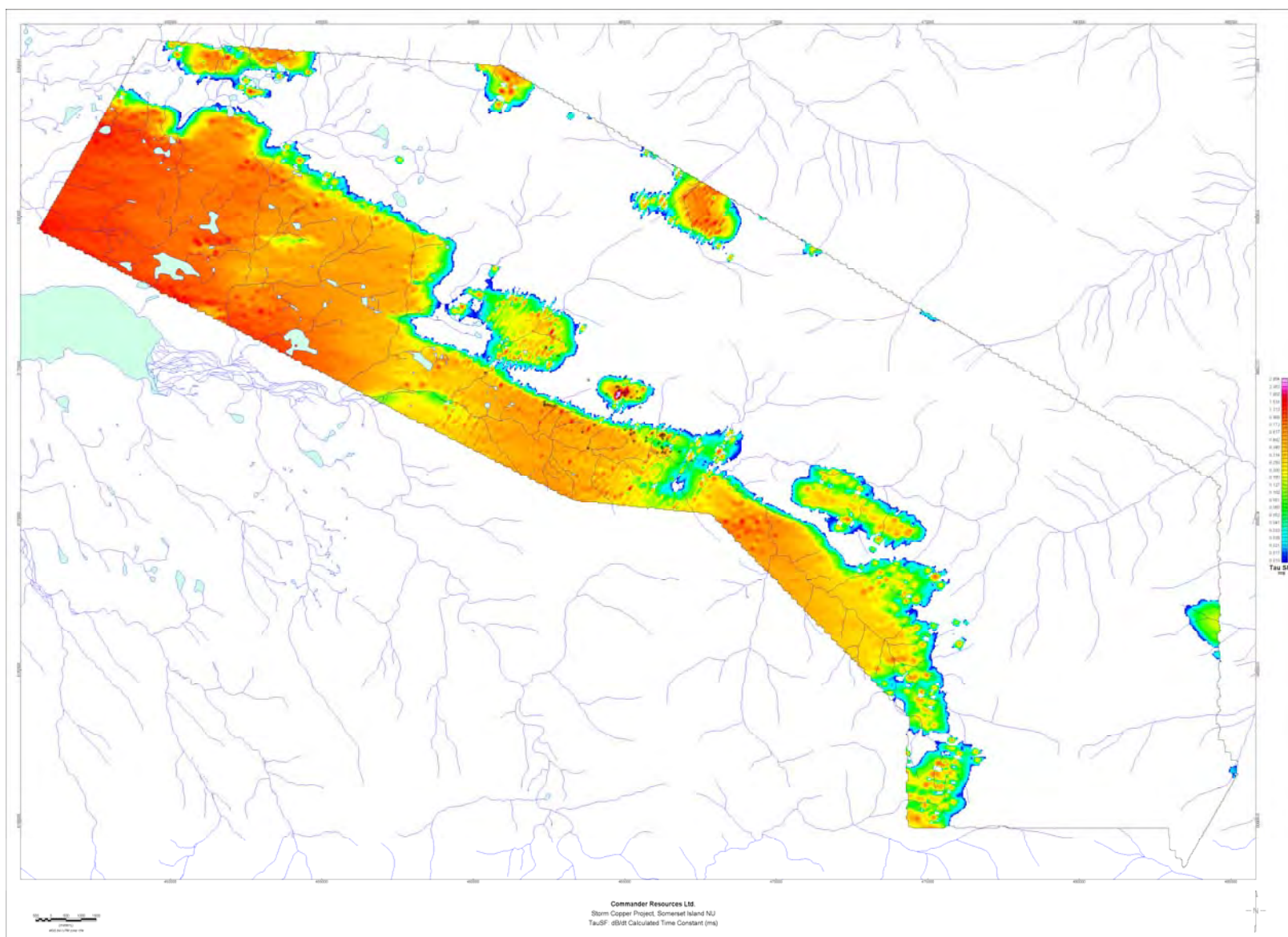


Figure 14. Time Constant (Tau) calculated from dB/dt data

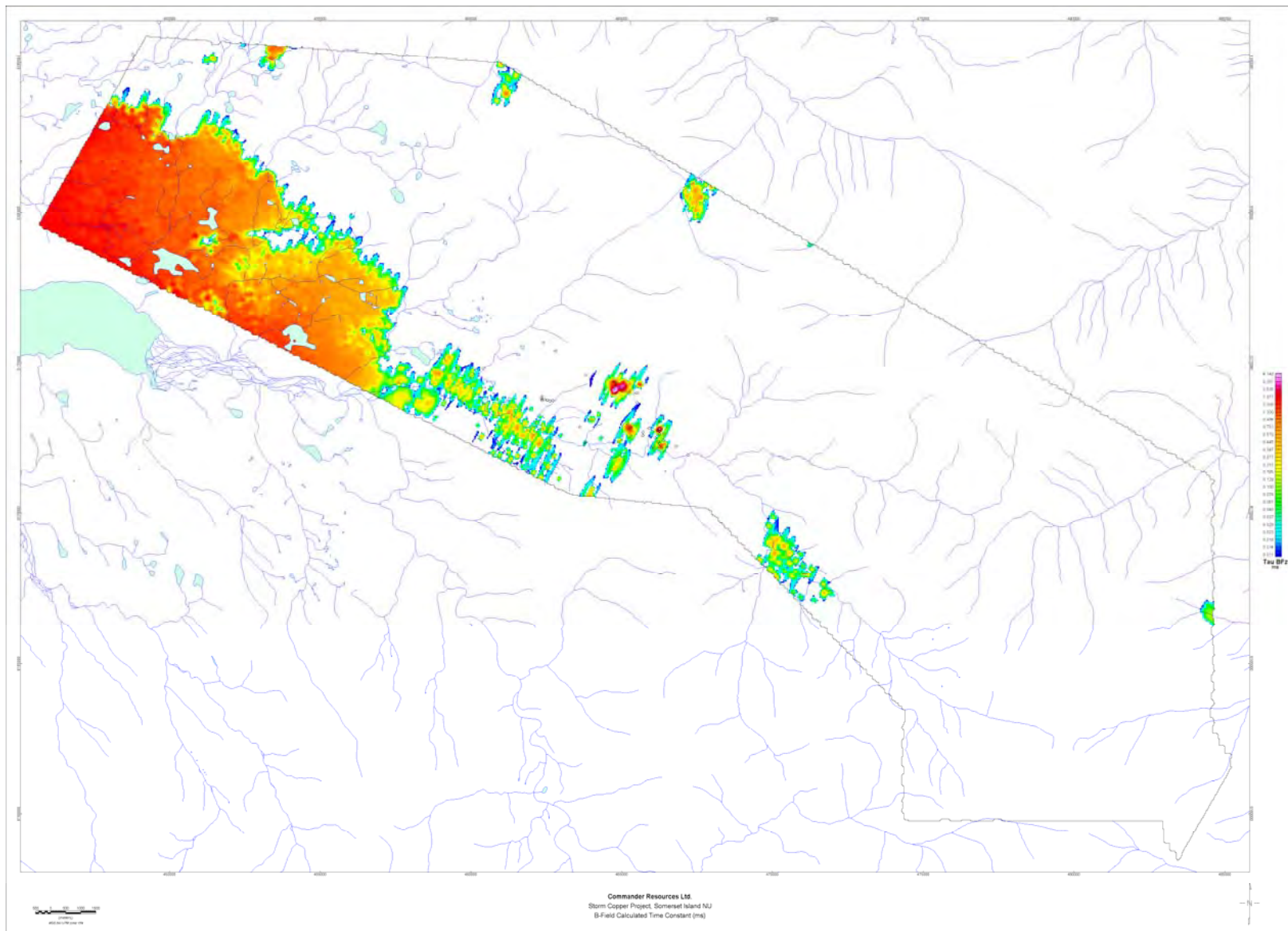


Figure 15. Time Constant (Tau) calculated from B-Field data

As mentioned in a preceding section, the B-field is less responsive to weaker conductors than dB/dt; hence this image is rel. constrained.

4. Data Interpretation

4.1. Overview — Magnetism/Electromagnetics

A first step in the interpretation is to compare the airborne geophysical response to the known showings on the property; thereafter, parallels to these are sought and identified throughout the survey as a whole. As previously stated, 4 main zones of anomalous copper mineralization have been identified by Cominco; these are the so-called 4100N, 2200N, 2750N and 3500N zones. Responses on the AEM data vary from very strong conductivity at the 4100N Zone to not readily discernible on the 3500N Zone. There also appears to be no direct correlation to magnetics.

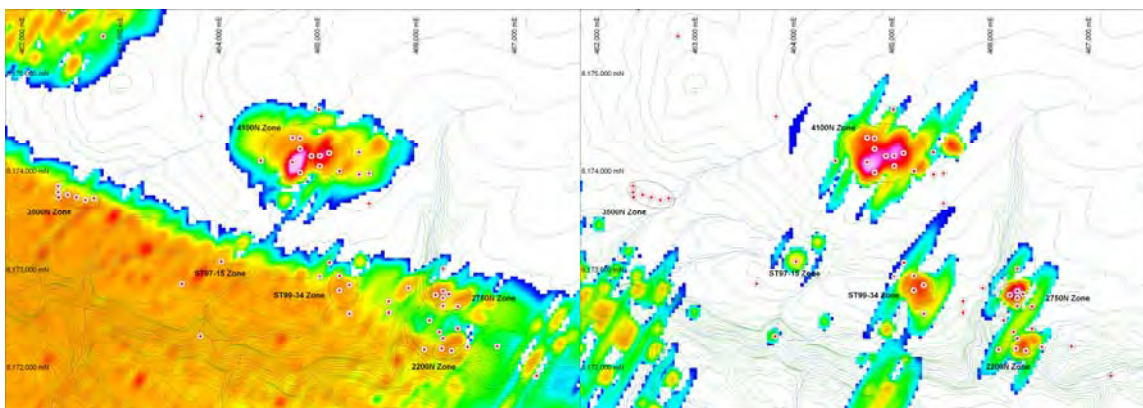


Figure 16a. dB/dt Tau Storm Cu mineralization

Figure 16b. B-field Tau Storm Cu mineralization

There occur two further 'zones' which are apparent on the AEM data; although drilled by Cominco, there are no names assigned in the various reports; accordingly, these have been named by their central drill hole as ST97-15 and ST99-34 respectively.

4.2. Magnetism

Overall, the magnetics are dominated by a relatively intense, irregular magnetic anomaly at the northwest end of the surveyed area; extending from this anomaly is a southeast-trending dyke-like high. The source of these two magnetic anomalies is felt to lay in the Proterozoic basement; modelling of the SE-dyke feature indicates a depth to source of ~534 m below sea level, having a reasonable fit on the anomaly as it extends away from the more extensive intrusion on the very western end of the survey (this latter feature is not resolved sufficiently by this airborne survey to permit reliable modelling or depth estimates). A summary model is shown on the following page.

Enhancement filters applied to the magnetic grid have highlighted a limited number of structural orientations and trends. The aeromagnetic data is primarily reflecting very long wavelength, buried features believed to be sourced in the Proterozoic basement at some depth (i.e., ≥ 500 m). However, a high-frequency, shallow component is evident throughout; this is felt to be due to magnetic minerals contained within the Paleozoic platform carbonates (extending from Silurian Douro and Cape Strom formations through to Upper Ordovician Allen Bay Formation), possibly originating in magnetite-precipitating bacteria, or possibly related to detrital materials themselves related to variation in sea levels. It may be that the carbonate susceptibilities (if and when these could be determined in future exploration and drilling campaigns) can therefore be considered as one of the environmental proxy data for the research of sequence stratigraphy. A degree of remanence is also suspected, although there is no evidence to support or deny this concept at the present time. A simple 10-group classification was run on the magnetic intensity to isolate and identify the main 'bands' of these intra-sedimentary magnetic patterns; results are shown in a following figure.

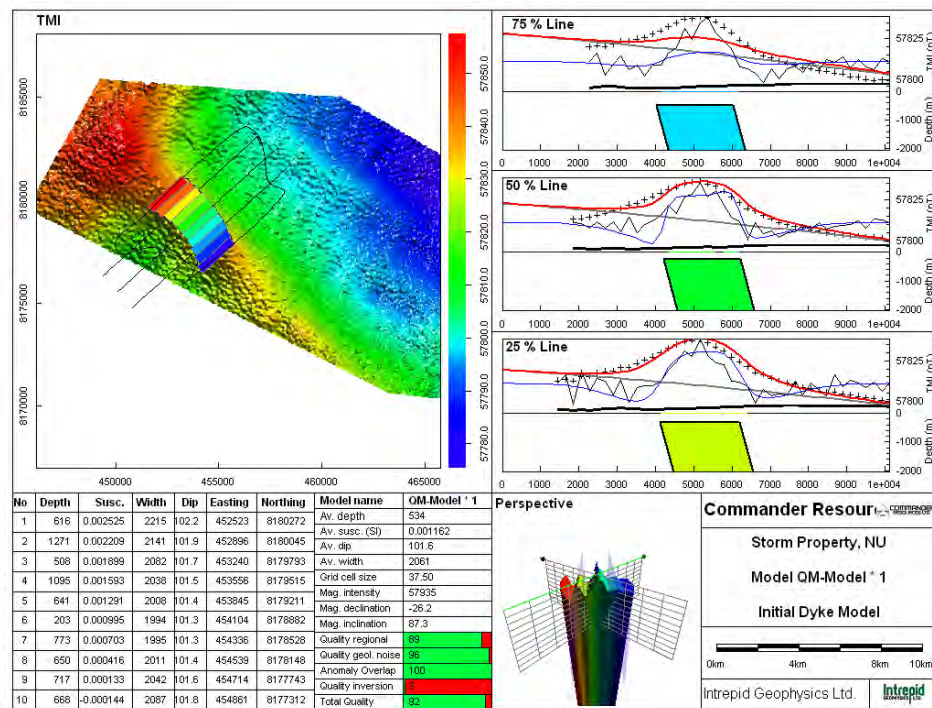


Figure 17 QuickMag model – SE dyke feature

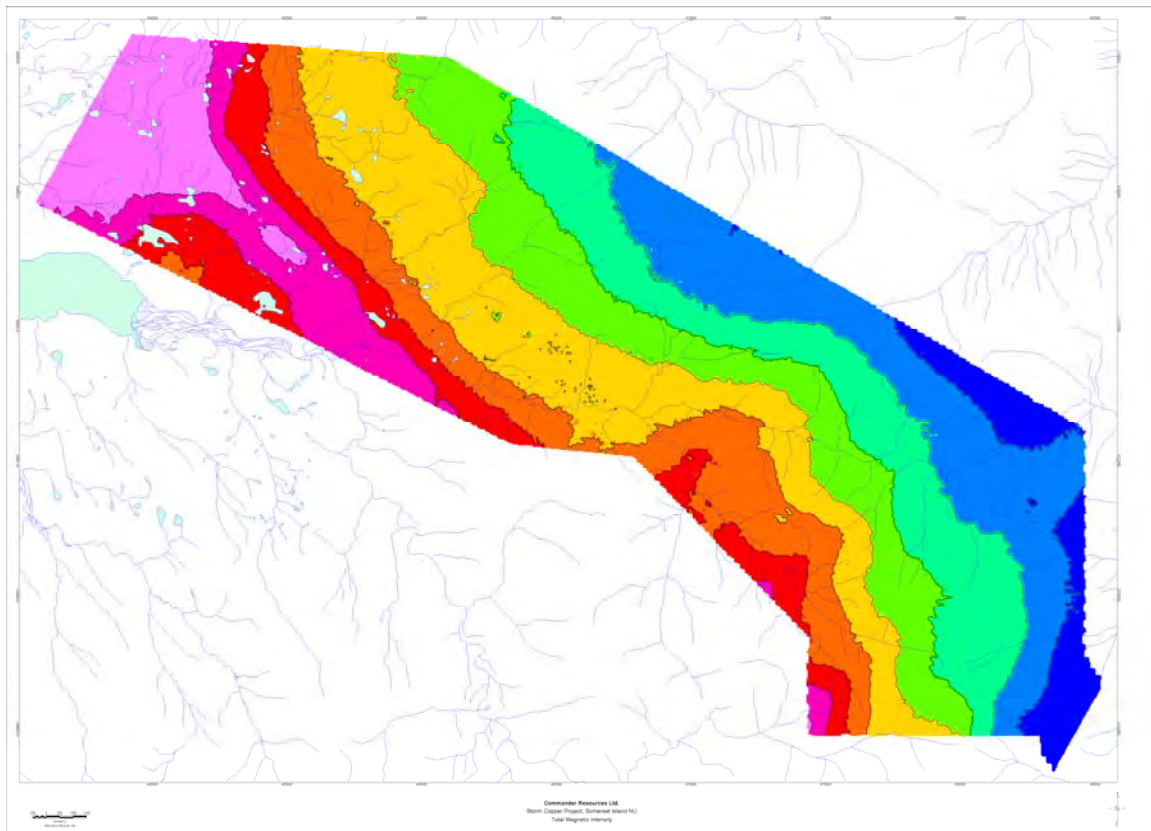


Figure 18. Unsupervised Classification of Magnetic Intensity

A combination of the total horizontal and tilt derivative are typically suitable for mapping shallow basement structure and mineral exploration targets; they have distinct advantages over many

conventional derivatives. The total horizontal derivative provides an effective alternative to the vertical derivative to map continuity of structures and enhance magnetic fabric. The advantages of the tilt derivative are its abilities to normalize a magnetic field image and to discriminate between signal and noise.

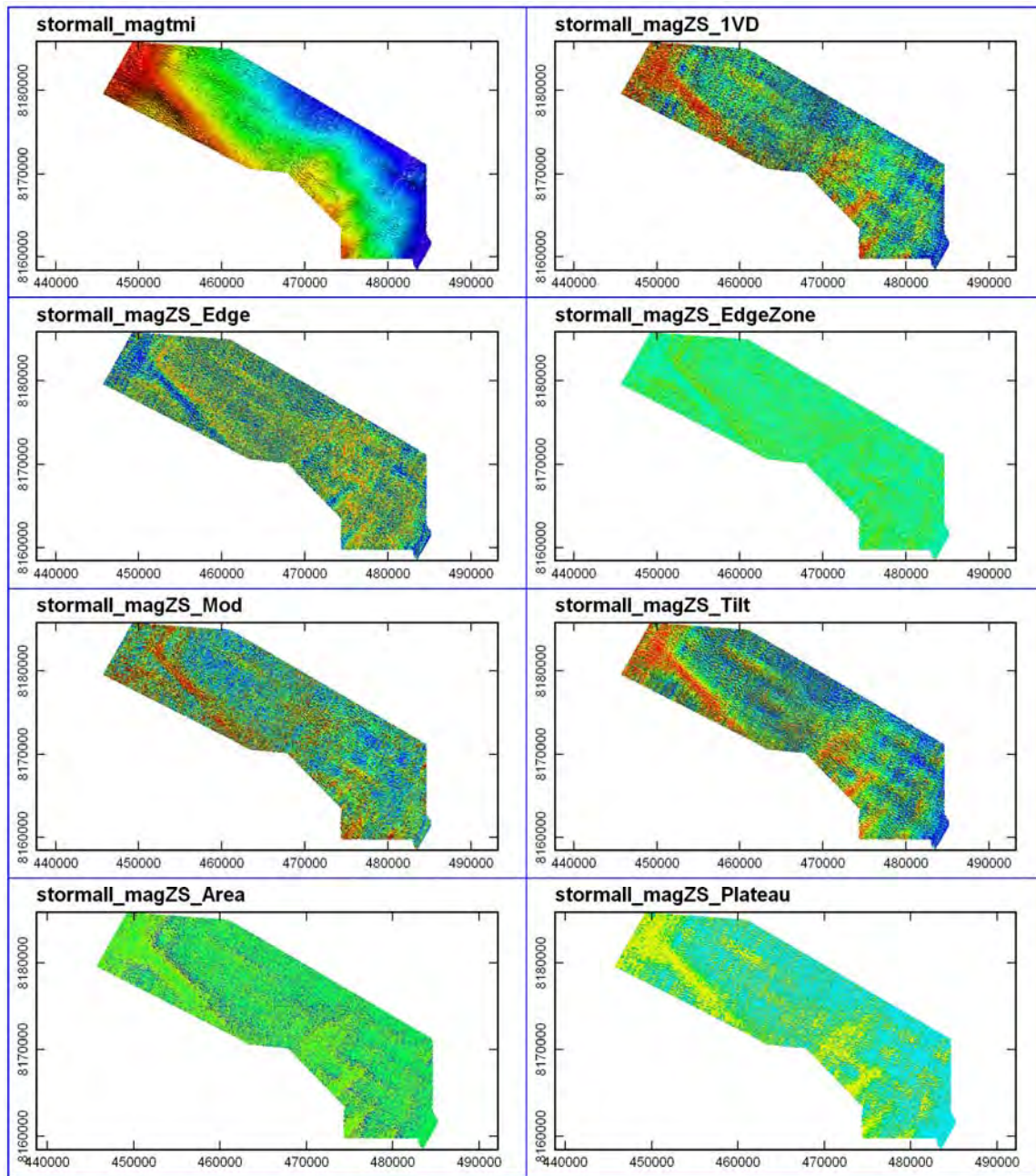


Figure 19. ZS Filter (magnetics) mosaic

Additionally, a suite of filters known as the 'ZS' filters¹⁷ (after Zhiqun Shi, the primary author of this development) were employed and are depicted in summary form on Figure 19 above. Two types of filters have been developed for the purpose of enhancing weak magnetic anomalies from

¹⁷ Shi, Z. and Butt, G., 2004, New enhancement filters for geological mapping, Extended Abstracts, ASEG 17th Geophysical Conference and Exhibition, Sydney 2004.

near-surface sources while simultaneously enhancing low-amplitude, long-wavelength magnetic anomalies from deep-seated or regional sources. The Edge filter group highlights edges surrounding both shallow and deeper magnetic sources. The results are used to infer the location of the boundaries of magnetized lithologies. The Block filter group has the effect of transforming the data into 'zones' which, similar to image classification systems, segregate anomalous zones into apparent lithological categories. Both filter groups change the textural character of a dataset and thereby facilitate interpretation of geological structures.

4.2.1. Multiscale edge analysis

The analysis of lineaments is of fundamental importance to understanding geological structures and the stress regimes in which they are produced. Automatic analysis of lineaments has previously been done with information mapped from remotely sensed data, using either satellite-based imagery or aerial photographs. Potential field data may also be analyzed in terms of their lineament content. Edge detection and automatic trend analysis using gradients in such data are methods for producing unbiased estimates of sharp lateral changes in physical properties of rocks. The assumption is made that the position of the maxima in the horizontal gradient of gravity or magnetic data represents the edges of the source bodies, although this should be used with caution. Such maxima can be detected and mapped as points, providing the interpreter with an unbiased estimate of their positions. The process of mapping maxima as points can be extended to many different levels of upward continuation, thus providing sets of points that can be displayed in three dimensions, using the height of upward continuation as the z-dimension. There have been recent developments and use of this method for interpretation of potential field data (e.g. Archibald *et al*, 1999¹⁸ and Hornby *et al*, 1999¹⁹). Archibald (1999) refers to this process as 'multiscale edge analysis.'

In multiscale edge analysis the assumption is made that lower levels of upward continuation map near-surface sources while higher levels of continuation map deeper sources. This assumption is generally true but must be treated with caution, due to the non-uniqueness of potential field solutions. The INTREPID software's unique implementation of multiscale edge analysis includes the use of Euler 'worms' which provide a view of structural geology obtained directly from potential field geophysical data. The method is based on Fourier techniques for continuation, reduction to pole and total horizontal derivatives coupled with automatic edge detection.

¹⁸ Archibald, N., Gow, P. and Boschetti, F., 1999, Multiscale edge analysis of potential field data: Exploration Geophysics, 30, 38-44.

¹⁹ Hornby, P., Boschetti, F. and Horowitz, F.G., 1999, Analysis of potential field data in the wavelet domain: Geophysical Journal International, 137, 175-196.

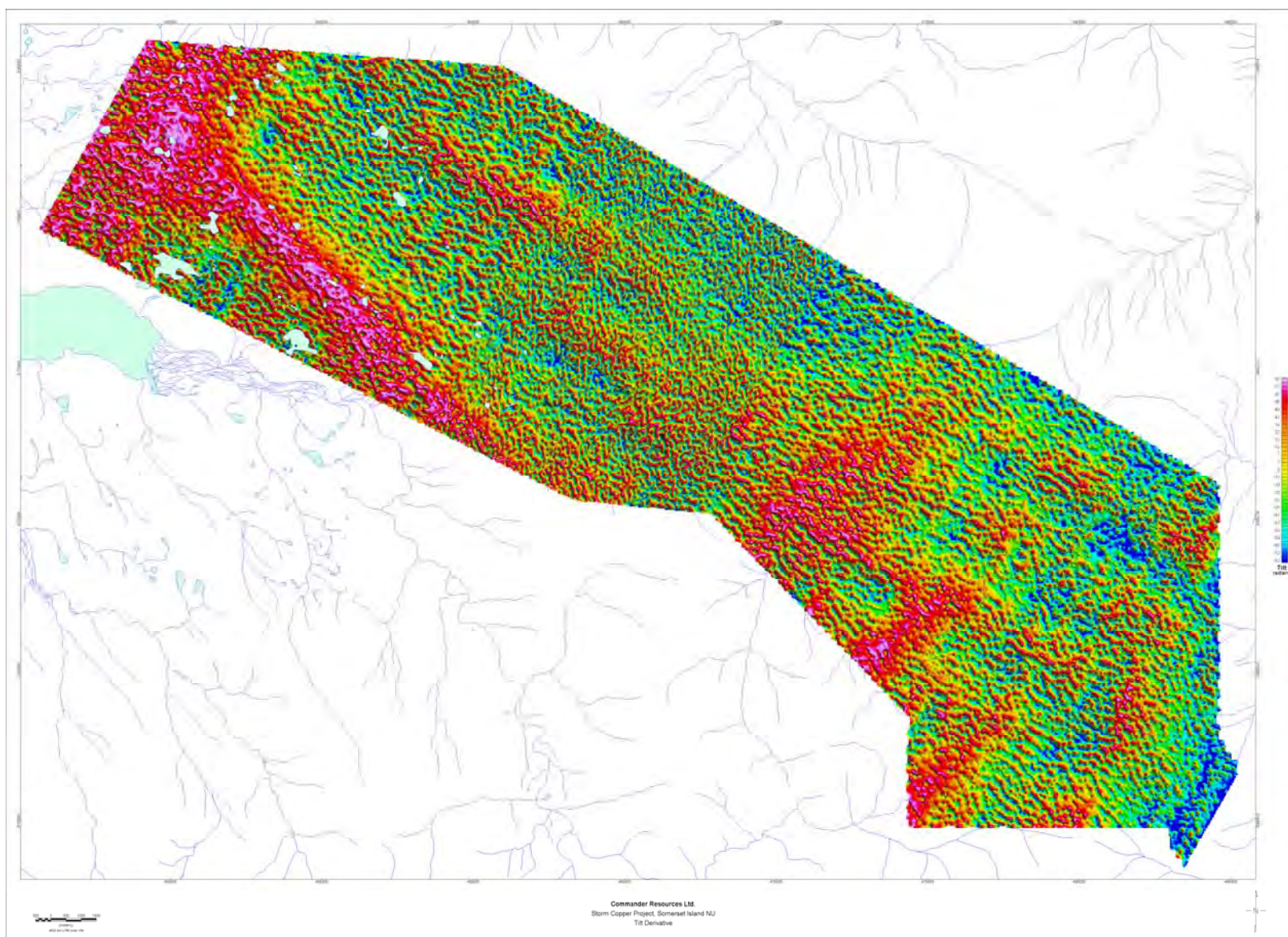


Figure 20. ZS Filter: Tilt Derivative

The tilt derivative above provides a substitute for both the vertical derivative and the high-frequency band pass residual anomaly.

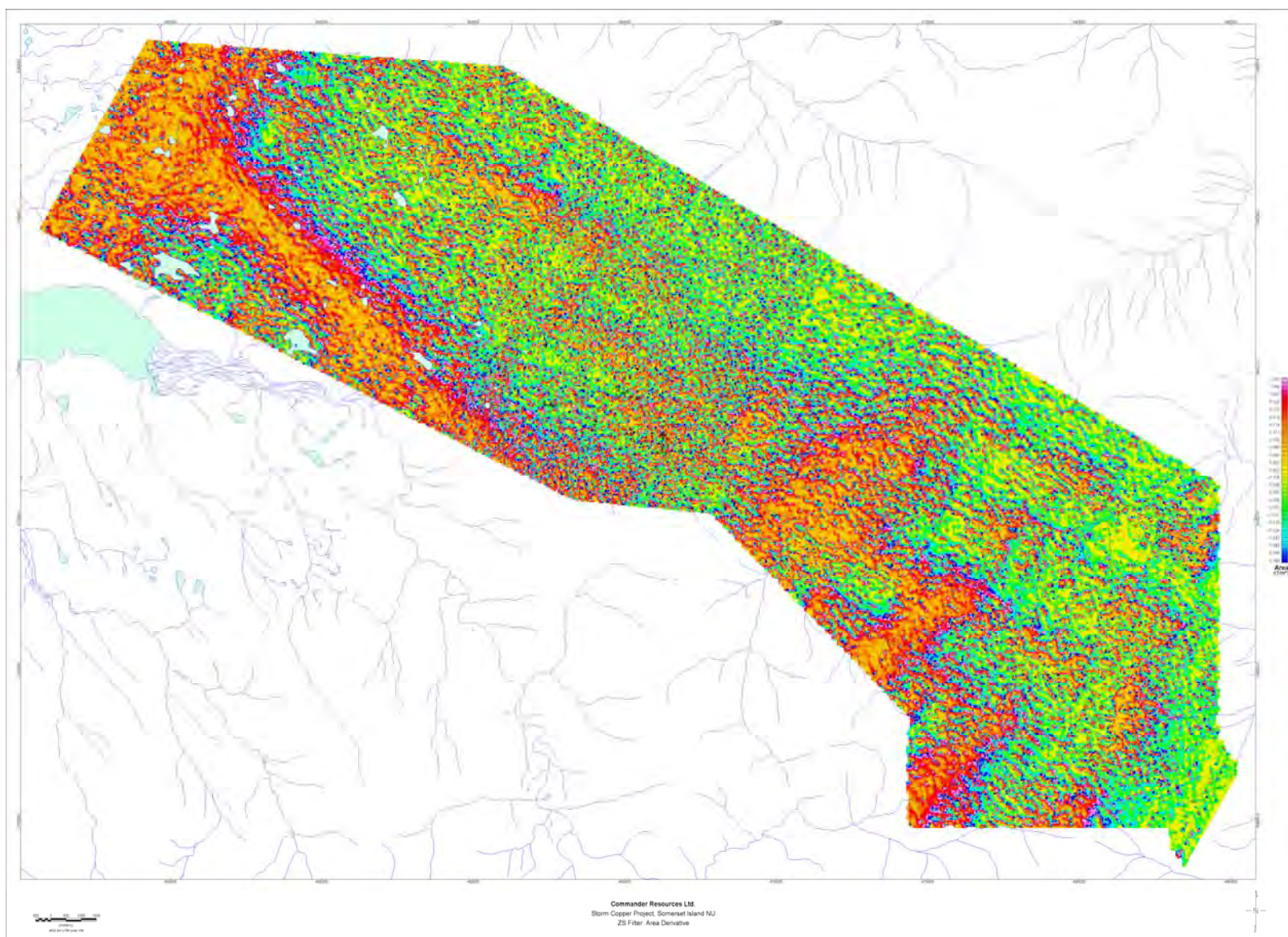


Figure 21. ZS Filter: Area Derivative

The 'Area' filter above serves to effectively segregate anomalous zones into apparent lithological categories.

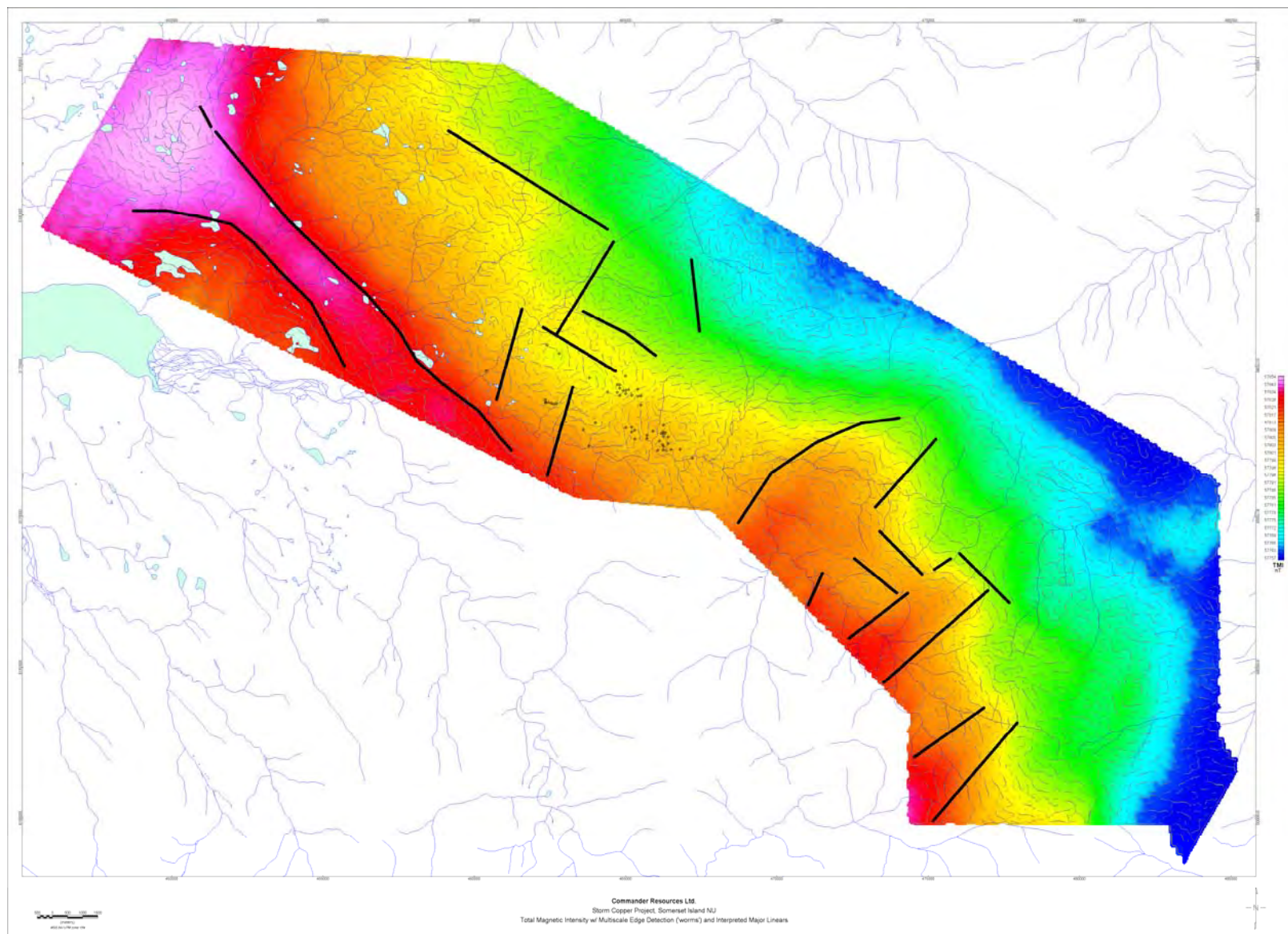


Figure 22. Multiscale edge detection ('worms') with interpreted major linears

Multiscale edge detection ('worms') with interpreted major linears from analysis of all derivatives, superimposed on magnetic intensity.

4.3. Electromagnetics

The airborne electromagnetic images are dominated by obvious, positive zones at the western-most extents of the survey; these are interpreted as broad, formational type responses and are very likely due at least in part to salt water incursion into near-surface sediments / bedrock from Aston Bay and Pelly Sound. However, a sharply-defined gradient is seen to extend southeast from these positive zones through the 3500N Zone before 'bending' south-southeast and following the trend of a tributary to the Aston River. The prominent 'edge' mapped by the AEM is interpreted to map or delineate the southern margin of the Central Graben reported by McRobbie *et al* (2000) and later reiterated by Cook and Moreton (2009).

Three pronounced negative zones of AEM response are also seen on this data (following figure); two are approximately elliptical in shape, while the eastern-most zone is elongated. These negative zones are a peculiar phenomena²⁰; sign reversals (negatives) arising from coincident loop time-domain e.m. (such as the VTEM system) can occur when the polarization decay becomes greater than the fundamental inductive response. For most conductivity structures, negatives will not be observed unless the IP chargeability of the ground is exceptionally large. However, in special circumstances the fundamental inductive response is particularly small, and thus negatives can be produced by conductivity structures with geologically feasible chargeabilities. Examples of such circumstances are: in localised zones between inductively interacting conductors, at the edge of overburdens, and over relatively resistive grounds which have a thin polarisable surficial layer. In this case, near-surface polarizable material (e.g., glacial clays) lying over more resistive bedrocks are considered as the being the probable cause of these negative AEM anomalies on the Storm property.

Broad positives and peculiar negatives aside, the principle anomalies of interest occur coincident to the known 4100N, 2750N and 2200N; also responding well to the VTEM system are the ST97-15 and ST99-34 zones; these 5 zones comprise the sole, unambiguous bedrock responses in the entire survey. The 3500N zone does not have a significant positive AEM response, but does lay right along the gradient edge from positive (extended and layered conductive zone) to negative response, apparently at the southern edge of the NW-trending graben. All of these conductive responses are distinguished by a complete lack of direct magnetic correlation.

Based on initial modelling of selected lines, a consecutive series of 41 flight lines over the main Storm copper zone were chosen for detailed resistivity depth imaging (RDI); this work was carried out by Geotech Ltd. using their in-house implementation of the method. This technique is used to rapidly convert EM profile decay data into an equivalent resistivity versus depth cross-section, by deconvolving the measured TEM data. The Resistivity-Depth transformation is based on the apparent resistivity transform of Meju²¹ and the TEM response from a conductive half-space. The program was developed by Alexander Prikhodko of Geotech Ltd., and depth-calibrated based on forward plate modeling using the Maxwell plate modelling software of ElectroMagnetic Imaging Technology Pty. Ltd. (EMIT). Further details of this process are supplied in an appendix to the Geotech logistics report (Appendix A to this report). Basically, the recorded TEM apparent resistivity data are transformed to an effective subsurface resistivity at an approximate exploration depth to yield an almost continuous picture of the resistivity distribution beneath the observational location.

²⁰ Smith, R.S. and G.F., 1988, TEM coincident loop negatives and the loop effect. *Exploration Geophysics*, vol. 19 (1988), p. 354–357

²¹ Meju, M.A., 1998, Short Note: A simple method of transient electromagnetic data analysis. *Geophysics*, vol. 63, no.2, p. 405–410.

The RDIs provide reasonable indications of conductor relative depth and vertical extent, as well as accurate 1D layered-earth apparent conductivity/resistivity structure across VTEM flight lines.

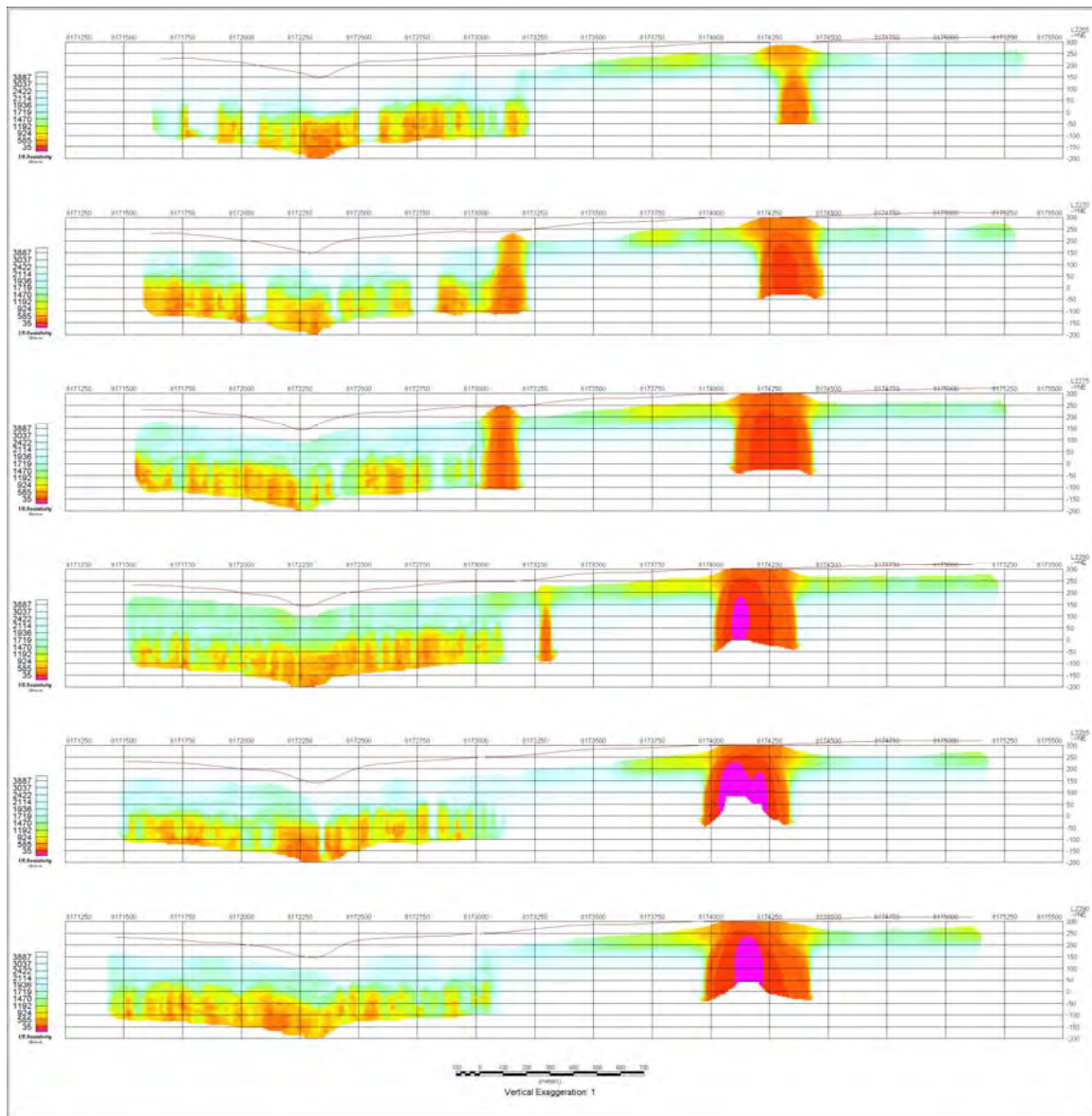


Figure 23. Example of stacked RDIs, Lines 2265-2290 inclusive

The series or stacked set of RDIs above displays 5-6 lines approaching the 4100N Zone from the west; the centre of 4100N Zone itself is shown on L2290 (bottom RDI), with the very conductive response at surface corresponding (more or less) to DDH ST00-60. The individual RDI for L2290 itself is shown on the following image, along with the historical drill collars and subsurface traces.

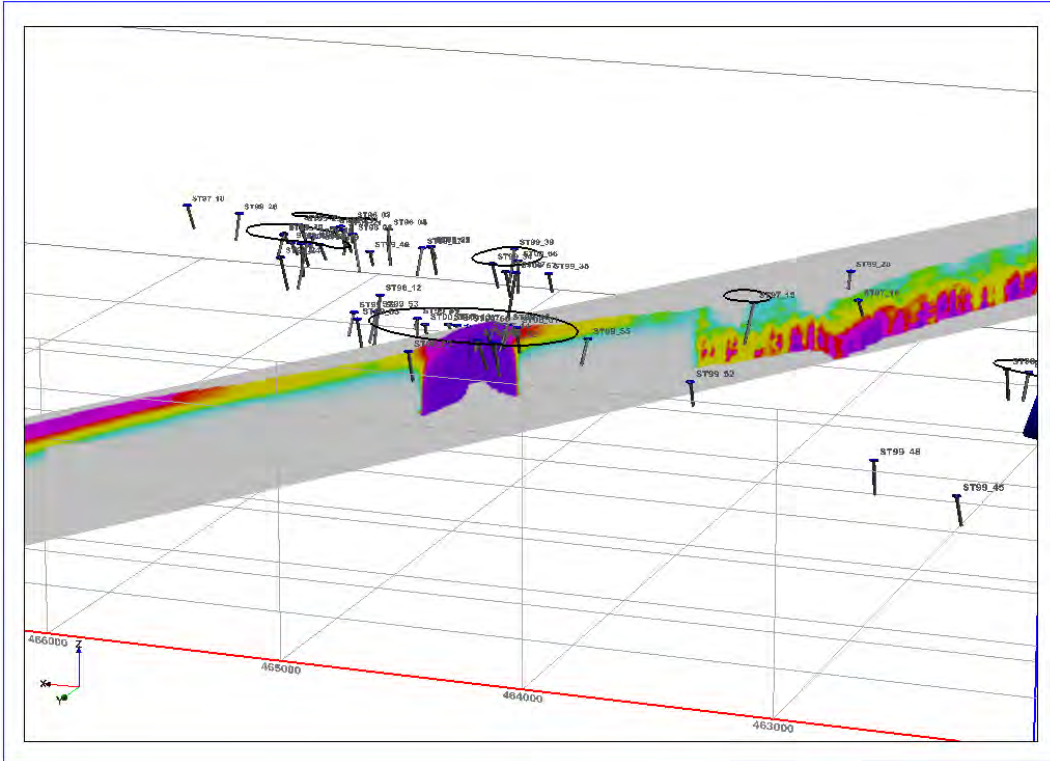


Figure 24. RDI section – Line 2290 looking toward 160° at inclination -15° (drill holes indicated)

The full set of RDIs are then gridded in a 3-dimensional context to produce a voxel model (a 3-dimensional solid representation of the Earth's apparent resistivity). Example results of this process are displayed following.

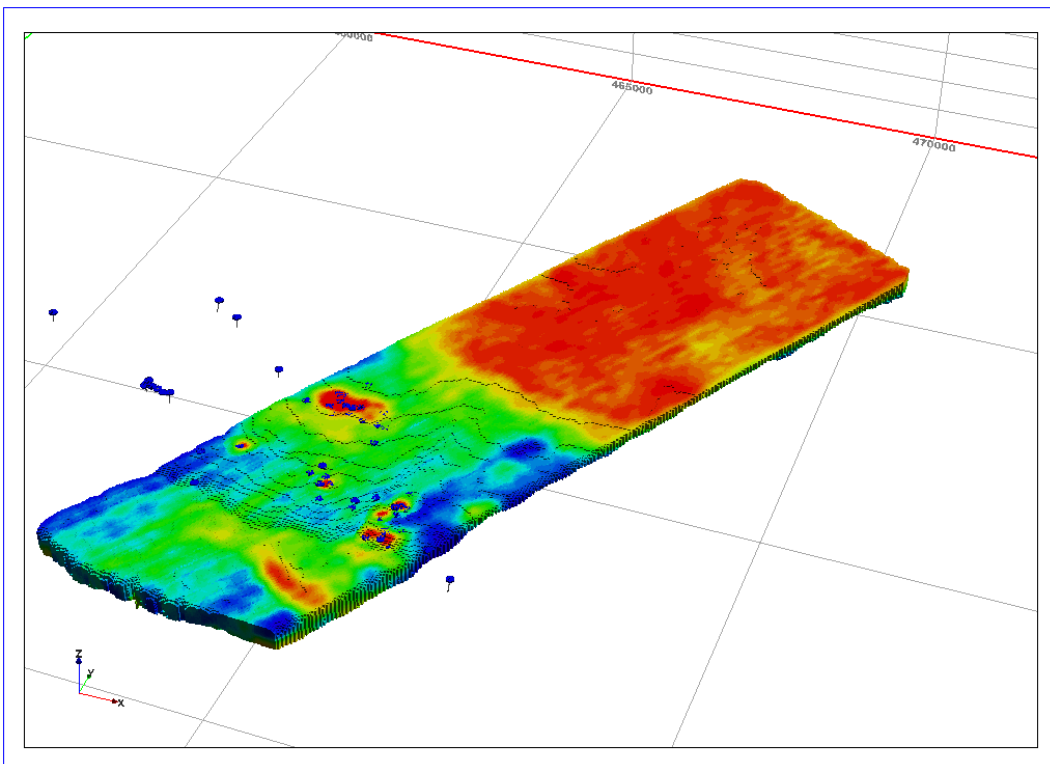


Figure 25. RDI voxel – overview using reverse colour lookup (red denotes higher conductivity)

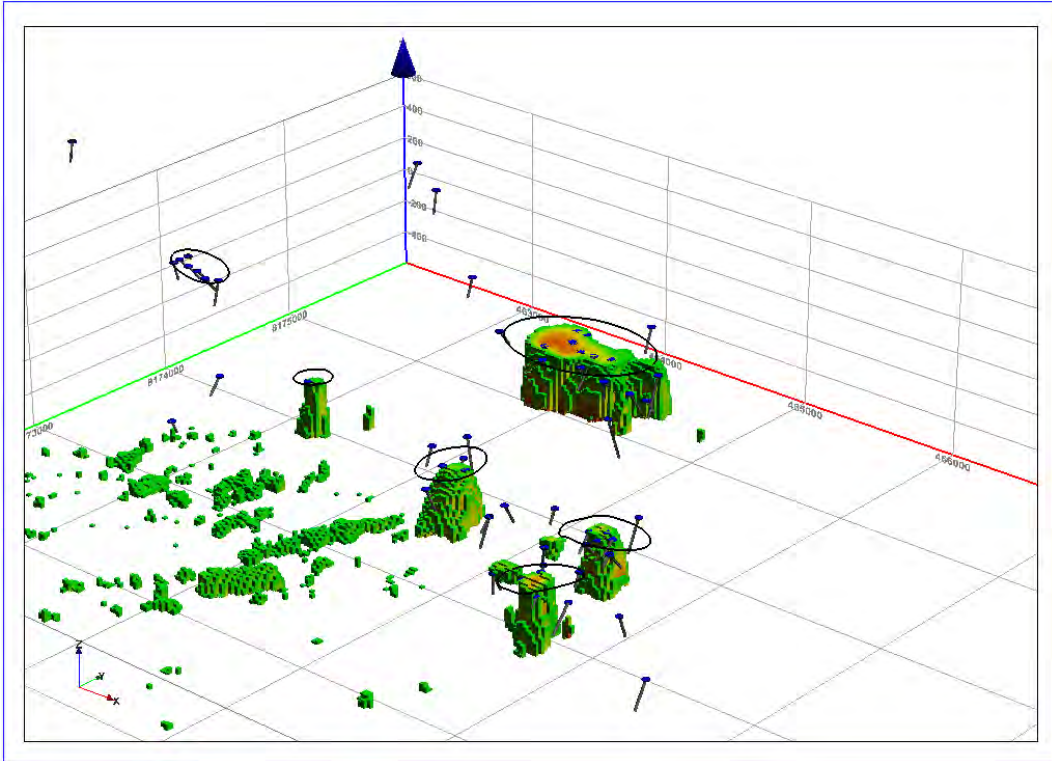


Figure 26. RDI – close-in view toward 320° and inclination -25° with RDI clipped to 500 ohm-m maximum

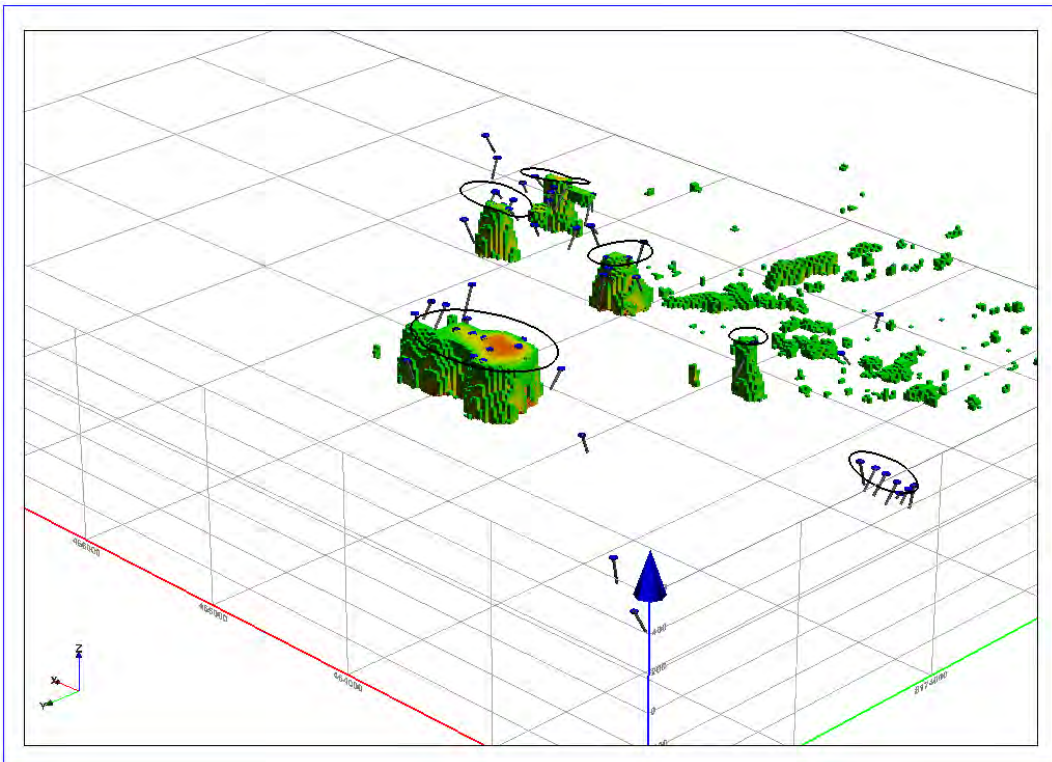


Figure 27. RDI – close-in view toward 135° and inclination -25° with RDI clipped to 500 ohm-m maximum

Analysis of the RDI inversions in conjunction with the historical drilling suggests that there remain portions of the 4100N, ST97-15, ST99-34 and 2200N Zones in particular, that have not been drill

tested adequately. Further, the deep (100 to 200 m below sea level) conductive trends shown to be extending southward from the 4100N Zone have not been tested at all.

Additional modeling using the Maxwell plate modelling software should permit precise drill targeting for these bodies; this is currently being undertaken but will not be included in this report due to time constraints (assessment filing deadlines).

Notwithstanding the lack or absence of unambiguous bedrock conductors removed from the above, drilled zones, 9 target 'areas of interest' are identified on the following image as A-I; without exception, all represent primarily surficial or near-surface conductivity with very weak mid-time decays (and little or no late-time decays). These targets do not have similar characteristics to the main Storm zones discussed above, but nonetheless present themselves as possible areas for ground follow-up and geochemical sampling. They may reflect sulphides deficient in copper, or sulphides dominant in zinc and/or lead mineralization and thus not amenable to direct detection by electromagnetic methods.

| ID | Xnutm15nad83 | Ynutm15nad83 |
|----|--------------|--------------|
| A | 472700 | 8170375 |
| D | 461055 | 8184305 |
| E | 457600 | 8181900 |
| C | 467636 | 8180289 |
| B | 462101 | 8176193 |
| F | 453330 | 8185405 |
| G | 452640 | 8184185 |
| H | 451485 | 8185280 |
| I | 484100 | 8166650 |

Table 2. VTEM Secondary 'areas of interest'

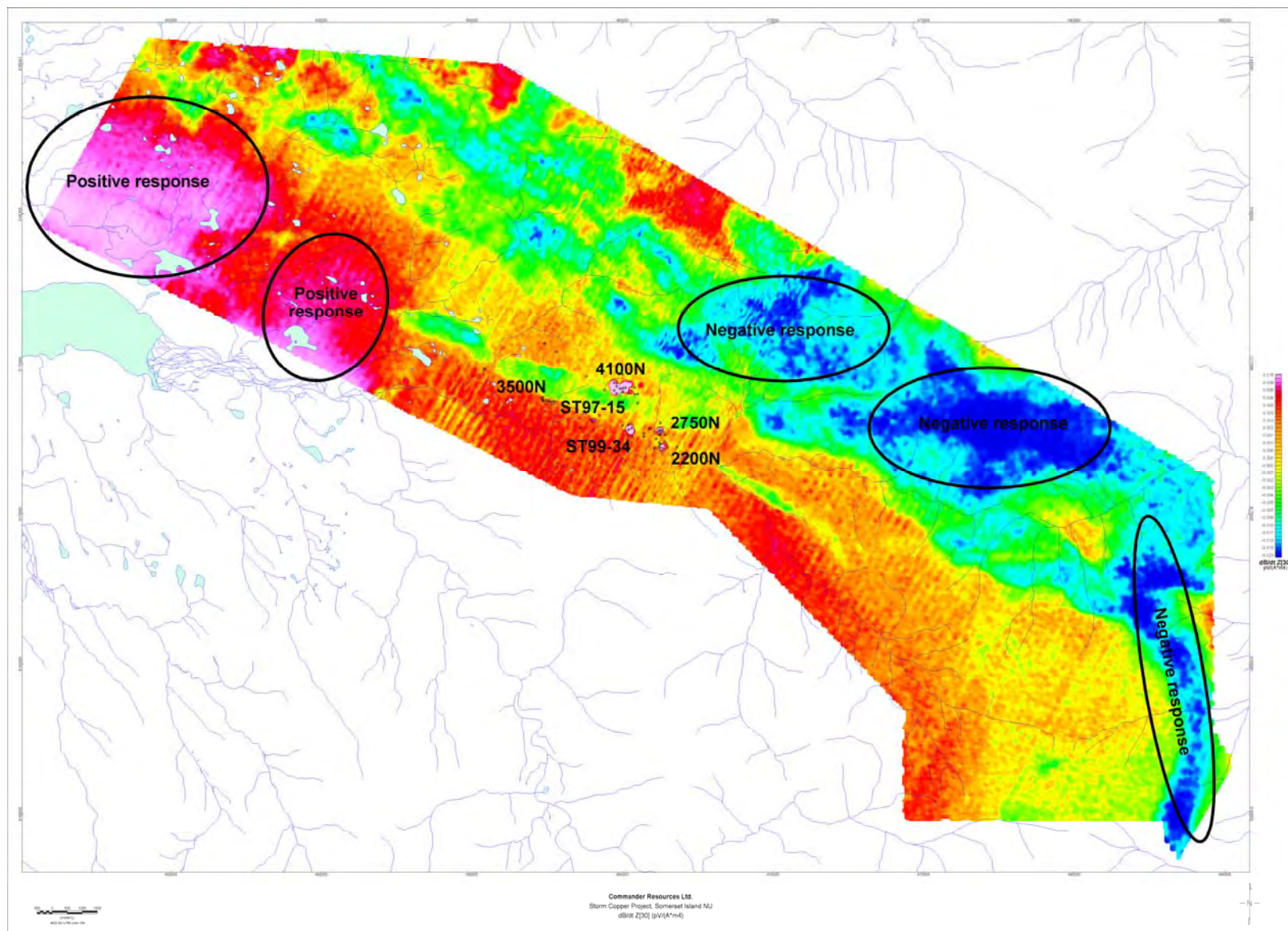


Figure 28. dB/dt Z[30] pseudocolour image with anomalous zones indicated

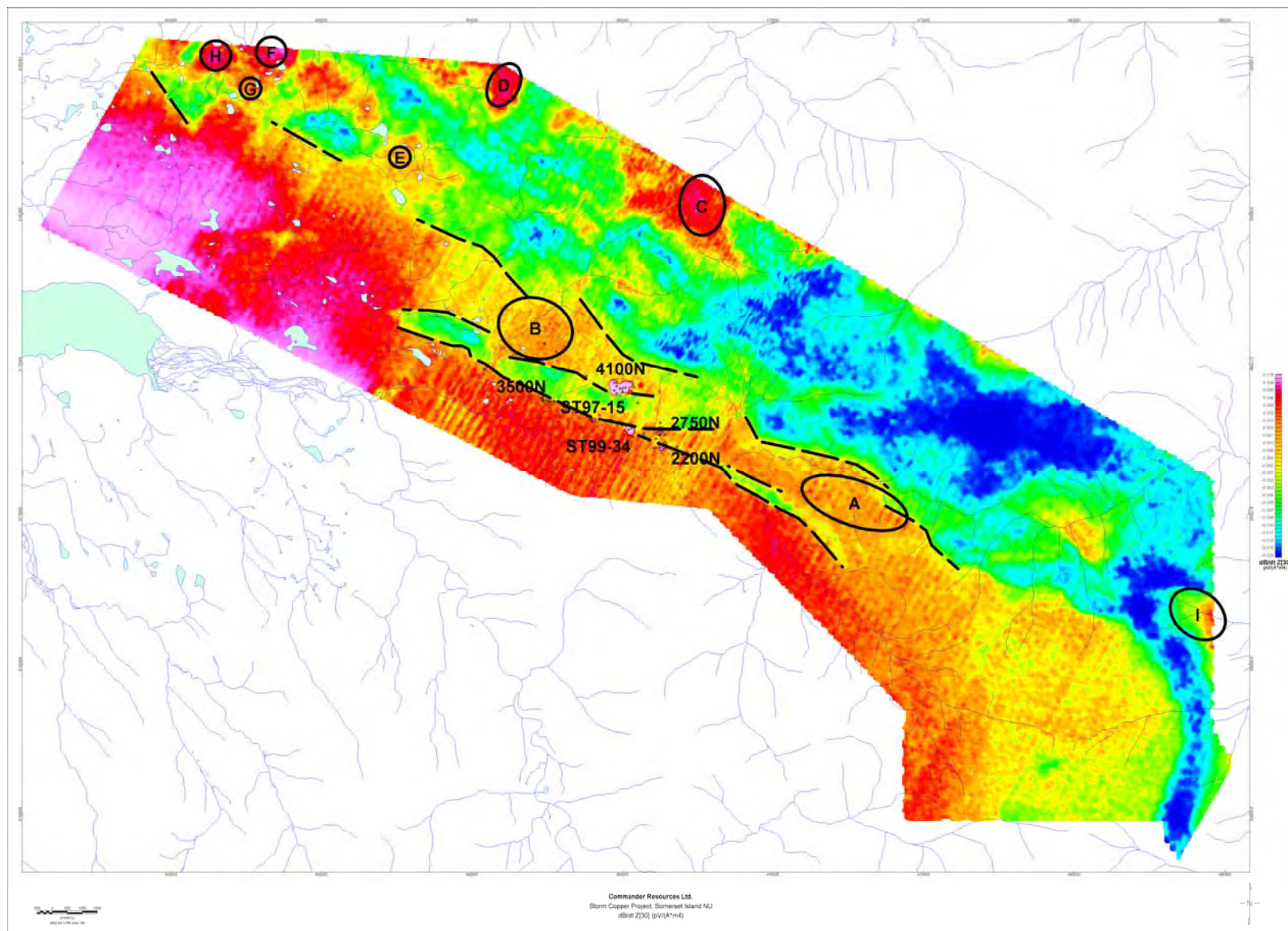


Figure 29. dB/dt Z[30] pseudocolour image with prospective target zones indicated

5. Conclusions and Recommendations

A helicopter-borne electromagnetic and magnetic survey was flown by Geotech Ltd. in July 2011 over the Storm Property on Somerset Island, Nunavut; the survey is comprised of ~3,970 line-kilometres of data acquired on a grid pattern of 300 and 150 m spaced traverses oriented at N030°E, controlled by 1,500 m spaced tie lines oriented at right angles toward N120°E. The electromagnetic technology utilized is Geotech's *VTEM Plus* time-domain system in a towed-loop configuration. Products obtained from this airborne geophysical survey include the total magnetic intensity, calculated (magnetic) vertical derivative, dB/dt and B-field both X- and Z-components, both dB/dt and B-field calculated Time Constants Tau, and a digital elevation model. Resistivity depth imaging (RDI) sections and apparent resistivity depth slices were also subsequently supplied as part of the interpretation phase of this project. A geosoft-format database of the profile data, as well as grids of total magnetic intensity, calculated vertical derivative, a single mid-time B-field Z-axis component, dB/dt and B-field time constants and the digital elevation model were provided by the contractor.

Enhanced derivative grids of the magnetics were generated and imaged as part of this study and which have highlighted a limited number of structural orientations and trends. The aeromagnetic data is primarily reflecting very long wavelength, buried features believed to be sourced in the Proterozoic basement at some depth; a high-frequency, shallow component is, however, evident throughout and is possibly related to detrital materials themselves related to variation in sea levels. Significant linears are mapped based upon analysis of all derivatives; these are interpreted as most likely occurring within the sedimentary section (based on frequency content) and may be related to equivalent horizons to the known Storm copper zones. These features are presented as possible structural controls impacting the stratiform sulphide mineralization.

The principle airborne electromagnetic anomalies of interest occur coincident to the known 4100N, 2750N and 2200N zones; also responding well to the VTEM system are the ST97-15 and ST99-34 zones; these 5 zones comprise the sole, unambiguous bedrock responses in the entire survey. The 3500N zone does not have a significant positive AEM response, but does lay right along the gradient edge from positive (extended and layered conductive zone) to negative response, apparently at the southern edge of the NW-trending graben. All of these conductive responses are distinguished by a complete lack of direct magnetic correlation.

Based on initial test modelling of selected lines, a consecutive series of 41 flight lines over the main Storm copper zone were chosen for detailed resistivity depth imaging (RDI) by the airborne contractor; results were provided as section images and grids for each line as well as a 3D voxel model of the apparent resistivity. This data was analyzed in 3D using Encom PA (visualization and interpretation software). Analysis of the RDI inversions in conjunction with the historical drilling suggests that there remain portions of the 4100N, ST97-15, ST99-34 and 2200N Zones that have not been drill tested adequately. Further, the deep (100 to 200 m below sea level) conductive trends shown to be extending southward from the 4100N Zone have not been tested at all. Additional modeling of the VTEM data using the Maxwell plate modelling software should permit precise drill targeting for these bodies.

Notwithstanding the lack of absence of unambiguous bedrock conductors removed from the above, and drilled zones, 9 target 'areas of interest' are identified on the following image as A-I; without exception, all represent primarily surficial or near-surface conductivity with very weak mid-time decays. These targets do not have similar characteristics to the main Storm zones discussed above, but nonetheless present themselves as possible areas for ground follow-up and geochemical sampling. They may reflect sulphides deficient in copper, or sulphides dominant in zinc and/or lead mineralization and thus not amenable to direct detection by electromagnetics.

A program of geological prospecting, sampling and ground geophysics consisting of 3D induced polarization / resistivity is recommended to further delineate the conductive zones and possible identify disseminated sulphides which in turn could indicate anomalous Cu mineralization.

All targets and zones or areas of interest are supplied separately to Commander Resources Ltd. as Mapinfo *.tab files with accompanying annotation and geo-referencing.

6. Certificate of Professional Qualifications

I, Christopher J. Campbell, with business address of 4505 Cove Cliff Road, North Vancouver British Columbia V7G 1H7, hereby certify that:

- ◆ I am a graduate (1972) of the University of British Columbia, with a Bachelor of Science degree in Geophysics.
- ◆ I am a graduate (1986) of the University of Denver, with a Masters of Business Administration.
- ◆ I am a registered member in good standing of the Association of Professional Engineers and Geoscientists of British Columbia.
- ◆ I have practiced my profession for approximately thirty-nine years in Canada (British Columbia, Alberta, Saskatchewan, Manitoba, Ontario, Quebec, Newfoundland/Labrador, Yukon and Northwest Territories / Nunavut), United States of America, Australia, Russia, and Africa.
- ◆ I have no interest, direct or indirect, in the properties or securities of Commander Resources Ltd., or in any of their related companies or joint venture partners anywhere in Canada.

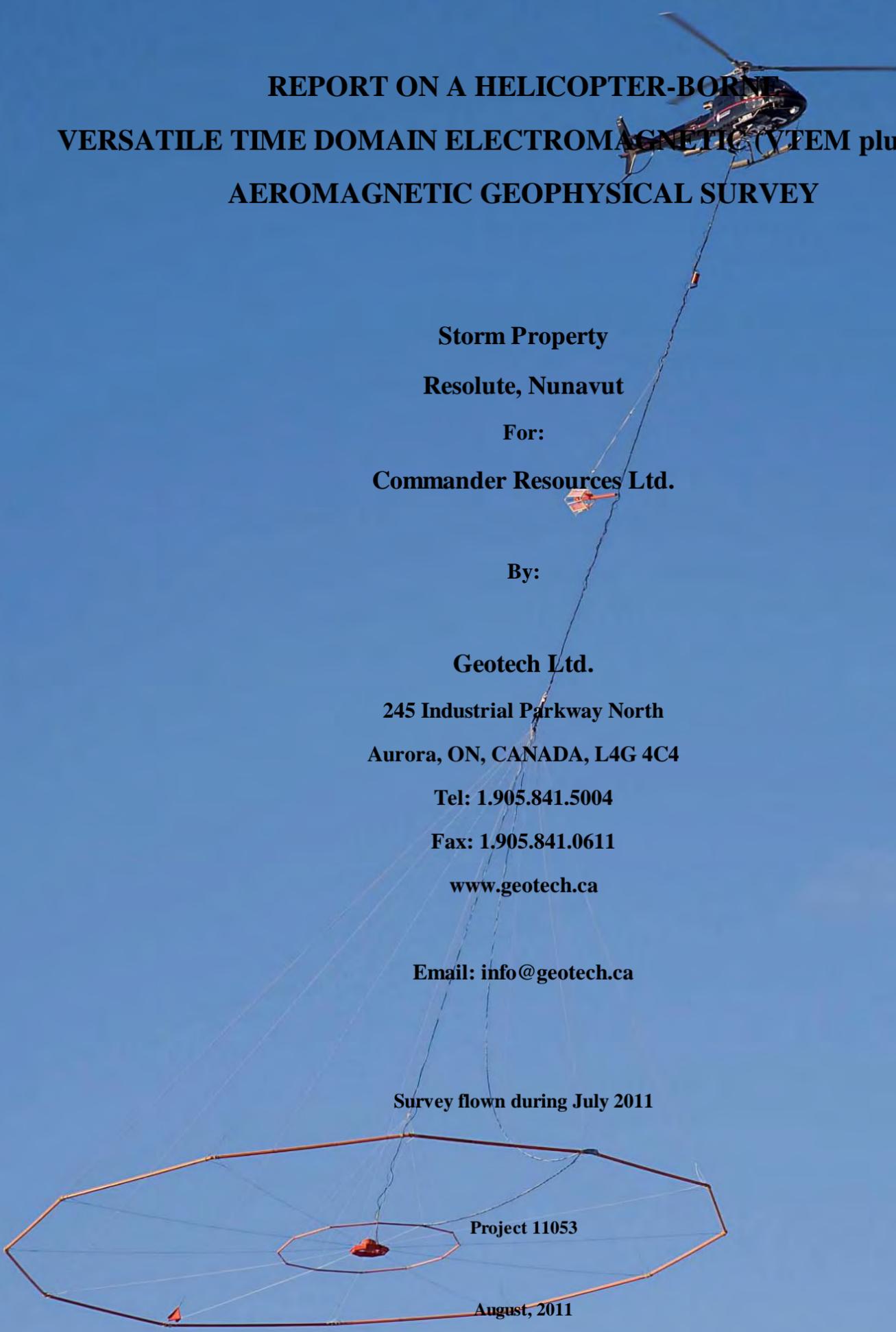
Dated this day November 18, 2011 in North Vancouver, British Columbia.



Christopher J. Campbell, P. Geo.

Appendix A

Airborne Contractor's Logistics and Processing Report



**REPORT ON A HELICOPTER-BORNE
VERSATILE TIME DOMAIN ELECTROMAGNETIC (VTEM plus) AND
AEROMAGNETIC GEOPHYSICAL SURVEY**

**Storm Property
Resolute, Nunavut**

**For:
Commander Resources Ltd.**

**By:
Geotech Ltd.
245 Industrial Parkway North
Aurora, ON, CANADA, L4G 4C4
Tel: 1.905.841.5004
Fax: 1.905.841.0611
www.geotech.ca**

Email: info@geotech.ca

Survey flown during July 2011

Project 11053

August, 2011

TABLE OF CONTENTS

| | |
|---|-----------|
| Executive Summary | ii |
| 1. INTRODUCTION | 1 |
| 1.1 General Considerations | 1 |
| 1.2 Survey and System Specifications..... | 2 |
| 1.3 Topographic Relief and Cultural Features..... | 3 |
| 2. DATA ACQUISITION | 4 |
| 2.1 Survey Area | 4 |
| 2.2 Survey Operations | 4 |
| 2.3 Flight Specifications..... | 6 |
| 2.4 Aircraft and Equipment..... | 6 |
| 2.4.1 Survey Aircraft | 6 |
| 2.4.2 Electromagnetic System | 6 |
| 2.4.3 Airborne magnetometer..... | 10 |
| 2.4.4 Radar Altimeter | 10 |
| 2.4.5 GPS Navigation System | 10 |
| 2.4.6 Digital Acquisition System..... | 10 |
| 2.5 Base Station | 11 |
| 3. PERSONNEL | 12 |
| 4. DATA PROCESSING AND PRESENTATION | 13 |
| 4.1 Flight Path..... | 13 |
| 4.2 Electromagnetic Data..... | 13 |
| 4.3 Magnetic Data..... | 14 |
| 5. DELIVERABLES..... | 16 |
| 5.1 Survey Report..... | 16 |
| 5.2 Maps..... | 16 |
| 5.3 Digital Data | 16 |
| 6. CONCLUSIONS AND RECOMMENDATIONS | 21 |
| 6.1 Conclusions | 21 |
| 6.2 Recommendations | 21 |

LIST OF FIGURES

| | |
|--|-----------|
| FIGURE 1 - PROPERTY LOCATION | 1 |
| FIGURE 2 - SURVEY AREAS LOCATION ON GOOGLE EARTH | 2 |
| FIGURE 3 - FLIGHT PATH OVER A GOOGLE EARTH IMAGE – STORM PROPERTY..... | 3 |
| FIGURE 4 - VTEM PLUS CONFIGURATION, WITH MAGNETOMETER. | 7 |
| FIGURE 5 - VTEM PLUS WAVEFORM & SAMPLE TIMES..... | 7 |
| FIGURE 6 - VTEM PLUS SYSTEM CONFIGURATION..... | 9 |
| FIGURE 7 - Z, X AND FRASER FILTERED X (FFX) COMPONENTS FOR “THIN” TARGET..... | 14 |

LIST OF TABLES

| | |
|---|-----------|
| TABLE 1 - SURVEY SPECIFICATIONS..... | 4 |
| TABLE 2 - SURVEY SCHEDULE | 4 |
| TABLE 3 - DECAY SAMPLING SCHEME..... | 8 |
| TABLE 4 - ACQUISITION SAMPLING RATES | 10 |
| TABLE 5 - GEOSOFTE GDB DATA FORMAT..... | 17 |

APPENDICES

| | |
|--|--|
| A. Survey location maps..... | |
| B. Survey Block Coordinates..... | |
| C. VTEM Waveform..... | |
| D. Geophysical Maps | |
| E. Generalized Modelling Results of the VTEM System..... | |
| F. EM Time Constant (TAU) Analysis | |
| G. TEM Resistivity Depth Imaging (RDI) | |

REPORT ON A HELICOPTER-BORNE VERSATILE TIME DOMAIN ELECTROMAGNETIC (VTEM plus) and AEROMAGNETIC SURVEY

Storm Property
Resolute, Nunavut

Executive Summary

During July 6th to July 24th, 2011 Geotech Ltd. carried out a helicopter-borne geophysical survey over the Storm Property situated approximately 107 kilometres southeast of Resolute, Nunavut.

Principal geophysical sensors included a versatile time domain electromagnetic (VTEM plus) system, and a caesium magnetometer. Ancillary equipment included a GPS navigation system and a radar altimeter. A total of 3819.7 line-kilometres of geophysical data were acquired during the survey.

In-field data quality assurance and preliminary processing were carried out on a daily basis during the acquisition phase. Preliminary and final data processing, including generation of final digital data and map products were undertaken from the office of Geotech Ltd. in Aurora, Ontario.

The processed survey results are presented as the following maps:

- Electromagnetic stacked profiles of the B-field Z Component,
- Electromagnetic stacked profiles of dB/dt Z Components,
- Colour grids of a B-Field Z Component Channel,
- Total Magnetic Intensity (TMI), and
- EM Time-constant dB/dt Z Component (Tau), are presented.

Digital data includes all electromagnetic and magnetic products, plus ancillary data including the waveform.

The survey report describes the procedures for data acquisition, processing, final image presentation and the specifications for the digital data set.

1. INTRODUCTION

1.1 General Considerations

Geotech Ltd. performed a helicopter-borne geophysical survey over the Storm Property situated approximately 107 kilometres southeast of Resolute, Nunavut (Figure 1 & Figure 2).

Gordon Davidson represented Commander Resources Ltd. during the data acquisition and data processing phases of this project.

The geophysical surveys consisted of helicopter borne EM using the versatile time-domain electromagnetic (VTEM plus) system with Z and X component measurements and aeromagnetics using a caesium magnetometer. A total of 3819.7 line-km of geophysical data were acquired during the survey.

The crew was based out of Resolute Bay (Figure 2) in Nunavut for the acquisition phase of the survey. Survey flying started on July 6th and was completed on July 24th, 2011.

Data quality control and quality assurance, and preliminary data processing were carried out on a daily basis during the acquisition phase of the project. Final data processing followed immediately after the end of the survey. Final reporting, data presentation and archiving were completed from the Aurora office of Geotech Ltd. in August, 2011.

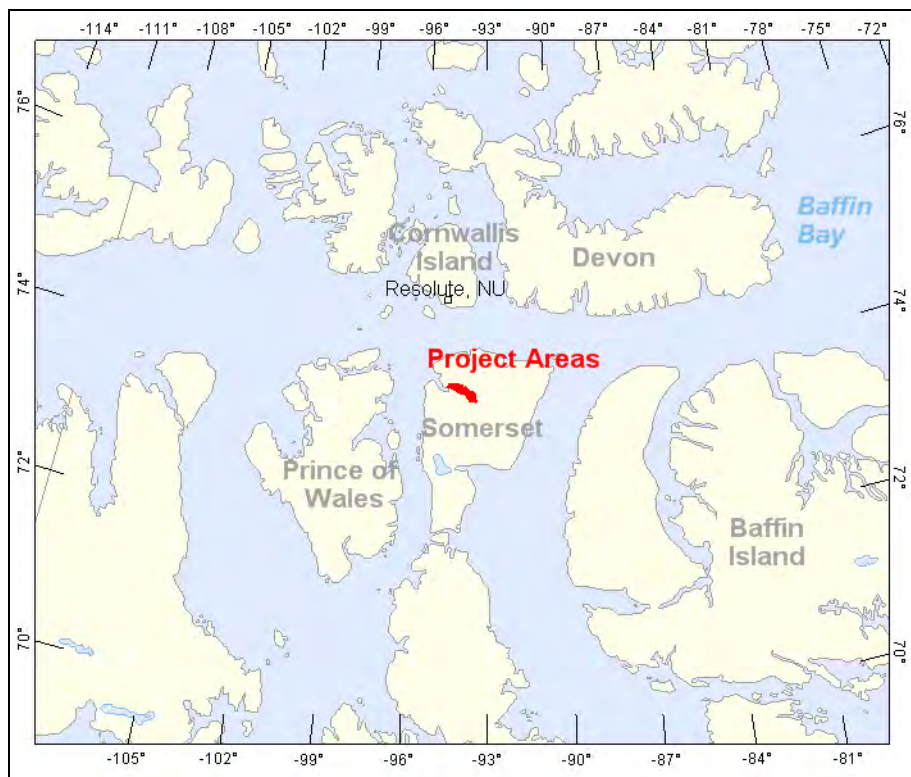


Figure 1 - Property Location

1.2 Survey and System Specifications

The Storm Property is located approximately 107 kilometres southeast of Resolute, Nunavut (Figure 2).



Figure 2 - Survey areas location on Google Earth

The survey block was flown in a southwest to northeast ($N 30^{\circ} E$ azimuth) direction, with traverse line spacing of 150 metres and 75 metres for the Infills as depicted in Figure 3. Tie lines were flown perpendicular to the traverse lines ($N 120^{\circ} E$ azimuth) at a spacing of 1500 metres respectively. For more detailed information on the flight spacing and direction see Table 1.

1.3 Topographic Relief and Cultural Features

Topographically, the Storm Property exhibits a shallow relief with an elevation ranging from 39 to 395 metres above mean sea level over an area of 430 square kilometres (Figure 3).

The survey block has various rivers and streams running through the survey area which connect various lakes. There are no visible signs of culture located in the survey area.

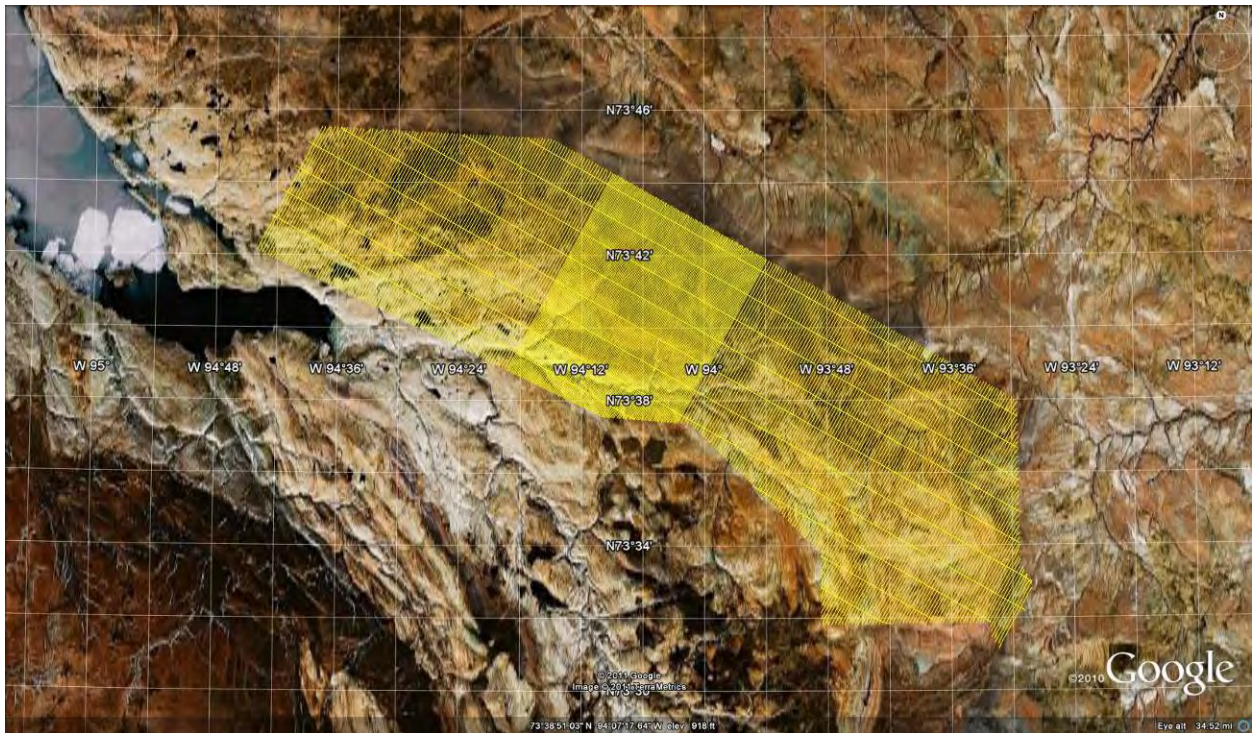


Figure 3 - Flight path over a Google Earth Image – Storm Property

The survey area is covered by NTS (National Topographic Survey) of Canada sheets 058C10, 058C11 and 058C14.

2. DATA ACQUISITION

2.1 Survey Area

The survey block (see Figure 3 and Appendix A) and general flight specifications are as follows:

Table 1 - Survey Specifications

| Survey block | Traverse Line spacing (m) | Area (Km ²) | Planned ¹ Line-km | Actual Line-km | Flight direction | Line numbers |
|----------------|---------------------------|-------------------------|------------------------------|----------------|---------------------|---------------|
| Storm Property | Traverse: 150 | 430 | 3186.6 | 2999.8 | N 30° E / N 210° E | L1000 – L3880 |
| | Tie: 1500 | | | 313.5 | N 120° E / N 300° E | T4000 – T4090 |
| Infills | Traverse: 75 | | 633.1 | 656.4 | N 30° E / N 210° E | L1955 – L2545 |
| TOTAL | | 430 | 3819.7 | 3969.7 | | |

Survey block boundaries co-ordinates are provided in Appendix B.

2.2 Survey Operations

Survey operations were based out of Resolute Bay, Nunavut from July 2nd to July 24th, 2011. The following table shows the timing of the flying.

Table 2 - Survey schedule

| Date | Flight # | Crew location | Comments |
|-----------|-------------|------------------|------------------|
| 2-Jul-11 | | | Resolute Bay, NU |
| 3-Jul-11 | | | Resolute Bay, NU |
| 4-Jul-11 | | | Resolute Bay, NU |
| 5-Jul-11 | | | Resolute Bay, NU |
| 6-Jul-11 | 1,2 | Storm Property | Resolute Bay, NU |
| 7-Jul-11 | 3,4,5 | Storm Property | Resolute Bay, NU |
| 8-Jul-11 | 6,7,8 | Storm Property | Resolute Bay, NU |
| 9-Jul-11 | 9,10,11 | Storm Property | Resolute Bay, NU |
| 10-Jul-11 | 12 | Storm Property | Resolute Bay, NU |
| 11-Jul-11 | | | Resolute Bay, NU |
| 12-Jul-11 | | | Resolute Bay, NU |
| 13-Jul-11 | 13,14 | Storm Property | Resolute Bay, NU |
| 14-Jul-11 | | | Resolute Bay, NU |
| 15-Jul-11 | 15,16 | Storm Property | Resolute Bay, NU |
| 16-Jul-11 | 17,18 | Storm Property | Resolute Bay, NU |
| 17-Jul-11 | 19,20 | Storm Property | Resolute Bay, NU |
| 18-Jul-11 | 21 | Storm Property | Resolute Bay, NU |
| 19-Jul-11 | 22,23,24,25 | Storm Property | Resolute Bay, NU |
| 20-Jul-11 | 26,27,28 | Storm Property - | Resolute Bay, NU |

¹ Note: Actual Line kilometres represent the total line kilometres in the final database. These line-km normally exceed the Planned line-km, as indicated in the survey NAV files.

| Date | Flight # | Crew location | Comments |
|-----------|----------|-----------------------------|------------------|
| | | Infills | |
| 21-Jul-11 | | | Resolute Bay, NU |
| 22-Jul-11 | | | Resolute Bay, NU |
| 23-Jul-11 | | | Resolute Bay, NU |
| 24-Jul-11 | 29,30 | Storm Property - Infills | Resolute Bay, NU |
| | | | |

2.3 Flight Specifications

During the survey the helicopter was maintained at a mean altitude of 77 metres above the ground with a nominal survey speed of 80 km/hour. This allowed for a nominal EM bird terrain clearance of 42 metres and a magnetic sensor clearance of 64 metres.

The on board operator was responsible for monitoring the system integrity. He also maintained a detailed flight log during the survey, tracking the times of the flight as well as any unusual geophysical or topographic features.

On return of the aircrew to the base camp the survey data was transferred from a compact flash card (PCMCIA) to the data processing computer. The data were then uploaded via ftp to the Geotech office in Aurora for daily quality assurance and quality control by qualified personnel.

2.4 Aircraft and Equipment

2.4.1 Survey Aircraft

The survey was flown using a Eurocopter Aerospatiale (Astar) 350 B3 helicopter, registration C-GXGX. The helicopter is owned and operated by Geotech Aviation. Installation of the geophysical and ancillary equipment was carried out by a Geotech Ltd crew.

2.4.2 Electromagnetic System

The electromagnetic system was a Geotech Time Domain EM (VTEM plus) system. The configuration is as indicated in Figure 4.

The VTEM plus Receiver and transmitter coils were in concentric-coplanar and Z-direction oriented configuration. The receiver system for the project also included a coincident-coaxial X-direction coil to measure the in-line dB/dt and calculate B-Field responses. The EM bird was towed at a mean distance of 35 metres below the aircraft as shown in Figure 4 and Figure 6. The receiver decay recording scheme is shown in Figure 5.

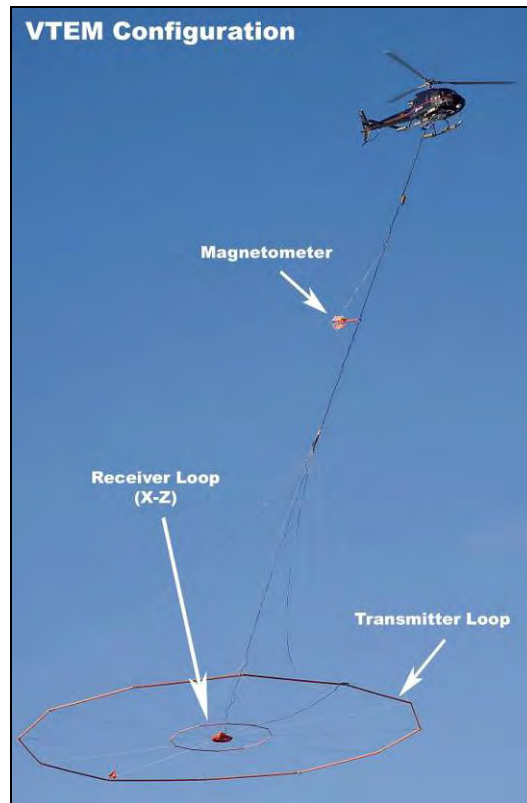


Figure 4 - VTEM plus Configuration, with magnetometer.

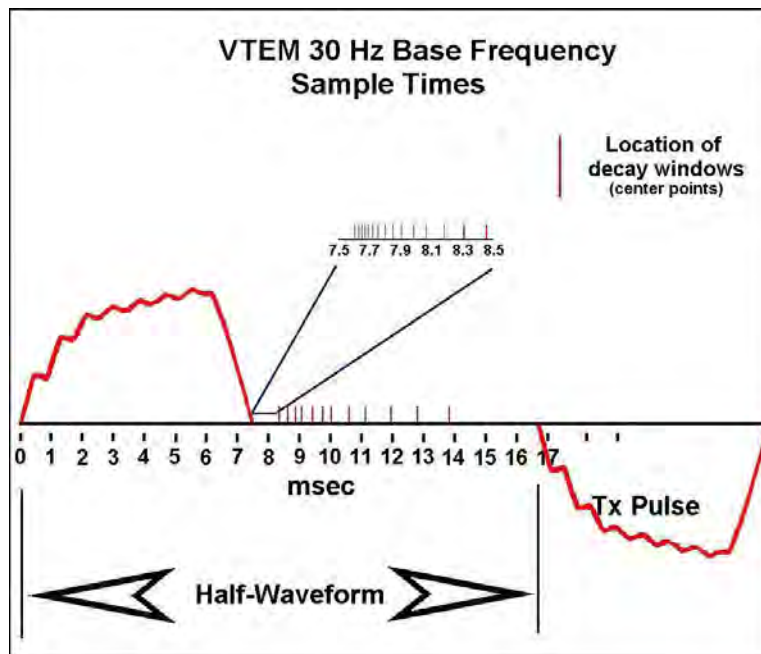


Figure 5 - VTEM plus Waveform & Sample Times

The VTEM plus decay sampling scheme is shown in Table 3 below. Thirty-two time measurement gates were used for the final data processing in the range from 96 to 7036 μ sec.

Table 3 - Decay Sampling Scheme

| VTEM plus Decay Sampling Scheme | | | | |
|--|---------------------|--------------|------------|---------------|
| Index | Middle | Start | End | Window |
| | Microseconds | | | |
| 14 | 96 | 90 | 103 | 13 |
| 15 | 110 | 103 | 118 | 15 |
| 16 | 126 | 118 | 136 | 18 |
| 17 | 145 | 136 | 156 | 20 |
| 18 | 167 | 156 | 179 | 23 |
| 19 | 192 | 179 | 206 | 27 |
| 20 | 220 | 206 | 236 | 30 |
| 21 | 253 | 236 | 271 | 35 |
| 22 | 290 | 271 | 312 | 40 |
| 23 | 333 | 312 | 358 | 46 |
| 24 | 383 | 358 | 411 | 53 |
| 25 | 440 | 411 | 472 | 61 |
| 26 | 505 | 472 | 543 | 70 |
| 27 | 580 | 543 | 623 | 81 |
| 28 | 667 | 623 | 716 | 93 |
| 29 | 766 | 716 | 823 | 107 |
| 30 | 880 | 823 | 945 | 122 |
| 31 | 1,010 | 945 | 1,086 | 141 |
| 32 | 1,161 | 1,086 | 1,247 | 161 |
| 33 | 1,333 | 1,247 | 1,432 | 185 |
| 34 | 1,531 | 1,432 | 1,646 | 214 |
| 35 | 1,760 | 1,646 | 1,891 | 245 |
| 36 | 2,021 | 1,891 | 2,172 | 281 |
| 37 | 2,323 | 2,172 | 2,495 | 323 |
| 38 | 2,667 | 2,495 | 2,865 | 370 |
| 39 | 3,063 | 2,865 | 3,292 | 427 |
| 40 | 3,521 | 3,292 | 3,781 | 490 |
| 41 | 4,042 | 3,781 | 4,341 | 560 |
| 42 | 4,641 | 4,341 | 4,987 | 646 |
| 43 | 5,333 | 4,987 | 5,729 | 742 |
| 44 | 6,125 | 5,729 | 6,581 | 852 |
| 45 | 7,036 | 6,581 | 7,560 | 979 |

VTEM plus system parameters:

Transmitter Section

- Transmitter coil diameter: 26.1 m
- Number of turns: 4
- Transmitter base frequency: 30 Hz
- Peak current: 171 A
- Pulse width: 7.119 ms
- Duty cycle: 43 %
- Wave form shape: trapezoid
- Peak dipole moment: 365,954.42 nIA
- Nominal EM Bird terrain clearance: 46 metres above the ground
- Effective coil area: 2123 m²

Receiver Section

X-Coil

- X Coil diameter: 0.32 m
- Number of turns: 245
- Effective coil area: 19.69 m²

Z-Coil

- Z-Coil coil diameter: 1.2 m
- Number of turns: 100
- Effective coil area: 113.04 m²

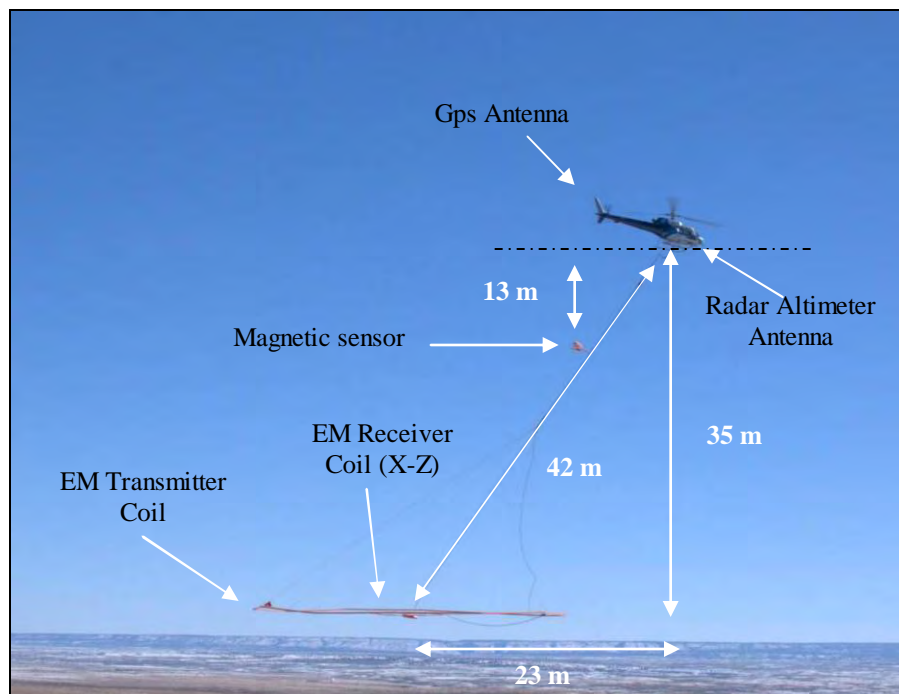


Figure 6 - VTEM plus System Configuration

2.4.3 Airborne magnetometer

The magnetic sensor utilized for the survey was Geometrics optically pumped caesium vapour magnetic field sensor mounted 13 metres below the helicopter, as shown in Figure 6. The sensitivity of the magnetic sensor is 0.02 nanoTesla (nT) at a sampling interval of 0.1 seconds.

2.4.4 Radar Altimeter

A Terra TRA 3000/TRI 40 radar altimeter was used to record terrain clearance. The antenna was mounted beneath the bubble of the helicopter cockpit (Figure 6).

2.4.5 GPS Navigation System

The navigation system used was a Geotech PC104 based navigation system utilizing a NovAtel's CDGPS (Canada-Wide Differential Global Positioning System Correction Service) enable OEM4-G2-3151W GPS receiver, Geotech navigate software, a full screen display with controls in front of the pilot to direct the flight and an NovAtel GPS antenna mounted on the helicopter tail (Figure 6). As many as 11 GPS and two CDGPS satellites may be monitored at any one time. The positional accuracy or circular error probability (CEP) is 1.8 m, with CDGPS active, it is 1.0 m. The co-ordinates of the block were set-up prior to the survey and the information was fed into the airborne navigation system.

2.4.6 Digital Acquisition System

A Geotech data acquisition system recorded the digital survey data on an internal compact flash card. Data is displayed on an LCD screen as traces to allow the operator to monitor the integrity of the system. The data type and sampling interval as provided in Table 4.

Table 4 - Acquisition Sampling Rates

| DATA TYPE | SAMPLING |
|-----------------|----------|
| TDEM | 0.1 sec |
| Magnetometer | 0.1 sec |
| GPS Position | 0.2 sec |
| Radar Altimeter | 0.2 sec |

2.5 Base Station

A combined magnetometer/GPS base station was utilized on this project. A Geometrics Caesium vapour magnetometer was used as a magnetic sensor with a sensitivity of 0.001 nT. The base station was recording the magnetic field together with the GPS time at 1 Hz on a base station computer.

The base station magnetometer sensor was installed east of fuel cache close to the block – removed from Resolute (73° 41.1249' N, 94° 47.8301' W); away from electric transmission lines and moving ferrous objects such as motor vehicles. The base station data were backed-up to the data processing computer at the end of each survey day.

3. PERSONNEL

The following Geotech Ltd. personnel were involved in the project.

Field:

| | |
|------------------|----------------------|
| Project Manager: | Darren Tuck (Office) |
| Data QC: | Nick Venter (Office) |
| Crew chief: | Alex Smirnov |
| Operator: | Greg Luus |

The survey pilot and the mechanical engineer were employed directly by the helicopter operator – Heli Carrier.

| | |
|----------------------|--------------------|
| Pilot: | Jean Michel Dumont |
| Mechanical Engineer: | Philip Levasseur |

Office:

| | |
|------------------------------|---------------------|
| Preliminary Data Processing: | Nick Venter |
| Final Data Processing: | Karl Kwan |
| Final Data QA/QC: | Alexander Prikhodko |
| Reporting/Mapping: | Liz Johnson |

Data acquisition phase was carried out under the supervision of Andrei Bagrianski, P. Geo, Chief Operating Officer. The processing and interpretation phase was under the supervision of Alexander Prikhodko, P. Geo. The customer relations were looked after by Blair Walker.

4. DATA PROCESSING AND PRESENTATION

Data compilation and processing were carried out by the application of Geosoft OASIS Montaj and programs proprietary to Geotech Ltd.

4.1 Flight Path

The flight path, recorded by the acquisition program as WGS 84 latitude/longitude, was converted into the NAD83 Datum, UTM Zone 15 North coordinate system in Oasis Montaj.

The flight path was drawn using linear interpolation between x, y positions from the navigation system. Positions are updated every second and expressed as UTM easting's (x) and UTM northing's (y).

4.2 Electromagnetic Data

A three stage digital filtering process was used to reject major sferic events and to reduce system noise. Local sferic activity can produce sharp, large amplitude events that cannot be removed by conventional filtering procedures. Smoothing or stacking will reduce their amplitude but leave a broader residual response that can be confused with geological phenomena. To avoid this possibility, a computer algorithm searches out and rejects the major sferic events.

The signal to noise ratio was further improved by the application of a low pass linear digital filter. This filter has zero phase shift which prevents any lag or peak displacement from occurring, and it suppresses only variations with a wavelength less than about 1 second or 15 metres. This filter is a symmetrical 1 sec linear filter.

The results are presented as stacked profiles of EM voltages for the time gates, in linear - logarithmic scale for the B-field Z component and dB/dt responses in the Z and X components. B-field Z component time channel recorded at 2.021 milliseconds after the termination of the impulse is also presented as contour colour images. Calculated Time Constant (TAU) with anomaly contours of Calculated Vertical Derivative of TMI is presented in Appendix D and F. Resistivity Depth Image (RDI) is also presented in Appendix D and G.

VTEM plus has two receiver coil orientations. Z-axis coil is oriented parallel to the transmitter coil axis and both are horizontal to the ground. The X-axis coil is oriented parallel to the ground and along the line-of-flight. This combined two coil configuration provides information on the position, depth, dip and thickness of a conductor. Generalized modeling results of VTEM plus data are shown in Appendix E.

In general X-component data produce cross-over type anomalies: from “+ to –” in flight direction of flight for “thin” sub vertical targets and from “- to +” in direction of flight for “thick” targets. Z component data produce double peak type anomalies for “thin” sub vertical targets and single peak for “thick” targets.

The limits and change-over of “thin-thick” depends on dimensions of a TEM system.

Because of X component polarity is under line-of-flight, convolution Fraser filter (FF, Figure 7) is applied to X component data to represent axes of conductors in the form of grid map. In this case positive FF anomalies always correspond to “plus-to-minus” X data crossovers independently of direction of flight.

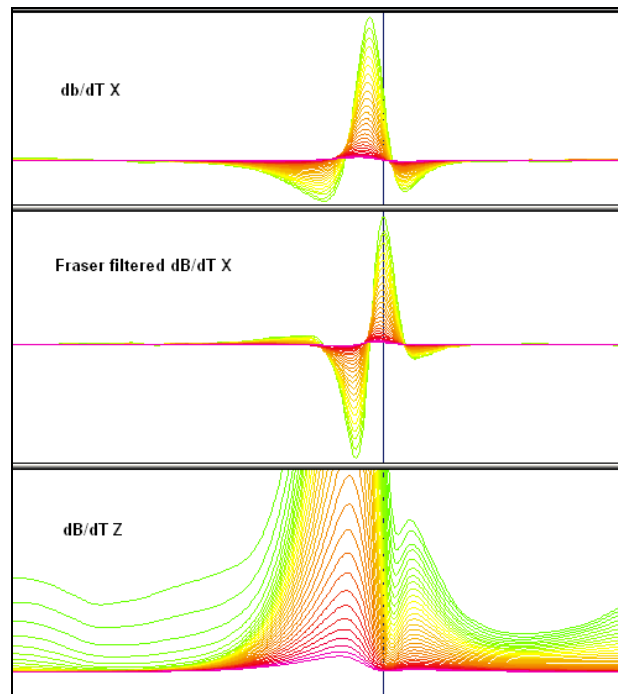


Figure 7 - Z, X and Fraser filtered X (FFx) components for “thin” target

Graphical representations of the VTEM plus transmitter input current and the output voltage of the receiver coil are shown in Appendix C.

4.3 Magnetic Data

The processing of the magnetic data involved the correction for diurnal variations by using the digitally recorded ground base station magnetic values. The base station magnetometer data was edited and merged into the Geosoft GDB database on a daily basis. The aeromagnetic data was corrected for diurnal variations by subtracting the observed magnetic base station deviations.

Tie line levelling was carried out by adjusting intersection points along traverse lines. A micro-levelling procedure was applied to remove persistent low-amplitude components of flight-line noise remaining in the data.

The corrected magnetic data was interpolated between survey lines using a random point gridding method to yield x-y grid values for a standard grid cell size of approximately 37.5 metres for the entire property and 15 metres for the Infills area at the mapping scale. The Minimum Curvature algorithm was used to interpolate values onto a rectangular regular spaced grid.

5. DELIVERABLES

5.1 Survey Report

The survey report describes the data acquisition, processing, and final presentation of the survey results. The survey report is provided in two paper copies and digitally in PDF format.

5.2 Maps

Final maps were produced at a scale of 1:20,000 for the Infill area, and 1:25,000 with the survey block split in two map sheets for best representation of the survey size and line spacing. The coordinate/projection system used was NAD83 Datum, UTM Zone 15 North. All maps show the mining claims, flight path trace and topographic data; latitude and longitude are also noted on maps.

The preliminary and final results of the survey are presented as EM profiles, a late-time gate gridded EM channel, and a color magnetic TMI contour map. The following maps are presented on paper;

- VTEM dB/dt profiles Z Component, Time Gates 0.220 – 7.036 ms in linear – logarithmic scale.
- VTEM B-Field profiles Z Component, Time Gates 0.220 – 7.036 ms in linear – logarithmic scale.
- VTEM B-field late time Z Component Channel 36, Time Gate 2.021 ms colour image.
- VTEM dB/dt Calculated Time Constant (TAU) with contours of anomaly areas of the Total Magnetic Intensity
- Total Magnetic Intensity (TMI) colour image and contours.

5.3 Digital Data

- Two copies of the data and maps on DVD were prepared to accompany the report. Each DVD contains a digital file of the line data in GDB Geosoft Montaj format as well as the maps in Geosoft Montaj Map and PDF format.
- DVD structure.

| | |
|---------------|---|
| Data | contains databases, grids and maps, as described below. |
| Report | contains a copy of the report and appendices in PDF format. |

Databases in Geosoft GDB format, containing the channels listed in Table 5.

Table 5 - Geosoft GDB Data Format

| Channel name | Units | Description |
|--------------|--------------------|---|
| X: | metres | UTM Easting NAD83 Zone 15 North |
| Y: | metres | UTM Northing NAD83 Zone 15 North |
| Z: | metres | GPS antenna elevation (above Geoid) |
| Longitude: | Decimal Degrees | WGS 84 Longitude data |
| Latitude: | Decimal Degrees | WGS 84 Latitude data |
| Radar: | metres | helicopter terrain clearance from radar altimeter |
| Radarb: | metres | Calculated EM bird terrain clearance from radar altimeter |
| DEM: | metres | Digital Elevation Model |
| Gtime: | Seconds of the day | GPS time |
| Mag1: | nT | Raw Total Magnetic field data |
| Basemag: | nT | Magnetic diurnal variation data |
| Mag2: | nT | Diurnal corrected Total Magnetic field data |
| Mag3: | nT | Levelled Total Magnetic field data |
| CVG | nT | Calculated Vertical Derivative of TMI |
| SFz[14]: | $pV/(A \cdot m^4)$ | Z dB/dt 96 microsecond time channel |
| SFz[15]: | $pV/(A \cdot m^4)$ | Z dB/dt 110 microsecond time channel |
| SFz[16]: | $pV/(A \cdot m^4)$ | Z dB/dt 126 microsecond time channel |
| SFz[17]: | $pV/(A \cdot m^4)$ | Z dB/dt 145 microsecond time channel |
| SFz[18]: | $pV/(A \cdot m^4)$ | Z dB/dt 167 microsecond time channel |
| SFz[19]: | $pV/(A \cdot m^4)$ | Z dB/dt 192 microsecond time channel |
| SFz[20]: | $pV/(A \cdot m^4)$ | Z dB/dt 220 microsecond time channel |
| SFz[21]: | $pV/(A \cdot m^4)$ | Z dB/dt 253 microsecond time channel |
| SFz[22]: | $pV/(A \cdot m^4)$ | Z dB/dt 290 microsecond time channel |
| SFz[23]: | $pV/(A \cdot m^4)$ | Z dB/dt 333 microsecond time channel |
| SFz[24]: | $pV/(A \cdot m^4)$ | Z dB/dt 383 microsecond time channel |
| SFz[25]: | $pV/(A \cdot m^4)$ | Z dB/dt 440 microsecond time channel |
| SFz[26]: | $pV/(A \cdot m^4)$ | Z dB/dt 505 microsecond time channel |
| SFz[27]: | $pV/(A \cdot m^4)$ | Z dB/dt 580 microsecond time channel |
| SFz[28]: | $pV/(A \cdot m^4)$ | Z dB/dt 667 microsecond time channel |
| SFz[29]: | $pV/(A \cdot m^4)$ | Z dB/dt 766 microsecond time channel |
| SFz[30]: | $pV/(A \cdot m^4)$ | Z dB/dt 880 microsecond time channel |
| SFz[31]: | $pV/(A \cdot m^4)$ | Z dB/dt 1010 microsecond time channel |
| SFz[32]: | $pV/(A \cdot m^4)$ | Z dB/dt 1161 microsecond time channel |
| SFz[33]: | $pV/(A \cdot m^4)$ | Z dB/dt 1333 microsecond time channel |
| SFz[34]: | $pV/(A \cdot m^4)$ | Z dB/dt 1531 microsecond time channel |
| SFz[35]: | $pV/(A \cdot m^4)$ | Z dB/dt 1760 microsecond time channel |
| SFz[36]: | $pV/(A \cdot m^4)$ | Z dB/dt 2021 microsecond time channel |
| SFz[37]: | $pV/(A \cdot m^4)$ | Z dB/dt 2323 microsecond time channel |
| SFz[38]: | $pV/(A \cdot m^4)$ | Z dB/dt 2667 microsecond time channel |
| SFz[39]: | $pV/(A \cdot m^4)$ | Z dB/dt 3063 microsecond time channel |
| SFz[40]: | $pV/(A \cdot m^4)$ | Z dB/dt 3521 microsecond time channel |
| SFz[41]: | $pV/(A \cdot m^4)$ | Z dB/dt 4042 microsecond time channel |
| SFz[42]: | $pV/(A \cdot m^4)$ | Z dB/dt 4641 microsecond time channel |
| SFz[43]: | $pV/(A \cdot m^4)$ | Z dB/dt 5333 microsecond time channel |
| SFz[44]: | $pV/(A \cdot m^4)$ | Z dB/dt 6125 microsecond time channel |
| SFz[45]: | $pV/(A \cdot m^4)$ | Z dB/dt 7036 microsecond time channel |
| SFx[20]: | $pV/(A \cdot m^4)$ | X dB/dt 220 microsecond time channel |
| SFx[21]: | $pV/(A \cdot m^4)$ | X dB/dt 253 microsecond time channel |
| SFx[22]: | $pV/(A \cdot m^4)$ | X dB/dt 290 microsecond time channel |
| SFx[23]: | $pV/(A \cdot m^4)$ | X dB/dt 333 microsecond time channel |

| Channel name | Units | Description |
|--------------|---|---|
| SFx[24]: | $\text{pV}/(\text{A}\cdot\text{m}^4)$ | X dB/dt 383 microsecond time channel |
| SFx[25]: | $\text{pV}/(\text{A}\cdot\text{m}^4)$ | X dB/dt 440 microsecond time channel |
| SFx[26]: | $\text{pV}/(\text{A}\cdot\text{m}^4)$ | X dB/dt 505 microsecond time channel |
| SFx[27]: | $\text{pV}/(\text{A}\cdot\text{m}^4)$ | X dB/dt 580 microsecond time channel |
| SFx[28]: | $\text{pV}/(\text{A}\cdot\text{m}^4)$ | X dB/dt 667 microsecond time channel |
| SFx[29]: | $\text{pV}/(\text{A}\cdot\text{m}^4)$ | X dB/dt 766 microsecond time channel |
| SFx[30]: | $\text{pV}/(\text{A}\cdot\text{m}^4)$ | X dB/dt 880 microsecond time channel |
| SFx[31]: | $\text{pV}/(\text{A}\cdot\text{m}^4)$ | X dB/dt 1010 microsecond time channel |
| SFx[32]: | $\text{pV}/(\text{A}\cdot\text{m}^4)$ | X dB/dt 1161 microsecond time channel |
| SFx[33]: | $\text{pV}/(\text{A}\cdot\text{m}^4)$ | X dB/dt 1333 microsecond time channel |
| SFx[34]: | $\text{pV}/(\text{A}\cdot\text{m}^4)$ | X dB/dt 1531 microsecond time channel |
| SFx[35]: | $\text{pV}/(\text{A}\cdot\text{m}^4)$ | X dB/dt 1760 microsecond time channel |
| SFx[36]: | $\text{pV}/(\text{A}\cdot\text{m}^4)$ | X dB/dt 2021 microsecond time channel |
| SFx[37]: | $\text{pV}/(\text{A}\cdot\text{m}^4)$ | X dB/dt 2323 microsecond time channel |
| SFx[38]: | $\text{pV}/(\text{A}\cdot\text{m}^4)$ | X dB/dt 2667 microsecond time channel |
| SFx[39]: | $\text{pV}/(\text{A}\cdot\text{m}^4)$ | X dB/dt 3063 microsecond time channel |
| SFx[40]: | $\text{pV}/(\text{A}\cdot\text{m}^4)$ | X dB/dt 3521 microsecond time channel |
| SFx[41]: | $\text{pV}/(\text{A}\cdot\text{m}^4)$ | X dB/dt 4042 microsecond time channel |
| SFx[42]: | $\text{pV}/(\text{A}\cdot\text{m}^4)$ | X dB/dt 4641 microsecond time channel |
| SFx[43]: | $\text{pV}/(\text{A}\cdot\text{m}^4)$ | X dB/dt 5333 microsecond time channel |
| SFx[44]: | $\text{pV}/(\text{A}\cdot\text{m}^4)$ | X dB/dt 6125 microsecond time channel |
| SFx[45]: | $\text{pV}/(\text{A}\cdot\text{m}^4)$ | X dB/dt 7036 microsecond time channel |
| BFz | $(\text{pV}\cdot\text{ms})/(\text{A}\cdot\text{m}^4)$ | Z B-Field data for time channels 14 to 45 |
| BFx | $(\text{pV}\cdot\text{ms})/(\text{A}\cdot\text{m}^4)$ | X B-Field data for time channels 20 to 45 |
| SFxFF | $\text{pV}/(\text{A}\cdot\text{m}^4)$ | Fraser filtered X dB/dt |
| PLM: | | 60 Hz power line monitor |
| TauSF | milliseconds | Time Constant (Tau) calculated from dB/dt data |
| TauBF | milliseconds | Time Constant (Tau) calculated from B-Field data |
| NchanBF | | Last channel where the Tau algorithm stops calculation, B-Field |
| NchanSF | | Last channel where the Tau algorithm stops calculation, dB/dt |

Electromagnetic B-field and dB/dt Z component data is found in array channel format between indexes 14 – 45, and X component data from 20 – 45, as described above.

- Database of the VTEM Waveform “11053_waveform_final.gdb” in Geosoft GDB format, containing the following channels:

Time: Sampling rate interval, 5.2083 microseconds
Rx_Volt: Output voltage of the receiver coil (Volt)
Tx_Current: Output current of the transmitter (Amp)

- Grids in Geosoft GRD format, as follows:

BFz36: B-Field Z Component Channel 36 (Time Gate 2.021 ms)
TMI: Total Magnetic Intensity (nT)
CVG: Calculated Vertical Derivative of TMI (nT/m)
TauBF: B-Field Calculated Time Constant (ms)
TauSF: dB/dt Calculated Time Constant (ms)
SFxFF30: Fraser Filter X Component dB/dt Channel 30 (Time Gate 0.880 ms)
DEM: Digital Elevation Model (metres)
PLM: Power Line Monitor (60Hz)

A Geosoft .GRD file has a .GI metadata file associated with it, containing grid projection information. A grid cell size of 37.5 metres for the entire property and 15 metres for the Infills area was used.

- Maps at 1:20,000 for the Infill area, and 1:25,000 with the survey block split in two map sheets (Plate 1 and Plate 2) in Geosoft MAP format, as follows:

11053_ *scalek* _*bb* _dBdtz: dB/dt profiles Z Component, Time Gates 0.220 – 7.036 ms in linear – logarithmic scale.
11053_ *scalek* _*bb* _Bfield: B-field profiles Z Component, Time Gates 0.220 – 7.036 ms in linear – logarithmic scale over total magnetic intensity.
11053_ *scalek* _*bb* _BFz36: B-field late time Z Component Channel 36, Time Gate 2.021 ms color image.
11053_ *scalek* _*bb* _TMI: Total magnetic intensity (TMI) color image and contours.
11053_ *scalek* _*bb* _TauSF: dB/dt Calculated Time Constant (TAU) with contours of anomaly areas of the Total Magnetic Intensity

where *scale* represents the scale of the map
bb represents the map name

Maps are also presented in PDF format.

1:50,000 topographic vectors were taken from the NRCAN Geogratis database at;
<http://geogratis.gc.ca/geogratis/en/index.html>.

- A Google Earth file *11053_Flight Path.kml* showing the flight path of the block is included. Free versions of Google Earth software from:
<http://earth.google.com/download-earth.html>

6. CONCLUSIONS AND RECOMMENDATIONS

6.1 Conclusions

A helicopter-borne versatile time domain electromagnetic (VTEM plus) geophysical survey has been completed over the Storm Property near Resolute, Nunavut.

The total area coverage for all properties is 430 km². Total survey line coverage is 3969.7 line kilometres. The principal sensors included a Time Domain EM system and a magnetometer. Results have been presented as stacked profiles, and contour color images at a scale of 1:20,000 for the Infill area, and 1:25,000 with the survey block split in two map sheets (Plate 1 and Plate 2).

Time constants TAU's from dB/dt and B-field are calculated. The TAU's from dB/dt are presented as color image overlain with TMI contours.

6.2 Recommendations

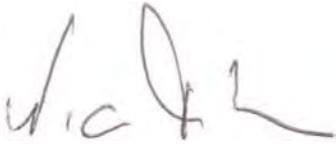
A strong, near circular magnetic anomaly is observed at the west end of the surveyed area. Originating from this anomaly, an SE trending dyke can be seen. The sources of these magnetic anomalies are in the Proterozoic basement.

A sharp magnetic gradient (high rate of change in magnetic values) can also be seen over the entire area, trending in NW-SE direction in a “zigzag” fashion. The gradient may reflect a graben-type contact in the basement.

An extended and layered conductive zone is detected on the south side of the contact in the southwest end of the area. Four discrete, pipe-like conductors near the surface are visible in the middle (infill area) of the property. These vertical conductors may correspond to copper (Cu) mineralization.

We recommend detailed interpretations of the VTEM and magnetic data prior to any ground follow-up or drill testing. The interpretations should include magnetic 2D/3D modeling, Resistivity Depth Imaging (RDI) sections, Apparent Resistivity depth slices and Maxwell 2.5D modeling of discrete conductors.

Respectfully submitted⁵,



Nick Venter
Geotech Ltd.

Alexander Prikhodko, P.Geo.
Geotech Ltd.

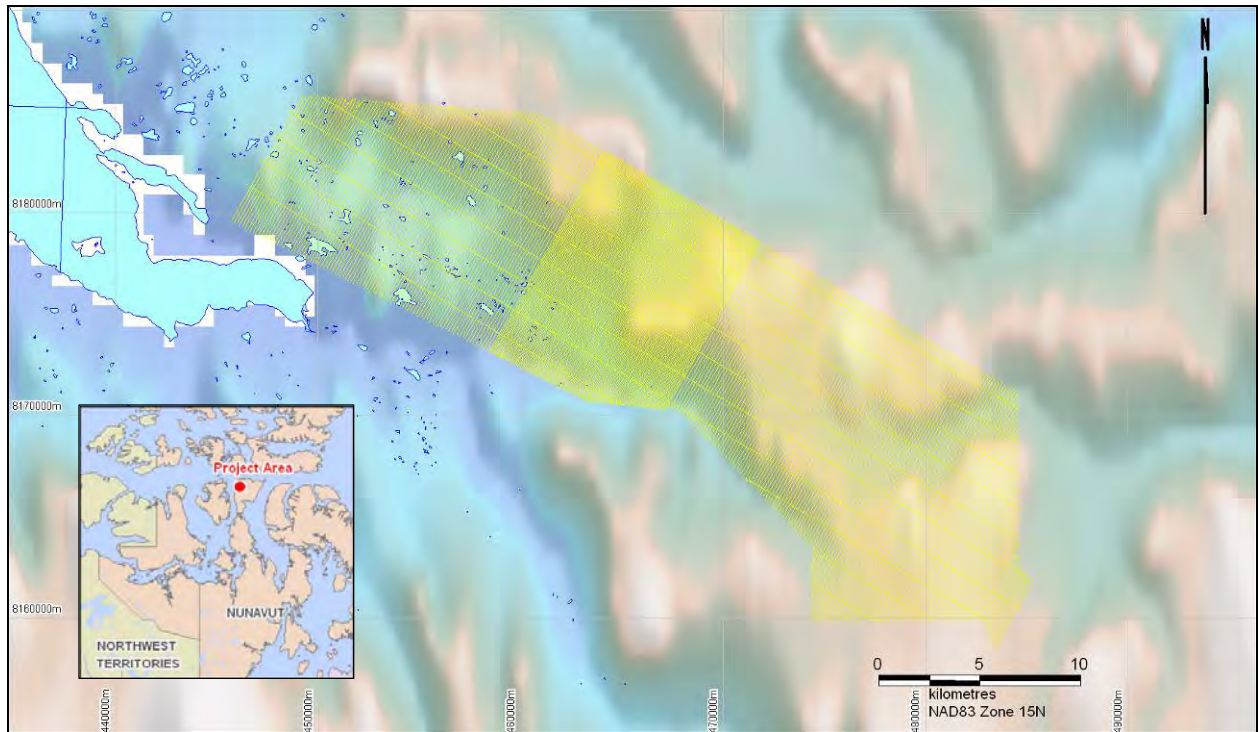
Karl Kwan
Geotech Ltd.

August 2011

⁵Final data processing of the EM and magnetic data were carried out by Karl Kwan, from the office of Geotech Ltd. in Aurora, Ontario, under the supervision of Alexander Prikhodko, P.Geo., PhD, Senior Geophysicist, VTEM Interpretation Supervisor.

APPENDIX A

SURVEY BLOCK LOCATION MAP



Survey Overview of the Blocks

APPENDIX B

SURVEY BLOCK COORDINATES

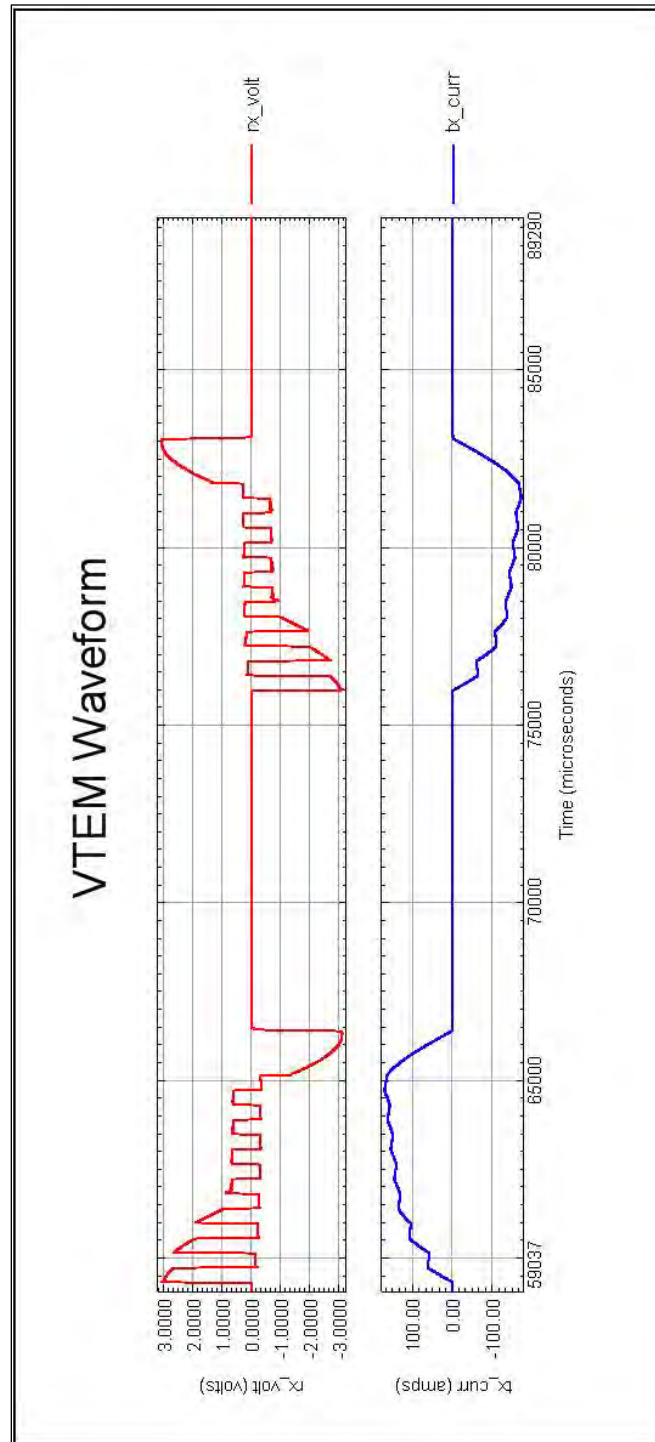
(WGS 84, UTM Zone 15 North)

Storm Property

| X | Y |
|--------|---------|
| 449085 | 8185650 |
| 445695 | 8179810 |
| 463365 | 8170850 |
| 467920 | 8170390 |
| 474525 | 8163600 |
| 474525 | 8160000 |
| 484395 | 8160000 |
| 484395 | 8171045 |
| 460935 | 8184755 |
| 449085 | 8185650 |

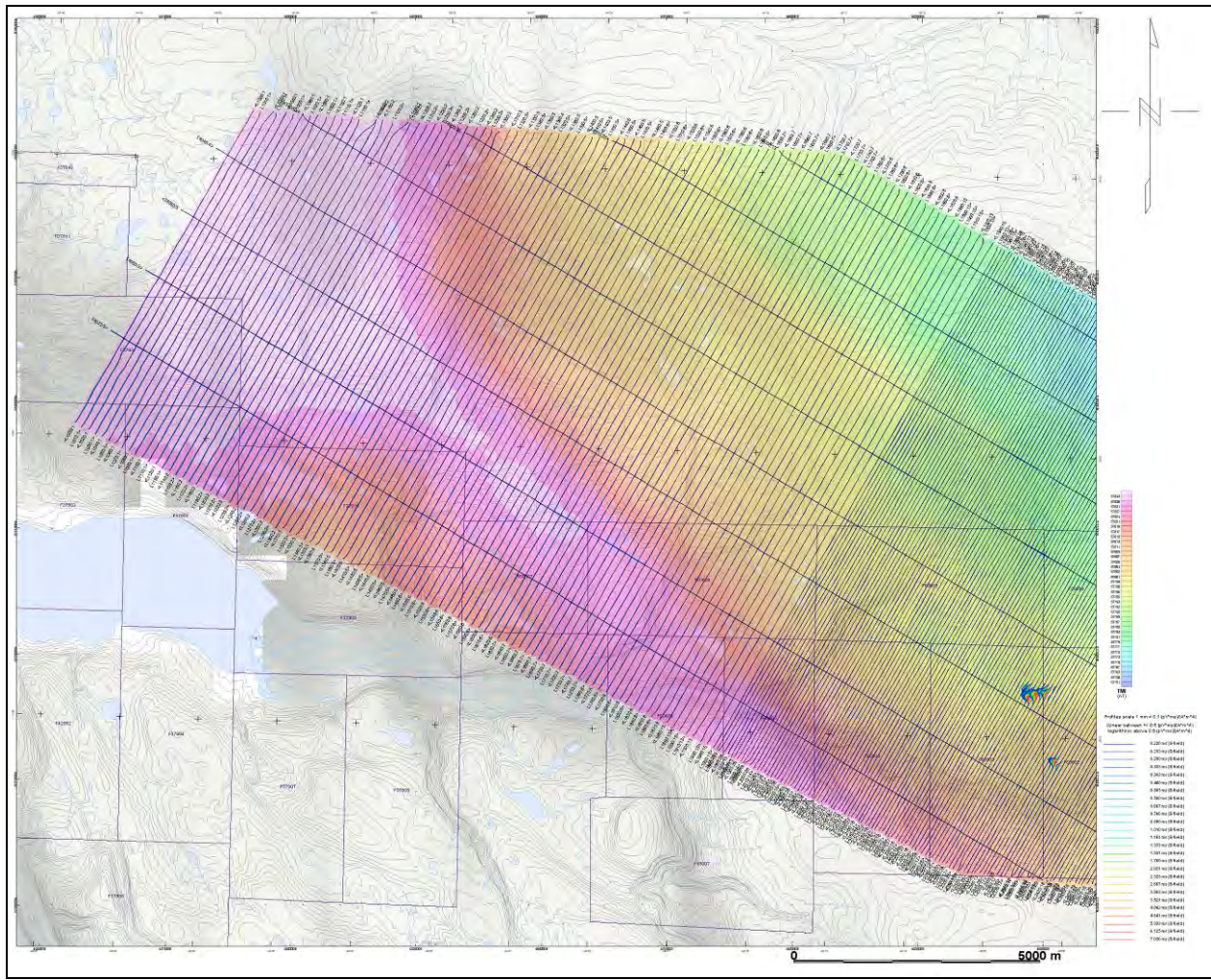
APPENDIX C

VTEM WAVEFORM



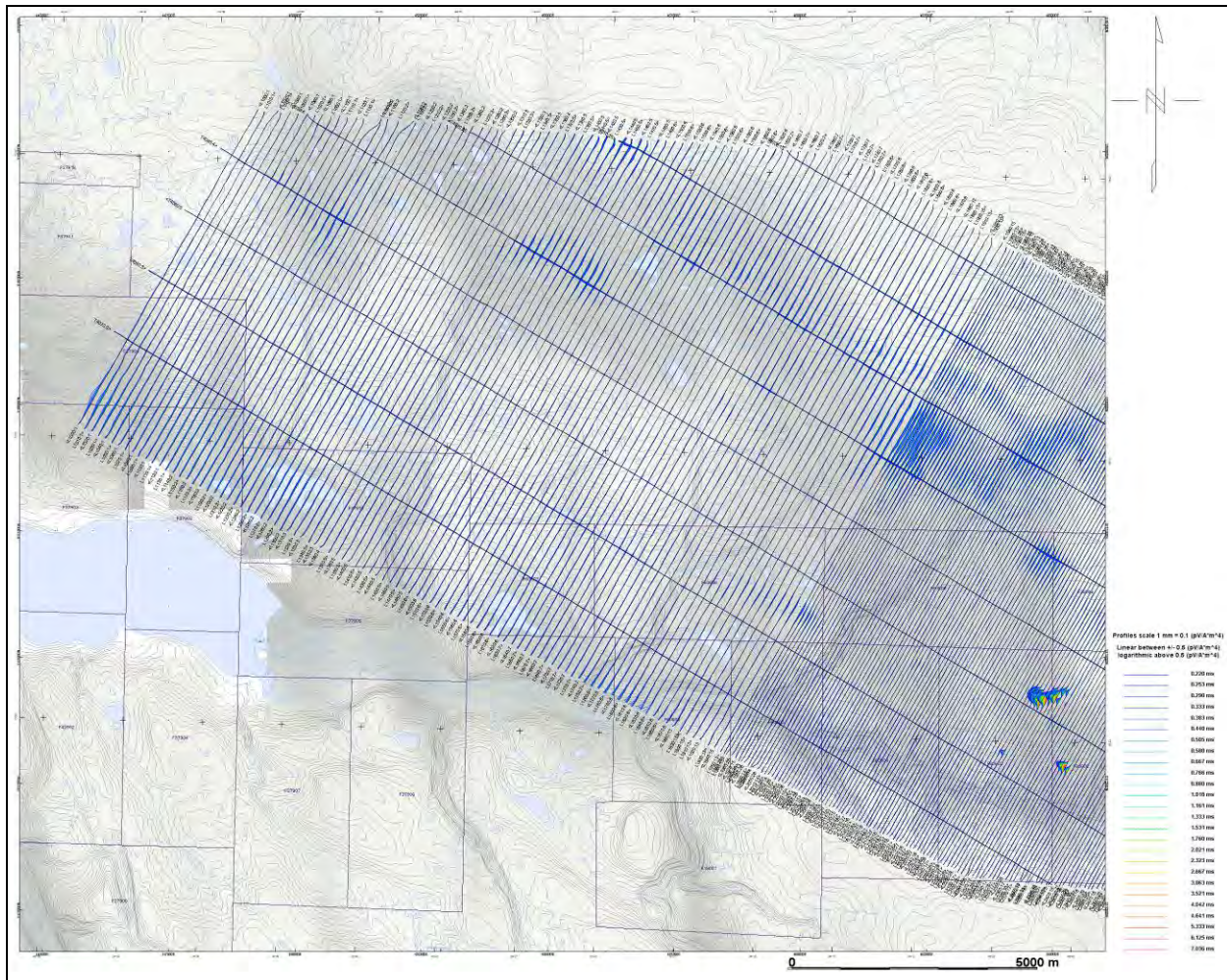
APPENDIX D

GEOPHYSICAL MAPS¹

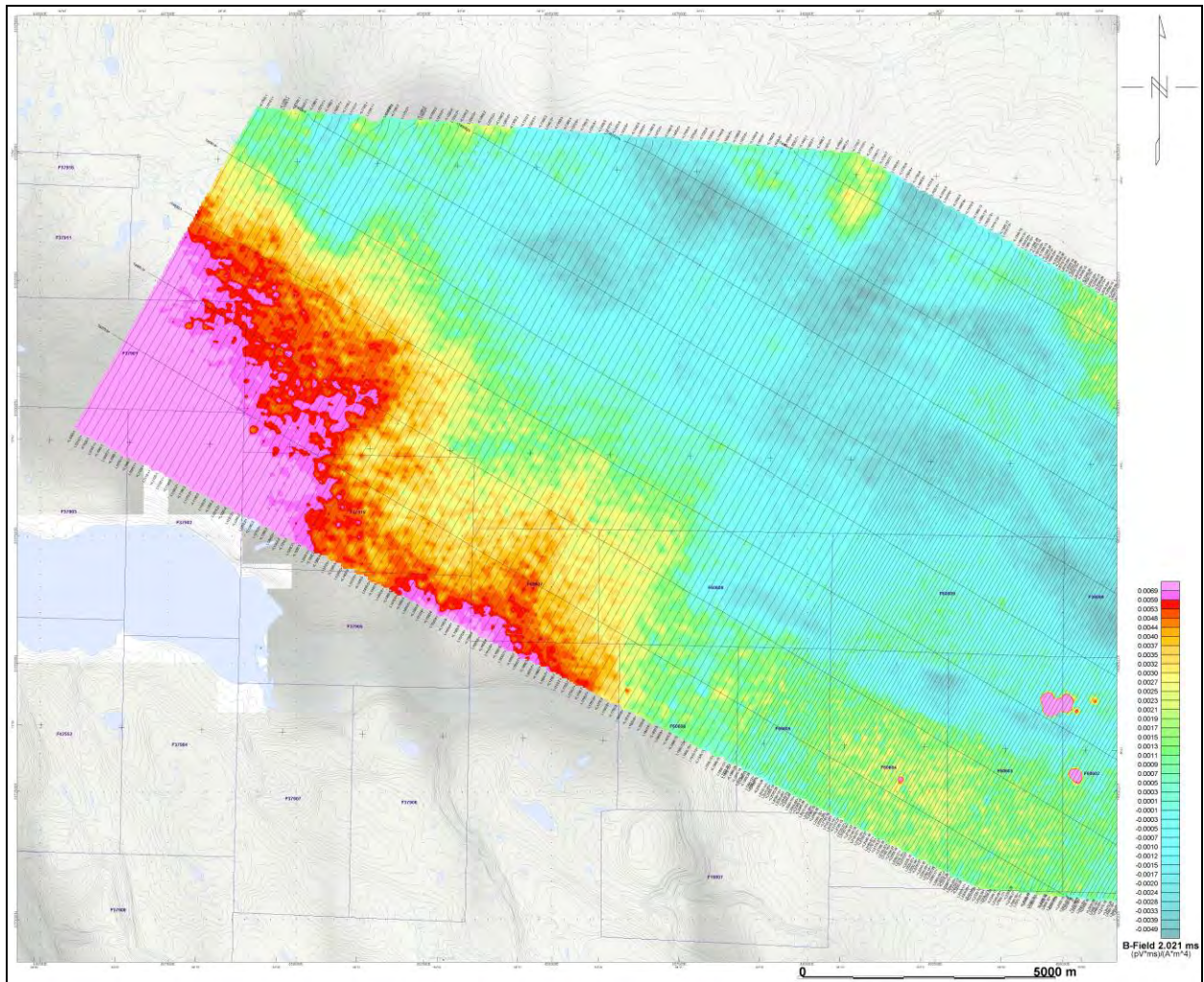


Storm Property (Plate 1) - VTEM B-Field Z Component Profiles, Time Gates 0.220 to 7.036 ms

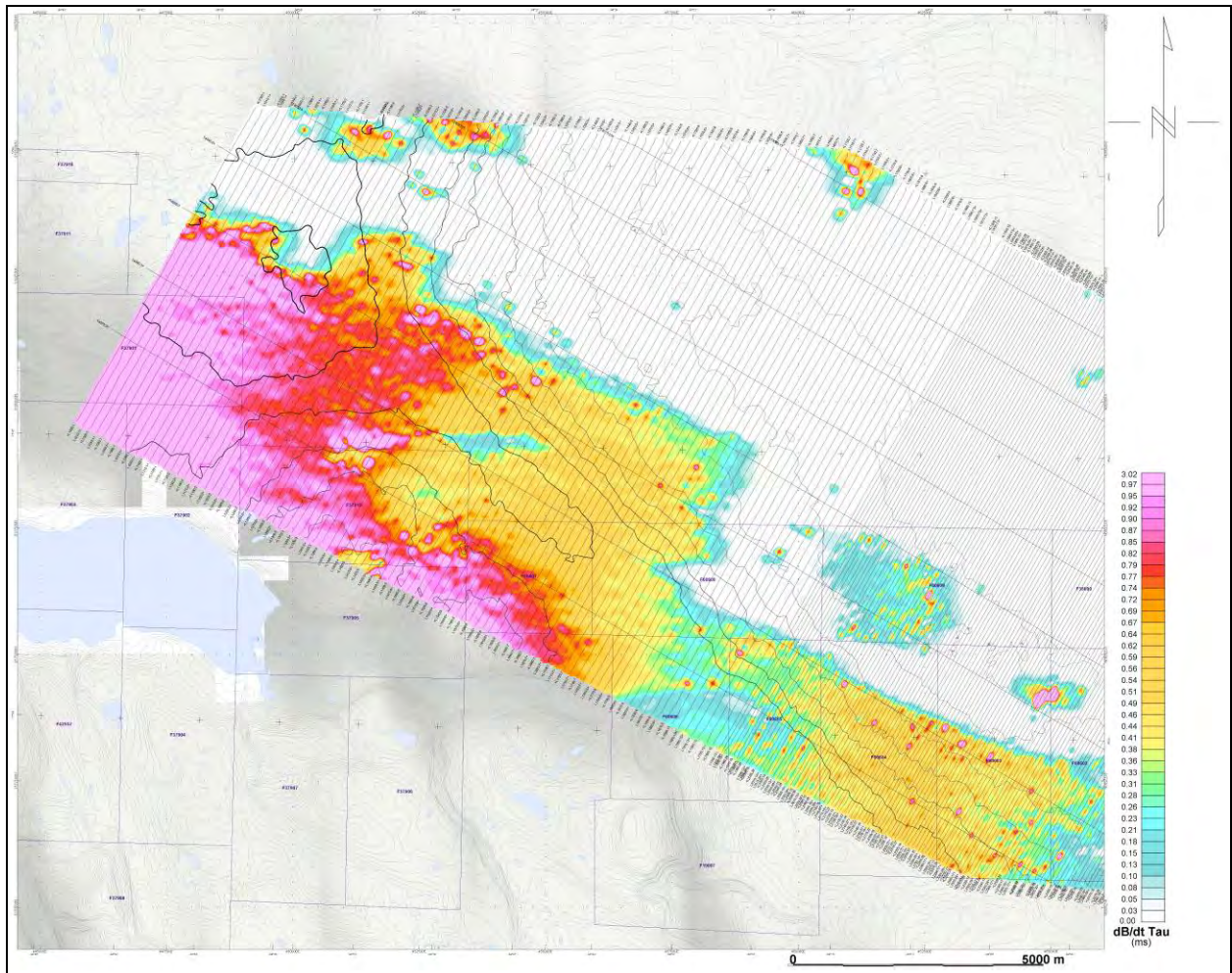
¹ Full size geophysical maps are also available in PDF format on the final DVD



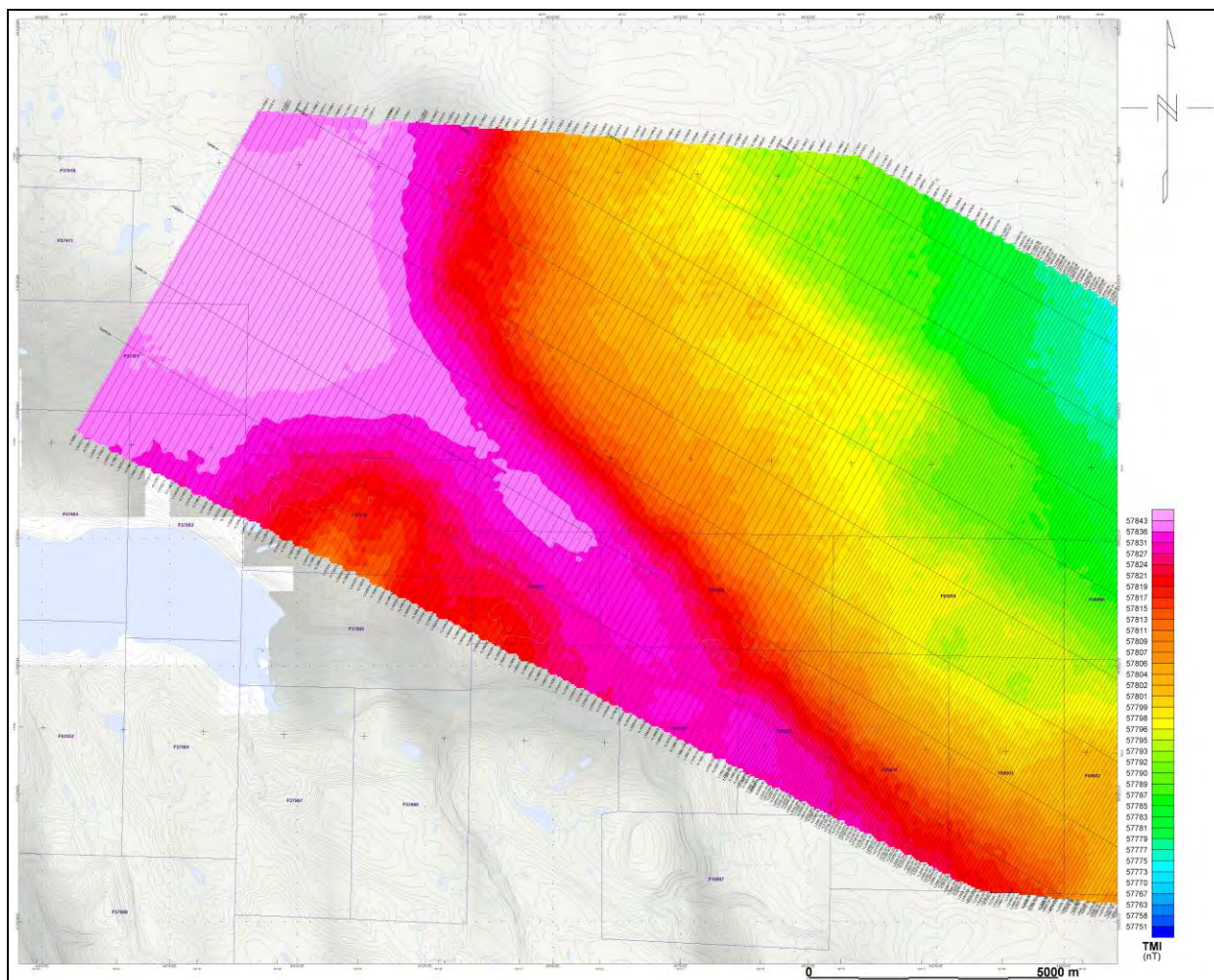
Storm Property (Plate 1) - VTEM dB/dt Z Component Profiles, Time Gates 0.220 to 7.036 ms



Storm Property (Plate 1) - VTEM B-Field Z Component Channel 36, Time Gate 2.021 ms

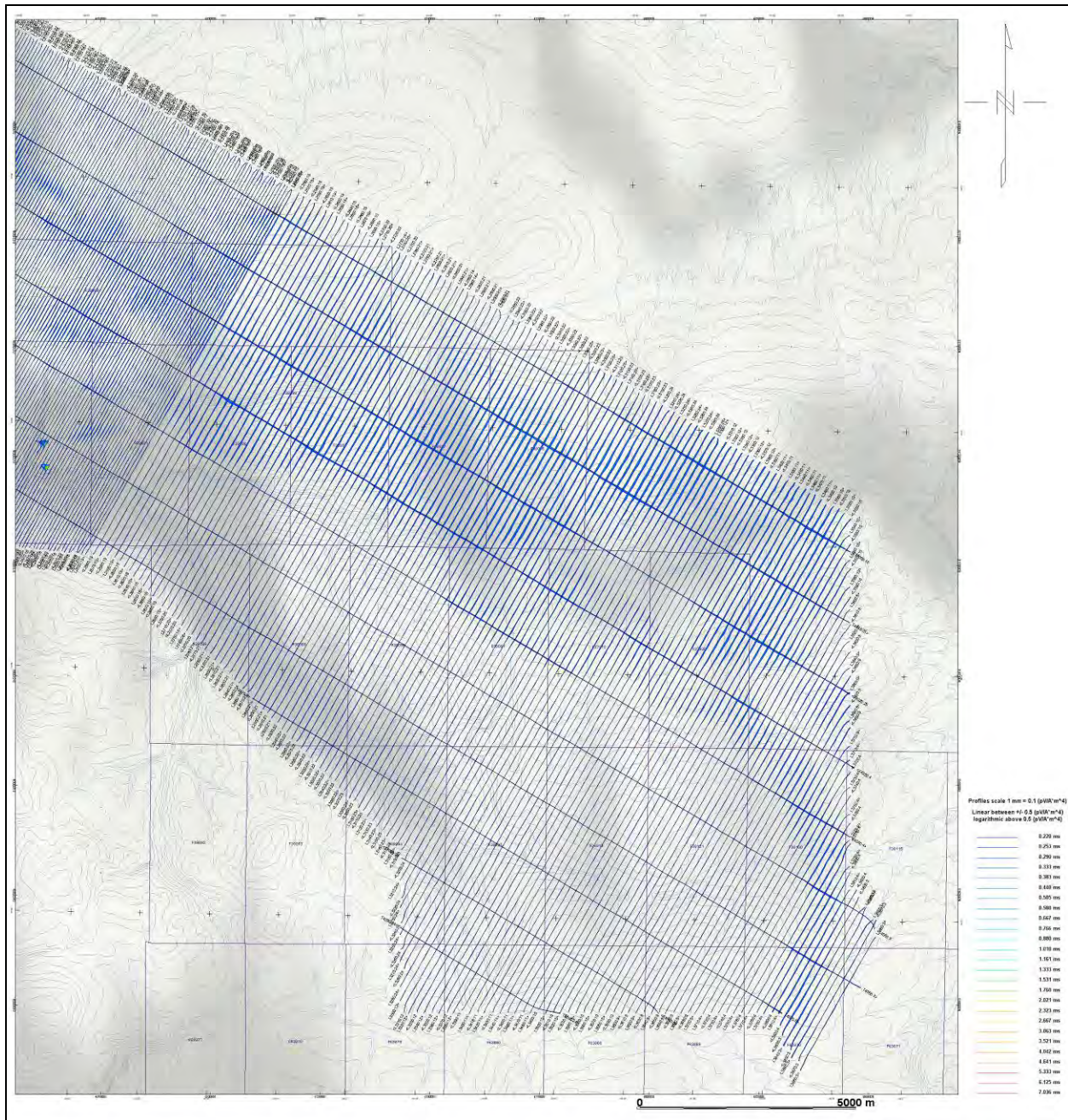


Storm Property (Plate 1) – dB/dt Calculated Time Constant (τ) with contours of anomaly areas of the Calculated Vertical Derivative of TMI

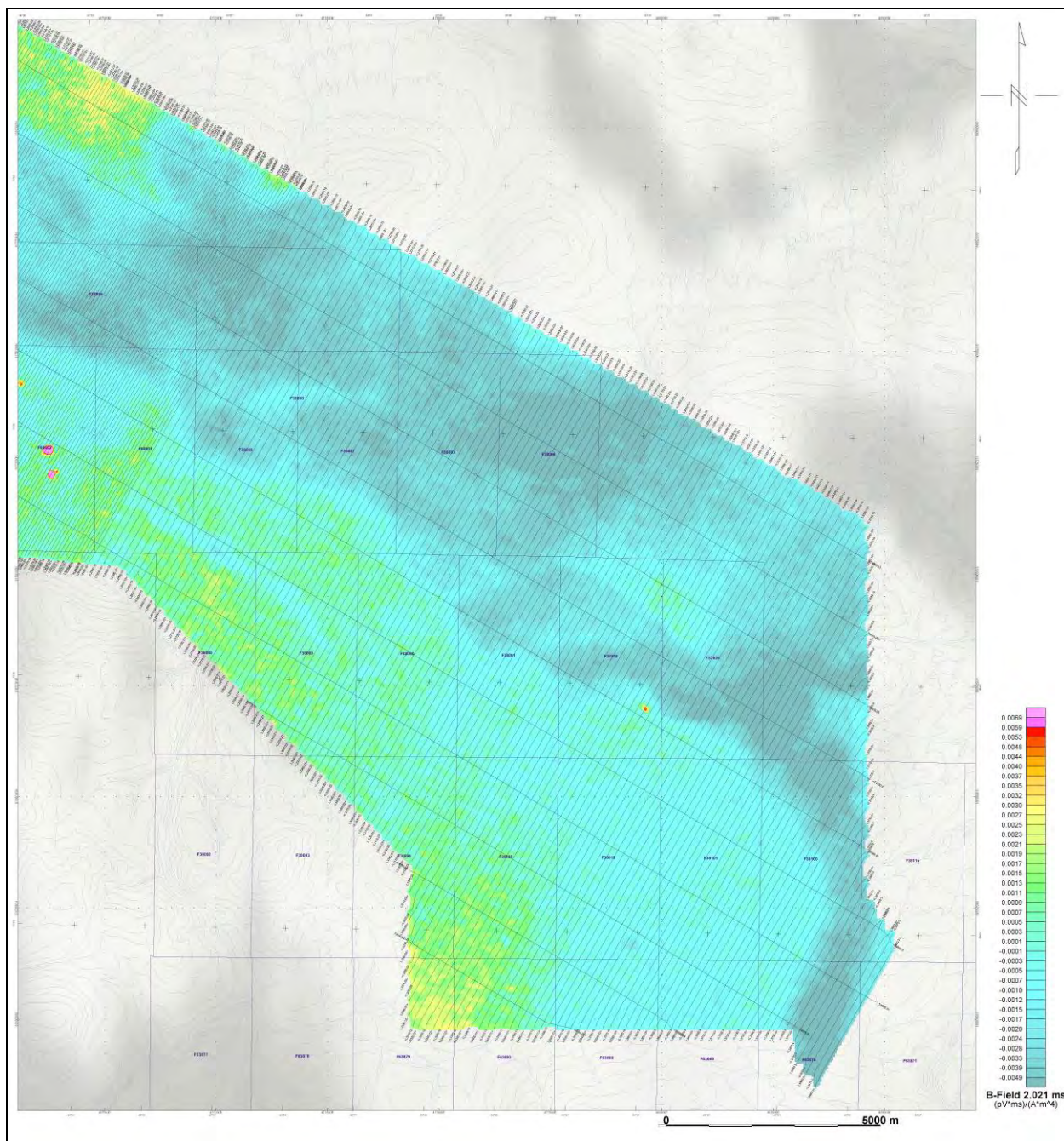


Storm Property (Plate 1) - Total Magnetic Intensity (TMI)

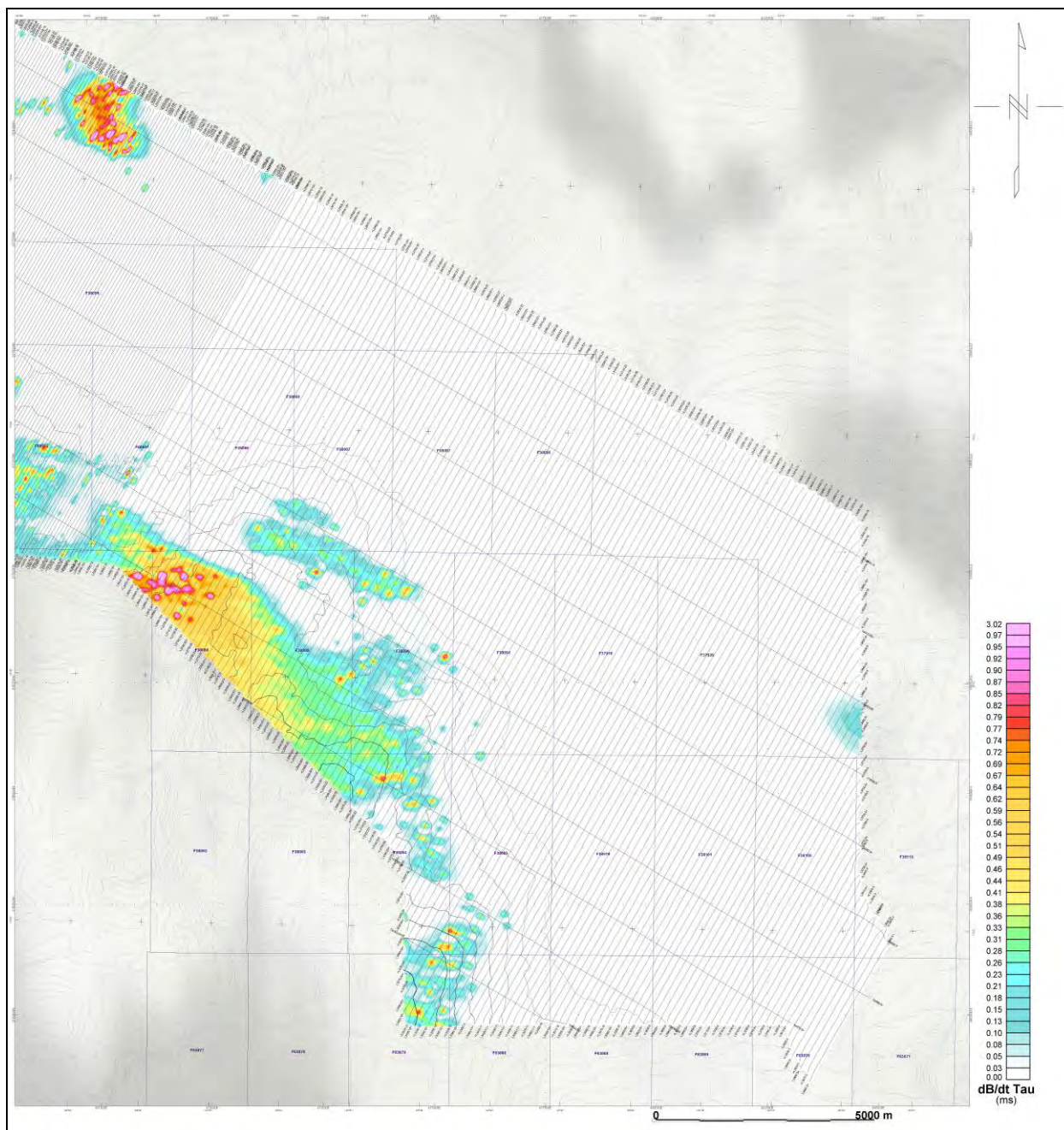




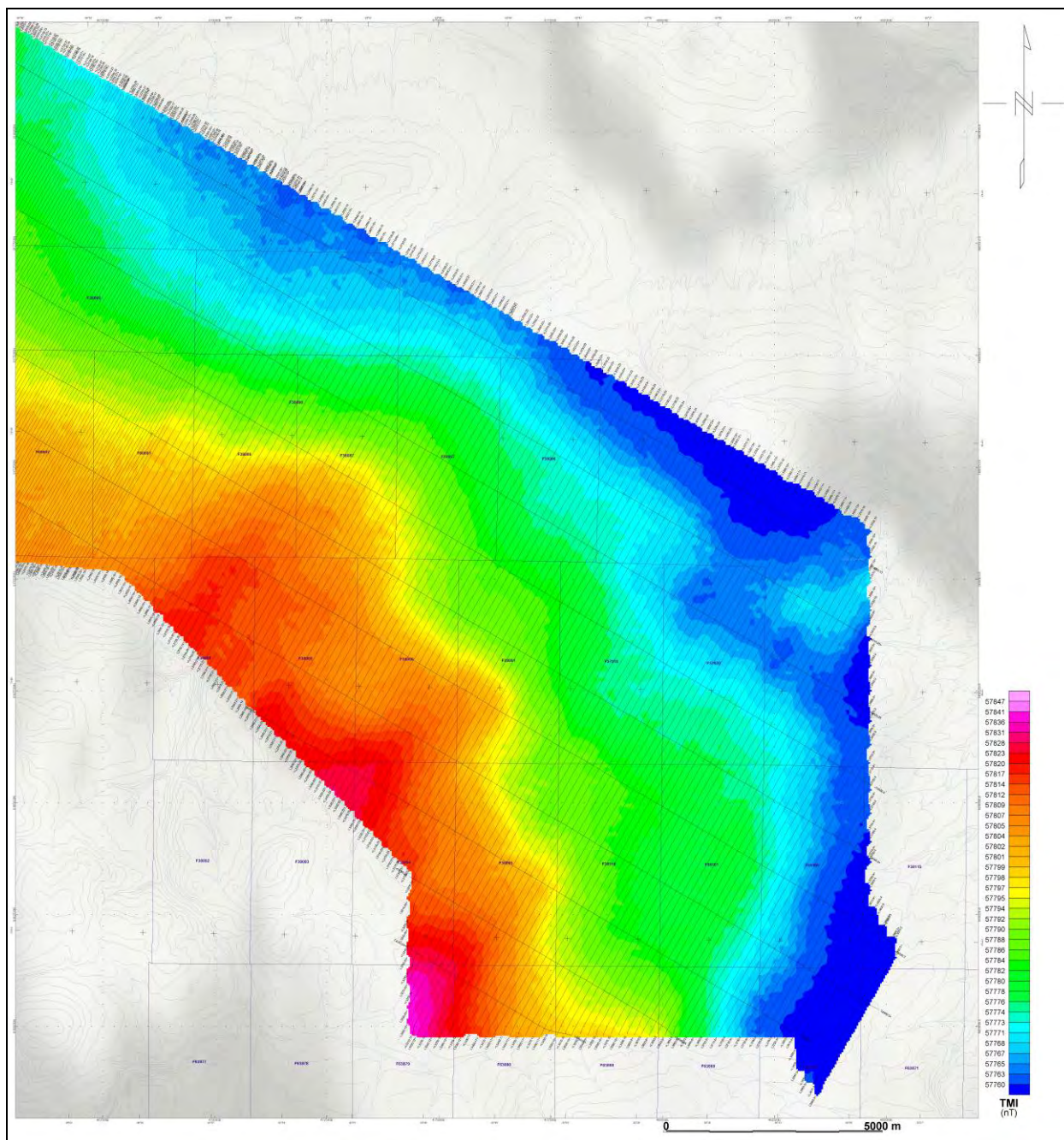
Storm Property (Plate 2) - VTEM dB/dt Z Component Profiles, Time Gates 0.220 to 7.036 ms



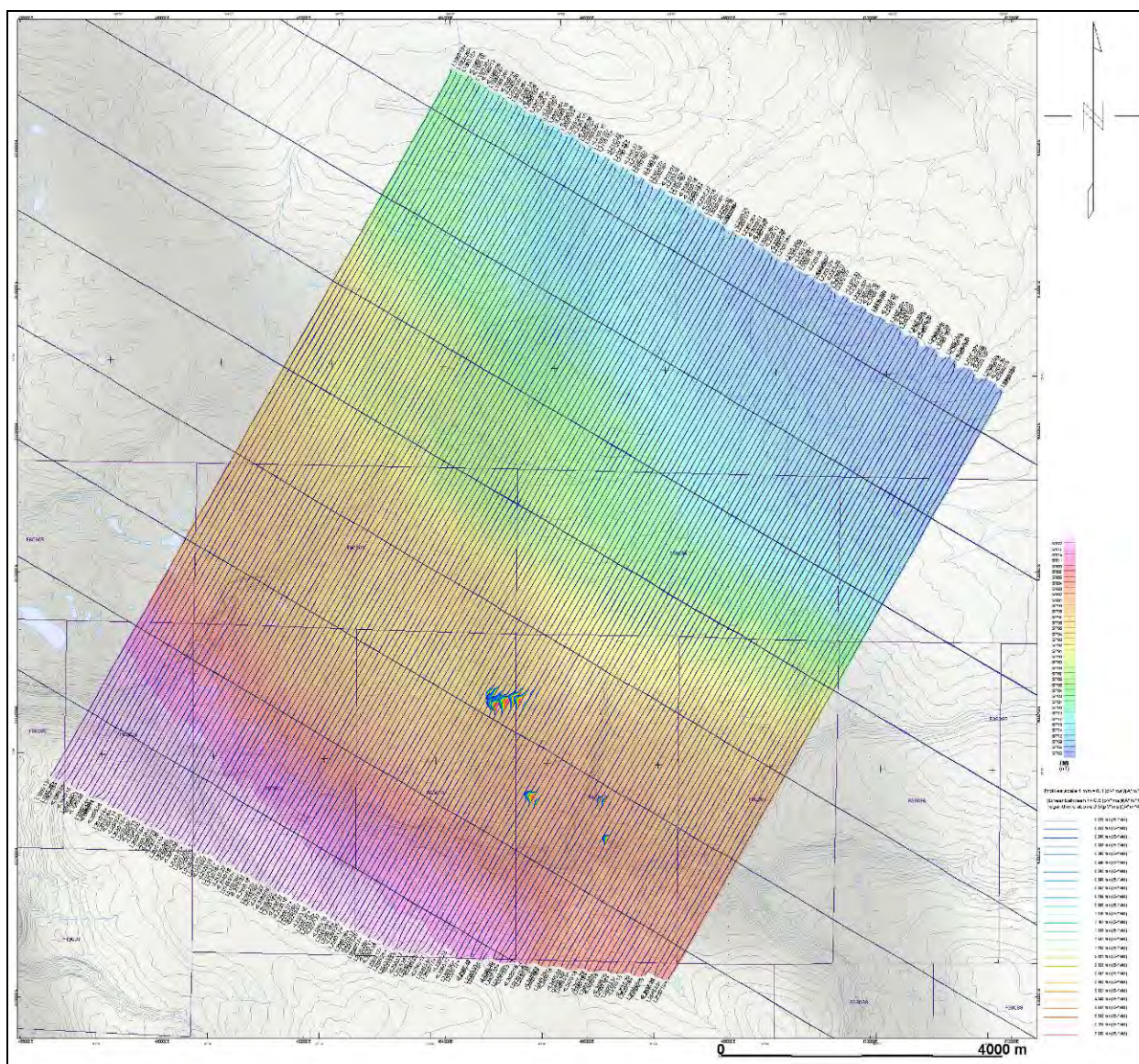
Storm Property (Plate 2) - VTEM B-Field Z Component Channel 36, Time Gate 2.021 ms

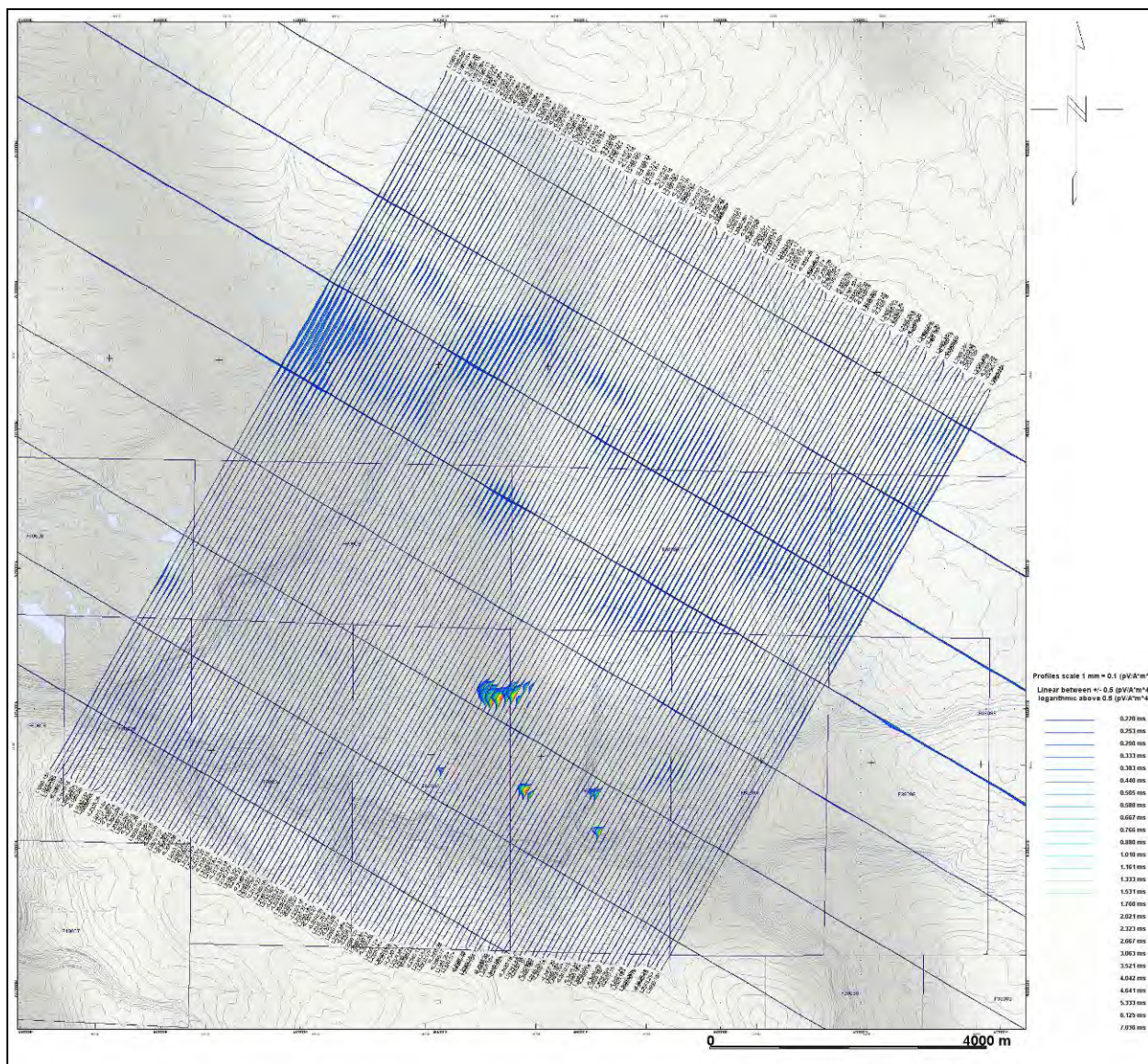


Storm Property (Plate 2) – dB/dt Calculated Time Constant (Tau) with contours of anomaly areas of the Calculated Vertical Derivative of TMI

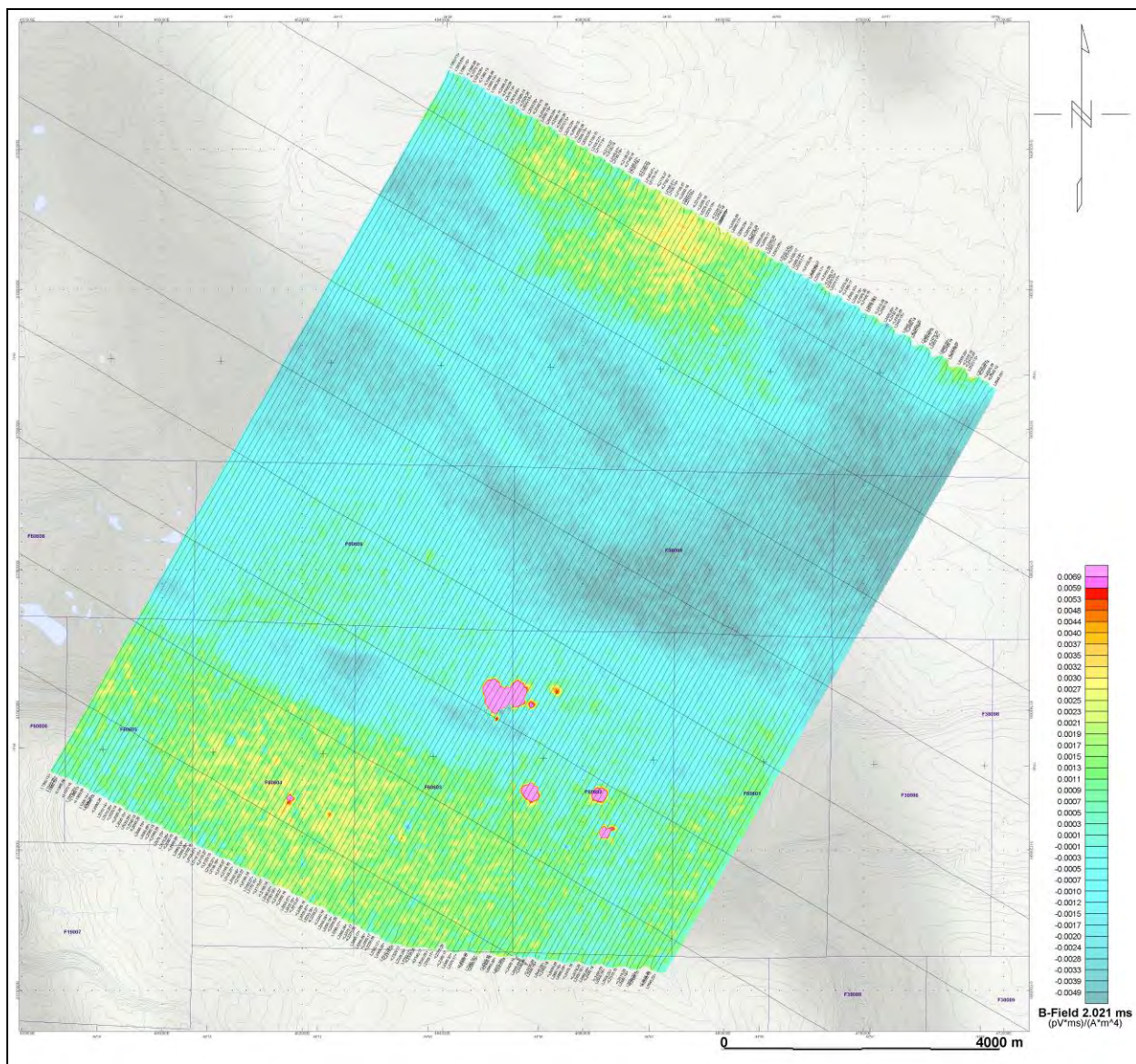


Storm Property (Plate 2) - Total Magnetic Intensity (TMI)

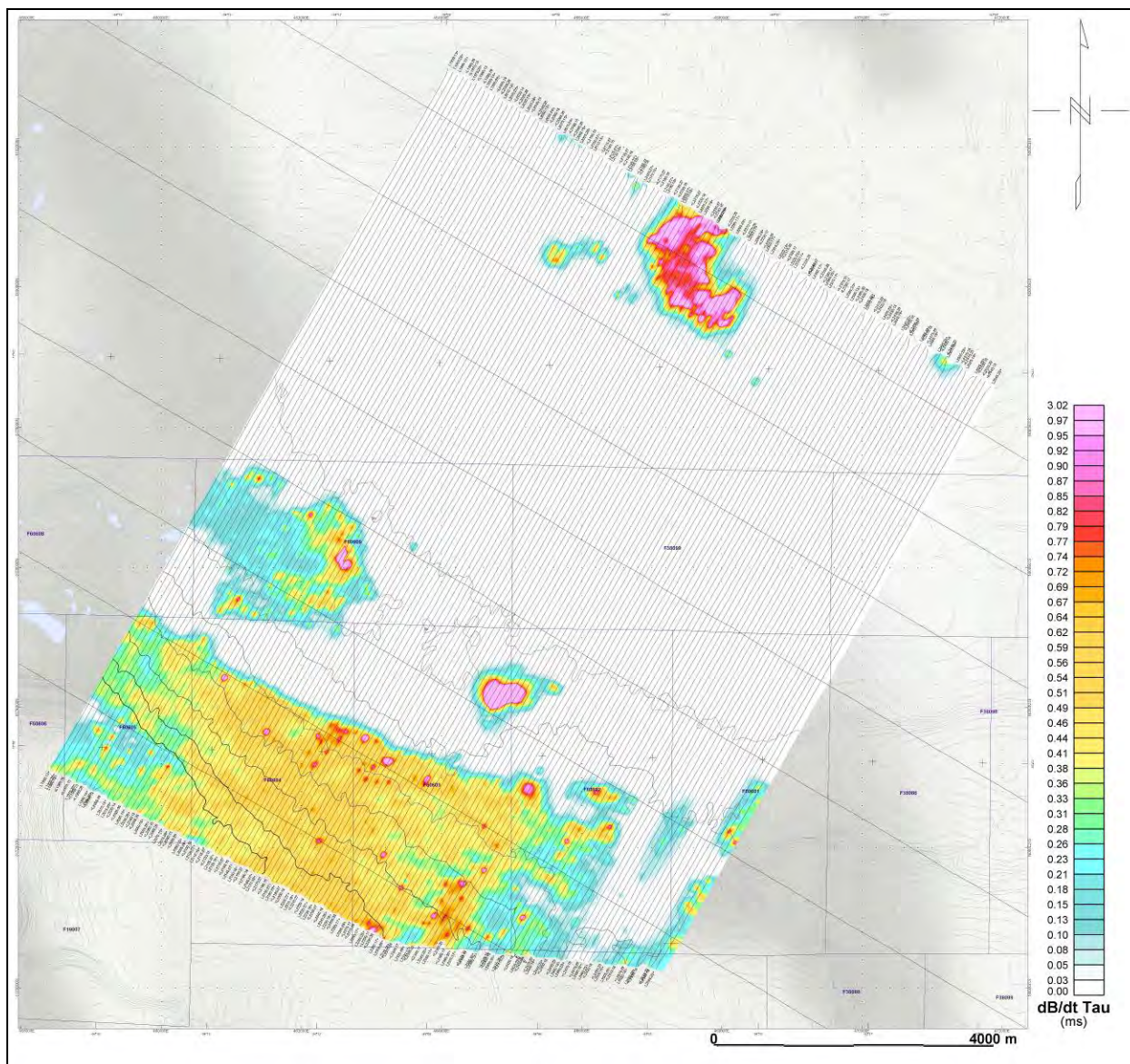




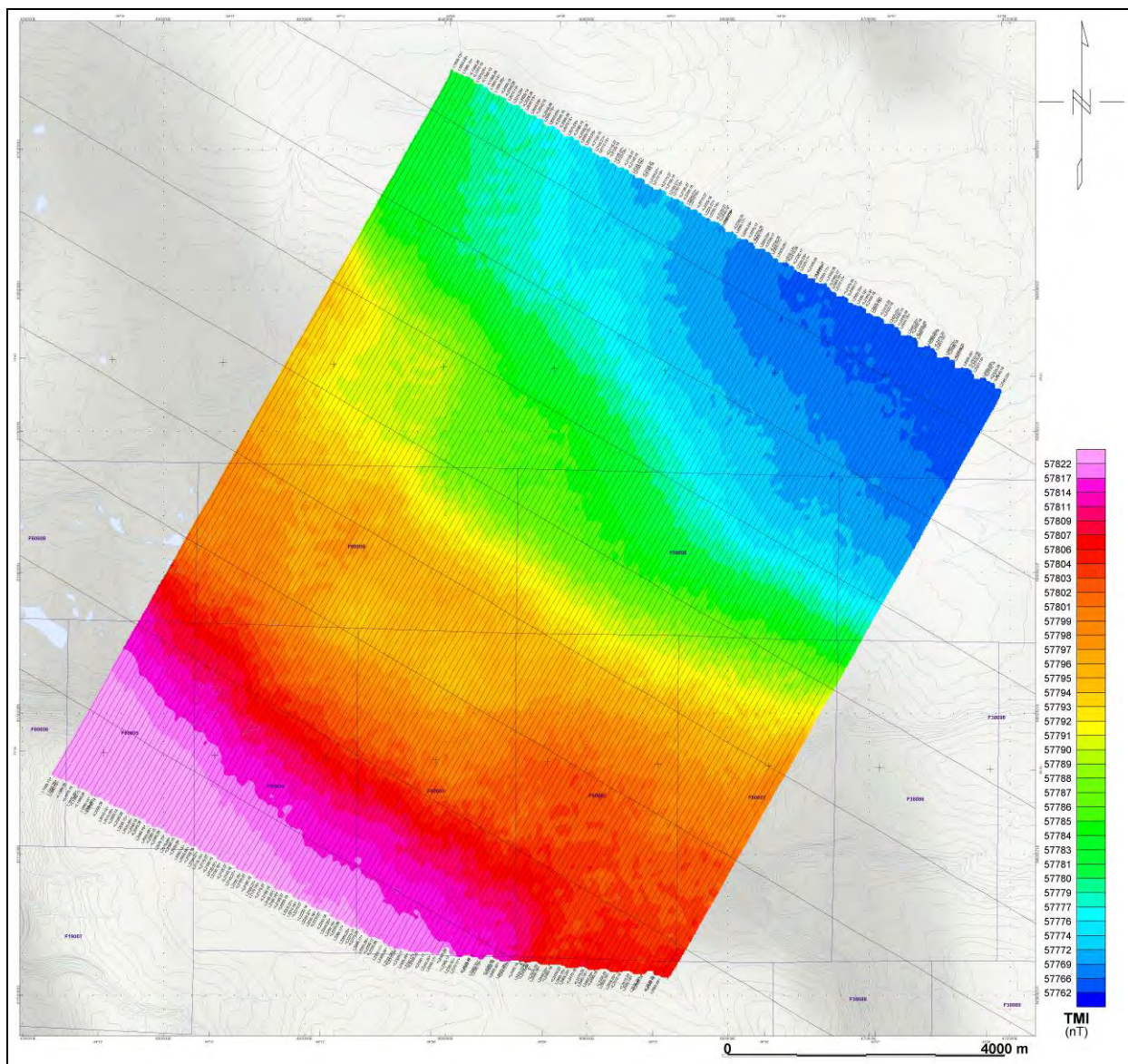
Storm Property (Infills) - VTEM dB/dt Z Component Profiles, Time Gates 0.220 to 7.036 ms



Storm Property (Infills) - VTEM B-Field Z Component Channel 36, Time Gate 2.021 ms



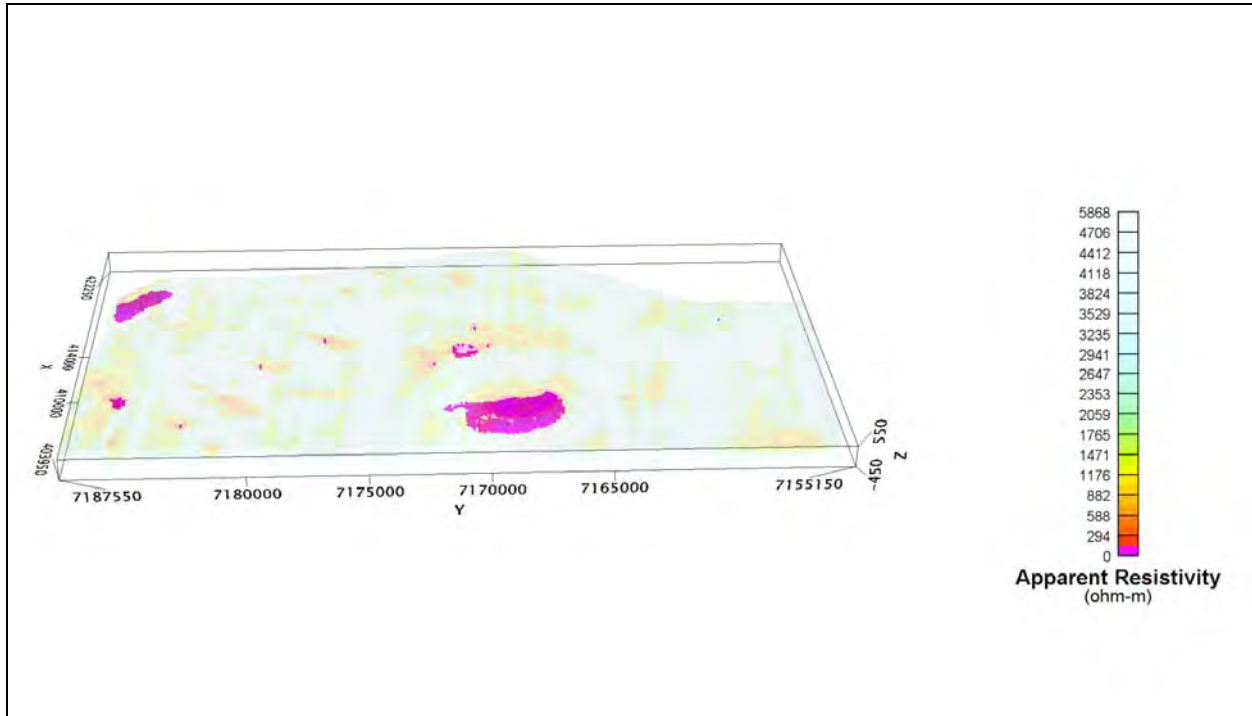
Storm Property (Infills) – dB/dt Calculated Time Constant (Tau) with contours of anomaly areas of the Calculated Vertical Derivative of TMI



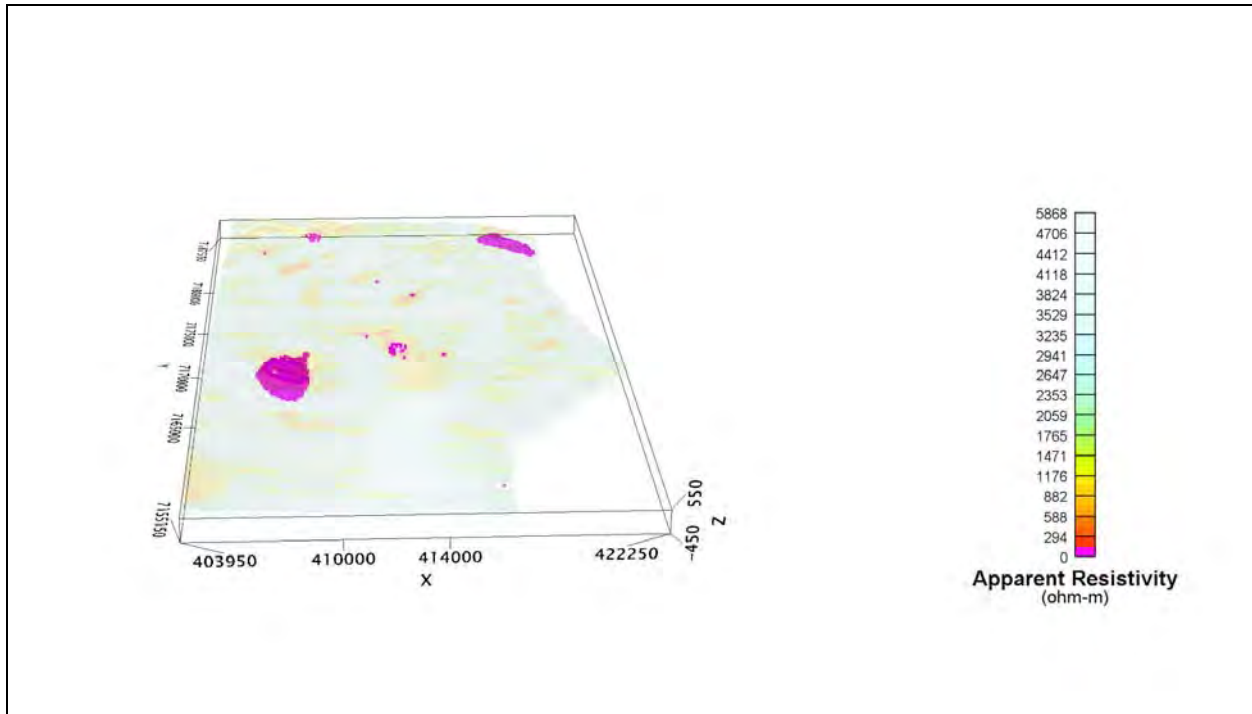
Storm Property (Infills) - Total Magnetic Intensity (TMI)

Resistivity Depth Image (RDI) MAPS

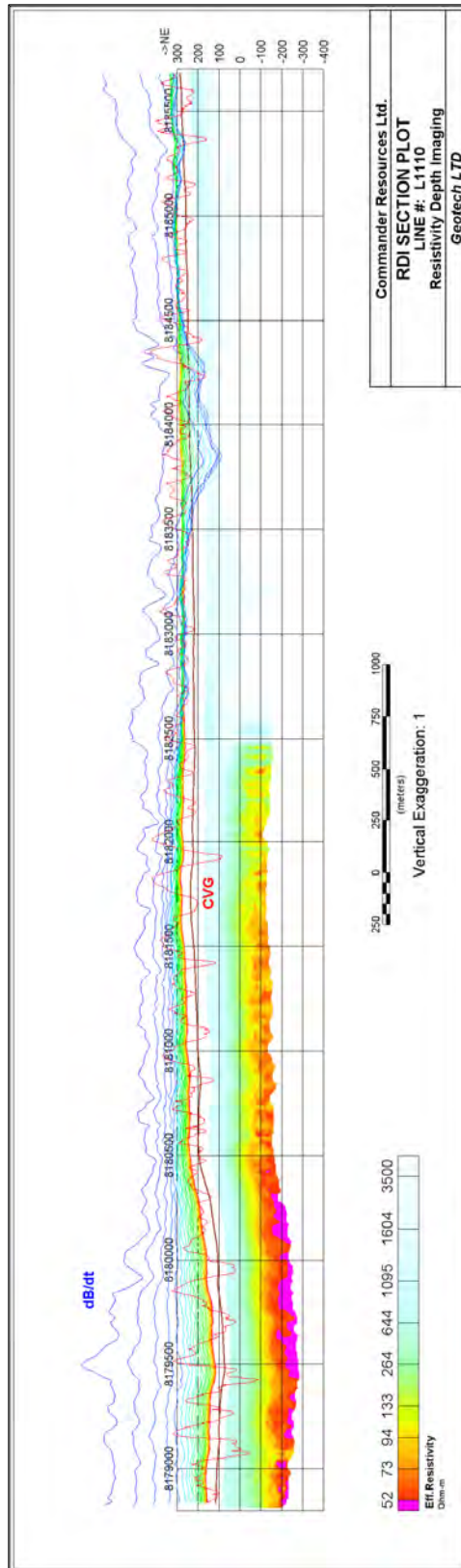
3D Resistivity Depth Images (RDI)



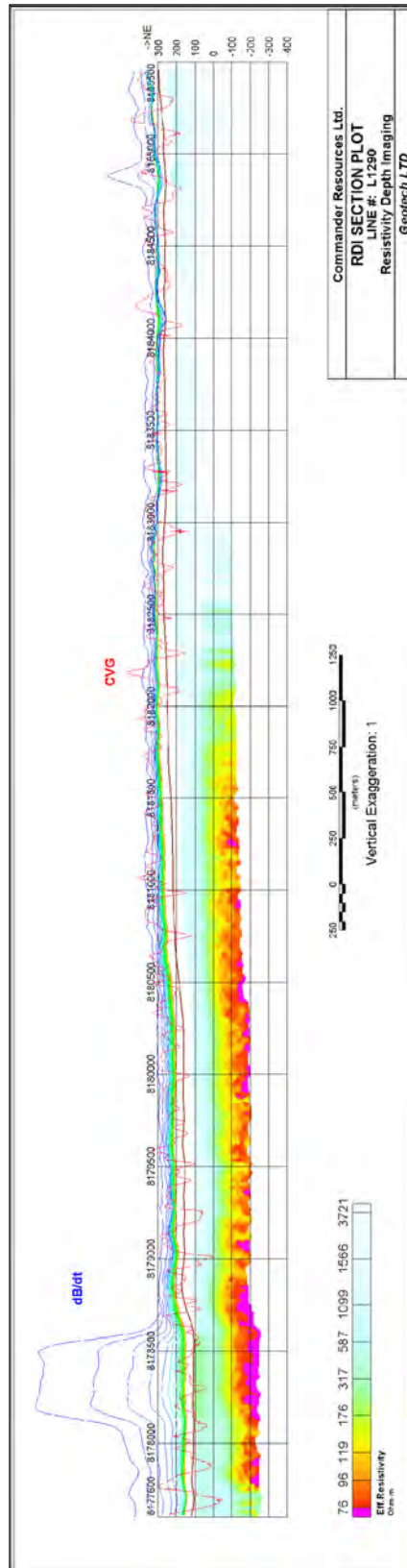
Storm Property (looking East)



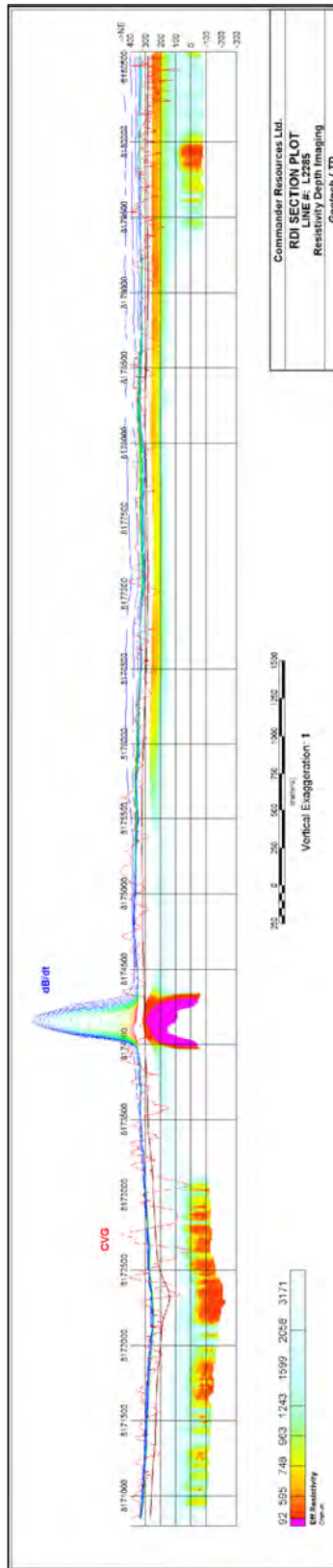
Storm Property (looking North)



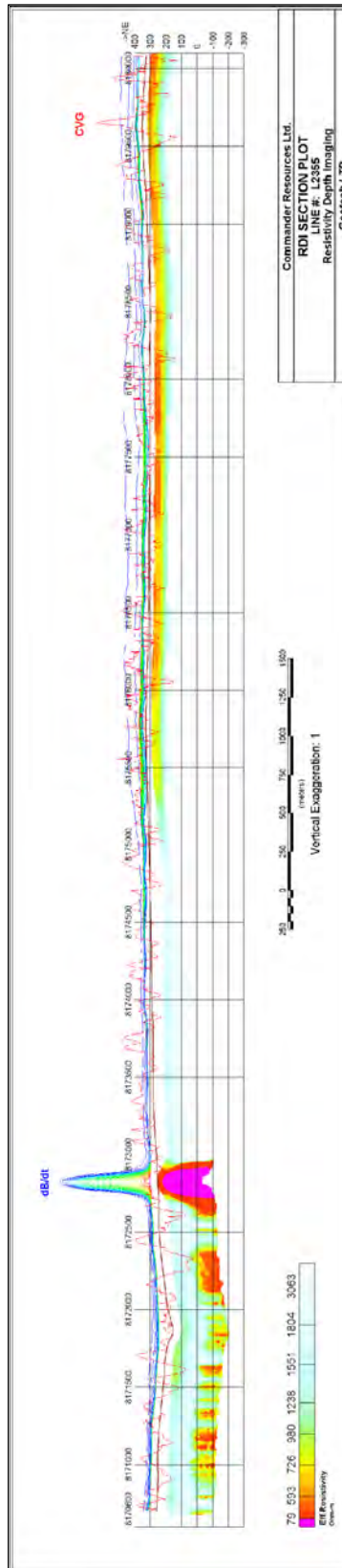
RDI Sections - Line 1110



RDI Sections - Line 1290



RDI Sections - Line 2285



RDI Sections - Line 2355

APPENDIX E

GENERALIZED MODELING RESULTS OF THE VTEM SYSTEM

Introduction

The VTEM system is based on a concentric or central loop design, whereby, the receiver is positioned at the centre of a transmitter loop that produces a primary field. The wave form is a bi-polar, modified square wave with a turn-on and turn-off at each end.

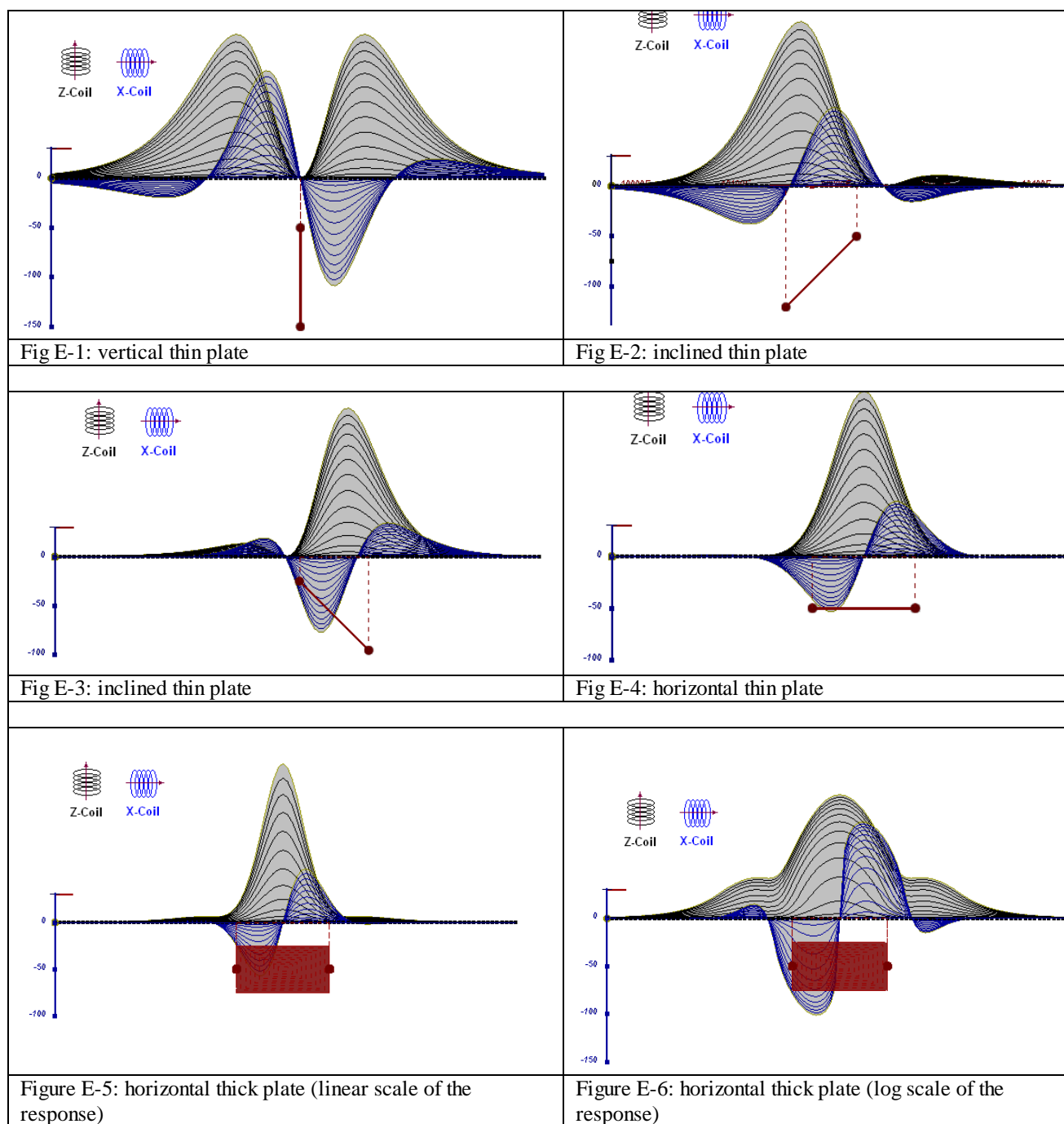
During turn-on and turn-off, a time varying field is produced (dB/dt) and an electro-motive force (emf) is created as a finite impulse response. A current ring around the transmitter loop moves outward and downward as time progresses. When conductive rocks and mineralization are encountered, a secondary field is created by mutual induction and measured by the receiver at the centre of the transmitter loop.

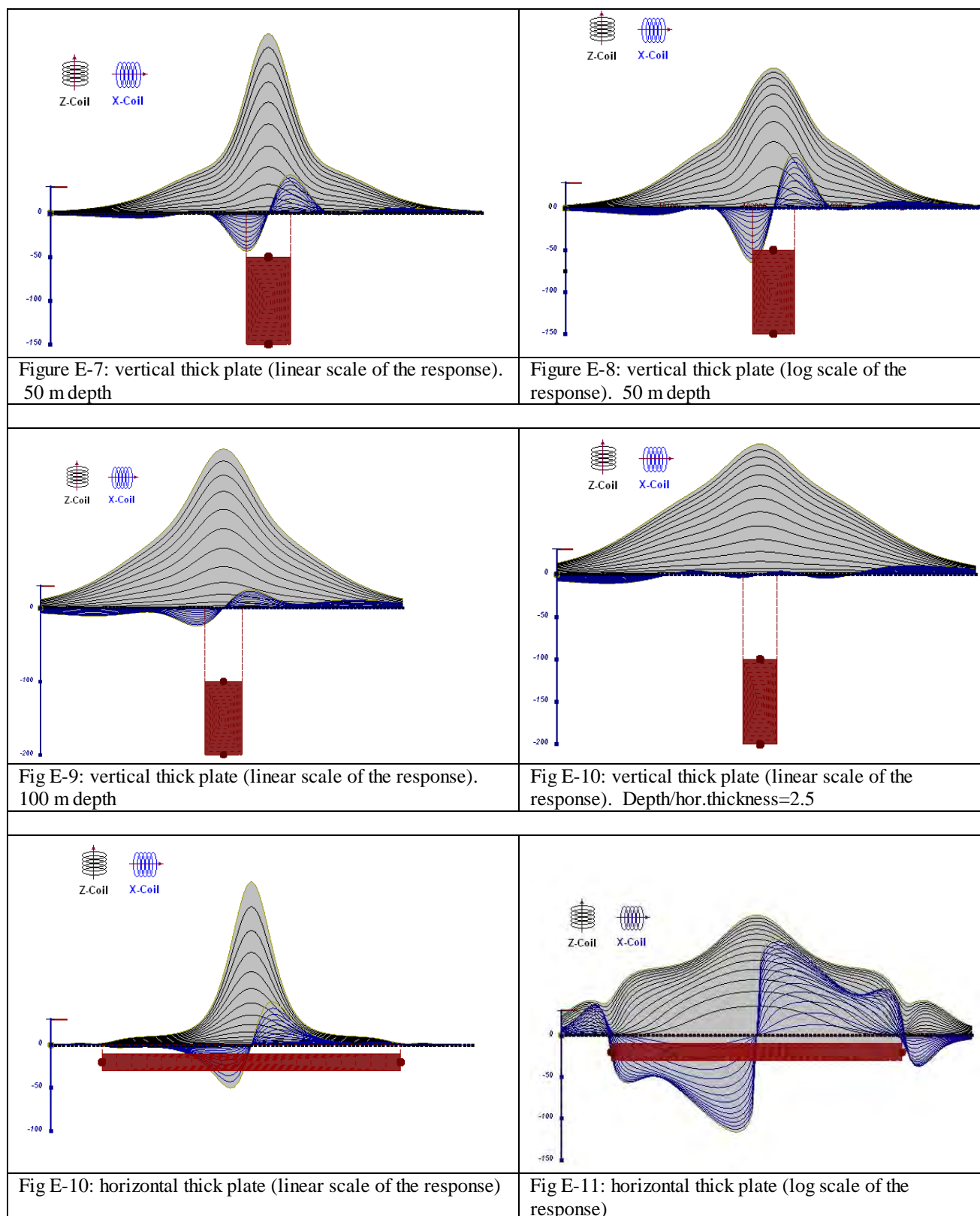
Efficient modeling of the results can be carried out on regularly shaped geometries, thus yielding close approximations to the parameters of the measured targets. The following is a description of a series of common models made for the purpose of promoting a general understanding of the measured results.

A set of models has been produced for the Geotech VTEM® system dB/dT Z and X components (see models E1 to E15). The MaxwellTM modeling program (EMIT Technology Pty. Ltd. Midland, WA, AU) used to generate the following responses assumes a resistive half-space. The reader is encouraged to review these models, so as to get a general understanding of the responses as they apply to survey results. While these models do not begin to cover all possibilities, they give a general perspective on the simple and most commonly encountered anomalies.

As the plate dips and departs from the vertical position, the peaks become asymmetrical.

As the dip increases, the aspect ratio (Min/Max) decreases and this aspect ratio can be used as an empirical guide to dip angles from near 90° to about 30°. The method is not sensitive enough where dips are less than about 30°.





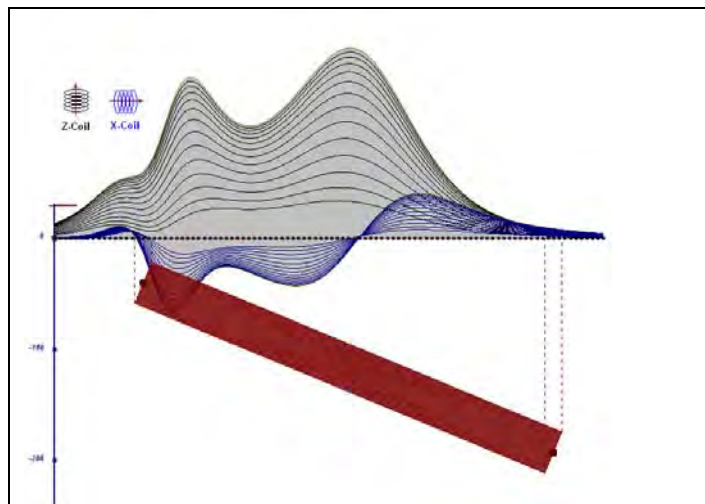


Fig E-12: inclined long thick plate

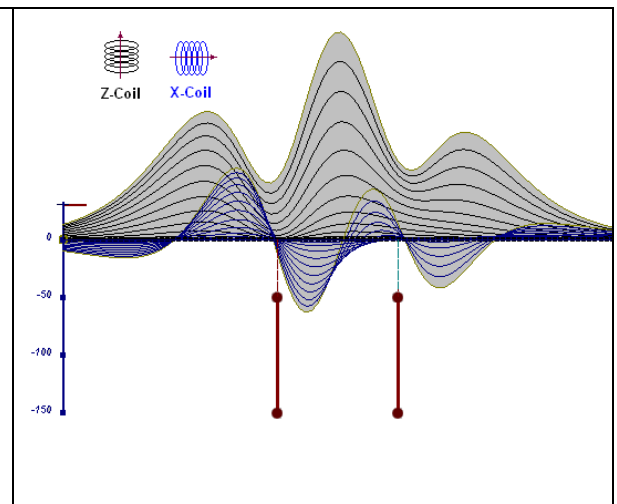


Fig E-13: two vertical thin plates

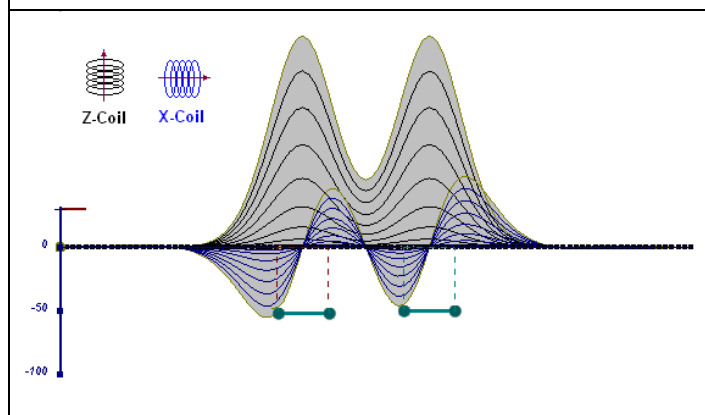


Fig E-14: two horizontal thin plates

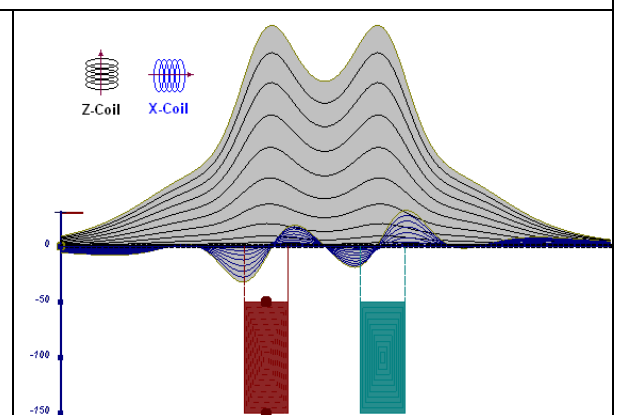


Fig E-15: two vertical thick plates

The same type of target but with different thickness, for example, creates different form of the response:

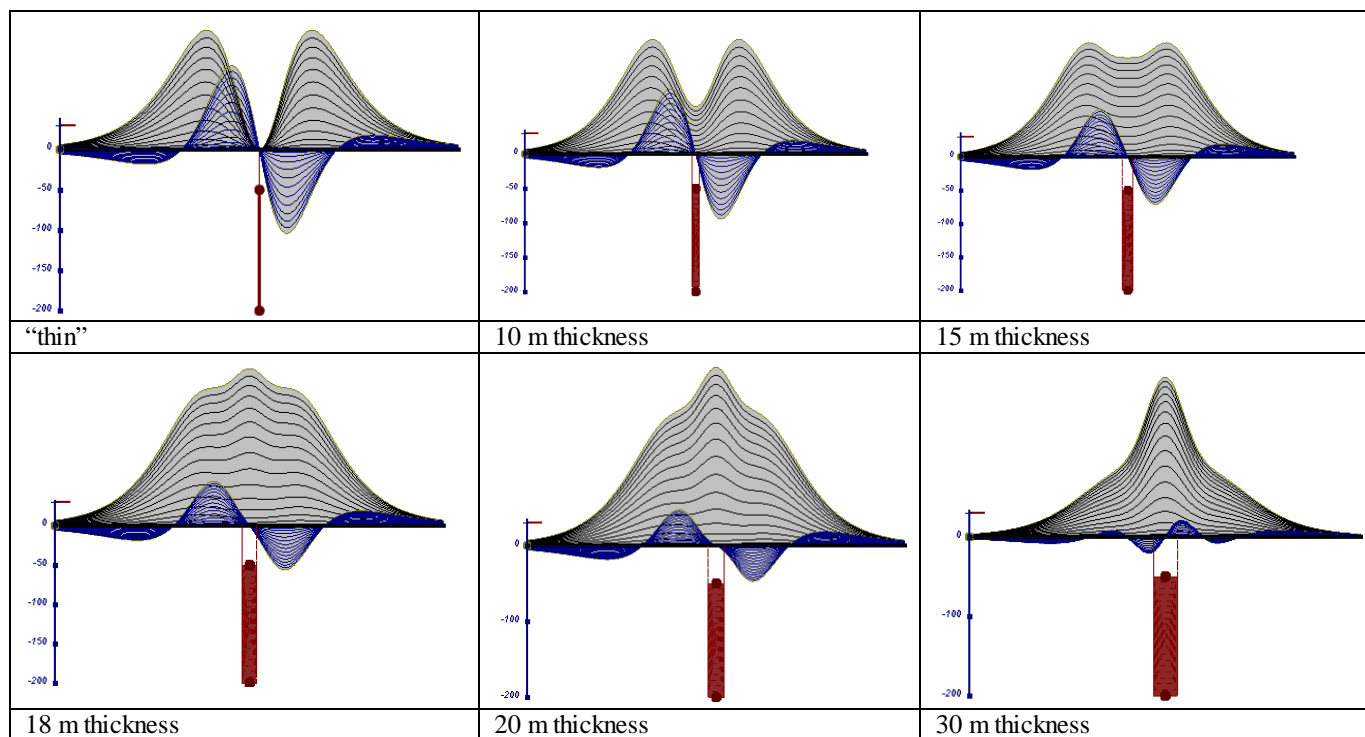


Fig.E-16 Conductive vertical plate, depth 50 m, strike length 200 m, depth extend 150 m.

Alexander Prihodko, PhD, P.Geol
Geotech Ltd.

September 2010

APPENDIX F

EM TIME CONSTANT (TAU) ANALYSIS

Estimation of time constant parameter¹ in transient electromagnetic method is one of the steps toward the extraction of the information about conductance's beneath the surface from TEM measurements.

The most reliable method to discriminate or rank conductors from overburden, background or one and other is by calculating the EM field decay time constant (TAU parameter), which directly depends on conductance despite their depth and accordingly amplitude of the response.

Theory

As established in electromagnetic theory, the magnitude of the electro-motive force (emf) induced is proportional to the time rate of change of primary magnetic field at the conductor. This emf causes eddy currents to flow in the conductor with a characteristic transient decay, whose Time Constant (Tau) is a function of the conductance of the survey target or conductivity and geometry (including dimensions) of the target. The decaying currents generate a proportional secondary magnetic field, the time rate of change of which is measured by the receiver coil as induced voltage during the Off time.

The receiver coil output voltage (e_0) is proportional to the time rate of change of the secondary magnetic field and has the form,

$$e_0 \propto (1 / \tau) e^{-(t / \tau)}$$

Where,

$\tau = L/R$ is the characteristic time constant of the target (TAU)

R = resistance

L = inductance

From the expression, conductive targets that have small value of resistance and hence large value of τ yield signals with small initial amplitude that decays relatively slowly with progress of time. Conversely, signals from poorly conducting targets that have large resistance value and small τ , have high initial amplitude but decay rapidly with time¹ (Fig. F1).

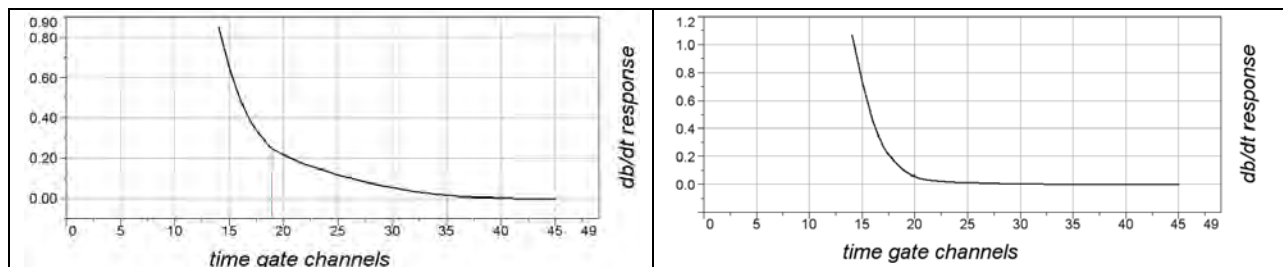


Figure F1 Left – presence of good conductor, right – poor conductor.

¹ McNeill, JD, 1980, “Applications of Transient Electromagnetic Techniques”, Technical Note TN-7 page 5, Geonics Limited, Mississauga, Ontario.

EM Time Constant (Tau) Calculation

The EM Time-Constant (TAU) is a general measure of the speed of decay of the electromagnetic response and indicates the presence of eddy currents in conductive sources as well as reflecting the “conductance quality” of a source. Although TAU can be calculated using either the measured dB/dt decay or the calculated B-field decay, dB/dt is commonly preferred due to better stability (S/N) relating to signal noise. Generally, TAU calculated on base of early time response reflects both near surface overburden and poor conductors whereas, in the late ranges of time, deep and more conductive sources, respectively. For example early time TAU distribution in an area that indicates conductive overburden is shown in Figure 2.

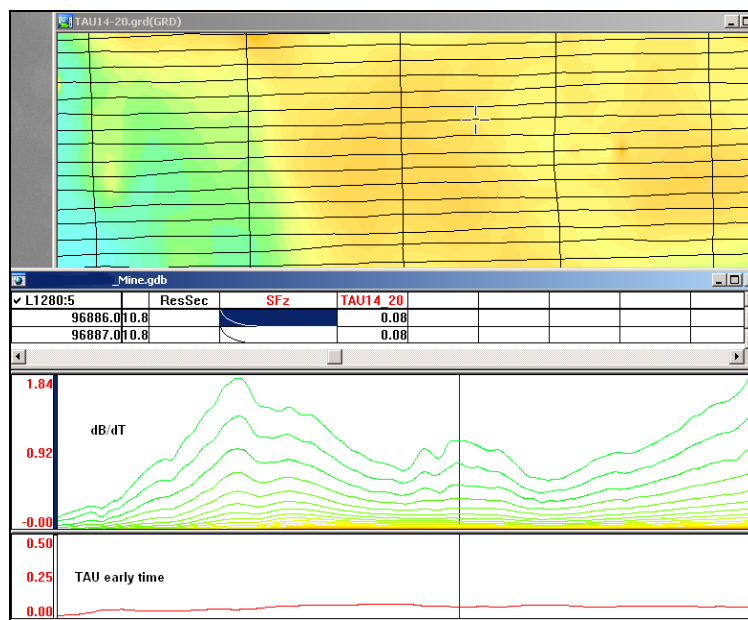


Figure F2 – Map of early time TAU. Area with overburden conductive layer and local sources.

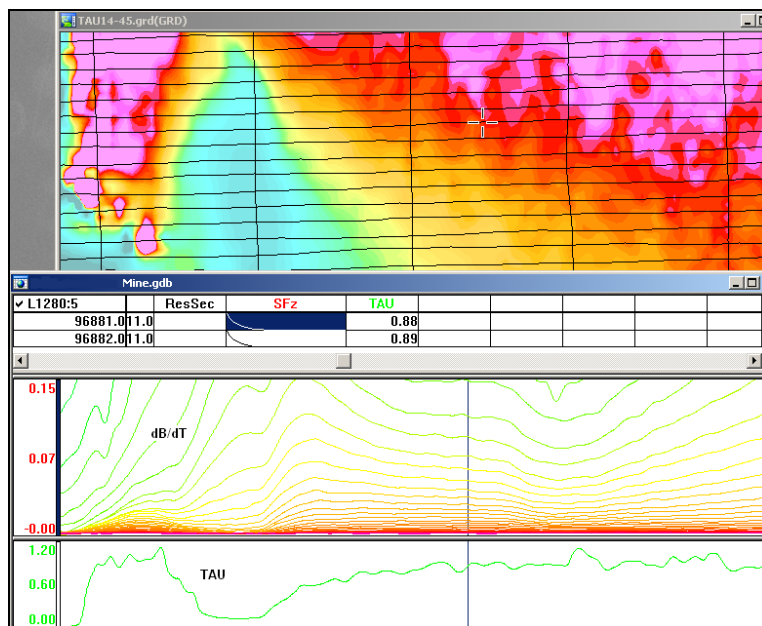


Figure F3 – Map of full time range TAU with EM anomaly due to deep highly conductive target.

There are many advantages of TAU maps:

- TAU depends only on one parameter (conductance) in contrast to response magnitude;
- TAU is integral parameter, which covers time range and all conductive zones and targets are displayed independently of their depth and conductivity on a single map.
- Very good differential resolution in complex conductive places with many sources with different conductivity.
- Signs of the presence of good conductive targets are amplified and emphasized independently of their depth and level of response accordingly.

In the example shown in Figure 4 and 5, three local targets are defined, each of them with a different depth of burial, as indicated on the resistivity depth image (RDI). All are very good conductors but the deeper target (number 2) has a relatively weak dB/dt signal yet also features the strongest total TAU (Figure 4). This example highlights the benefit of TAU analysis in terms of an additional target discrimination tool.

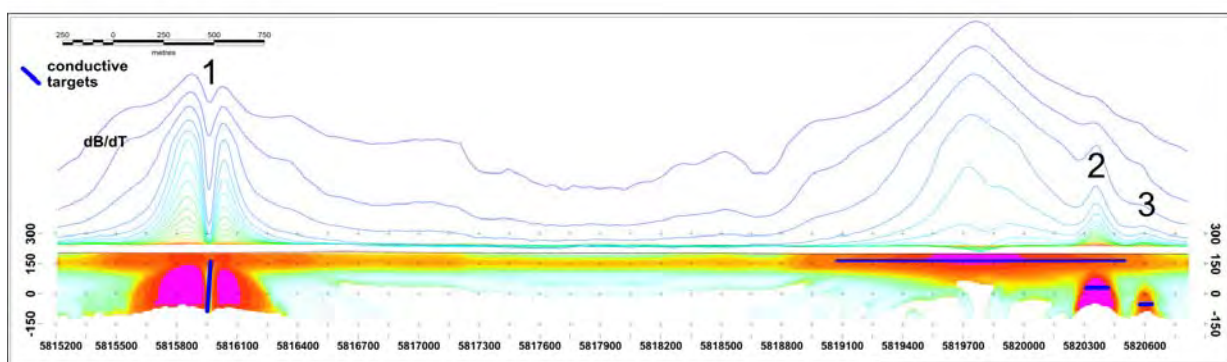


Figure F4 – dB/dt profile and RDI with different depths of targets.

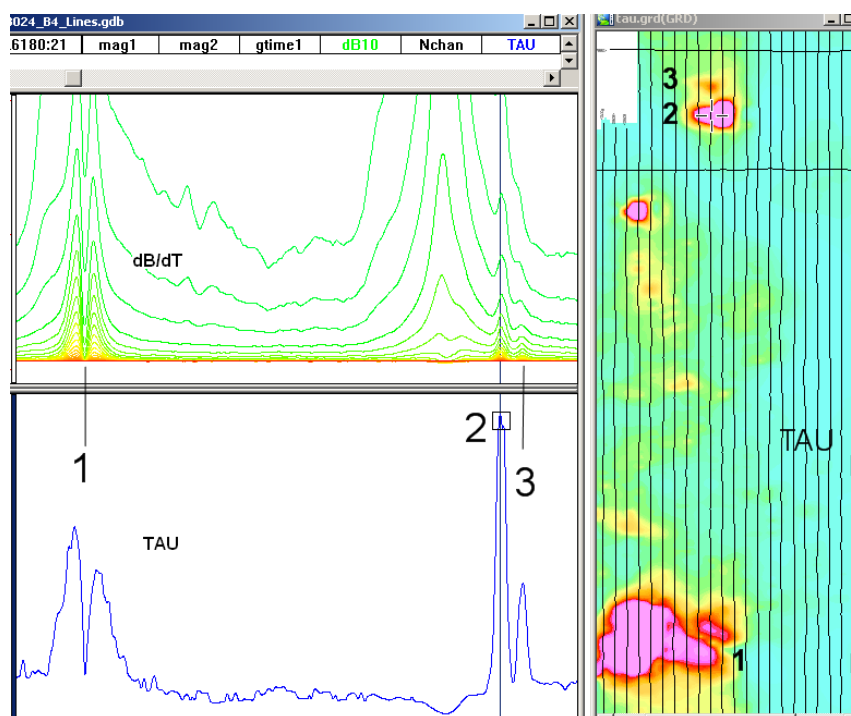


Figure F5 – Map of total TAU and dB/dt profile.

The EM Time Constants for dB/dt and B-field were calculated using the “sliding Tau” in-house program developed at Geotech2. The principle of the calculation is based on using of time window (4 time channels) which is sliding along the curve decay and looking for latest time channels which have a response above the level of noise and decay. The EM decays are obtained from all available decay channels, starting at the latest channel. Time constants are taken from a least square fit of a straight-line (log/linear space) over the last 4 gates above a pre-set signal threshold level (Figure F6). Threshold settings are pointed in the “label” property of TAU database channels. The sliding Tau method determines that, as the amplitudes increase, the time-constant is taken at progressively later times in the EM decay. Conversely, as the amplitudes decrease, Tau is taken at progressively earlier times in the decay. If the maximum signal amplitude falls below the threshold, or becomes negative for any of the 4 time gates, then Tau is not calculated and is assigned a value of “dummy” by default.

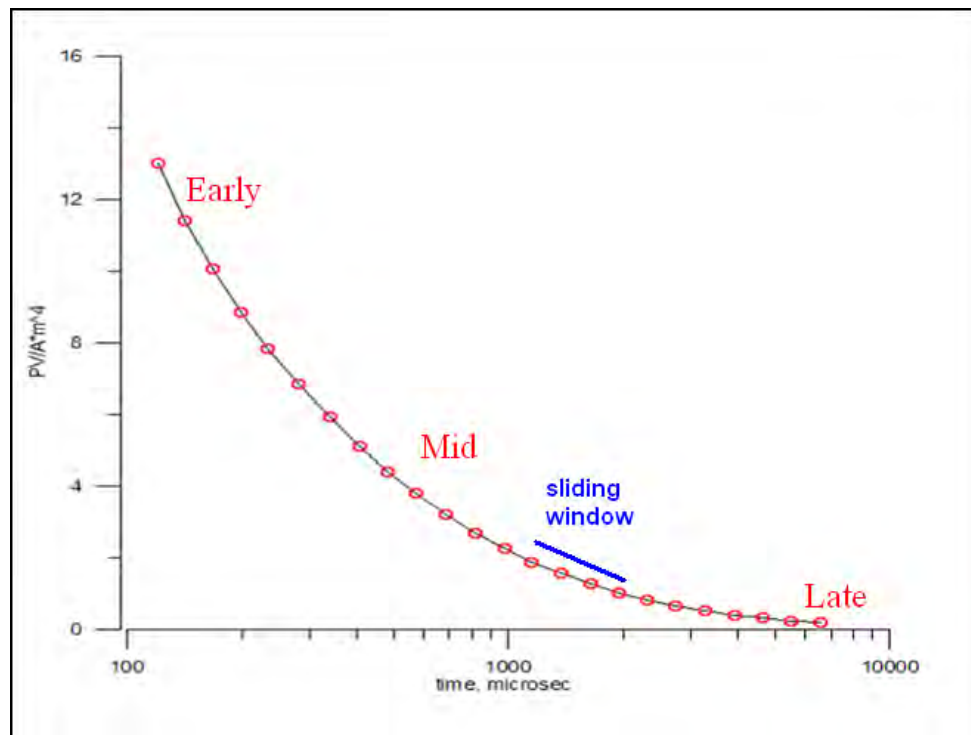


Figure F6 - Typical dB/dt decays of VTEM data

Alexander Prikhodko, PhD, P.Geo
Geotech Ltd.

September 2010

² by A.Prikhodko

APPENDIX G

TEM Resistivity Depth Imaging (RDI)

Resistivity depth imaging (RDI) is technique used to rapidly convert EM profile decay data into an equivalent resistivity versus depth cross-section, by deconvolving the measured TEM data.

The used RDI algorithm of Resistivity-Depth transformation is based on scheme of the apparent resistivity transform of Maxwell A.Meju (1998)¹ and TEM response from conductive half-space. The program is developed by Alexander Prihodko and depth calibrated based on forward plate modeling for VTEM system configuration (Fig. 1-10).

RDIs provide reasonable indications of conductor relative depth and vertical extent, as well as accurate 1D layered-earth apparent conductivity/resistivity structure across VTEM flight lines. Approximate depth of investigation of a TEM system, image of secondary field distribution in half space, effective resistivity, initial geometry and position of conductive targets is the information obtained on base of the RDIs.

Maxwell forward modeling with RDI sections from the synthetic responses (VTEM system)

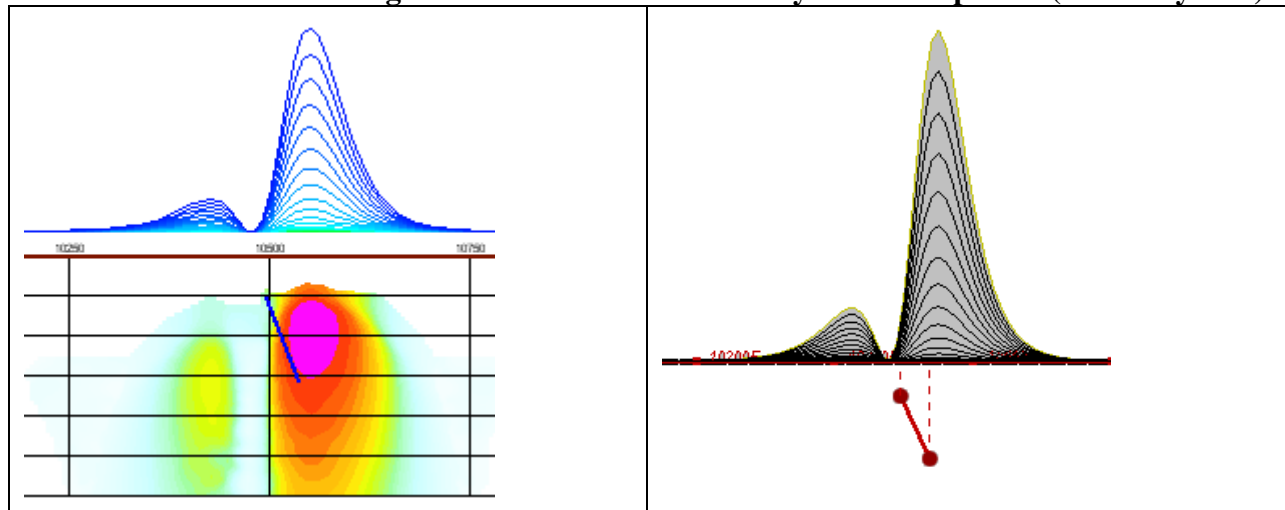


Fig. 1 Maxwell plate model and RDI from the calculated response for conductive “thin” plate (depth 50 m, dip 65 degree, depth extend 100 m).

¹ Maxwell A.Meju, 1998, Short Note: A simple method of transient electromagnetic data analysis, *Geophysics*, **63**, 405–410.

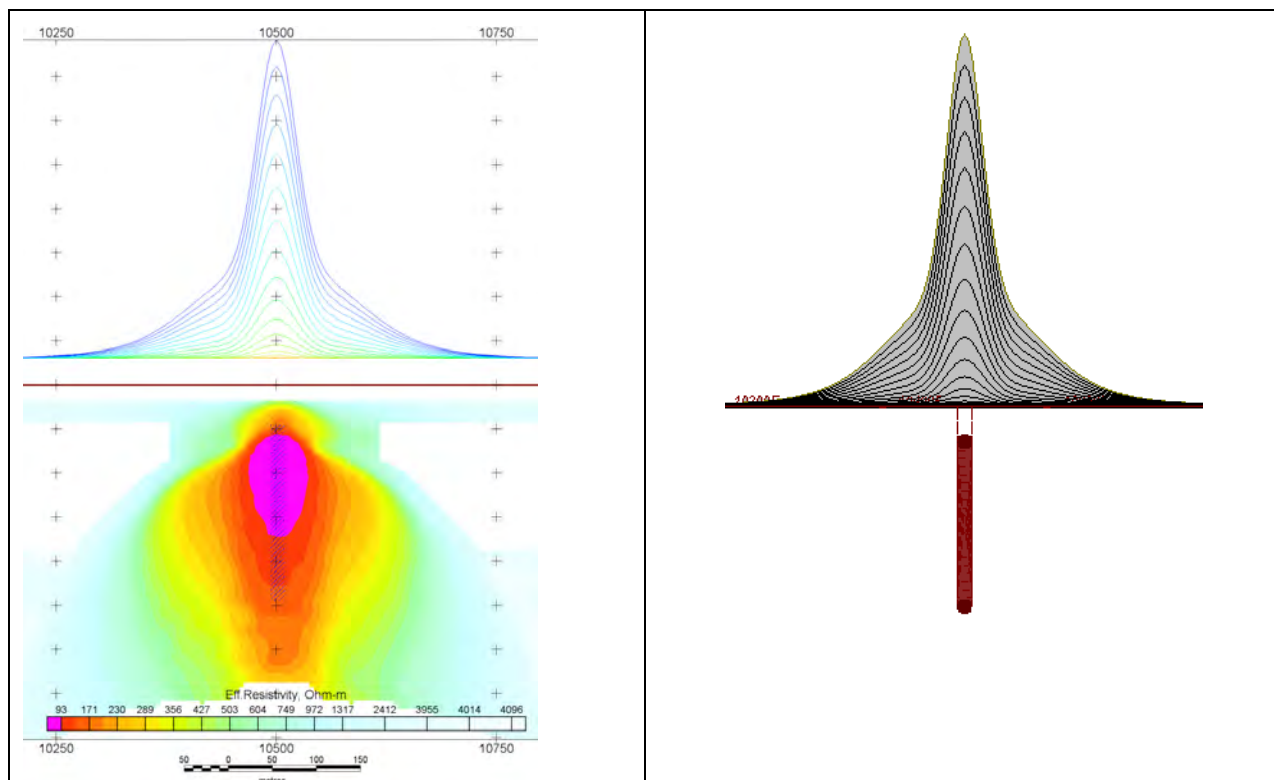


Fig. 2 Maxwell plate model and RDI from the calculated response for "thick" plate 18 m thickness, depth 50 m, depth extend 200 m).

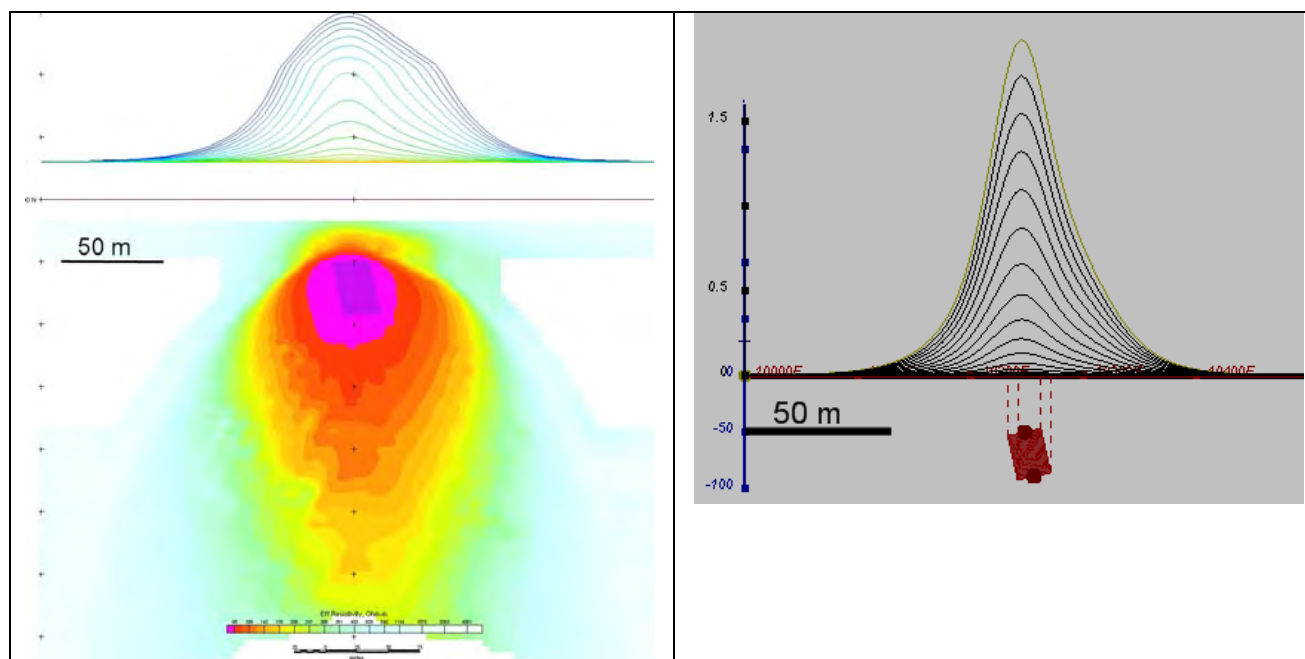


Fig.3 Maxwell plate model and RDI from the calculated response for bulk ("thick") 100 m length, 40 m depth extend, 30 m thickness

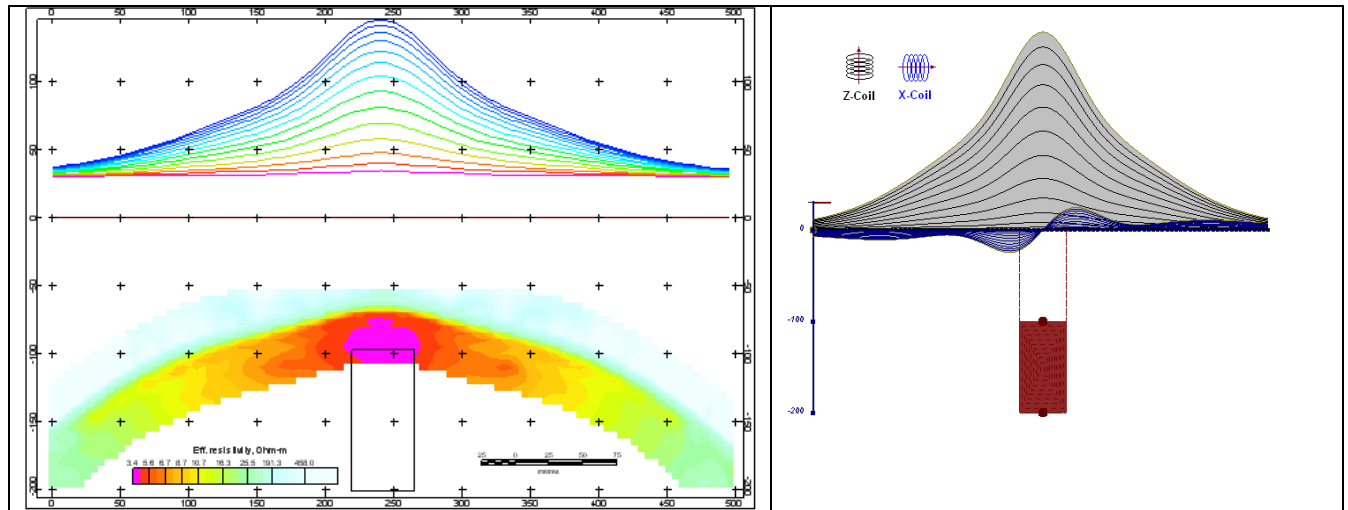


Fig. 4 Maxwell plate model and RDI from the calculated response for “thick” vertical target (depth 100 m, depth extend 100m). 19-44 chan.

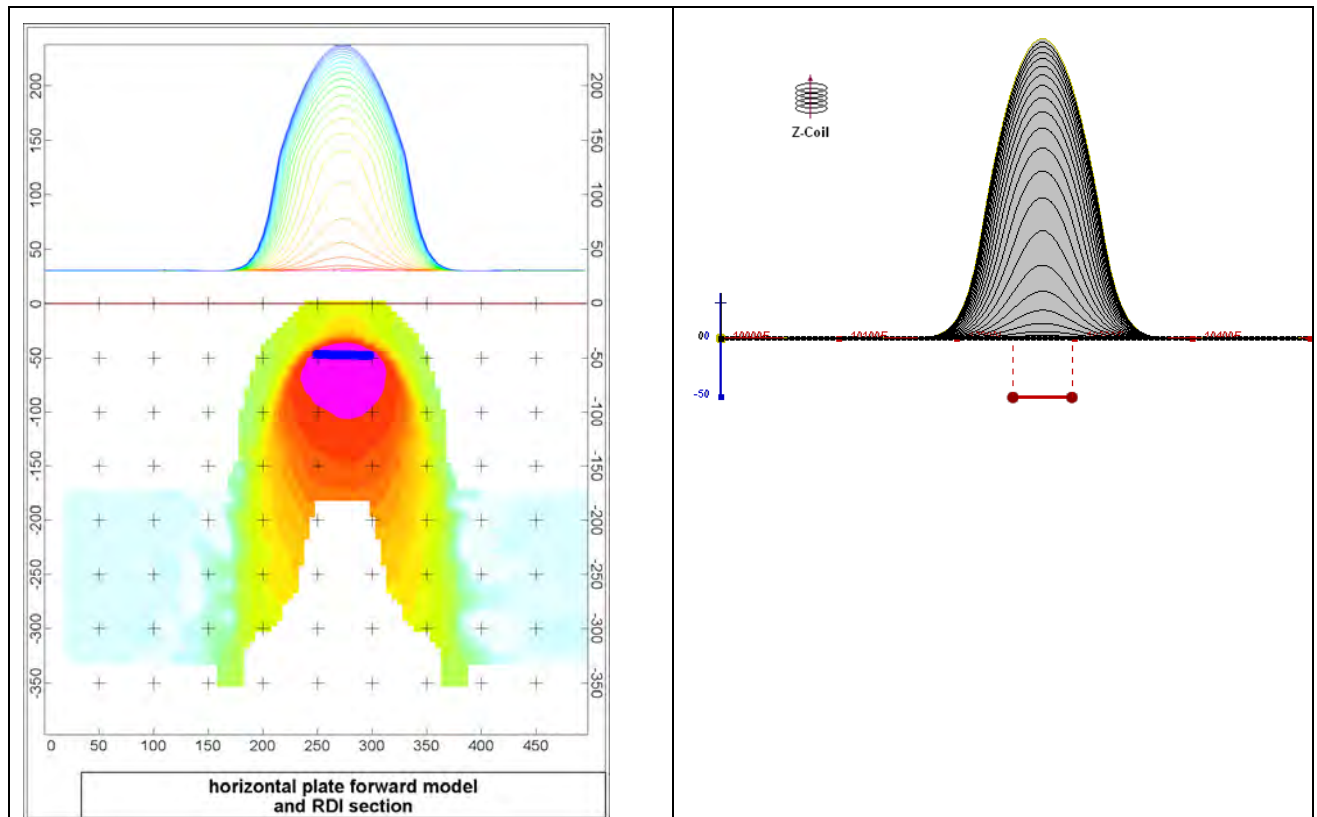


Fig. 5 Maxwell plate model and RDI from the calculated response for horizontal thin plate (depth 50 m, dim 50x100 m). 15-44 chan.

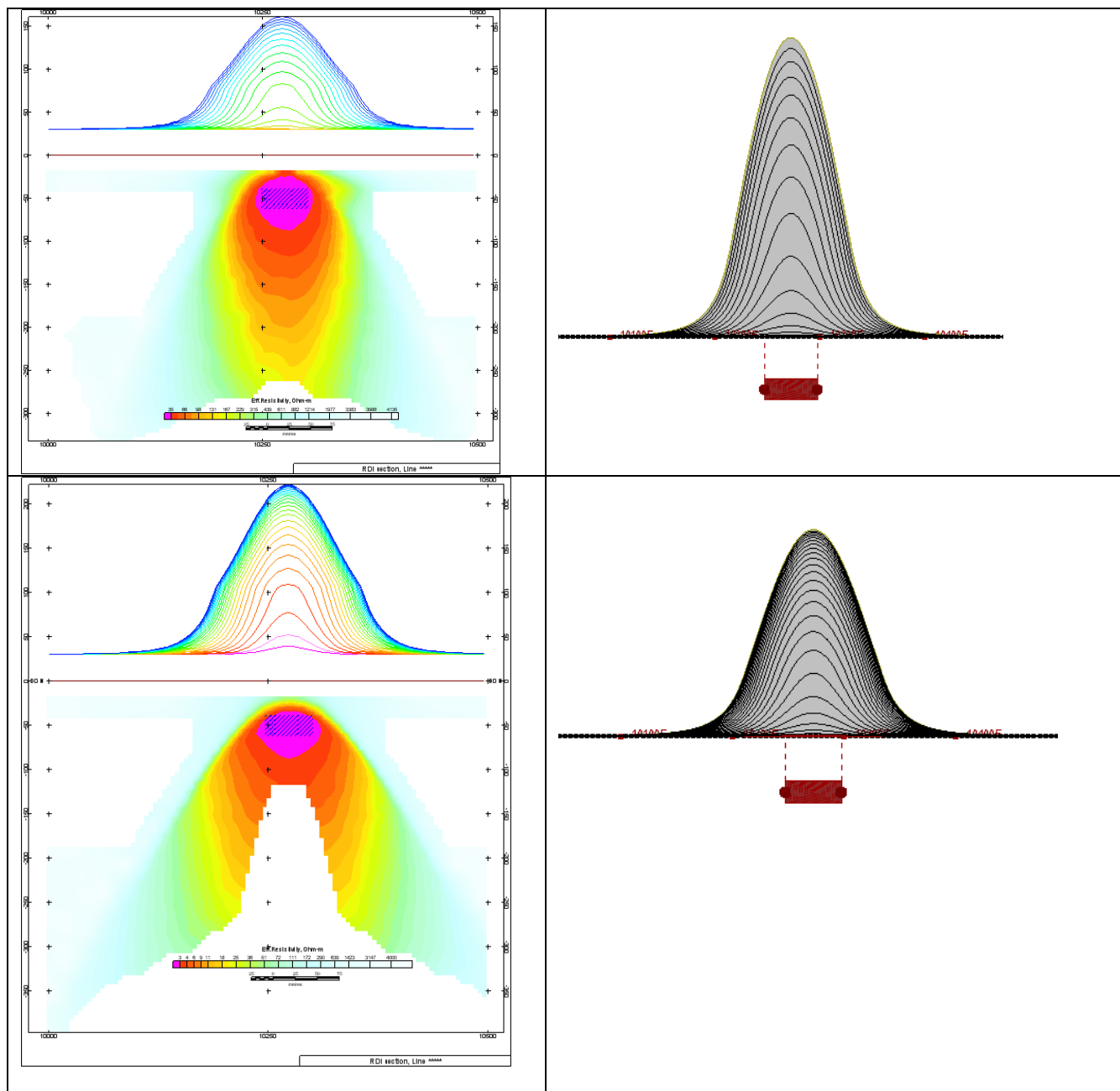


Fig.6 Maxwell plate model and RDI from the calculated response for horizontal thick (20m) plate – less conductive (on the top), more conductive (below)

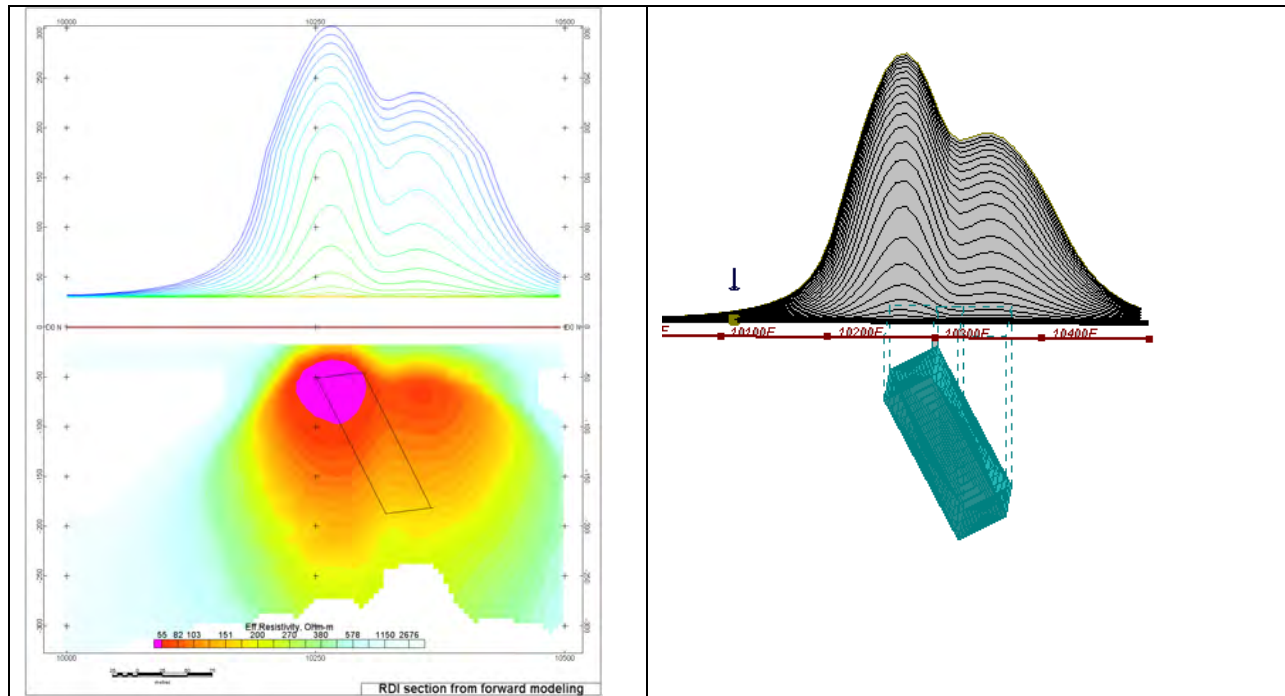


Fig.7 Maxwell plate model and RDI from the calculated response for inclined thick (50m) plate. Depth extend 150 m, depth to the target 50 m.

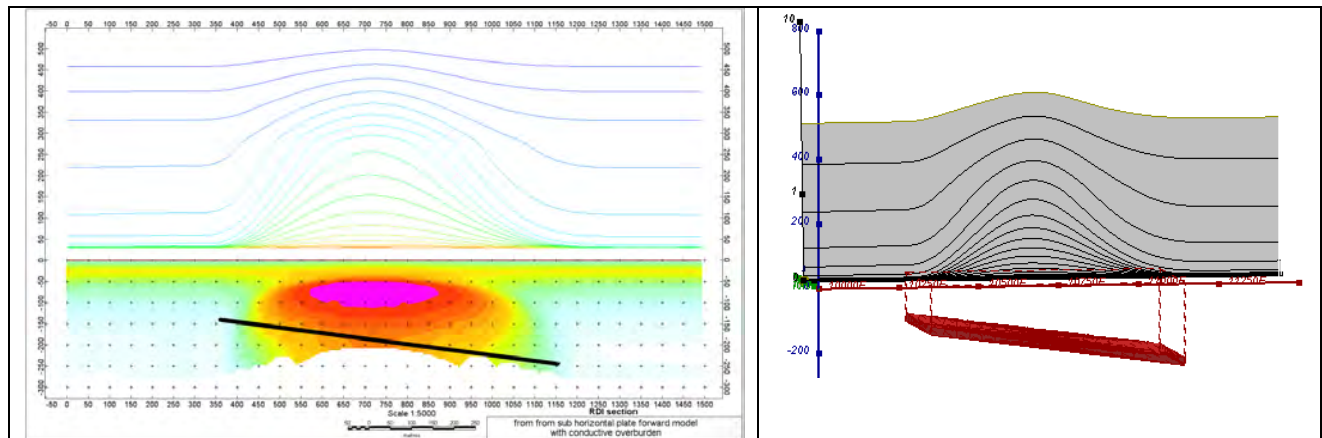


Fig.8 Maxwell plate model and RDI from the calculated response for the long, wide and deep sub horizontal plate (depth 140 m, dim 25x500x800 m) with conductive overburden.

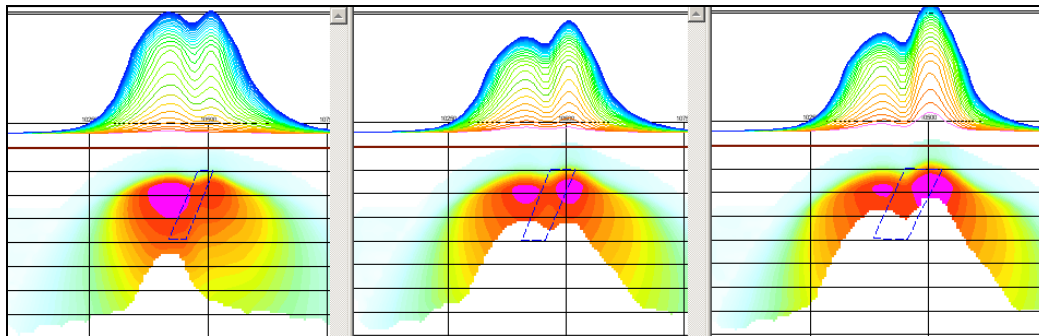


Fig.9 Maxwell plate models and RDIs from the calculated response for “thick” dipping plates (35, 50, 75 m thickness), depth 50 m, conductivity 2.5 S/m.

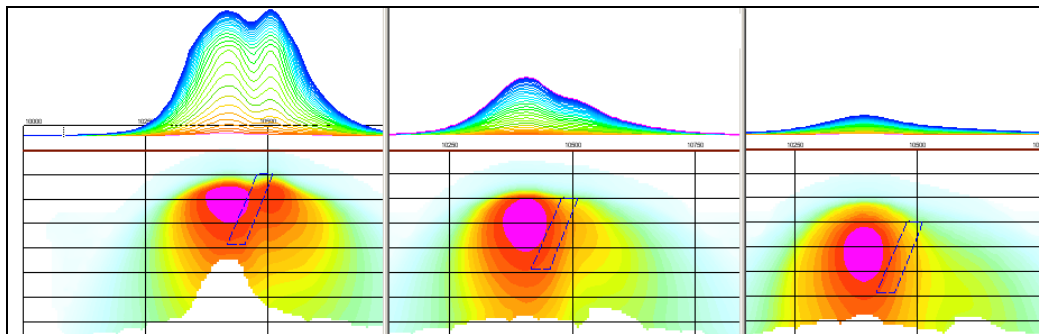


Fig.10 Maxwell plate models and RDIs from the calculated response for “thick” (35 m thickness) dipping plate on different depth (50, 100, 150 m), conductivity 2.5 S/m.

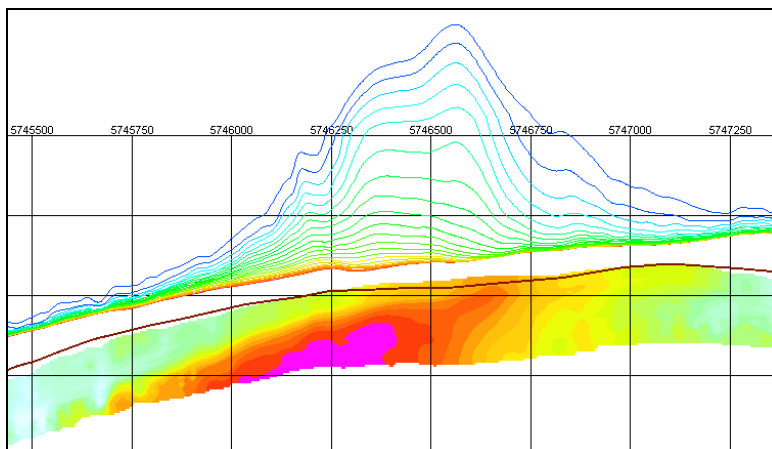
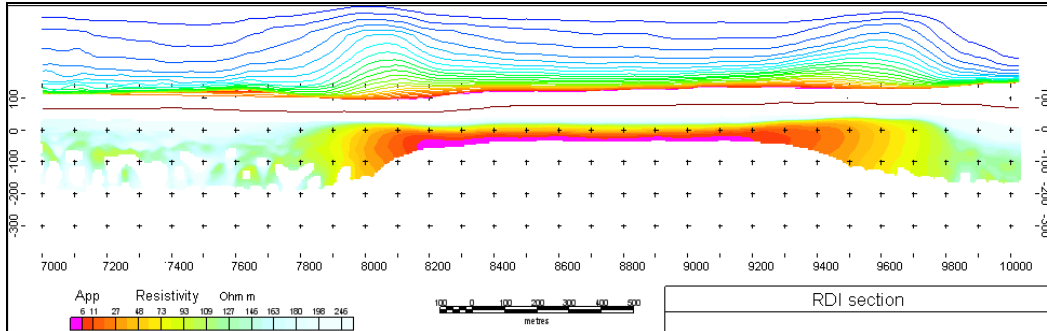
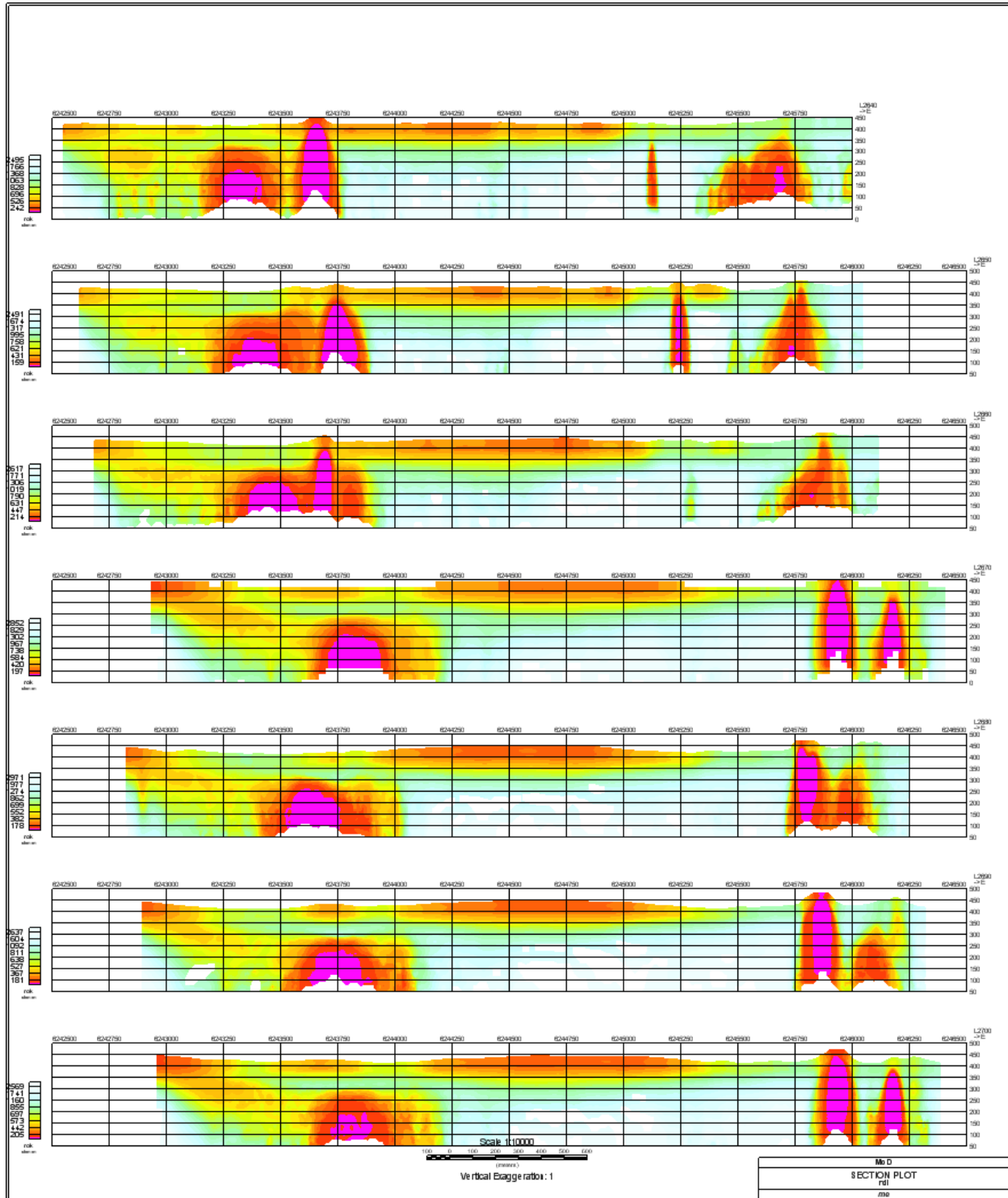


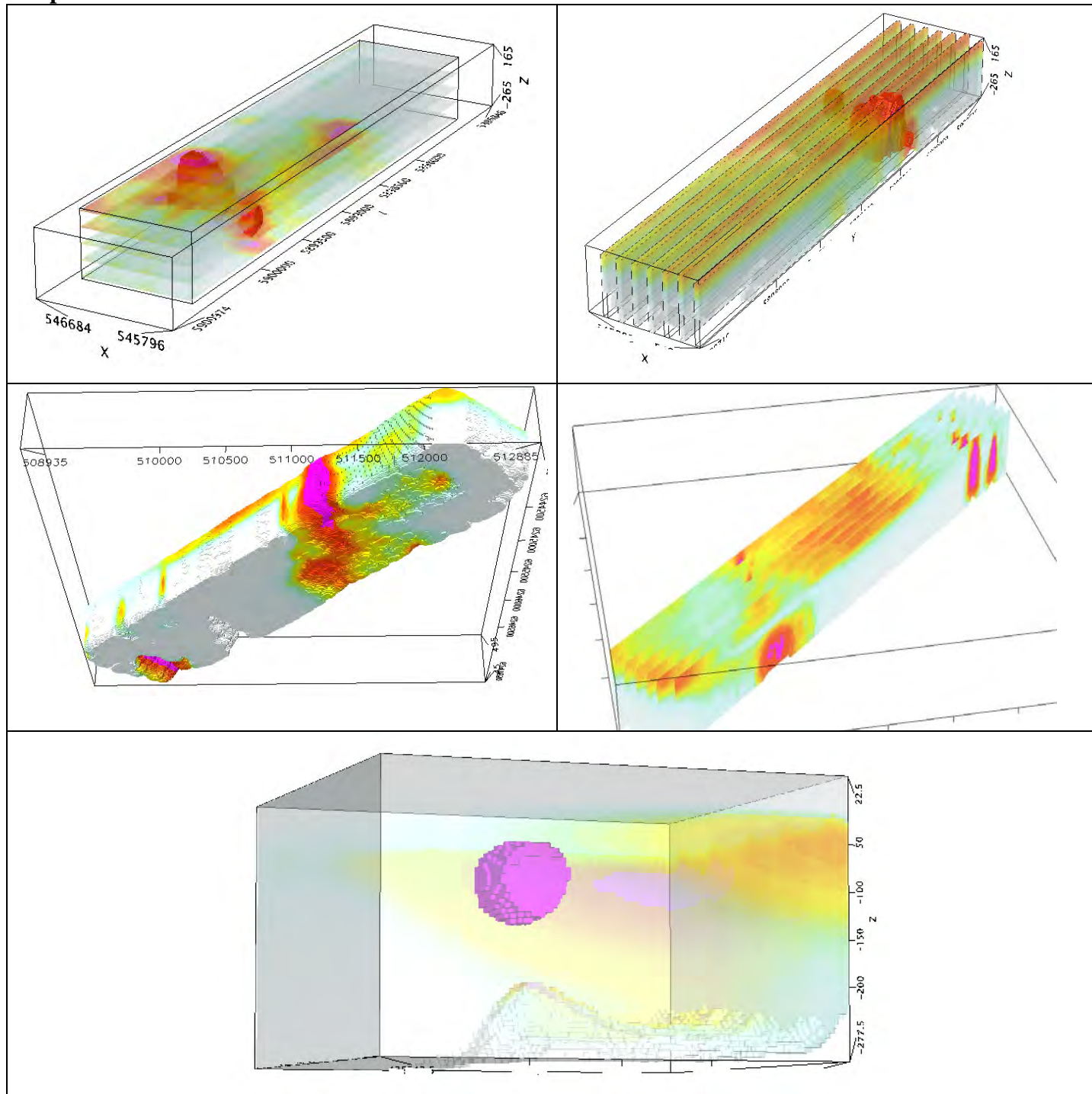
Fig.11 RDI section for the real horizontal and slightly dipping conductive layers

Forms of RDI presentation

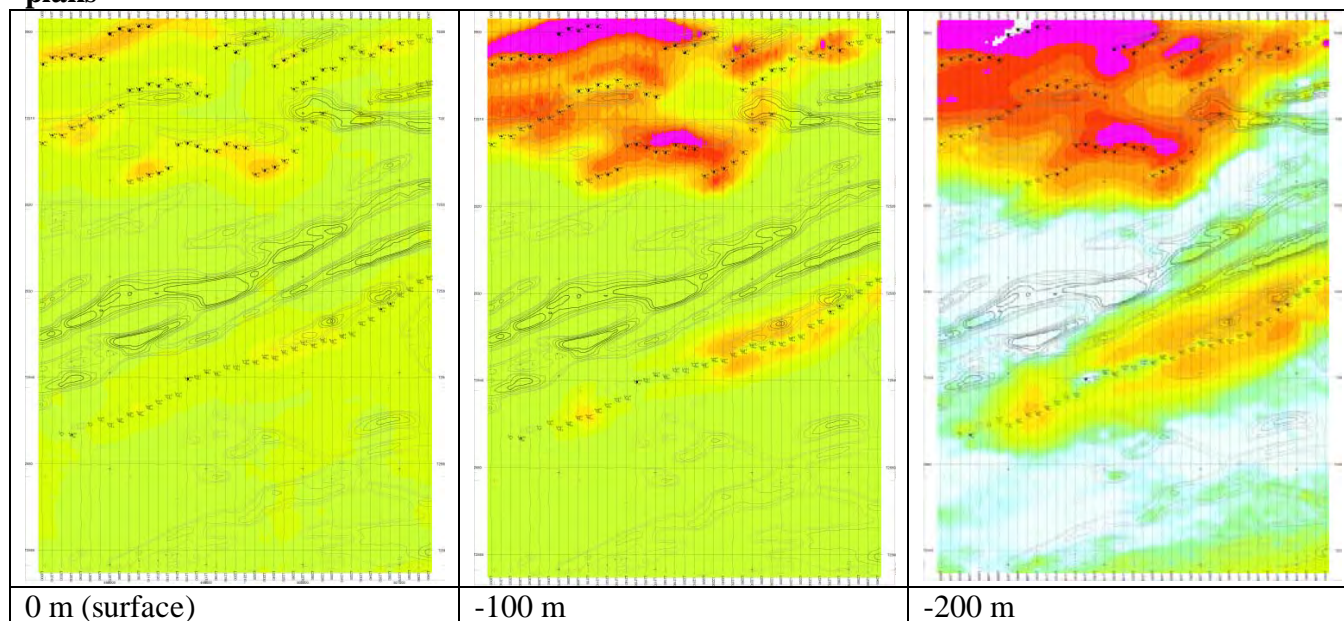
Presentation of series of lines



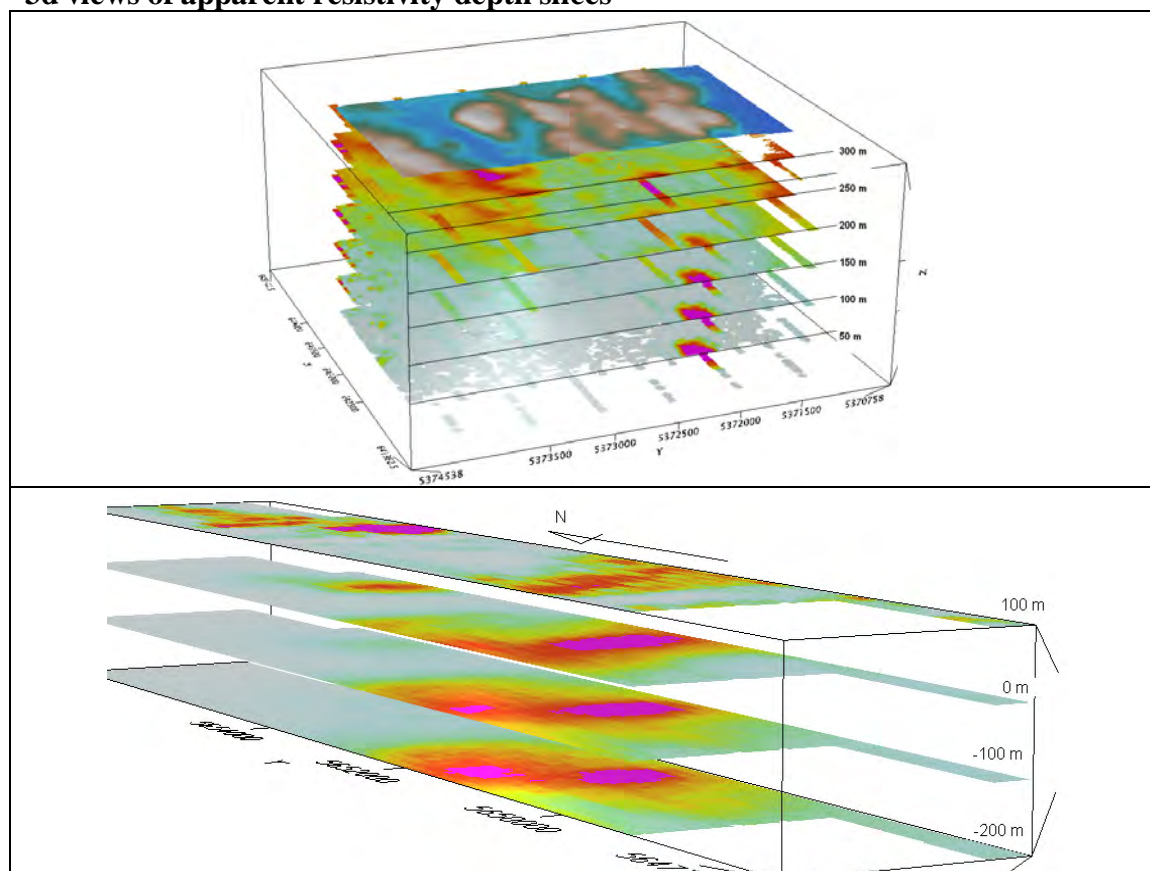
3d presentation of RDIs



Apparent Resistivity Depth Slices plans

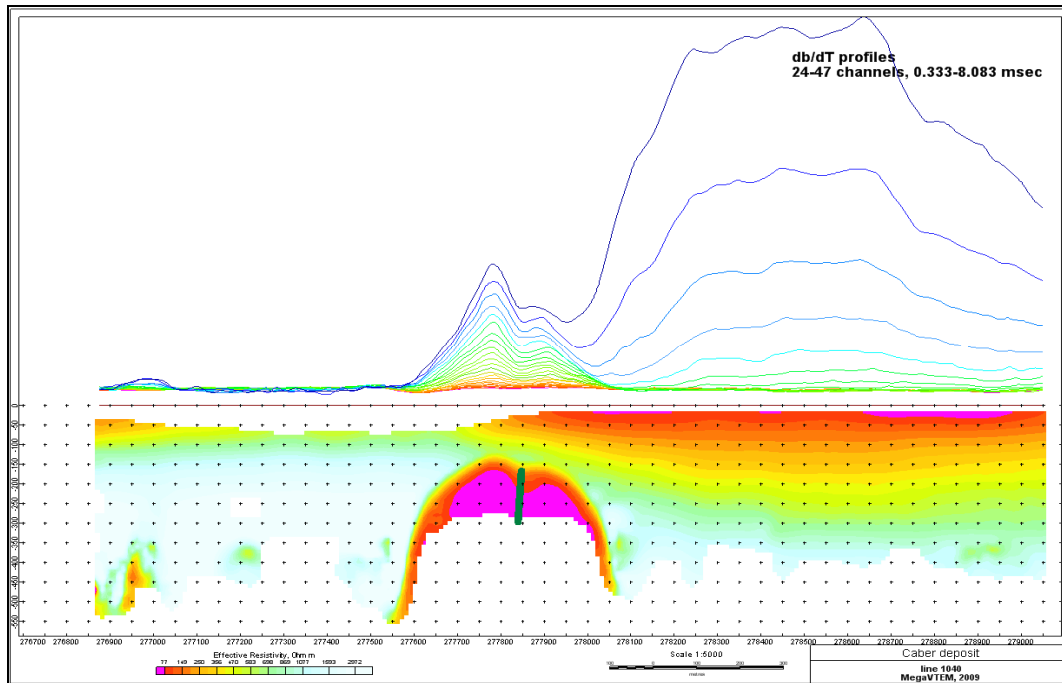


3d views of apparent resistivity depth slices

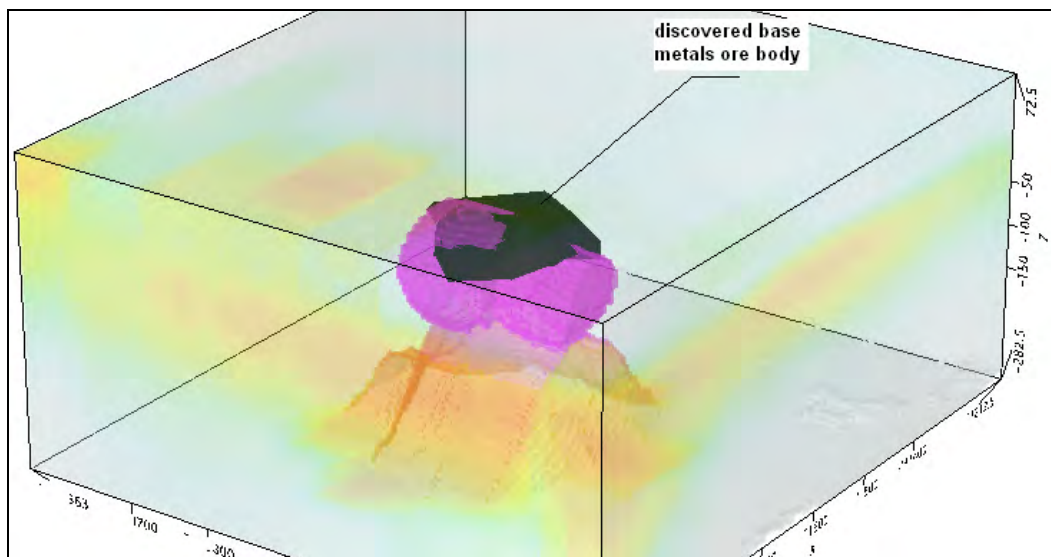


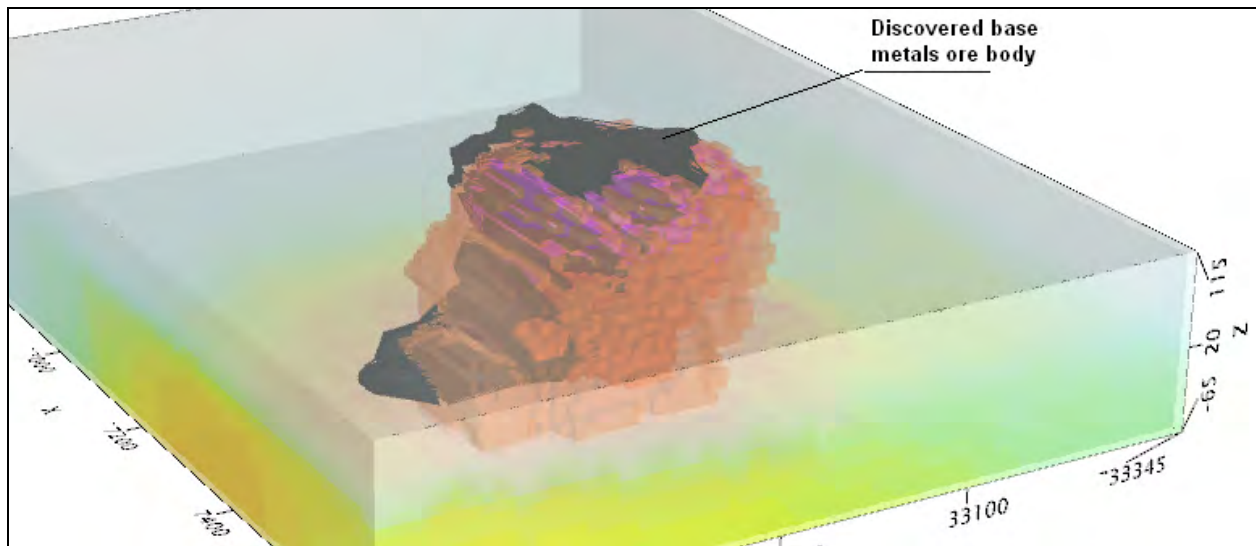
Real base metal targets in comparison with RDIs:

RDI section of the line over Caber deposit (“thin” sub vertical plate target and conductive overburden).



3d RDI voxels with base metals ore bodies (Middle East):





Alexander Prihodko, PhD, P.Geo
Geotech Ltd.
April 2011

Appendix 3

Grab Sample Results

| Sample ID | Date | Showing | Coordinates | | Lithology | Material Sampled | Grain Size | | | Altn Int | Altn Type | Veining | Relief | Strike | Dip |
|-----------|----------------|-------------|-------------|------------|-------------------------------------|------------------|------------|-----|-----|----------|-----------|---------|--------|--------|-----|
| | | | X_Nad83z15 | Y_Nad83z15 | | | fine | med | crs | | | | | | |
| 12CLP001 | August 1, 2012 | Seal Island | 438492 | 8178457 | Oolitic Sandstone | O/C | x | x | | | | | High | | |
| 12CLP002 | August 1, 2012 | Seal Island | 438707 | 8177936 | Sandstone | Bldr | | x | | | | | Low | | |
| 12CLP003 | August 1, 2012 | Seal Island | 438033 | 8178251 | Sandstone | O/C | | | | | | | Mod | | |
| 12BAP100 | August 1, 2012 | Seal Island | 438465 | 8178468 | Quartz Vein | O/C | | x | | Mod | | Stock | Mod | | |
| 12BAP101 | August 1, 2012 | Seal Island | 439211 | 8178168 | Quartzite | Talus | | x | | | | | Mod | | |
| 12BAP102 | August 1, 2012 | Seal Island | 438028 | 8178212 | Quartz Vein | O/C | x | | | | | | Low | | |
| 12TFP001 | July 21, 2012 | Seal | 439004 | 8183616 | Quartz Arenite | O/C | x | | | Str | Cbn | Mod | Mod | 198 | 60 |
| 12VSP001 | July 21, 2012 | Seal | 438966 | 8183578 | Quartz Arenite | Bldr | | | x | | Cbn | | Mod | | |
| 12VSP002 | July 21, 2012 | Seal | 439001 | 8183539 | Quartz Arenite | Gsn | | | x | | Cbn | | Mod | | |
| 12WBP101 | July 21, 2012 | Seal | 438887 | 8183695 | Quartz Arenite | Talus | x | | | | | | | | |
| 12WBP102 | July 21, 2012 | Seal | 438870 | 8183645 | Quartz Arenite | Talus | x | | | | | | | | |
| 12WBP103 | July 21, 2012 | Seal | 438928 | 8183614 | Quartz Arenite Gossan & Sphalerite | Talus | x | | | | | | | | |
| 12WBP104 | July 21, 2012 | 2200 Zone | 466296 | 8172208 | Cu-rich zone in Dolomitic Limestone | | | | | | | | | | |
| 12WBP105 | July 21, 2012 | 2750 Zone | 466264 | 8172795 | Cu-rich zone in Dolomitic Limestone | Talus | x | | | | | | | | |

| Sample ID | Composition (%) | | | | | | | | | | | | | | Sulphides (relative %) | | | | | | Remarks |
|-----------|-----------------|------|----|----|-----|-----|-----|----|-----|-----|-------|----|-------|-------|------------------------|----|-----|-----|----|-------|--|
| | qtz | flds | ms | bt | amp | chl | pyx | ol | gar | cbn | sulph | ox | other | other | py | po | cpy | gal | sp | other | |
| 12CLP001 | x | | | | | | | | | x | x | | | | x | | | | | Mcrs | Fine grained disseminated marcasite |
| 12CLP002 | x | | | | | | | | | | x | | | | x | | | | | Mcrs | Sandstone boulder with black cherty vein hosting disseminated marcasite |
| 12CLP003 | x | | | | | | | | | | x | x | | | x | | | | | Mcrs | Small pod (<50cm visible diameter) of highly oxidized sandstone; Blue mineral (lazurite?) |
| 12BAP100 | x | | | | | | | | | | | x | | | | | | | | | stockworked outcrop of laminated oolitic dolostone; Hematite staining associated with the veining; Quartz veins along beds / laminations are boudinaged; colloform and comb textures observed in veins |
| 12BAP101 | x | | | | | | | | | | x | | | | x | | | | | | medium grained massive quartzite with fine grained disseminated pyrite. |
| 12BAP102 | x | | | | | | | | | x | x | | | | x | | | | x | Mcrs | Fine grained banded vein associated with quartz carbonate (dolomite) flooding. |
| 12TFP001 | | | | | | | | | | | | | | | | | | | 5 | | 5% Marcasite; Brecciation |
| 12VSP001 | 85 | | | | | | | | | 10 | 5 | | | | tr. | | | | 5 | | |
| 12VSP002 | 60 | | | | | 25 | | | | | 15 | | | | 5 | | | | 10 | | |
| 12WBP101 | | | | | | | | | | | 5 | | | | | | | | | | String of very strongly oxidized talus piles along slope of ridge; Quartz clasts subrounded, <1mm; Sulphides are very fine grained, cannot ID, mineralization marked by darker colour than regular white quartz arenite, 50% grey; Sampled from numerous boulders in talus pile, all 7 <30x20x20cm |
| 12WBP102 | 95 | | | | | | | | | | 5 | | | | | | | | | | Boulder A - 25x15x50cm, in talus, mid-slope; Very well sorted, sub-rounded quartz grains; Sulphide nodules are dark grey and marcasite is included in sulphide content |
| 12WBP103 | 20 | | | | | | | | | | 80 | | | | | | | | 75 | | Gossanous talus mid-slope; Up to golf ball sized pieces of massive to semi-massive sphalerite; Jet black colour |
| 12WBP104 | | | | | | | | | | 20 | | | | | | | | | | | Pieces of Cu mineral rich rock in a small area; Strongly weathered; Unable to ID all Cu minerals; Malachite and azurite coating |
| 12WBP105 | | | | | | | | | | 40 | | | CC | BN | | | | | | | Frost boil and talus material rich in Cu minerals; 25% MAL, 25% AZ, 5% BN, 5% CC; chalcocite is very fine grained |

Appendix 4

Core Intervals and Descriptions

| Hole ID | Sample ID | Lab Certificate | DH From (m) | DH To (m) | Interval Length (m) | Ag_ppm | Cu_% | Pb_% | Zn_% | Lithology | Description |
|---------|-----------|-----------------|-------------|-----------|---------------------|-------------|-------|-------|---------------|---|--|
| AB95-02 | M999301 | YW12175933 | 49.00 | 50.40 | 1.40 | 0.9 | 0.003 | 0.001 | 0.122 | Dolomiticrite / Sandy Dolostone | Interbedded dolomiticrite and sandy dolostone; dm scale sandstone interbeds; bedded, often disturbed from 47.5 |
| AB95-02 | M999302 | YW12175933 | 50.40 | 51.80 | 1.40 | 0.5 | 0.002 | 0.002 | 0.083 | Dolostone | |
| AB95-02 | M999303 | YW12175933 | 51.80 | 52.80 | 1.00 | 14.0 | 0.003 | 0.011 | 6.040 | Semi-Sulphide Rock | Broken zone; highly oxidized and weathered to un lithified state; MRC/PY + SPH |
| AB95-02 | M999304 | YW12175933 | 52.80 | 54.30 | 1.50 | 41.2 | 0.008 | 0.040 | 19.450 | | |
| AB95-02 | M999305 | YW12175933 | 54.30 | 55.30 | 1.00 | 28.8 | 0.007 | 0.039 | 15.100 | Sulphide Rock | Broken zone; highly oxidized and weathered to un lithified state; MRC/PY + SPH |
| AB95-02 | M999306 | YW12175933 | 55.30 | 57.00 | 1.70 | 19.9 | 0.005 | 0.039 | 8.570 | | |
| AB95-02 | M999307 | YW12175933 | 57.00 | 58.00 | 1.00 | 37.2 | 0.004 | 0.022 | 13.250 | Sandstone | Well sorted, quartz rich; disseminated PY/MRC |
| AB95-02 | M999308 | YW12175933 | 58.00 | 59.10 | 1.10 | 35.9 | 0.003 | 0.022 | 9.580 | | |
| AB95-02 | M999309 | YW12175933 | 59.10 | 60.00 | 0.90 | 9.7 | 0.002 | 0.013 | 2.340 | | |
| AB95-02 | M999310 | YW12175933 | 60.00 | 60.70 | 0.70 | 59.1 | 0.004 | 0.020 | 16.700 | | |
| AB95-02 | M999311 | YW12175933 | 60.70 | 62.00 | 1.30 | 4.8 | 0.001 | 0.006 | 1.210 | | |
| AB95-02 | M999312 | YW12175933 | 62.00 | 63.00 | 1.00 | 1.0 | 0.002 | 0.003 | 0.143 | | |
| AB95-02 | M999313 | YW12175933 | 63.00 | 64.00 | 1.00 | 0.5 | 0.000 | 0.002 | 0.124 | | |
| AB95-02 | M999314 | YW12175933 | 64.00 | 65.00 | 1.00 | 0.7 | 0.001 | 0.003 | 0.070 | | |
| AB95-02 | M999315 | YW12179287 | 65.00 | 66.40 | 1.40 | 9.2 | 0.003 | 0.011 | 2.750 | | |
| AB95-02 | M999316 | YW12179287 | 66.40 | 67.00 | 0.60 | 42.9 | 0.008 | 0.030 | 13.100 | Semi-Sulphide Rock | Broken zone; highly oxidized and weathered to un lithified state; MRC/PY + SPH |
| AB95-02 | M999317 | YW12179287 | 67.00 | 68.00 | 1.00 | 58.9 | 0.007 | 0.026 | 19.850 | | |
| AB95-02 | M999318 | YW12179287 | 68.00 | 69.00 | 1.00 | 19.7 | 0.003 | 0.025 | 5.820 | | |
| AB95-02 | M999319 | YW12179287 | 69.00 | 69.80 | 0.80 | 14.5 | 0.002 | 0.021 | 5.240 | | |
| AB95-02 | M999320 | YW12179287 | 69.80 | 70.60 | 0.80 | 65.6 | 0.008 | 0.029 | 16.450 | | |
| AB95-02 | M999321 | YW12179287 | 70.60 | 72.30 | 1.70 | 1.9 | 0.001 | 0.005 | 0.341 | Pyritic Sandstone / Dolomitic Sandstone | Fractured and vuggy sandstone; disseminated and void filling pyrite; chlorite alteration associated with fractures |
| AB95-02 | M999322 | YW12179287 | 72.30 | 73.50 | 1.20 | 0.6 | 0.001 | 0.003 | 0.093 | | |
| AB95-03 | M999323 | YW12179287 | 75.00 | 76.00 | 1.00 | 0.5 | 0.001 | 0.002 | 0.121 | Massive Sulphide | massive, oxidized, crumbled, sulphide - top 0.5m is broken down sandstone |
| AB95-03 | M999324 | YW12179287 | 76.00 | 76.60 | 0.60 | 2.4 | 0.001 | 0.006 | 0.650 | | |
| AB95-03 | M999325 | YW12179287 | 76.60 | 77.70 | 1.10 | 54.8 | 0.004 | 0.015 | 21.800 | | |
| AB95-03 | M999326 | YW12179287 | 77.70 | 78.50 | 0.80 | 20.6 | 0.002 | 0.016 | 4.590 | | |
| AB95-03 | M999327 | YW12179287 | 78.50 | 80.00 | 1.50 | 43.8 | 0.002 | 0.015 | 12.950 | | |
| AB95-03 | M999328 | YW12179287 | 80.00 | 81.00 | 1.00 | 30.5 | 0.002 | 0.013 | 6.720 | Quartz Sandstone | Massive, medium grained. |
| AB95-03 | M999329 | YW12179287 | 81.00 | 82.60 | 1.60 | -0.5 | 0.000 | 0.001 | 0.057 | | |
| AB95-03 | M999331 | YW12179287 | 82.60 | 84.00 | 1.40 | 0.5 | 0.001 | 0.001 | 0.030 | | |
| AB95-03 | M999332 | YW12179287 | 84.00 | 85.50 | 1.50 | 0.5 | 0.001 | 0.002 | 0.042 | | |
| AB95-03 | M999333 | YW12179287 | 85.50 | 87.00 | 1.50 | -0.5 | 0.000 | 0.002 | 0.065 | | |
| AB95-03 | M999334 | YW12179287 | 87.00 | 88.00 | 1.00 | -0.5 | 0.001 | 0.004 | 0.042 | Sulphidic Sandstone | Nearly massive, medium grained marcasite. |
| AB95-03 | M999335 | YW12179287 | 88.00 | 89.00 | 1.00 | 9.5 | 0.001 | 0.004 | 1.030 | | |
| AB95-03 | M999336 | YW12179287 | 89.00 | 89.50 | 0.50 | 20.2 | 0.002 | 0.019 | 6.900 | | |
| AB95-03 | M999337 | YW12179287 | 89.50 | 90.50 | 1.00 | 18.3 | 0.003 | 0.031 | 2.500 | | |
| AB95-03 | M999338 | YW12179287 | 90.50 | 91.25 | 0.75 | 86.3 | 0.008 | 0.043 | 16.200 | | |
| AB95-03 | M999339 | YW12179287 | 91.25 | 92.25 | 1.00 | 11.3 | 0.002 | 0.019 | 1.990 | Dolo Sandstone | oxidized, broken down, sideritic sandstone |
| AB95-03 | M999341 | YW12179287 | 92.25 | 93.50 | 1.25 | 4.7 | 0.002 | 0.017 | 0.733 | | |
| AB95-03 | M999342 | YW12179287 | 93.50 | 94.90 | 1.40 | 37.0 | 0.006 | 0.022 | 14.400 | | |
| AB95-03 | M999343 | YW12179287 | 94.90 | 95.90 | 1.00 | 71.8 | 0.007 | 0.021 | 26.200 | | |
| AB95-03 | M999344 | YW12179287 | 95.90 | 96.50 | 0.60 | 51.5 | 0.008 | 0.029 | 18.100 | | |
| AB95-03 | M999345 | YW12179287 | 96.50 | 97.70 | 1.20 | 6.8 | 0.003 | 0.007 | 1.930 | Dolo Sandstone | oxidized, broken down, sideritic sandstone |
| AB95-03 | M999346 | YW12179287 | 97.70 | 98.80 | 1.10 | 15.2 | 0.011 | 0.048 | 5.350 | | |
| AB95-03 | M999347 | YW12179287 | 98.80 | 100.00 | 1.20 | 24.9 | 0.004 | 0.033 | 0.505 | | |
| AB95-03 | M999348 | YW12179287 | 100.00 | 101.70 | 1.70 | 80.4 | 0.018 | 0.135 | 2.480 | | |
| AB95-03 | M999349 | YW12179287 | 101.70 | 103.00 | 1.30 | 3.3 | 0.001 | 0.006 | 0.256 | | |
| AB95-04 | M999012 | YW12188552 | 74.00 | 75.50 | 1.50 | -0.5 | 0.001 | 0.001 | 0.016 | Dolomitic Sandstone | Lithic sandstone; massive to laminated; occasional MRC/PY stringers; weak oxide stain |
| AB95-04 | M999013 | YW12188552 | 75.50 | 77.00 | 1.50 | -0.5 | 0.001 | 0.001 | 0.040 | | |
| AB95-04 | M999014 | YW12188552 | 77.00 | 78.50 | 1.50 | -0.5 | 0.001 | 0.001 | 0.045 | | |
| AB95-04 | M999015 | YW12188552 | 78.50 | 80.00 | 1.50 | -0.5 | 0.000 | 0.001 | 0.020 | | |
| AB95-04 | M999016 | YW12188552 | 80.00 | 81.50 | 1.50 | -0.5 | 0.001 | 0.001 | 0.028 | | |
| AB95-04 | M999017 | YW12188552 | 81.50 | 83.00 | 1.50 | -0.5 | 0.001 | 0.003 | 0.084 | Dolo Sandstone | fine grained |
| AB95-05 | M999001 | YW12188552 | 119.00 | 120.50 | 1.50 | -0.5 | 0.002 | 0.000 | 0.007 | | |
| AB95-05 | M999002 | YW12188552 | 120.50 | 122.00 | 1.50 | -0.5 | 0.001 | 0.002 | 0.043 | | |
| AB95-05 | M999003 | YW12188552 | 122.00 | 123.50 | 1.50 | -0.5 | 0.001 | 0.001 | 0.010 | | |
| AB95-05 | M999004 | YW12188552 | 123.50 | 125.00 | 1.50 | -0.5 | 0.001 | 0.001 | 0.010 | | |
| AB95-05 | M999005 | YW12188552 | 125.00 | 126.00 | 1.00 | -0.5 | 0.001 | 0.002 | 0.011 | | |
| AB95-05 | M999006 | YW12188552 | 126.00 | 127.50 | 1.50 | -0.5 | 0.001 | 0.002 | 0.011 | | |

| | | | | | | | | | | | |
|---------|---------|------------|--------|--------|------|--------------|-------|-------|---------------|---------------------------|---|
| AB95-06 | M999351 | YW12179287 | 97.00 | 98.50 | 1.50 | -0.5 | 0.000 | 0.002 | 0.041 | Rubble Zone | Rubble zone (fault?); clay & fine sand particles with intervals of lithified sandstone |
| AB95-06 | M999352 | YW12179287 | 98.50 | 100.00 | 1.50 | 1.3 | 0.001 | 0.007 | 0.098 | | |
| AB95-06 | M999353 | YW12179287 | 100.00 | 101.50 | 1.50 | 5.9 | 0.001 | 0.004 | 2.160 | | |
| AB95-06 | M999354 | YW12179287 | 101.50 | 102.30 | 0.80 | 15.1 | 0.002 | 0.018 | 9.440 | Semi-Sulphide Rock | Dark grey to reddish brown semi-sulphide and sulphide rock; MRC/PY with SPH; oxide staining of variable intensity; mainly rubble with coherent intervals up to 40cm |
| AB95-06 | M999355 | YW12179287 | 102.30 | 103.30 | 1.00 | 5.5 | 0.001 | 0.029 | 1.650 | | |
| AB95-06 | M999356 | YW12179287 | 103.30 | 104.30 | 1.00 | 23.8 | 0.002 | 0.025 | 13.900 | | |
| AB95-06 | M999357 | YW12179287 | 104.30 | 105.50 | 1.20 | 55.1 | 0.003 | 0.029 | 7.830 | | |
| AB95-06 | M999358 | YW12179287 | 105.50 | 106.60 | 1.10 | 58.5 | 0.003 | 0.035 | 12.450 | | |
| AB95-06 | M999359 | YW12179287 | 106.60 | 107.50 | 0.90 | 1.4 | 0.000 | 0.007 | 0.158 | Sandstone | Quartz and lithic rich sandstone; beige - grey with orange - brown oxide stain |
| AB95-06 | M999361 | YW12179287 | 107.50 | 108.60 | 1.10 | 1.2 | 0.002 | 0.006 | 0.099 | | |
| AB95-06 | M999362 | YW12179287 | 108.60 | 109.60 | 1.00 | 3.2 | 0.001 | 0.010 | 0.518 | Semi-Sulphide Rock | Dark grey to reddish brown semi-sulphide and sulphide rock; MRC/PY with SPH; oxide staining of variable intensity; mainly rubble with coherent intervals up to 40cm |
| AB95-06 | M999363 | YW12179287 | 109.60 | 110.70 | 1.10 | 13.0 | 0.001 | 0.005 | 4.260 | | |
| AB95-06 | M999364 | YW12179287 | 110.70 | 111.70 | 1.00 | 75.6 | 0.008 | 0.013 | 18.950 | | |
| AB95-06 | M999365 | YW12179287 | 111.70 | 112.70 | 1.00 | 52.4 | 0.004 | 0.013 | 14.850 | | |
| AB95-06 | M999366 | YW12179287 | 112.70 | 113.70 | 1.00 | 5.9 | 0.001 | 0.013 | 0.989 | | |
| AB95-06 | M999367 | YW12179287 | 113.70 | 114.70 | 1.00 | 3.1 | 0.001 | 0.010 | 0.282 | | |
| AB95-06 | M999368 | YW12179287 | 114.70 | 115.70 | 1.00 | 7.0 | 0.001 | 0.020 | 1.260 | | |
| AB95-06 | M999369 | YW12179287 | 115.70 | 116.80 | 1.10 | 9.2 | 0.002 | 0.021 | 0.974 | | |
| AB95-06 | M999371 | YW12179287 | 116.80 | 117.80 | 1.00 | 13.9 | 0.002 | 0.016 | 4.440 | | |
| AB95-06 | M999372 | YW12179287 | 117.80 | 118.50 | 0.70 | 48.1 | 0.002 | 0.020 | 10.800 | | |
| AB95-06 | M999373 | YW12179287 | 118.50 | 119.10 | 0.60 | 66.0 | 0.003 | 0.017 | 14.850 | | |
| AB95-06 | M999374 | YW12179287 | 119.10 | 120.20 | 1.10 | 28.4 | 0.002 | 0.028 | 4.660 | | |
| AB95-06 | M999375 | YW12179287 | 120.20 | 121.20 | 1.00 | 9.2 | 0.002 | 0.010 | 0.921 | Sandstone | Quartz and lithic rich sandstone; beige - grey with orange - brown oxide stain |
| AB95-06 | M999376 | YW12179287 | 121.20 | 122.20 | 1.00 | -0.5 | 0.001 | 0.002 | 0.091 | | |
| AB95-06 | M999377 | YW12179287 | 122.20 | 123.20 | 1.00 | 0.5 | 0.001 | 0.002 | 0.065 | | |
| AB95-06 | M999378 | YW12179287 | 123.20 | 124.30 | 1.10 | 0.6 | 0.001 | 0.002 | 0.093 | | |
| AB95-06 | M999379 | YW12179287 | 124.30 | 125.30 | 1.00 | 0.5 | 0.001 | 0.003 | 0.062 | | |
| AB95-06 | M999381 | YW12179287 | 125.30 | 126.30 | 1.00 | -0.5 | 0.001 | 0.002 | 0.062 | | |
| AB95-06 | M999382 | YW12179287 | 126.30 | 127.30 | 1.00 | -0.5 | 0.001 | 0.004 | 0.055 | | |
| AB95-06 | M999383 | YW12179287 | 127.30 | 128.30 | 1.00 | 4.8 | 0.001 | 0.003 | 0.081 | | |
| AB95-06 | M999384 | YW12179287 | 128.30 | 129.30 | 1.00 | 52.6 | 0.002 | 0.026 | 6.750 | Semi-Sulphide Rock | Dark grey to reddish brown semi-sulphide and sulphide rock; MRC/PY with SPH; oxide staining of variable intensity |
| AB95-06 | M999385 | YW12179287 | 129.30 | 130.00 | 0.70 | 136.0 | 0.003 | 0.032 | 14.750 | | |
| AB95-06 | M999386 | YW12179287 | 130.00 | 131.00 | 1.00 | 26.8 | 0.002 | 0.033 | 4.860 | | |
| AB95-06 | M999387 | YW12179287 | 131.00 | 132.20 | 1.20 | 25.1 | 0.001 | 0.026 | 3.140 | | |
| AB95-06 | M999388 | YW12179287 | 132.20 | 133.30 | 1.10 | 3.5 | 0.001 | 0.006 | 0.470 | Dolomiticrite | Beige - light grey bedded dolomiticrite; rubble zone from 150-156 |
| AB95-06 | M999389 | YW12179287 | 133.30 | 134.50 | 1.20 | 3.3 | 0.001 | 0.004 | 0.359 | | |
| AB95-07 | M999391 | YW12179287 | 114.00 | 115.50 | 1.50 | 1.1 | 0.001 | 0.005 | 0.148 | Laminated Dolomiticrite | Variably oxidized, highly broken and weathered interbedded sandy dolostone dolomiticrite and sandstone. Bituminous intervals. Trace sulphides. |
| AB95-07 | M999392 | YW12179287 | 115.50 | 117.00 | 1.50 | 1.8 | 0.005 | 0.020 | 0.631 | | |
| AB95-07 | M999393 | YW12179287 | 117.00 | 118.00 | 1.00 | 0.6 | 0.001 | 0.002 | 0.119 | | |
| AB95-07 | M999394 | YW12179287 | 118.00 | 119.50 | 1.50 | 2.4 | 0.003 | 0.010 | 0.282 | | |
| AB95-07 | M999395 | YW12179287 | 119.50 | 121.00 | 1.50 | 5.3 | 0.004 | 0.015 | 0.593 | | |
| AB95-07 | M999396 | YW12179287 | 121.00 | 122.50 | 1.50 | 1.0 | 0.001 | 0.003 | 0.159 | | |
| AB95-07 | M999397 | YW12179287 | 122.50 | 124.00 | 1.50 | -0.5 | 0.000 | 0.002 | 0.032 | | |
| AB95-07 | M999398 | YW12179287 | 124.00 | 125.40 | 1.40 | 0.7 | 0.000 | 0.003 | 0.151 | | |
| AB95-07 | M999399 | YW12179287 | 125.40 | 126.80 | 1.40 | 6.6 | 0.001 | 0.023 | 0.556 | Sulphidic Sandstone | Dark grey, highly broken vuggy sandstone. Abundant marcasite. |
| AB95-07 | M999401 | YW12179287 | 126.80 | 128.00 | 1.20 | 5.3 | 0.001 | 0.007 | 0.715 | Sandstone | Beige-rusty brown, well sorted, fine to medium grained sandstone. Oxide staining. Trace sulphides. |
| AB95-07 | M999402 | YW12179287 | 128.00 | 129.50 | 1.50 | 1.4 | 0.001 | 0.005 | 0.209 | | |
| AB95-07 | M999403 | YW12179287 | 129.50 | 131.00 | 1.50 | 0.5 | 0.000 | 0.002 | 0.108 | | |
| AB95-07 | M999404 | YW12179287 | 131.00 | 132.00 | 1.00 | 1.4 | 0.000 | 0.003 | 0.122 | | |
| AB95-07 | M999405 | YW12179287 | 132.00 | 133.00 | 1.00 | 27.5 | 0.002 | 0.023 | 8.620 | | |
| AB95-07 | M999406 | YW12179287 | 133.00 | 133.90 | 0.90 | 39.4 | 0.002 | 0.206 | 1.415 | | |
| AB95-07 | M999407 | YW12179287 | 133.90 | 135.00 | 1.10 | 123.0 | 0.008 | 0.024 | 13.150 | Massive Sulphide | Grey to red-brown crumbled and broken sulphide rock. Marcasite with lesser sphalerite. |
| AB95-07 | M999408 | YW12179287 | 135.00 | 135.85 | 0.85 | 15.7 | 0.002 | 0.022 | 2.400 | | |
| AB95-07 | M999409 | YW12179287 | 135.85 | 137.00 | 1.15 | 118.0 | 0.003 | 0.024 | 22.500 | | |
| AB95-07 | M999411 | YW12179287 | 137.00 | 138.00 | 1.00 | -0.5 | 0.001 | 0.003 | 0.075 | Dolomiticrite | Light grey-beige laminated and bioturbated dolomiticrite with sandy interbeds. |
| AB95-07 | M999412 | YW12179287 | 138.00 | 139.00 | 1.00 | -0.5 | 0.001 | 0.003 | 0.044 | | |
| AB95-08 | M999007 | YW12188552 | 107.00 | 108.00 | 1.00 | -0.5 | 0.001 | 0.001 | 0.004 | Laminated Dolomiticrite | Bioturbated interbeds. Greywacke interbed at 18-21m. Core is blocky. |
| AB95-08 | M999008 | YW12188552 | 108.00 | 109.00 | 1.00 | -0.5 | 0.001 | 0.003 | 0.010 | Dolostone Breccia | light, pink pyritic. |
| AB95-08 | M999009 | YW12188552 | 109.00 | 110.00 | 1.00 | -0.5 | 0.001 | 0.001 | 0.005 | Bioturbated Dolomiticrite | bioturbated interbeds. Muddy horizons are broken down. Minor vuggy sections in bioturbated beds along with minor algal beds. |
| AB95-08 | M999010 | YW12188552 | 110.00 | 111.00 | 1.00 | -0.5 | 0.001 | 0.001 | 0.003 | | |
| AB95-08 | M999011 | YW12188552 | 111.00 | 112.00 | 1.00 | -0.5 | 0.000 | 0.001 | 0.003 | | |

| | | | | | | | | | | | |
|---------|---------|------------|--------|--------|------|-------|-------|-------|-------|-------------------------|--|
| AB95-10 | M999413 | YW12179287 | 128.00 | 129.50 | 1.50 | 6.0 | 0.001 | 0.007 | 1.845 | Laminated Dolomicrite | interbedded with bioturbated dolostone. Muddy and sandy horizons causing the core to be blocky and broken down. |
| AB95-10 | M999414 | YW12179287 | 129.50 | 131.00 | 1.50 | 1.2 | 0.002 | 0.004 | 0.370 | | |
| AB95-10 | M999415 | YW12179287 | 131.00 | 132.00 | 1.00 | 1.0 | 0.001 | 0.002 | 0.148 | | |
| AB95-10 | M999416 | YW12179287 | 132.00 | 133.00 | 1.00 | 4.6 | 0.013 | 0.010 | 2.600 | Massive Sulphide | medium grained. |
| AB95-10 | M999417 | YW12179287 | 133.00 | 134.50 | 1.50 | 5.5 | 0.001 | 0.003 | 0.348 | Sulphidic Sandstone | broken down, fine grained dolomitic. |
| AB95-10 | M999418 | YW12179287 | 134.50 | 136.00 | 1.50 | 3.8 | 0.001 | 0.004 | 0.460 | | |
| AB95-10 | M999419 | YW12179287 | 136.00 | 137.00 | 1.00 | 2.9 | 0.001 | 0.001 | 0.159 | | |
| AB95-10 | M999421 | YW12179287 | 137.00 | 138.50 | 1.50 | 5.7 | 0.002 | 0.004 | 0.450 | | |
| AB95-10 | M999422 | YW12179287 | 138.50 | 140.00 | 1.50 | 3.9 | 0.001 | 0.002 | 0.192 | | |
| AB95-10 | M999423 | YW12179287 | 140.00 | 141.50 | 1.50 | 5.3 | 0.001 | 0.003 | 0.514 | | |
| AB95-10 | M999424 | YW12179287 | 141.50 | 143.00 | 1.50 | 57.1 | 0.007 | 0.038 | 2.740 | | |
| AB95-10 | M999425 | YW12179287 | 143.00 | 144.00 | 1.00 | 58.9 | 0.009 | 0.022 | 2.080 | | |
| AB95-10 | M999426 | YW12179287 | 144.00 | 146.00 | 2.00 | 16.7 | 0.005 | 0.049 | 1.785 | Dolomicrite | blocky and broken core |
| AB95-10 | M999427 | YW12179287 | 146.00 | 147.50 | 1.50 | 5.0 | 0.002 | 0.030 | 0.954 | | |
| AB95-10 | M999428 | YW12179287 | 147.50 | 149.00 | 1.50 | 2.6 | 0.002 | 0.010 | 0.935 | | |
| AB95-11 | M999429 | YW12179287 | 189.50 | 191.00 | 1.50 | -0.5 | 0.000 | 0.001 | 0.015 | Dolo Sandstone | fine grained, interbedded, with muddy horizons and minor bioturbated Dolostone. Sandstone layers are broken down. |
| AB95-11 | M999431 | YW12179287 | 191.00 | 192.00 | 1.00 | 11.3 | 0.003 | 0.006 | 0.768 | Sulphidic Sandstone | Dolomitic |
| AB95-11 | M999432 | YW12179287 | 192.00 | 193.00 | 1.00 | 84.0 | 0.004 | 0.013 | 2.270 | | |
| AB95-11 | M999433 | YW12179287 | 193.00 | 194.00 | 1.00 | 9.3 | 0.002 | 0.008 | 0.402 | Massive Sulphide | Massive, medium grained Marcasite. |
| AB95-11 | M999434 | YW12179287 | 194.00 | 195.00 | 1.00 | 9.4 | 0.002 | 0.017 | 0.180 | | |
| AB95-11 | M999435 | YW12179287 | 195.00 | 196.00 | 1.00 | 6.6 | 0.002 | 0.017 | 0.092 | | |
| AB95-11 | M999436 | YW12179287 | 196.00 | 197.50 | 1.50 | 12.8 | 0.003 | 0.023 | 0.492 | | |
| AB95-11 | M999437 | YW12179287 | 197.50 | 198.50 | 1.00 | 1.6 | 0.001 | 0.006 | 0.068 | Dolo Sandstone | Fine grained. Massive, oxidized. |
| AB95-11 | M999438 | YW12179287 | 198.50 | 200.00 | 1.50 | 1.4 | 0.001 | 0.008 | 0.084 | | |
| AB95-11 | M999439 | YW12179287 | 200.00 | 201.50 | 1.50 | 0.8 | 0.001 | 0.008 | 0.047 | | |
| AB95-11 | M999441 | YW12179287 | 201.50 | 203.00 | 1.50 | 1.6 | 0.002 | 0.016 | 0.098 | | |
| AB95-11 | M999442 | YW12179287 | 203.00 | 204.00 | 1.00 | 6.1 | 0.001 | 0.008 | 0.280 | | |
| AB95-11 | M999443 | YW12179287 | 204.00 | 205.00 | 1.00 | 155.0 | 0.011 | 0.065 | 1.565 | Sulphidic Sandstone | Dolomitic |
| AB95-11 | M999444 | YW12179287 | 205.00 | 206.00 | 1.00 | 82.0 | 0.005 | 0.041 | 6.160 | | |
| AB95-11 | M999445 | YW12179287 | 206.00 | 207.00 | 1.00 | 16.1 | 0.002 | 0.010 | 0.378 | Dolomicrite | interbedded with bioturbated dolostone and lesser muddy interbeds. Muddy horizons cause the core to be blocky. |
| AB95-11 | M999446 | YW12179287 | 207.00 | 208.00 | 1.00 | 8.7 | 0.002 | 0.006 | 0.566 | | |
| AB95-12 | M999021 | YW12188552 | 89.00 | 90.50 | 1.50 | -0.5 | 0.001 | 0.001 | 0.038 | Dolo Sandstone | fine grained. Vuggy. Broken down to blocky in places. Vugs are filled with late medium grained euheudral dolomite. |
| AB95-12 | M999022 | YW12188552 | 90.50 | 92.00 | 1.50 | -0.5 | 0.001 | 0.001 | 0.028 | | |
| AB95-12 | M999023 | YW12188552 | 92.00 | 93.50 | 1.50 | -0.5 | 0.001 | 0.001 | 0.032 | | |
| AB95-12 | M999024 | YW12188552 | 93.50 | 94.50 | 1.00 | -0.5 | 0.001 | 0.001 | 0.020 | | |
| AB95-13 | M999018 | YW12188552 | 196.50 | 197.20 | 0.70 | -0.5 | 0.001 | 0.001 | 0.006 | Sandstone | Beige quartz rich sandstone. Increasing lithic content down interval. |
| AB95-13 | M999019 | YW12188552 | 197.20 | 198.50 | 1.30 | -0.5 | 0.001 | 0.002 | 0.019 | Sandstone | Lithic sandstone. Minor marcasite. |
| AB95-13 | M999020 | YW12188552 | 198.50 | 199.20 | 0.70 | -0.5 | 0.002 | 0.004 | 0.009 | | |
| ST97-07 | M999051 | YW12188552 | 32.00 | 33.50 | 1.50 | 0.5 | 0.168 | 0.001 | 0.002 | Laminated Dolomicrite | finely laminated beige with local muddy interbeds (broken down) and bioturbated beds. Green smectite at 5.6m. |
| ST97-07 | M999052 | YW12188552 | 33.50 | 35.00 | 1.50 | 1.8 | 1.655 | 0.001 | 0.002 | Bioturbated Dolomicrite | beige with moderate patchy malachite staining with medium grained euheudral clotty pyrite. |
| ST97-07 | M999053 | YW12188552 | 35.00 | 36.50 | 1.50 | -0.5 | 0.038 | 0.001 | 0.001 | | |
| ST97-07 | M999054 | YW12188552 | 36.50 | 38.00 | 1.50 | -0.5 | 0.121 | 0.001 | 0.002 | | |
| ST97-07 | M999055 | YW12188552 | 38.00 | 39.50 | 1.50 | -0.5 | 0.160 | 0.001 | 0.001 | | |
| ST97-07 | M999056 | YW12188552 | 39.50 | 41.00 | 1.50 | -0.5 | 0.074 | 0.001 | 0.001 | Bioturbated Dolomicrite | local crackle breccia. Chalcopyrite and pyrite infilling large flooded spaces in the breccia. |
| ST97-07 | M999057 | YW12188552 | 41.00 | 42.00 | 1.00 | -0.5 | 0.139 | 0.001 | 0.001 | | |
| ST97-07 | M999058 | YW12188552 | 42.00 | 43.00 | 1.00 | 3.2 | 0.300 | 0.003 | 0.001 | | |
| ST97-07 | M999059 | YW12188552 | 43.00 | 44.00 | 1.00 | 28.9 | 0.248 | 0.016 | 0.001 | | |
| ST97-07 | M999060 | YW12188552 | 44.00 | 45.00 | 1.00 | 15.8 | 0.085 | 0.007 | 0.001 | | |
| ST97-07 | M999061 | YW12188552 | 45.00 | 46.00 | 1.00 | 2.4 | 0.132 | 0.002 | 0.001 | | |
| ST97-07 | M999062 | YW12188552 | 46.00 | 47.00 | 1.00 | 2.0 | 0.068 | 0.004 | 0.001 | | |
| ST97-07 | M999063 | YW12188552 | 47.00 | 48.00 | 1.00 | 3.3 | 0.249 | 0.003 | 0.001 | Bioturbated Dolomicrite | Minor breccia horizons with sparse malachite, chalcopyrite, and pyrite. |
| ST97-07 | M999064 | YW12188552 | 48.00 | 49.00 | 1.00 | 7.3 | 0.892 | 0.016 | 0.001 | | |
| ST97-07 | M999065 | YW12188552 | 49.00 | 50.00 | 1.00 | 2.2 | 1.260 | 0.005 | 0.001 | | |
| ST97-07 | M999066 | YW12188552 | 50.00 | 51.00 | 1.00 | -0.5 | 0.094 | 0.001 | 0.001 | | |
| ST97-07 | M999067 | YW12188552 | 51.00 | 52.00 | 1.00 | -0.5 | 0.069 | 0.000 | 0.001 | | |
| ST97-07 | M999068 | YW12188552 | 52.00 | 53.00 | 1.00 | 1.4 | 1.470 | 0.001 | 0.001 | | |
| ST97-07 | M999069 | YW12188552 | 53.00 | 54.00 | 1.00 | 1.4 | 0.481 | 0.001 | 0.001 | | |
| ST97-07 | M999070 | YW12188552 | 54.00 | 55.00 | 1.00 | 4.1 | 0.567 | 0.001 | 0.001 | | |
| ST97-07 | M999071 | YW12188552 | 55.00 | 56.00 | 1.00 | -0.5 | 0.423 | 0.001 | 0.001 | | |
| ST97-07 | M999072 | YW12188552 | 56.00 | 57.00 | 1.00 | -0.5 | 0.636 | 0.001 | 0.000 | | |
| ST97-07 | M999073 | YW12188552 | 57.00 | 58.00 | 1.00 | -0.5 | 0.203 | 0.000 | 0.000 | | |
| ST97-07 | M999074 | YW12188552 | 58.00 | 59.00 | 1.00 | 1.1 | 0.492 | 0.002 | 0.000 | | |

| | | | | | | | | | | | |
|---------|---------|------------|--------|--------|------|-------------|--------------|-------|-------|-------------------------|--|
| ST97-07 | M999075 | YW12188552 | 59.00 | 60.00 | 1.00 | 0.5 | 0.242 | 0.001 | 0.001 | Polymictic Breccia | 2-5% chalcopyrite and pyrite in cement. Clast supported breccia. Clasts are 0.5-2cm and subangular. Sulphides occur as fine grained clots. Clasts range in composition from dolomicrite to milky quartz. |
| ST97-07 | M999076 | YW12188552 | 60.00 | 61.00 | 1.00 | 3.3 | 0.110 | 0.004 | 0.001 | Dolomicrite | 2-5% chalcopyrite and pyrite in cement. Clast supported breccia. Clasts are 0.5-2cm and subangular. Sulphides occur as fine grained clots. Clasts range in composition from dolomicrite to milky quartz. |
| ST97-07 | M999077 | YW12188552 | 61.00 | 62.00 | 1.00 | 2.1 | 0.137 | 0.002 | 0.001 | | |
| ST97-07 | M999078 | YW12188552 | 62.00 | 63.00 | 1.00 | 2.2 | 0.030 | 0.002 | 0.000 | | |
| ST97-07 | M999079 | YW12188552 | 63.00 | 64.00 | 1.00 | 2.9 | 0.083 | 0.004 | 0.000 | | |
| ST97-07 | M999081 | YW12188552 | 64.00 | 65.00 | 1.00 | 0.9 | 0.033 | 0.002 | 0.000 | | |
| ST97-07 | M999082 | YW12188552 | 65.00 | 66.00 | 1.00 | 3.4 | 0.064 | 0.006 | 0.000 | | |
| ST97-07 | M999083 | YW12188552 | 66.00 | 67.00 | 1.00 | 2.4 | 0.014 | 0.003 | 0.001 | | |
| ST97-07 | M999084 | YW12188552 | 67.00 | 68.00 | 1.00 | -0.5 | 0.014 | 0.002 | 0.001 | | |
| ST97-07 | M999085 | YW12188552 | 68.00 | 69.00 | 1.00 | -0.5 | 0.083 | 0.001 | 0.000 | | |
| ST97-07 | M999086 | YW12188552 | 69.00 | 70.00 | 1.00 | 0.7 | 0.114 | 0.002 | 0.001 | | |
| ST97-07 | M999087 | YW12188552 | 70.00 | 71.00 | 1.00 | 1.1 | 0.110 | 0.003 | 0.000 | | |
| ST97-07 | M999088 | YW12188552 | 71.00 | 72.50 | 1.50 | 0.8 | 0.190 | 0.001 | 0.001 | | |
| ST97-07 | M999089 | YW12188552 | 72.50 | 74.00 | 1.50 | -0.5 | 0.072 | 0.001 | 0.000 | | |
| ST97-07 | M999091 | YW12188552 | 74.00 | 75.50 | 1.50 | -0.5 | 0.013 | 0.001 | 0.006 | | |
| ST97-07 | M999092 | YW12188552 | 75.50 | 77.00 | 1.50 | -0.5 | 0.005 | 0.000 | 0.001 | | |
| ST97-07 | M999093 | YW12188552 | 77.00 | 78.50 | 1.50 | -0.5 | 0.015 | 0.000 | 0.000 | | |
| ST97-07 | M999094 | YW12188552 | 78.50 | 80.00 | 1.50 | -0.5 | 0.008 | 0.000 | 0.000 | | |
| ST97-07 | M999095 | YW12188552 | 80.00 | 81.50 | 1.50 | -0.5 | 0.068 | 0.000 | 0.000 | | |
| ST97-07 | M999096 | YW12188552 | 81.50 | 83.00 | 1.50 | -0.5 | 0.026 | 0.000 | 0.000 | | |
| ST97-07 | M999097 | YW12188552 | 83.00 | 84.50 | 1.50 | -0.5 | 0.014 | 0.000 | 0.000 | | |
| ST97-07 | M999098 | YW12188552 | 84.50 | 86.00 | 1.50 | -0.5 | 0.291 | 0.002 | 0.000 | | |
| ST97-07 | M999099 | YW12188552 | 86.00 | 87.50 | 1.50 | -0.5 | 0.057 | 0.001 | 0.001 | | |
| ST97-07 | M999451 | YW12188552 | 87.50 | 89.00 | 1.50 | -0.5 | 0.088 | 0.002 | 0.016 | Bioturbated Dolomicrite | Local Breccia horizons. Vugs are infilled by dark green to black Chlorite. Minor disseminated Malachite staining associated with fractures and vugs. |
| ST97-07 | M999452 | YW12188552 | 89.00 | 90.50 | 1.50 | -0.5 | 0.024 | 0.001 | 0.002 | | |
| ST97-07 | M999453 | YW12188552 | 90.50 | 92.00 | 1.50 | 0.9 | 0.284 | 0.001 | 0.001 | Dolomicrite | Local stylolitic horizons and Crackle Breccia. |
| ST97-07 | M999454 | YW12188552 | 92.00 | 93.00 | 1.00 | 0.6 | 0.161 | 0.001 | 0.002 | | |
| ST97-07 | M999455 | YW12188552 | 93.00 | 94.50 | 1.50 | -0.5 | 0.013 | 0.000 | 0.001 | | |
| ST97-07 | M999456 | YW12188552 | 94.50 | 96.00 | 1.50 | 1.6 | 0.581 | 0.001 | 0.001 | | |
| ST97-07 | M999457 | YW12188552 | 96.00 | 97.00 | 1.00 | 0.9 | 0.099 | 0.001 | 0.001 | | |
| ST97-07 | M999458 | YW12188552 | 97.00 | 98.00 | 1.00 | <0.5 | 0.127 | 0.003 | 0.001 | Cataclastic Fault Zone | Clast supported cemented Breccia. Cement is Dolomitic. Clasts are subangular - subrounded. Clasts themselves are Crackle Brecciated. |
| ST97-07 | M999459 | YW12188552 | 98.00 | 99.00 | 1.00 | 1.0 | 0.034 | 0.001 | 0.001 | | |
| ST97-07 | M999461 | YW12188552 | 99.00 | 100.50 | 1.50 | -0.5 | 0.018 | 0.000 | 0.001 | Bioturbated Dolomicrite | Beige |
| ST97-07 | M999462 | YW12188552 | 100.50 | 102.00 | 1.50 | 0.6 | 0.088 | 0.001 | 0.001 | | |
| ST97-07 | M999463 | YW12188552 | 102.00 | 103.50 | 1.50 | 0.6 | 0.024 | 0.001 | 0.001 | Dolomicrite | Weakly brecciated. Fine grained, dusty Pyrite and Chalcopyrite along with Dolomite as cement. Dark Chlorite in cement as well. |
| ST97-07 | M999464 | YW12188552 | 103.50 | 105.00 | 1.50 | 5.8 | 0.031 | 0.001 | 0.001 | | |
| ST97-07 | M999465 | YW12188552 | 105.00 | 106.50 | 1.50 | 1.1 | 0.067 | 0.001 | 0.000 | | |
| ST97-07 | M999466 | YW12188552 | 106.50 | 108.00 | 1.50 | 60.5 | 1.310 | 0.003 | 0.000 | | |
| ST97-07 | M999467 | YW12188552 | 108.00 | 109.50 | 1.50 | 25.7 | 0.396 | 0.002 | 0.001 | | |
| ST97-07 | M999654 | YW12175936 | 109.50 | 111.00 | 1.50 | 3.9 | 0.018 | 0.000 | 0.000 | Laminated Dolomicrite | Beige, finely laminated. Interbedded with bioturbated / weakly brecciated zones. Dark Chlorite and dusty Pyrite in matrix. |
| ST97-07 | M999655 | YW12175936 | 111.00 | 112.50 | 1.50 | 1.2 | 0.157 | 0.000 | 0.000 | | |
| ST97-07 | M999656 | YW12175936 | 112.50 | 114.00 | 1.50 | -0.5 | 0.085 | 0.000 | 0.000 | | |
| ST97-07 | M999657 | YW12175936 | 114.00 | 115.50 | 1.50 | -0.5 | 0.041 | 0.000 | 0.000 | | |
| ST97-07 | M999658 | YW12175936 | 115.50 | 117.00 | 1.50 | -0.5 | 0.006 | 0.000 | 0.000 | | |
| ST97-07 | M999659 | YW12175936 | 117.00 | 118.50 | 1.50 | -0.5 | 0.058 | 0.001 | 0.000 | | |
| ST97-07 | M999661 | YW12175936 | 118.50 | 120.00 | 1.50 | -0.5 | 0.019 | 0.001 | 0.001 | | |
| ST97-07 | M999662 | YW12175936 | 120.00 | 121.50 | 1.50 | 2.0 | 0.162 | 0.001 | 0.000 | | |
| ST97-07 | M999663 | YW12175936 | 121.50 | 123.00 | 1.50 | 1.8 | 0.151 | 0.001 | 0.000 | | |
| ST97-07 | M999664 | YW12175936 | 123.00 | 124.50 | 1.50 | 0.9 | 0.107 | 0.001 | 0.000 | | |
| ST97-07 | M999665 | YW12175936 | 124.50 | 126.00 | 1.50 | 0.6 | 0.083 | 0.000 | 0.000 | Dolomicrite | Upper Crackle Breccia contact, matrix is stained with Malachite. Dolomicrite is weakly brecciated and beige. |
| ST97-07 | M999666 | YW12175936 | 126.00 | 127.50 | 1.50 | -0.5 | 0.104 | 0.000 | 0.000 | | |
| ST97-08 | M999468 | YW12184046 | 0.00 | 1.20 | 1.20 | 7.9 | 4.550 | 0.005 | 0.040 | Laminated Dolomicrite | Finely laminated with minor breccia interbeds. Muddier horizons are broken down. Core is blocky. Minor Calcite in matrix of breccias. |
| ST97-08 | M999469 | YW12184046 | 1.20 | 2.20 | 1.00 | 8.2 | 4.850 | 0.005 | 0.040 | | |
| ST97-08 | M999471 | YW12184046 | 2.20 | 3.50 | 1.30 | -0.5 | 0.146 | 0.001 | 0.009 | | |
| ST97-08 | M999472 | YW12184046 | 3.50 | 5.00 | 1.50 | 6.9 | 3.260 | 0.003 | 0.014 | | |
| ST97-08 | M999473 | YW12184046 | 5.00 | 6.50 | 1.50 | 19.3 | 7.870 | 0.014 | 0.014 | | |
| ST97-08 | M999474 | YW12184046 | 6.50 | 8.00 | 1.50 | -0.5 | 0.136 | 0.001 | 0.004 | | |
| ST97-08 | M999475 | YW12184046 | 8.00 | 9.00 | 1.00 | -0.5 | 0.203 | 0.002 | 0.004 | | |
| ST97-08 | M999476 | YW12184046 | 9.00 | 10.00 | 1.00 | 1.7 | 1.300 | 0.005 | 0.005 | | |
| ST97-08 | M999477 | YW12184046 | 10.00 | 11.00 | 1.00 | 0.5 | 0.812 | 0.000 | 0.003 | | |
| ST97-08 | M999478 | YW12184046 | 11.00 | 12.00 | 1.00 | -0.5 | 0.239 | 0.001 | 0.003 | | |
| ST97-08 | M999479 | YW12184046 | 12.00 | 13.00 | 1.00 | 1.5 | 0.784 | 0.001 | 0.003 | | |
| ST97-08 | M999481 | YW12184046 | 13.00 | 14.00 | 1.00 | 4.1 | 0.904 | 0.003 | 0.007 | | |
| ST97-08 | M999482 | YW12184046 | 14.00 | 15.00 | 1.00 | 2.7 | 0.690 | 0.006 | 0.019 | | |

| | | | | | | | | | | |
|---------|---------|------------|-------|-------|------|------|--------|-------|-------|------------------------------|
| ST97-08 | M999483 | YW12184046 | 15.00 | 16.30 | 1.30 | 10.3 | 0.644 | 0.020 | 0.014 | |
| ST97-08 | M999484 | YW12184046 | 16.30 | 17.30 | 1.00 | 9.0 | 3.65 | 0.030 | 0.010 | |
| ST97-08 | M999485 | YW12184046 | 17.30 | 18.70 | 1.40 | 5.8 | 1.21 | 0.015 | 0.006 | |
| ST97-08 | M999486 | YW12184046 | 18.70 | 19.50 | 0.80 | 1.0 | 0.044 | 0.005 | 0.003 | |
| ST97-08 | M999487 | YW12184046 | 19.50 | 21.00 | 1.50 | 0.8 | 0.056 | 0.003 | 0.005 | |
| ST97-08 | M999488 | YW12184046 | 21.00 | 22.50 | 1.50 | 1.9 | 0.257 | 0.005 | 0.008 | |
| ST97-08 | M999489 | YW12184046 | 22.50 | 24.00 | 1.50 | 2.4 | 0.410 | 0.003 | 0.004 | |
| ST97-08 | M999491 | YW12184046 | 24.00 | 25.20 | 1.20 | 2.1 | 0.499 | 0.011 | 0.011 | |
| ST97-08 | M999492 | YW12184046 | 25.20 | 26.00 | 0.80 | 9.7 | 4.12 | 0.017 | 0.025 | |
| ST97-08 | M999493 | YW12184046 | 26.00 | 26.80 | 0.80 | 2.7 | 1.945 | 0.003 | 0.008 | |
| ST97-08 | M999494 | YW12184046 | 26.80 | 27.80 | 1.00 | 3.3 | 1.815 | 0.002 | 0.006 | |
| ST97-08 | M999495 | YW12184046 | 27.80 | 28.60 | 0.80 | 19.5 | 7.51 | 0.006 | 0.022 | |
| ST97-08 | M999496 | YW12184046 | 28.60 | 29.10 | 0.50 | 37.3 | 26.5 | 0.017 | 0.071 | |
| ST97-08 | M999497 | YW12184046 | 29.10 | 30.10 | 1.00 | 8.9 | 6.94 | 0.003 | 0.008 | |
| ST97-08 | M999498 | YW12184046 | 30.10 | 30.90 | 0.80 | 1.4 | 0.858 | 0.001 | 0.003 | |
| ST97-08 | M999499 | YW12184046 | 30.90 | 31.80 | 0.90 | <0.5 | 0.248 | 0.001 | 0.002 | |
| ST97-08 | M999501 | YW12184046 | 31.80 | 32.50 | 0.70 | <0.5 | 0.197 | 0.001 | 0.001 | |
| ST97-08 | M999502 | YW12184046 | 32.50 | 33.50 | 1.00 | 2.0 | 1.395 | 0.004 | 0.003 | |
| ST97-08 | M999503 | YW12184046 | 33.50 | 35.00 | 1.50 | 2.9 | 2.5 | 0.002 | 0.002 | |
| ST97-08 | M999504 | YW12184046 | 35.00 | 36.50 | 1.50 | 3.8 | 3.31 | 0.001 | 0.007 | |
| ST97-08 | M999505 | YW12184046 | 36.50 | 37.20 | 0.70 | 1.1 | 1.155 | 0.001 | 0.007 | |
| ST97-08 | M999506 | YW12184046 | 37.20 | 38.10 | 0.90 | 6.8 | 9.09 | 0.023 | 0.036 | |
| ST97-08 | M999507 | YW12184046 | 38.10 | 38.70 | 0.60 | 1.2 | 0.599 | 0.004 | 0.003 | |
| ST97-08 | M999508 | YW12184046 | 38.70 | 40.40 | 1.70 | 3.1 | 2.38 | 0.007 | 0.006 | |
| ST97-08 | M999509 | YW12184046 | 40.40 | 41.40 | 1.00 | 0.7 | 1.87 | 0.003 | 0.061 | |
| ST97-08 | M999511 | YW12184046 | 41.40 | 42.80 | 1.40 | 0.6 | 0.908 | 0.004 | 0.049 | |
| ST97-08 | M999512 | YW12184046 | 42.80 | 43.80 | 1.00 | 1.2 | 4.26 | 0.004 | 0.043 | |
| ST97-08 | M999513 | YW12184046 | 43.80 | 45.00 | 1.20 | 1.7 | 8.43 | 0.010 | 0.038 | |
| ST97-08 | M999514 | YW12184046 | 45.00 | 46.00 | 1.00 | 0.5 | 0.463 | 0.002 | 0.008 | |
| ST97-08 | M999515 | YW12184046 | 46.00 | 47.00 | 1.00 | 1.1 | 0.890 | 0.004 | 0.009 | |
| ST97-08 | M999516 | YW12184046 | 47.00 | 48.50 | 1.50 | 0.6 | 0.387 | 0.003 | 0.004 | |
| ST97-08 | M999517 | YW12184046 | 48.50 | 50.00 | 1.50 | 3.9 | 1.025 | 0.022 | 0.003 | |
| ST97-08 | M999518 | YW12184046 | 50.00 | 51.00 | 1.00 | 1.6 | 0.709 | 0.009 | 0.005 | |
| ST97-08 | M999519 | YW12184046 | 51.00 | 52.00 | 1.00 | 6.8 | 0.863 | 0.031 | 0.024 | |
| ST97-08 | M999521 | YW12184046 | 52.00 | 53.00 | 1.00 | 5.3 | 19.950 | 0.026 | 0.015 | |
| ST97-08 | M999522 | YW12184046 | 53.00 | 54.00 | 1.00 | 3.2 | 17.150 | 0.018 | 0.020 | |
| ST97-08 | M999523 | YW12184046 | 54.00 | 55.00 | 1.00 | 2.1 | 1.830 | 0.006 | 0.007 | |
| ST97-08 | M999524 | YW12184046 | 55.00 | 56.50 | 1.50 | 1.1 | 0.662 | 0.003 | 0.004 | |
| ST97-08 | M999525 | YW12184046 | 56.50 | 58.00 | 1.50 | 2.7 | 2.810 | 0.017 | 0.005 | |
| ST97-08 | M999526 | YW12184046 | 58.00 | 59.50 | 1.50 | -0.5 | 0.107 | 0.001 | 0.003 | |
| ST97-08 | M999527 | YW12184046 | 59.50 | 60.50 | 1.00 | -0.5 | 0.164 | 0.001 | 0.001 | |
| ST97-08 | M999528 | YW12184046 | 60.50 | 62.00 | 1.50 | -0.5 | 0.277 | 0.001 | 0.000 | |
| ST97-08 | M999529 | YW12184046 | 62.00 | 63.50 | 1.50 | -0.5 | 0.213 | 0.001 | 0.001 | |
| ST97-08 | M999531 | YW12184046 | 63.50 | 65.00 | 1.50 | -0.5 | 0.235 | 0.001 | 0.002 | |
| ST97-08 | M999532 | YW12184046 | 65.00 | 66.00 | 1.00 | -0.5 | 0.171 | 0.001 | 0.002 | Sulphidic Dolomitic Breccia |
| ST97-08 | M999533 | YW12184046 | 66.00 | 67.50 | 1.50 | 1.4 | 0.636 | 0.003 | 0.002 | |
| ST97-08 | M999534 | YW12184046 | 67.50 | 69.00 | 1.50 | -0.5 | 0.127 | 0.001 | 0.002 | Brecciated Dolomitic Breccia |
| ST97-08 | M999535 | YW12184046 | 69.00 | 70.50 | 1.50 | -0.5 | 0.030 | 0.001 | 0.002 | |
| ST97-08 | M999536 | YW12184046 | 70.50 | 72.00 | 1.50 | 0.8 | 0.221 | 0.003 | 0.003 | |
| ST97-08 | M999537 | YW12184046 | 72.00 | 73.00 | 1.00 | 8.5 | 1.715 | 0.018 | 0.010 | |
| ST97-08 | M999538 | YW12184046 | 73.00 | 74.00 | 1.00 | 2.6 | 0.411 | 0.004 | 0.005 | |
| ST97-08 | M999539 | YW12184046 | 74.00 | 76.00 | 2.00 | 3.6 | 1.620 | 0.005 | 0.010 | |
| ST97-08 | M999541 | YW12184046 | 76.00 | 78.00 | 2.00 | 10.0 | 4.780 | 0.005 | 0.007 | |
| ST97-08 | M999542 | YW12184046 | 78.00 | 79.40 | 1.40 | 4.2 | 0.884 | 0.003 | 0.003 | Brecciated Dolomitic Breccia |
| ST97-08 | M999543 | YW12184046 | 79.40 | 80.50 | 1.10 | 4.7 | 1.035 | 0.004 | 0.002 | |
| ST97-08 | M999544 | YW12184046 | 80.50 | 81.50 | 1.00 | 6.5 | 3.400 | 0.005 | 0.002 | Brecciated Dolomitic Breccia |
| ST97-08 | M999545 | YW12184046 | 81.50 | 82.50 | 1.00 | 1.4 | 0.935 | 0.001 | 0.001 | |
| ST97-08 | M999546 | YW12184046 | 82.50 | 84.00 | 1.50 | 1.0 | 0.129 | 0.001 | 0.001 | Brecciated Dolomitic Breccia |
| ST97-08 | M999547 | YW12184046 | 84.00 | 85.50 | 1.50 | -0.5 | 0.116 | 0.001 | 0.002 | |
| ST97-08 | M999548 | YW12184046 | 85.50 | 87.00 | 1.50 | -0.5 | 0.061 | 0.001 | 0.001 | |

Matrix is partially to completely comprised of Chalcopyrite and Pyrite. Chalcopyrite is coring Pyrite clots.

Clast supported, Dolomite matrix. Hematite along fractures locally.

Matrix supported, Dolomite matrix. Hematite along fractures locally. Minor Malachite in matrix.

Clast supported, dolomite matrix. Hematite along fractures locally.

Extremely blocky, strongly oxidized and broken down.

| | | | | | | | | | | | |
|---------|---------|------------|--------|--------|------|-------------|--------------|-------|-------|--------------------------|--|
| ST97-08 | M999549 | YW12184046 | 87.00 | 88.50 | 1.50 | -0.5 | 0.065 | 0.001 | 0.002 | Brecciated Dolomiticrite | Clast supported, Dolomite matrix. Hematite along fractures locally. |
| ST97-08 | M999551 | YW12184046 | 88.50 | 90.00 | 1.50 | -0.5 | 0.105 | 0.002 | 0.012 | Brecciated Dolomiticrite | Extremely blocky, strongly oxidized. Minor Malachite in cement locally. Broken down. |
| ST97-08 | M999552 | YW12184046 | 90.00 | 91.50 | 1.50 | -0.5 | 0.056 | 0.001 | 0.010 | | |
| ST97-08 | M999553 | YW12184046 | 91.50 | 93.00 | 1.50 | -0.5 | 0.188 | 0.003 | 0.006 | | |
| ST97-08 | M999554 | YW12184046 | 93.00 | 94.50 | 1.50 | -0.5 | 0.109 | 0.001 | 0.001 | | |
| ST97-08 | M999555 | YW12184046 | 94.50 | 96.00 | 1.50 | 5.5 | 1.745 | 0.003 | 0.004 | | |
| ST97-08 | M999556 | YW12184046 | 96.00 | 97.50 | 1.50 | 6.1 | 1.100 | 0.001 | 0.001 | | |
| ST97-08 | M999557 | YW12184046 | 97.50 | 99.00 | 1.50 | 1.1 | 0.195 | 0.001 | 0.002 | | |
| ST97-08 | M999558 | YW12184046 | 99.00 | 100.50 | 1.50 | 4.6 | 0.777 | 0.002 | 0.001 | | |
| ST97-08 | M999559 | YW12184046 | 100.50 | 102.00 | 1.50 | 13.4 | 0.856 | 0.003 | 0.001 | | |
| ST97-08 | M999561 | YW12184046 | 102.00 | 103.50 | 1.50 | 0.7 | 0.088 | 0.001 | 0.002 | | |
| ST97-08 | M999562 | YW12184046 | 103.50 | 105.00 | 1.50 | -0.5 | 0.022 | 0.001 | 0.001 | Brecciated Dolomiticrite | Calcite infilling fractures |
| ST97-08 | M999563 | YW12184046 | 105.00 | 106.50 | 1.50 | 0.5 | 0.035 | 0.001 | 0.001 | | |
| ST97-08 | M999564 | YW12184046 | 106.50 | 108.00 | 1.50 | 2.2 | 0.313 | 0.001 | 0.002 | | |
| ST97-08 | M999565 | YW12184046 | 108.00 | 109.50 | 1.50 | 1.5 | 0.183 | 0.002 | 0.003 | | |
| ST97-08 | M999566 | YW12184046 | 109.50 | 111.00 | 1.50 | 4.5 | 0.942 | 0.002 | 0.003 | | |
| ST97-08 | M999567 | YW12184046 | 111.00 | 112.50 | 1.50 | -0.5 | 0.029 | 0.001 | 0.001 | | |
| ST97-08 | M999568 | YW12184046 | 112.50 | 114.00 | 1.50 | -0.5 | 0.041 | 0.001 | 0.001 | | |
| ST97-08 | M999569 | YW12184046 | 114.00 | 115.00 | 1.00 | -0.5 | 0.017 | 0.001 | 0.001 | | |
| ST97-08 | M999571 | YW12184046 | 115.00 | 116.00 | 1.00 | -0.5 | 0.016 | 0.001 | 0.002 | | |
| ST97-09 | M999619 | YW12175936 | 53.00 | 54.50 | 1.50 | 0.5 | 0.109 | 0.003 | 0.001 | Brecciated Dolomiticrite | Med grey, variably clast to matrix supported, Hematite along fractures locally, minor rubby sections. |
| ST97-09 | M999621 | YW12175936 | 54.50 | 56.00 | 1.50 | -0.5 | 0.003 | 0.001 | 0.001 | Brecciated Dolomiticrite | Clast supported, strongly oxidized, Hematite along fractures and throughout matrix. |
| ST97-09 | M999622 | YW12175936 | 56.00 | 57.50 | 1.50 | -0.5 | 0.045 | 0.001 | 0.001 | | |
| ST97-09 | M999623 | YW12175936 | 57.50 | 59.00 | 1.50 | 0.8 | 0.055 | 0.002 | 0.001 | Brecciated Dolomiticrite | Beige , clast supported, localized minor matrix supported areas, blocky core |
| ST97-09 | M999624 | YW12175936 | 59.00 | 60.50 | 1.50 | -0.5 | 0.047 | 0.001 | 0.000 | | |
| ST97-09 | M999625 | YW12175936 | 60.50 | 62.00 | 1.50 | 0.5 | 0.053 | 0.001 | 0.001 | | |
| ST97-09 | M999626 | YW12175936 | 62.00 | 63.50 | 1.50 | 1.6 | 1.990 | 0.005 | 0.002 | | |
| ST97-09 | M999627 | YW12175936 | 63.50 | 64.75 | 1.25 | 1.2 | 3.580 | 0.011 | 0.002 | Brecciated Dolomiticrite | Med grey to beige in areas, mainly clast supported, matrix supported locally. Large rubblized sections. Trace hematite along fractures locally. |
| ST97-09 | M999628 | YW12175936 | 64.75 | 65.70 | 0.95 | 9.5 | 1.830 | 0.027 | 0.011 | | |
| ST97-09 | M999629 | YW12175936 | 65.70 | 67.00 | 1.30 | 2.6 | 1.975 | 0.010 | 0.003 | | |
| ST97-09 | M999631 | YW12175936 | 67.00 | 68.10 | 1.10 | 2.9 | 7.170 | 0.004 | 0.003 | | |
| ST97-09 | M999632 | YW12175936 | 68.10 | 69.10 | 1.00 | 1.6 | 8.780 | 0.002 | 0.005 | | |
| ST97-09 | M999633 | YW12175936 | 69.10 | 70.00 | 0.90 | 0.5 | 1.340 | 0.002 | 0.012 | | |
| ST97-09 | M999634 | YW12175936 | 70.00 | 71.50 | 1.50 | 1.0 | 3.380 | 0.002 | 0.011 | Dolomiticrite | Beige, clast supported brecciated sections, Malachite along fractures locally, large rubblized sections throughout, vuggy and pitted areas, laminated locally. |
| ST97-09 | M999635 | YW12175936 | 71.50 | 73.00 | 1.50 | 0.8 | 0.338 | 0.001 | 0.010 | | |
| ST97-09 | M999636 | YW12175936 | 73.00 | 74.50 | 1.50 | -0.5 | 0.959 | 0.005 | 0.010 | | |
| ST97-09 | M999637 | YW12175936 | 74.50 | 76.00 | 1.50 | 3.3 | 1.130 | 0.006 | 0.010 | | |
| ST97-09 | M999638 | YW12175936 | 76.00 | 77.50 | 1.50 | -0.5 | 0.409 | 0.000 | 0.002 | | |
| ST97-09 | M999639 | YW12175936 | 77.50 | 79.00 | 1.50 | -0.5 | 0.440 | 0.000 | 0.001 | | |
| ST97-09 | M999641 | YW12175936 | 79.00 | 80.50 | 1.50 | -0.5 | 3.060 | 0.001 | 0.001 | | |
| ST97-09 | M999642 | YW12175936 | 80.50 | 82.00 | 1.50 | -0.5 | 1.935 | 0.002 | 0.002 | | |
| ST97-09 | M999643 | YW12175936 | 82.00 | 83.50 | 1.50 | -0.5 | 0.802 | 0.004 | 0.002 | | |
| ST97-09 | M999644 | YW12175936 | 83.50 | 85.00 | 1.50 | 1.7 | 0.148 | 0.003 | 0.002 | Laminated Dolomiticrite | Med grey. Localized, clast supported brecciated areas. Blocky core. |
| ST97-09 | M999645 | YW12175936 | 85.00 | 86.50 | 1.50 | 3.8 | 0.850 | 0.021 | 0.001 | | |
| ST97-09 | M999646 | YW12175936 | 86.50 | 88.00 | 1.50 | 1.3 | 0.158 | 0.006 | 0.002 | | |
| ST97-09 | M999647 | YW12175936 | 88.00 | 89.00 | 1.00 | -0.5 | 0.062 | 0.005 | 0.002 | Laminated Dolomiticrite | Med grey to heavily oxidized areas, mainly blocky core, brecciated locally. Hematitic rubble at 90.30m |
| ST97-09 | M999648 | YW12175936 | 89.00 | 90.10 | 1.10 | 0.7 | 0.029 | 0.004 | 0.003 | | |
| ST97-09 | M999649 | YW12175936 | 90.10 | 92.00 | 1.90 | 1.2 | 0.085 | 0.002 | 0.003 | | |
| ST97-09 | M999651 | YW12175936 | 92.00 | 93.00 | 1.00 | -0.5 | 0.023 | 0.001 | 0.001 | Laminated Dolomiticrite | Med grey, well intact core, trace fracture surface oxidation. |
| ST97-09 | M999652 | YW12175936 | 93.00 | 94.00 | 1.00 | -0.5 | 0.016 | 0.001 | 0.001 | | |
| ST97-09 | M999653 | YW12175936 | 94.00 | 95.00 | 1.00 | -0.5 | 0.008 | 0.000 | 0.001 | Brecciated Dolomiticrite | Lt grey, blocky core, increasing oxidation and fractures from 63.5-64.5m. 65.1m to 66m: Major brecciation and hematite, dark grey in color. |
| ST97-10 | M999572 | YW12184046 | 61.00 | 62.50 | 1.50 | 1.4 | 0.016 | 0.005 | 0.001 | | |
| ST97-10 | M999573 | YW12184046 | 62.50 | 64.00 | 1.50 | 1.9 | 0.023 | 0.017 | 0.002 | Brecciated Dolomiticrite | |
| ST97-10 | M999574 | YW12184046 | 64.00 | 65.10 | 1.10 | 3.6 | 0.101 | 0.014 | 0.003 | | |
| ST97-10 | M999575 | YW12184046 | 65.10 | 66.60 | 1.50 | 7.7 | 0.310 | 0.088 | 0.001 | Laminated Dolomiticrite | Med grey, blocky core, rubby sections. Finely laminated. Minor localized brecciation with hematite matrix. |
| ST97-10 | M999576 | YW12184046 | 66.60 | 67.60 | 1.00 | 4.7 | 0.170 | 0.023 | 0.000 | | |
| ST97-10 | M999577 | YW12184046 | 67.60 | 69.00 | 1.40 | 1.5 | 0.054 | 0.009 | 0.000 | | |
| ST97-10 | M999578 | YW12184046 | 69.00 | 70.50 | 1.50 | -0.5 | 0.021 | 0.003 | 0.001 | | |
| ST97-10 | M999579 | YW12184046 | 70.50 | 72.00 | 1.50 | 1.1 | 0.019 | 0.006 | 0.001 | | |
| ST97-10 | M999581 | YW12184046 | 72.00 | 73.50 | 1.50 | -0.5 | 0.008 | 0.001 | 0.001 | | |

| | | | | | | | | | | | |
|---------|---------|------------|--------|--------|------|------------|--------------|-------|-------|------------------------|---|
| ST97-10 | M999582 | YW12184046 | 73.50 | 75.00 | 1.50 | -0.5 | 0.010 | 0.001 | 0.001 | Brecciated Dolomicrite | Med grey to beige, clast supported, blocky to rubblized sections, localized oxidation. |
| ST97-10 | M999583 | YW12184046 | 75.00 | 76.50 | 1.50 | -0.5 | 0.032 | 0.001 | 0.002 | | |
| ST97-10 | M999584 | YW12184046 | 76.50 | 78.00 | 1.50 | -0.5 | 0.083 | 0.001 | 0.002 | | |
| ST97-10 | M999585 | YW12184046 | 78.00 | 79.50 | 1.50 | 0.6 | 0.176 | 0.001 | 0.001 | | |
| ST97-10 | M999586 | YW12184046 | 79.50 | 81.00 | 1.50 | 0.9 | 0.504 | 0.002 | 0.002 | | |
| ST97-10 | M999587 | YW12184046 | 81.00 | 82.50 | 1.50 | 0.5 | 0.340 | 0.001 | 0.002 | | |
| ST97-10 | M999588 | YW12184046 | 82.50 | 84.00 | 1.50 | -0.5 | 0.065 | 0.001 | 0.002 | Brecciated Dolomicrite | Major oxidation throughout, locally hematitic. Heavily rubblized throughout. Clast supported. |
| ST97-10 | M999589 | YW12184046 | 84.00 | 85.50 | 1.50 | -0.5 | 0.061 | 0.001 | 0.001 | | |
| ST97-10 | M999591 | YW12184046 | 85.50 | 87.00 | 1.50 | -0.5 | 0.037 | 0.004 | 0.014 | | |
| ST97-10 | M999592 | YW12184046 | 87.00 | 88.50 | 1.50 | -0.5 | 0.011 | 0.001 | 0.001 | Brecciated Dolomicrite | Med grey, clast supported, blocky core, major hematite locally. |
| ST97-10 | M999593 | YW12184046 | 88.50 | 90.00 | 1.50 | 0.7 | 0.183 | 0.008 | 0.001 | | |
| ST97-10 | M999594 | YW12184046 | 90.00 | 91.50 | 1.50 | 0.7 | 0.201 | 0.002 | 0.002 | Brecciated Dolomicrite | Extremely rubblized section, heavily oxidized throughout, Hematite rich areas locally. Clast supported. Localized intact sections show hematite along fractures and in matrix. Minor localized laminated dolomicrite sections, trace hematite in fractures. |
| ST97-10 | M999595 | YW12184046 | 91.50 | 93.00 | 1.50 | 1.2 | 0.917 | 0.003 | 0.002 | | |
| ST97-10 | M999596 | YW12184046 | 93.00 | 94.50 | 1.50 | -0.5 | 0.278 | 0.002 | 0.001 | | |
| ST97-10 | M999597 | YW12184046 | 94.50 | 96.00 | 1.50 | 2.4 | 0.851 | 0.002 | 0.001 | | |
| ST97-10 | M999598 | YW12184046 | 96.00 | 97.50 | 1.50 | 2.8 | 1.805 | 0.002 | 0.002 | | |
| ST97-10 | M999599 | YW12184046 | 97.50 | 99.00 | 1.50 | 1.8 | 0.913 | 0.002 | 0.006 | | |
| ST97-10 | M999601 | YW12184046 | 99.00 | 100.50 | 1.50 | -0.5 | 0.091 | 0.001 | 0.002 | | |
| ST97-10 | M999602 | YW12184046 | 100.50 | 102.00 | 1.50 | -0.5 | 0.066 | 0.001 | 0.001 | | |
| ST97-10 | M999603 | YW12184046 | 102.00 | 103.50 | 1.50 | -0.5 | 0.299 | 0.001 | 0.003 | | |
| ST97-10 | M999604 | YW12184046 | 103.50 | 105.00 | 1.50 | -0.5 | 0.141 | 0.001 | 0.001 | | |
| ST97-10 | M999605 | YW12184046 | 105.00 | 106.50 | 1.50 | -0.5 | 0.111 | 0.001 | 0.000 | Brecciated Dolomicrite | Med grey, blocky core, clast supported. Trace oxidation on fracture faces. |
| ST97-10 | M999606 | YW12184046 | 106.50 | 108.00 | 1.50 | 0.5 | 0.053 | 0.001 | 0.003 | Rubble zone | Probable protolith Brecciated Dolomicrite. Heavily oxidized and unconsolidated material. Local hematite-rich breccia clasts. |
| ST97-10 | M999607 | YW12184046 | 108.00 | 109.50 | 1.50 | -0.5 | 0.030 | 0.001 | 0.002 | | |
| ST97-10 | M999608 | YW12184046 | 109.50 | 111.00 | 1.50 | -0.5 | 0.007 | 0.000 | 0.001 | Brecciated Dolomicrite | Med grey, well intact core, trace fracture surface oxidation. |
| ST97-11 | M999609 | YW12184046 | 64.60 | 66.00 | 1.40 | -0.5 | 0.024 | 0.001 | 0.002 | Dolomicrite | Siderite overprint, rust orange in colour. Minor vuggy bioturbated horizons. Trace Malachite along fractures. |
| ST97-11 | M999611 | YW12175936 | 66.00 | 67.50 | 1.50 | -0.5 | 0.037 | 0.001 | 0.002 | | |
| ST97-11 | M999612 | YW12175936 | 67.50 | 69.00 | 1.50 | 0.6 | 0.072 | 0.002 | 0.003 | | |
| ST97-11 | M999613 | YW12175936 | 69.00 | 70.50 | 1.50 | -0.5 | 0.056 | 0.001 | 0.002 | Laminated Dolomicrite | Finely laminated, weakly fractured - fractures are healed with Calcite. Interbedded breccia horizons. |
| ST97-11 | M999614 | YW12175936 | 70.50 | 71.50 | 1.00 | -0.5 | 0.020 | 0.001 | 0.001 | | |
| ST97-11 | M999615 | YW12175936 | 71.50 | 72.50 | 1.00 | 0.6 | 0.010 | 0.000 | 0.001 | | |
| ST97-11 | M999616 | YW12175936 | 160.00 | 161.50 | 1.50 | -0.5 | 0.018 | 0.001 | 0.002 | Laminated Dolomicrite | Finely laminated with interbeds of Framestone / Stromatolites. Local healed breccia zones. |
| ST97-11 | M999617 | YW12175936 | 161.50 | 163.00 | 1.50 | -0.5 | 0.029 | 0.001 | 0.004 | Dolo Sandstone | Oxidized and broken down. |